TABLE 1.0.1

HI-STORM FW SYSTEM COMPONENTS

Item	Designation (Model Number)
Overpack	HI-STORM FW
PWR Multi-Purpose Canisters	MPC-37, MPC-32ML
BWR Multi-Purpose Canister	MPC-89
Transfer Cask	HI-TRAC VW

1.1 INTRODUCTION TO THE HI-STORM FW SYSTEM

This section and the next section (Section 1.2) provide the necessary information on the HI-STORM FW System pursuant to 10CFR72 paragraphs 72.2(a)(1),(b); 72.122(a),(h)(1); 72.140(c)(2); 72.230(a),(b); and 72.236(a),(c),(h),(m).

HI-STORM (acronym for Holtec International Storage Module) FW System is a spent nuclear fuel storage system designed to be in full compliance with the requirements of 10CFR72. The model designation "FW" denotes this as a system which has been specifically engineered to withstand sustained Flood and Wind.

The HI-STORM FW System consists of a sealed metallic multi-purpose canister (MPC) contained within an overpack constructed from a combination of steel and concrete. The design features of the HI-STORM FW components are intended to simplify and reduce the on-site SNF loading and handling work effort, to minimize the burden of in-use monitoring, to provide utmost radiation protection to the plant personnel, and to minimize the site boundary dose.

The HI-STORM FW System can safely store either PWR or BWR fuel assemblies, in the MPC ~~-37 or MPC-89, respectively~~s identified in Table 1.0.1. The MPC is identified by the maximum number of fuel assemblies it can contain in the fuel basket. The MPC external diameters are identical to allow the use of a single overpack design, however the height of the MPC, as well as the overpack and transfer cask, are variable based on the SNF to be loaded.

Figure 1.1.1 shows the HI-STORM FW System with two of its major constituents, the MPC and the storage overpack, in a cut-away view. The MPC, shown partially withdrawn from the storage overpack, is an integrally welded pressure vessel designed to meet the stress limits of the ASME Boiler and Pressure Vessel Code, Section III, Subsection NB [1.1.1]. The MPC defines the Confinement Boundary for the stored spent nuclear fuel assemblies. The HI-STORM FW storage overpack provides structural protection, cooling, and radiological shielding for the MPC.

The HI-STORM FW overpack is equipped with thru-wall penetrations at the bottom of the overpack and in its lid to permit natural circulation of air to cool the MPC and the contained SNF. The HI-STORM FW System is autonomous inasmuch as it provides SNF and radioactive material confinement, radiation shielding, criticality control and passive heat removal independent of any other facility, structures, or components at the site. The surveillance and maintenance required by the plant's staff is minimized by the HI-STORM FW System since it is completely passive and is composed of proven materials. The HI-STORM FW System can be used either singly or as an array at an ISFSI. The site for an ISFSI can be located either at a nuclear reactor facility or an away-from-a-reactor (AFR) location.

The information presented in this report is intended to demonstrate the acceptability of the HI-STORM FW System for use under the general license provisions of Subpart K by meeting the criteria set forth in 10CFR72.236.

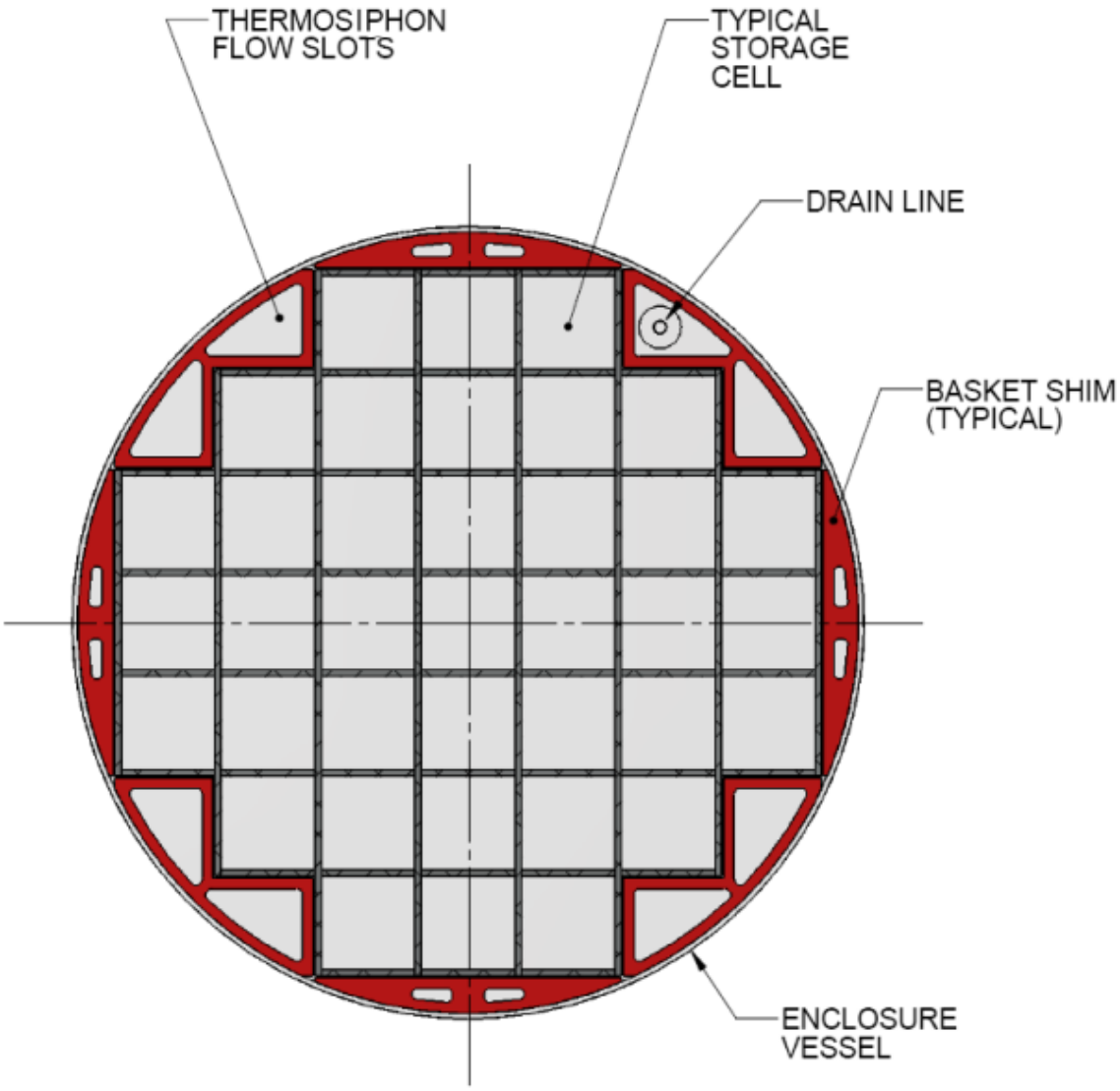

1.1.4A MPC-37 IN CROSS SECTION

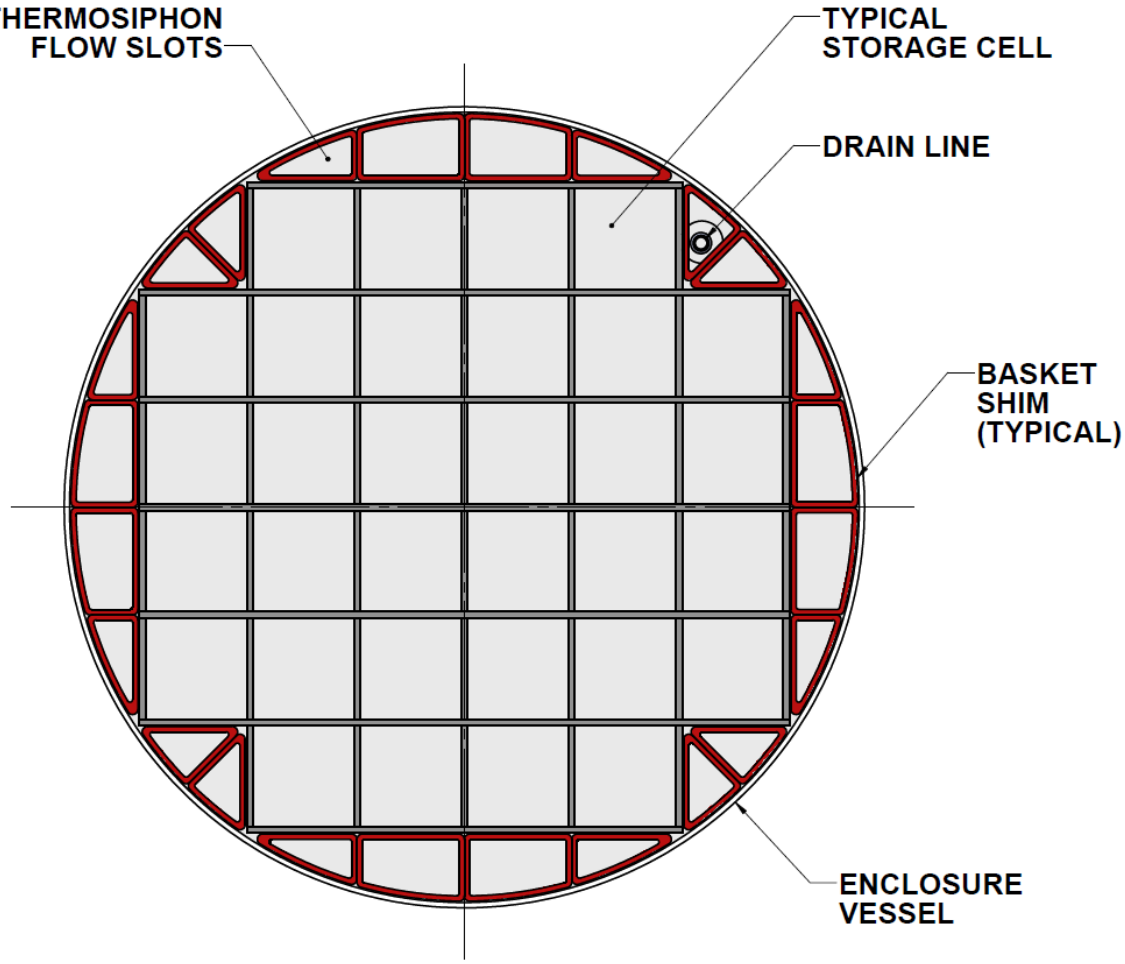

1.1.4B MPC-32ML IN CROSS SECTION

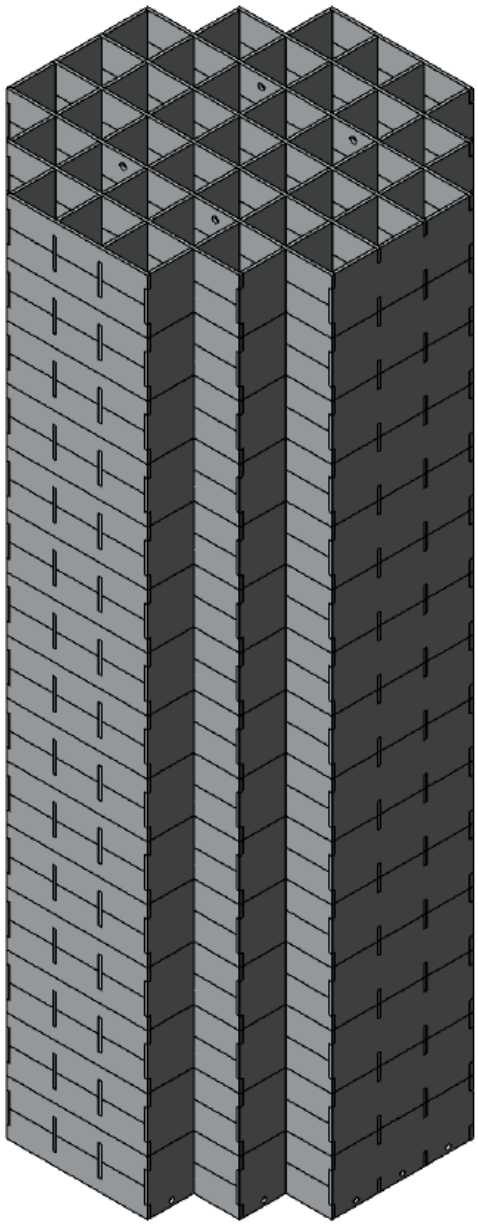

FIGURE 1.1.6A: MPC-37 PWR FUEL BASKET (37 STORAGE CELLS) IN PERSPECTIVE VIEW

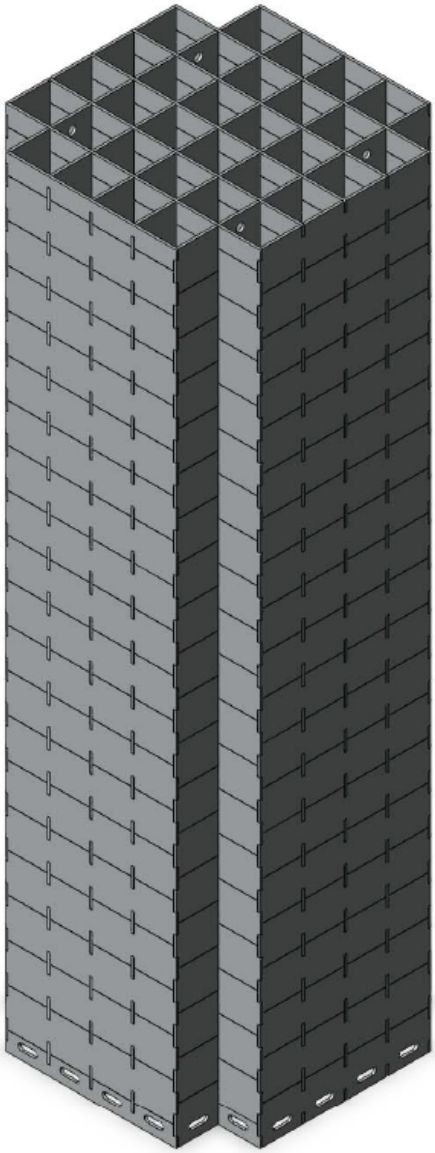

FIGURE 1.1.6B: MPC-32ML PWR FUEL BASKET (32 STORAGE CELLS) IN PERSPECTIVE VIEW

The HI-STORM FW System shares certain common attributes with the HI-STORM 100 System, Docket No. 72-1014, namely:

i. the honeycomb design of the MPC fuel basket;
ii. the effective distribution of neutron and gamma shielding materials within the system;
iii. the high heat dissipation capability;
iv. the engineered features to promote convective heat transfer by passive means;
v. a structurally robust steel-concrete-steel overpack construction.

The honeycomb design of the MPC fuel baskets renders the basket into a multi-flange egg-crate structure where all structural elements (i.e., cell walls) are arrayed in two orthogonal sets of plates. Consequently, the walls of the cells are either completely co-planar (i.e., no offset) or orthogonal with each other. There is complete edge-to-edge continuity between the contiguous cells to promote conduction of heat.

The composite shell construction in the overpack, steel-concrete-steel, allows ease of fabrication and eliminates the need for the sole reliance on the strength of concrete.

A description of each of the components is provided in this section, along with fabrication and safety feature information.

1.2.1.1 Multi-Purpose Canisters

The MPC enclosure vessels are cylindrical weldments with identical and fixed outside diameters. Each MPC is an assembly consisting of a honeycomb fuel basket (Figures 1.1.6 and 1.1.7), a baseplate, a canister shell, a lid, and a closure ring. The number of SNF storage locations in an MPC depends on the type of fuel assembly (PWR or BWR) to be stored in it.

Subsection 1.2.3 and Table 1.2.1 summarize the allowable contents for each MPC model listed in Table 1.0.1. Subsection 2.1.8 provides the detailed specifications for the contents authorized for storage in the HI-STORM FW System. Drawings for the MPCs are provided in Section 1.5.

The MPC enclosure vessel is a fully welded enclosure, which provides the confinement for the stored fuel and radioactive material. The MPC baseplate and shell are made of stainless steel (Alloy X, see Appendix 1.A). The lid is a two piece construction, with the top structural portion made of Alloy X. The confinement boundary is defined by the MPC baseplate, shell, lid, port covers, and closure ring.

The HI-STORM FW System MPCs shares external and internal features with the HI-STORM 100 MPCs certified in the §72-1014 docket, as summarized below.

i. ~~MPC-37 and MPC-89~~All HI-STORM FW MPCs have an identical enclosure vessel which mimics the enclosure vessel design details used in the HI-STORM 100 counterparts including the shell thickness, the vent and drain port sizes, construction details of the top lid and closure ring, and closure weld details. The baseplate is made slightly thicker to ensure its bending rigidity is comparable to its counterpart in the HI-STORM 100 system. The material

1.2.3 Cask Contents

This sub-section contains information on the cask contents pursuant to 10 CFR72, paragraphs 72.2(a)(1),(b) and 72.236(a),(c),(h),(m).

The HI-STORM FW System is designed to house both BWR and PWR spent nuclear fuel assemblies. Tables 1.2.1 and 1.2.2 provide key system data and parameters for the MPCs. A description of acceptable fuel assemblies for storage in the MPCs is provided in Section 2.1. This includes fuel assemblies classified as damaged fuel assemblies and fuel debris in accordance with the definitions of these terms in the Glossary. All fuel assemblies, non-fuel hardware, and neutron sources authorized for packaging in the MPCs must meet the fuel specifications provided in Section 2.1. All fuel assemblies classified as damaged fuel or fuel debris must be stored in damaged fuel containers (DFC).

As shown in Figure 1.2.1a (MPC-37) and Figure 1.2.2 (MPC-89), each storage location is assigned to one of three regions, denoted as Region 1, Region 2, and Region 3 with an associated cell identification number. For example, cell identified as 2-4 is Cell 4 in Region 2. A DFC can be stored in the outer peripheral locations of ~~both~~ the MPC-37/MPC-32ML and MPC-89 as shown in Figures 2.1.1 and 2.1.2, respectively. The permissible heat loads for each cell, region, and the total canister are given in Tables 1.2.3 and 1.2.4 for MPC-37/MPC-32ML and MPC-89, respectively. The sub-design heat loads for each cell, region and total canister are in Table 4.4.11.

TABLE 1.2.1

KEY SYSTEM DATA FOR HI-STORM FW SYSTEM

ITEM	QUANTITY	NOTES
Types of MPCs†	~~1~~2	~~1~~2 for PWR 1 for BWR
MPC storage capacity:	MPC-37	Up to 37 undamaged ZR clad PWR fuel assemblies with or without non-fuel hardware, of classes specified in Table 2.1.1a. Up to 12 damaged fuel containers containing PWR damaged fuel and/or fuel debris may be stored in the locations denoted in Figure 2.1.1a with the remaining basket cells containing undamaged fuel assemblies, up to a total of 37.
MPC storage capacity:	MPC-89	Up to 89 undamaged ZR clad BWR fuel assemblies. Up to 16 damaged fuel containers containing BWR damaged fuel and/or fuel debris may be stored in locations denoted in Figure 2.1.2 with the remaining basket cells containing undamaged fuel assemblies, up to a total of 89.
MPC storage capacity:	MPC-32ML	Up to 32 undamaged ZR clad PWR fuel assemblies, of classes specified in Table 2.1.1b. Up to 8 damaged fuel containers containing PWR damaged fuel and/or fuel debris may be stored in the locations denoted in Figure 2.1.1b with the remaining basket cells containing undamaged fuel assemblies, up to a total of 32.

† See Chapter 2 for a complete description of authorized cask contents and fuel specifications.

TABLE 1.2.2

KEY PARAMETERS FOR HI-STORM FW MULTI-PURPOSE CANISTERS

Parameter	PWR	BWR
Pre-disposal service life (years)	100	100
Design temperature, max./min. (°F)	752†/-40††	752†/-40††
Design internal pressure (psig) Normal conditions Off-normal conditions Accident Conditions	 100 120 200	 100 120 200
Total heat load, max. (kW)	See Table 1.2.3a/b	See Table 1.2.4
Maximum permissible peak fuel cladding temperature: Long Term Normal (°F) Short Term Operations (°F) Off-normal and Accident (°F)	 752 752 or 1058††† 1058	 752 752 or 1058††† 1058
Maximum permissible multiplication factor (k_{eff}) including all uncertainties and biases	< 0.95	< 0.95
B_4C content (by weight) (min.) in the Metamic-HT Neutron Absorber (storage cell walls)	10%	10%
[Withheld in Accordance with 10 CFR 2.390]	**[Withheld in Accordance with 10 CFR 2.390]**	**[Withheld in Accordance with 10 CFR 2.390]**
[Withheld in Accordance with 10 CFR 2.390]	**[Withheld in Accordance with 10 CFR 2.390]**	**[Withheld in Accordance with 10 CFR 2.390]**
End closure(s)	Welded	Welded
Fuel handling	Basket cell openings compatible with standard grapples	Basket cell openings compatible with standard grapples
Heat dissipation	Passive	Passive

† Maximum normal condition design temperatures for the MPC fuel basket. A complete listing of design temperatures for all components is provided in Table 2.2.3.

†† Temperature based on off-normal minimum environmental temperatures specified in Section 2.2.2 and no fuel decay heat load.

††† See Section 4.5 for discussion of the applicability of the 1058°F temperature limit during short-term operations, including MPC drying.

TABLE 1.2.3a
MPC-37 HEAT LOAD DATA (See Figure 1.2.1a)

Number of Regions: 3

Number of Storage Cells: 37

Maximum Design Basis Heat Load (kW): 44.09 (Pattern A); 45.0 (Pattern B)

Region No.	Decay Heat Limit per Cell, kW		Number of Cells per Region	Decay Heat Limit per Region, kW	
	Pattern A	Pattern B		Pattern A	Pattern B
1	1.05	1.0	9	9.45	9.0
2	1.70	1.2	12	20.4	14.4
3	0.89	1.35	16	14.24	21.6

Note: See Chapter 4 for decay heat limits per cell when vacuum drying high burnup fuel.

TABLE 1.2.3b MPC-32ML HEAT LOAD DATA (See Figure 1.2.1b)	
Number of Regions:	1
Number of Storage Cells:	32
Maximum Design Basis Heat Load (kW):	44.16
Decay Heat Limit per Cell, kW:	1.38

Note: See Chapter 4 for decay heat limits per cell when vacuum drying moderate or high burnup fuel.

TABLE 1.2.5 CRITICALITY AND SHIELDING SIGNIFICANT SYSTEM DATA		
Item	**Property**	**Value**
Metamic-HT Neutron Absorber	Nominal Thickness (mm)	10 (MPC-89) 15 (MPC-37) 15 (MPC-32ML)
	Minimum B_4C Weight %	10 (MPC-89) 10 (MPC-37) 10 (MPC-32ML)
Concrete in HI-STORM FW overpack body and lid	Installed Nominal Density (lb/ft^3)	150 (reference) 200 (maximum)

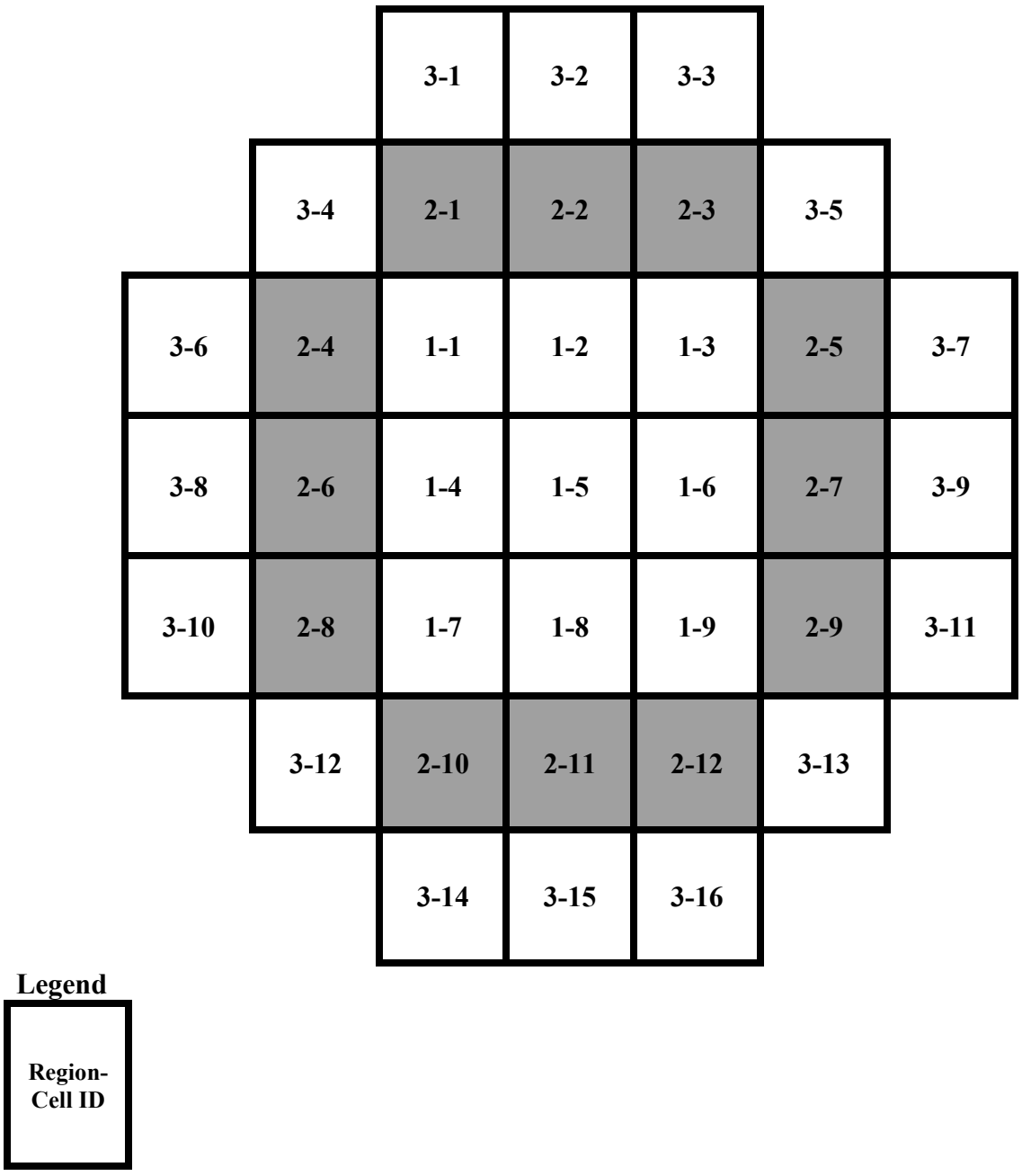

Figure 1.2.1a: MPC-37 Basket, Region and Cell Identification

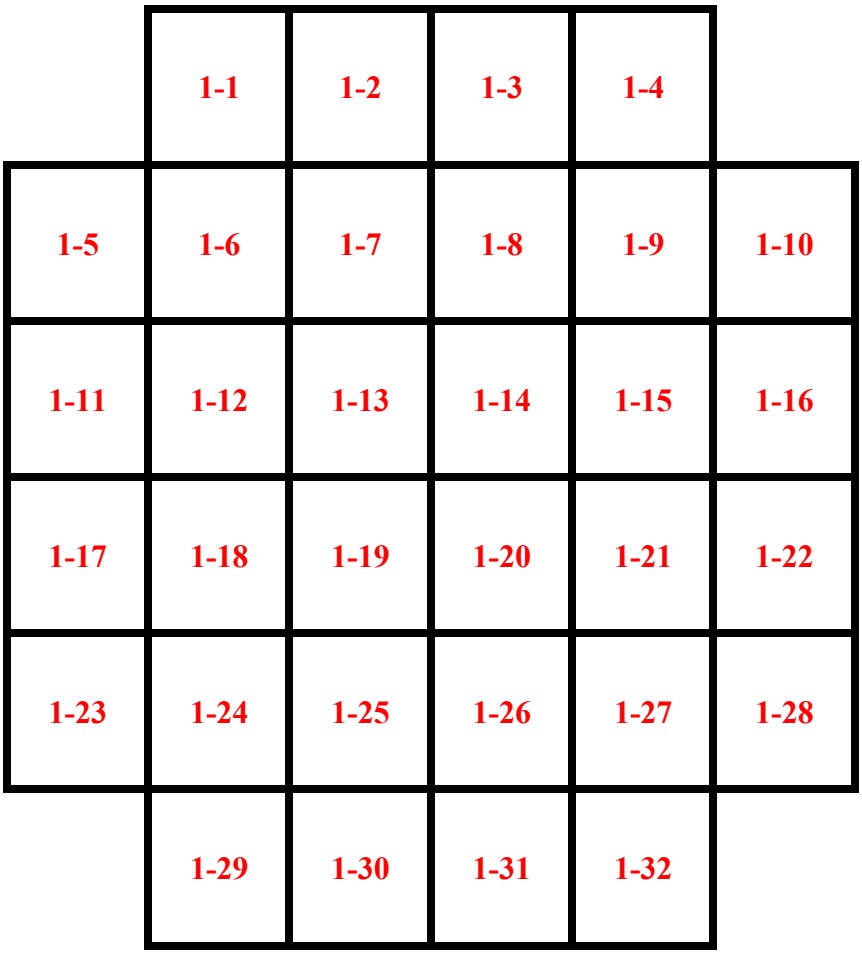

Figure 1.2.1b: MPC-32ML Basket Cell Identification

1.5 DRAWINGS

[Withheld in Accordance with 10 CFR 2.390]

CHAPTER 2†: PRINCIPAL DESIGN CRITERIA

2.0 INTRODUCTION

The design characteristics of the HI-STORM FW System are presented in Chapter 1, Section 1.2. This chapter contains a compilation of loadings and design criteria applicable to the HI-STORM FW System. The loadings and conditions prescribed herein for the MPC, particularly those pertaining to mechanical accidents, are consistent with those required for 10CFR72 compliance. This chapter sets forth the loading conditions and relevant acceptance criteria; it does not provide results of any analyses. The analyses and results carried out to demonstrate compliance with the structural design criteria are presented in the subsequent chapters of this FSAR.

This chapter is in full compliance with NUREG-1536, with the exceptions and clarifications provided in Table 1.0.3. Table 1.0.3 summarizes the NUREG-1536 review guidance, the justification for the exception or clarification, and the Holtec approach to meet the intent of the NUREG-1536 guidance.

The design criteria for the MPCs, HI-STORM FW overpack, and HI-TRAC VW transfer cask are summarized in Subsections 2.0.1, 2.0.2, and 2.0.3, respectively, and described in the sections that follow.

2.0.1 MPC Design Criteria

General

The MPC is engineered for a 60 year design life, while satisfying the requirements of 10CFR72. The adequacy of the MPC to meet the above design life is discussed in Section 3.4. The design characteristics of the MPC are described in Section 1.2.

Structural

The MPC is classified as important-to-safety. The MPC structural components include the fuel basket and the enclosure vessel. The fuel basket is designed and fabricated to meet a more stringent displacement limit under mechanical loadings than those implicit in the stress limits of the ASME code (see Section 2.2). The MPC enclosure vessel is designed and fabricated as a Class 1 pressure vessel in accordance with Section III, Subsection NB of the ASME Code, with

† This chapter has been prepared in the format and section organization set forth in Regulatory Guide 3.61. The material content of this chapter also fulfills the requirements of NUREG-1536. Pagination and numbering of sections, figures, and tables are consistent with the convention set down in Chapter 1, Section 1.0, herein. All terms-of-art used in this chapter are consistent with the terminology of the Glossary.

certain necessary alternatives, as discussed in Section 2.2. The principal exception to the above Code pertains to the MPC lid, vent and drain port cover plates, and closure ring welds to the MPC lid and shell, as discussed in Section 2.2. In addition, Threaded Anchor Locations (TALs) in the MPC lid are designed in accordance with the requirements of NUREG-0612 for critical lifts to facilitate handling of the loaded MPC.

The MPC closure welds are partial penetration welds that are structurally qualified by analysis in Chapter 3. The MPC lid and closure ring welds are inspected by performing a liquid penetrant examination in accordance with the drawings contained in Section 1.5. The integrity of the MPC lid-to-shell weld is further verified by performing a progressive liquid penetrant examination of the weld layers, and a Code pressure test.

The structural analysis of the MPC, in conjunction with the redundant closures and nondestructive examination, pressure testing, and helium leak testing provides assurance of canister closure integrity in lieu of the specific weld joint configuration requirements of Section III, Subsection NB.

Compliance with the ASME Code, with respect to the design and fabrication of the MPC, and the associated justification are discussed in Section 2.2. The MPC design is analyzed for all design basis normal, off-normal, and postulated accident conditions, as defined in Section 2.2. The required characteristics of the fuel assemblies to be stored in the MPC are limited in accordance with Section 2.1.

Thermal

The thermal design and operation of the MPC in the HI-STORM FW System meets the intent of the review guidance contained in ISG-11, Revision 3 [2.0.1]. Specifically, the ISG-11 provisions that are explicitly invoked and satisfied are:

i. The thermal acceptance criteria for all commercial spent fuel (CSF) authorized by the USNRC for operation in a commercial reactor are unified into one set of requirements.

ii. The maximum value of the calculated temperature for all CSF under long-term normal conditions of storage must remain below 400ºC (752ºF). For short-term operations, including canister drying, helium backfill, and on-site cask transport operations, the fuel cladding temperature must not exceed 400ºC (752ºF) for high burnup fuel (HBF) and 570ºC (1058ºF) for moderate burnup fuel.

iii. The maximum fuel cladding temperature as a result of an off-normal or accident event must not exceed 570ºC (1058ºF).

iv. For HBF, operating restrictions are imposed to limit the maximum temperature excursion during short-term operations to 65ºC (117ºF) and the number of excursions to less than 10.

To achieve compliance with the above criteria, certain design and operational changes are necessary, as summarized below.

i. The peak fuel cladding temperature limit (PCT) for long term storage operations and short term operations is generally set at 400ºC (752ºF). However, for MPCs containing all moderate burnup fuel, the fuel cladding temperature limit for short-term operations is set at 570ºC (1058ºF) because the nominal fuel cladding stress is shown to be less than 90 MPa [2.0.2]. Appropriate analyses have been performed as discussed in Chapter 4 and operating restrictions have been added to ensure these limits are met.

ii. A method of drying, such as forced helium dehydration (FHD) is used if the above temperature limits for short-term operations cannot be met.

iii. The off-normal and accident condition PCT limit remains unchanged at 570 ºC (1058ºF).

The MPC cavity is dried, either with FHD or vacuum drying, and then it is backfilled with high purity helium to promote heat transfer and prevent cladding degradation.

The normal condition design temperatures for the stainless steel components in the MPC are provided in Table 2.2.3.

~~Each~~ The MPC-37 and MPC-89 model~~s~~ allow~~s~~ for regionalized storage where the basket is segregated into three regions as shown in Figures 1.2.1a and 1.2.2. Decay heat limits for regionalized loading are presented in Tables 1.2.3a and 1.2.4 for MPC-37 and MPC-89 respectively. Specific requirements, such as approved locations for DFCs and non-fuel hardware are given in Section 2.1.

Shielding

The dose limits for an ISFSI using the HI-STORM FW System are delineated in 10CFR72.104 and 72.106. Compliance with these regulations for any particular array of casks at an ISFSI is necessarily site-specific and must be demonstrated by the licensee. Dose for a single cask and a representative cask array is illustrated in Chapter 5.

The MPC provides axial shielding at the top and bottom ends to maintain occupational exposures ALARA during canister closure and handling operations. The HI-TRAC VW bottom lid also contains shielding. The occupational doses are controlled in accordance with plant-specific procedures and ALARA requirements (discussed in Chapter 9).

The dose evaluation is performed for a reference fuel (Table 1.0.4) as described in Section 5.2. Calculated dose rates for each MPC are provided in Section 5.1. These dose rates are used to perform an occupational exposure (ALARA) evaluation, as discussed in Chapter 11.

Table 2.0.9 – MPC-32ML Enclosure Vessel (Drawing # 10464)		
Item Number*	Part Name	ITS QA Safety Category
1	Shell, Enclosure Vessel	A
2	Plate, Enclosure Vessel Base	A
3	Plate, Enclosure Vessel Lower Lid	B
4	Plate, Enclosure Vessel Upper Lid	A
5	Ring, Enclosure Vessel Closure	A
6	Plate, Enclosure Vessel Lift Lug	C
8	Block, Enclosure Vessel Vent/Drain Upper	B
9	Block, Enclosure Vessel Lower Drain Shield	C
10	Block, Enclosure Vessel Lower Vent Shield	C
11	Port, Enclosure Vessel Vent/Drain	C
12	Plug, Enclosure Vessel Vent /Drain	C
16	Purge Tool Port Plug	C
18	Plate, Enclosure Vessel Vent/Drain Port Cover	A

*Item Numbers are non-consecutive because they are consistent with Parts List on drawing.

Table 2.0.10 – Assembly, MPC-32ML Fuel Basket (Drawing # 10457)		
Item Number	Part Name	ITS QA Safety Category
1	Panel, Type 1 Cell Wall	A
2	Panel, Type 2 Cell Wall	A
3	Panel, Type 3 Cell Wall	A
4	Panel, Type 4 Cell Wall	A
5	Basket Shim, Type 1	C
6	Basket Shim, Type 2	C
7	Basket Shim, Type 3	C

reasonably conservative dose rates. The reference assemblies given in Table 1.0.4 are the predominant assemblies used in the industry.

The design basis dose rates can be met by a variety of burnup levels and cooling times. Table 2.1.1 provides the acceptable ranges of burnup, enrichment and cooling time for all of the authorized fuel assembly array/classes. Table 2.1.5 and Figures 2.1.3 and 2.1.4 provide the axial distribution for the radiological source terms for PWR and BWR fuel assemblies based on the axial burnup distribution. The axial burnup distributions are representative of fuel assemblies with the design basis burnup levels considered. These distributions are used for analyses only, and do not provide a criteria for fuel assembly acceptability for storage in the HI-STORM FW System.

Non-fuel hardware, as defined in the Glossary, has been evaluated and is also authorized for storage in the PWR MPCs as specified in Table 2.1.1.

2.1.7 Criticality Parameters for Design Basis SNF

Criticality control during loading of the MPC-37 is achieved through either meeting the soluble boron limits in Table 2.1.6 OR verifying that the assemblies meet the minimum burnup requirements in Table 2.1.7. Criticality control during loading of the MPC-32ML is achieved through meeting the soluble boron limits in Table 2.1.6.

For those spent fuel assemblies that need to meet the burnup requirements specified in Table 2.1.7, a burnup verification shall be performed in accordance with either Method A OR Method B described below.

Method A: Burnup Verification Through Quantitative Burnup Measurement

For each assembly in the MPC-37 where burnup credit is required, the minimum burnup is determined from the burnup requirement applicable to the loading configuration chosen for the cask (see Table 2.1.7). A measurement is then performed that confirms that the fuel assembly burnup exceeds this minimum burnup. The measurement technique may be calibrated to the reactor records for a representative set of assemblies. The assembly burnup value to be compared with the minimum required burnup should be the measured burnup value as adjusted by reducing the value by a combination of the uncertainties in the calibration method and the measurement itself.

Method B: Burnup Verification Through an Administrative Procedure and Qualitative Measurements

Depending on the location in the basket, assemblies loaded into a specific MPC-37 can either be fresh, or have to meet a single minimum burnup value. The assembly burnup value to be compared with the minimum required burnup should be the reactor record burnup value as adjusted by reducing the value by the uncertainties in the reactor record value. An administrative procedure shall be established that prescribes the following steps,

Table 2.1.1a

MATERIAL TO BE STORED

PARAMETER	VALUE	
	MPC-37	MPC-89
Fuel Type	Uranium oxide undamaged fuel assemblies, damaged fuel assemblies, and fuel debris meeting the limits in Table 2.1.2 for the applicable array/class.	Uranium oxide undamaged fuel assemblies, damaged fuel assemblies, with or without channels, fuel debris meeting the limits in Table 2.1.3 for the applicable array/class.
Cladding Type	ZR (see Glossary for definition)	ZR (see Glossary for definition)
Maximum Initial Rod Enrichment	Depending on soluble boron levels or burnup credit and assembly array/class as specified in Table 2.1.6 and Table 2.1.7.	≤ 5.0 wt. % U-235
Post-irradiation cooling time and average burnup per assembly	Minimum Cooling Time: 3 years Maximum Assembly Average Burnup: 68.2 GWd/mtU	Minimum Cooling Time: 3 years Maximum Assembly Average Burnup: 65 GWd/mtU
Non-fuel hardware post-irradiation cooling time and burnup	Minimum Cooling Time: 3 years Maximum Burnup†: - BPRAs, WABAs and vibration suppressors: 60 GWd/mtU - TPDs, NSAs, APSRs, RCCAs, CRAs, CEAs, water displacement guide tube plugs and orifice rod assemblies: 630 GWd/mtU - ITTRs: not applicable	N/A
Decay heat per fuel storage location	Regionalized Loading: See Table 1.2.3	Regionalized Loading: See Table 1.2.4

† Burnups for non-fuel hardware are to be determined based on the burnup and uranium mass of the fuel assemblies in which the component was inserted during reactor operation. Burnup not applicable for ITTRs since installed post-irradiation.

Table 2.1.1a (continued)

MATERIAL TO BE STORED

PARAMETER	VALUE	
	MPC-37	MPC-89
Fuel Assembly Nominal Length (in.)	Minimum: (1) All except 15x15I‡: 157 (with NFH); (2) 15x15I: 149 (with NFH)§ Reference: 167.2 (with NFH) Maximum: 199.2 (with NFH and DFC)	Minimum: 171 Reference: 176.5 Maximum: 181.5 (with DFC)
Fuel Assembly Width (in.)	≤ 8.54 (nominal design)	≤ 5.95 (nominal design)
Fuel Assembly Weight (lb)	Reference: 1600 (without NFH) 1750 (with NFH), 1850 (with NFH and DFC) Maximum: 2050 (including NFH and DFC)	Reference: 750 (without DFC), 850 (with DFC) Maximum: 850 (including DFC)

‡ See Table 2.1.2 for 15x15I fuel assembly array/class characteristics.
§ Minimum nominal fuel assembly length for 15x15I fuel assembly array/class is 149". The unique design of 15x15I fuel requires a 1" nominal fuel shim to properly support the assembly. Therefore the minimum MPC cavity height for 15x15I fuel is based on 150" fuel length.

HOLTEC INTERNATIONAL COPYRIGHTED MATERIAL

Table 2.1.1a (continued)

MATERIAL TO BE STORED

PARAMETER	VALUE	
	MPC-37	MPC-89
Other Limitations	▪ Quantity is limited to 37 undamaged ZR clad PWR fuel assemblies with or without non-fuel hardware. Up to 12 damaged fuel containers containing PWR damaged fuel and/or fuel debris may be stored in the locations denoted in Figure 2.1.1 with the remaining basket cells containing undamaged ZR fuel assemblies, up to a total of 37. ▪ One NSA. ▪ Up to 30 BPRAs. ▪ BPRAs, TPDs, WABAs, water displacement guide tube plugs, orifice rod assemblies, and/or vibration suppressor inserts, with or without ITTRs, may be stored with fuel assemblies in any fuel cell location. ▪ CRAs, RCCAs, CEAs, NSAs, and/or APSRs may be stored with fuel assemblies in fuel cell locations specified in Figure 2.1.5.	▪ Quantity is limited to 89 undamaged ZR clad BWR fuel assemblies. Up to 16 damaged fuel containers containing BWR damaged fuel and/or fuel debris may be stored in locations denoted in Figure 2.1.2 with the remaining basket cells containing undamaged ZR fuel assemblies, up to a total of 89.

Table 2.1.1b MATERIAL TO BE STORED	
PARAMETER	**VALUE**
	MPC-32ML
Fuel Type	Uranium oxide undamaged fuel assemblies, damaged fuel assemblies, and fuel debris meeting the limits in Table 2.1.2 for the 16x16D array/class only.
Cladding Type	ZR (see Glossary for definition)
Maximum Initial Rod Enrichment	Depending on soluble boron levels and assembly array/class as specified in Table 2.1.6.
Post-irradiation cooling time and average burnup per assembly	Minimum Cooling Time: 3 years Maximum Assembly Average Burnup: 68.2 GWd/mtU
Non-fuel hardware post-irradiation cooling time and burnup†	Minimum Cooling Time: 3 years Maximum Burnup: - BPRAs, WABAs and vibration suppressors: 60 GWd/mtU - TPDs, NSAs, APSRs, RCCAs, CRAs, CEAs, water displacement guide tube plugs and orifice rod assemblies: 630 GWd/mtU - ITTRs: not applicable
Decay heat per fuel storage location	Uniform Loading per Table 1.2.3b.
Fuel Assembly Nominal Length (in)	≤ 196~~3~~.122 (including NFH and DFC)
Fuel Assembly Width (in)	≤ 9.04 (nominal design)
Fuel Assembly Weight (lb)	≤ 1860 (without NFH) ≤ 2120 (with NFH) ≤ ~~1858~~2200 (including DFC and NFH).

† Burnups for non-fuel hardware are to be determined based on the burnup and uranium mass of the fuel assemblies in which the component was inserted during reactor operation. Burnup not applicable for ITTRs since installed post-irradiation.

Table 2.1.1b (continued) MATERIAL TO BE STORED	
PARAMETER	**VALUE**
	MPC-32ML
Other Limitations	▪ Quantity is limited to 32 undamaged ZR clad PWR class 16x16D fuel assemblies with or without non-fuel hardware. Up to 8 damaged fuel containers containing class 16x16D PWR damaged fuel and/or fuel debris may be stored in the locations denoted in Figure 2.1.1b with the remaining basket cells containing undamaged ZR fuel assemblies, up to a total of 32. ▪ One NSA. ▪ BPRAs, TPDs, WABAs, water displacement guide tube plugs, orifice rod assemblies, and/or vibration suppressor inserts, with or without ITTRs, may be stored with fuel assemblies in any fuel cell location. CRAs, RCCAs, CEAs, NSAs, and/or APSRs may be stored with fuel assemblies in fuel cell locations specified in Figure 2.1.5b.

Table 2.1.2 (continued)

PWR FUEL ASSEMBLY CHARACTERISTICS (Note 1)

Fuel Assembly Array and Class	**16x16 A**	**16x16B**	**16x16 C**	**16x16 D (MPC-32ML Only)**	**16x16E**
No. of Fuel Rod Locations	236	236	235	236	235
Fuel Clad O.D. (in.)	≥ 0.382	≥ 0.374	≥ 0.374	≥ 0.423	≥ 0.359
Fuel Clad I.D. (in.)	≤ 0.3350	≤ 0.3290	≤ 0.3290	≤ 0.3~~66~~73	≤ 0.3326
Fuel Pellet Dia. (in.) (Note 3)	≤ 0.3255	≤ 0.3225	≤ 0.3225	≤ 0.359	≤ 0.3225
Fuel Rod Pitch (in.)	≤ 0.506	≤ 0.506	≤ 0.485	≤ 0.563	≤ 0.485
Active Fuel length (in.)	≤ 150	≤ 150	≤ 150	≤ 154.5	≤ 150
No. of Guide and/or Instrument Tubes	5 (Note 2)	5 (Note 2)	21	20	21
Guide/Instrument Tube Thickness (in.)	≥ 0.0350	≥ 0.04	≥ 0.0157	≥ 0.015	≥ 0.0157

Table 2.1.2 (continued)

PWR FUEL ASSEMBLY CHARACTERISTICS (Note 1)

Fuel Assembly Array and Class	**17x17A**	**17x17 B**	**17x17 C**	**17x17 D**	**17x17 E**
No. of Fuel Rod Locations	264	264	264	264	265
Fuel Clad O.D. (in.)	≥ 0.360	≥ 0.372	≥ 0.377	≥ 0.372	≥ 0.372
Fuel Clad I.D. (in.)	≤ 0.3150	≤ 0.3310	≤ 0.3330	≤ 0.3310	≤ 0.3310
Fuel Pellet Dia. (in.) (Note 3)	≤ 0.3088	≤ 0.3232	≤ 0.3252	≤ 0.3232	≤ 0.3232
Fuel Rod Pitch (in.)	≤ 0.496	≤ 0.496	≤ 0.502	≤ 0.496	≤ 0.496
Active Fuel length (in.)	≤ 150	≤ 150	≤ 150	≤ 170	≤ 170
No. of Guide and/or Instrument Tubes	25	25	25	25	24
Guide/Instrument Tube Thickness (in.)	≥ 0.016	≥ 0.014	≥ 0.020	≥ 0.014	≥ 0.014

Notes:

1. All dimensions are design nominal values. Maximum and minimum dimensions are specified to bound variations in design nominal values among fuel assemblies within a given array/class.
2. Each guide tube replaces four fuel rods.
3. Annular fuel pellets are allowed in the top and bottom 12” of the active fuel length.
4. Assemblies have one Instrument Tube and eight Guide Bars (Solid ZR). Some assemblies have up to 16 fuel rods removed or replaced by Guide Tubes.

Table 2.1.6

Soluble Boron Requirements for MPC-37 and MPC-32ML Wet Loading and Unloading Operations

MPC	Array/Class	All Undamaged Fuel Assemblies		One or More Damaged Fuel Assemblies and/or Fuel Debris	
		Maximum Initial Enrichment $\leq$ 4.0 wt% ^{235}U (ppmb)	Maximum Initial Enrichment 5.0 wt% ^{235}U (ppmb)	Maximum Initial Enrichment $\leq$ 4.0 wt% ^{235}U (ppmb)	Maximum Initial Enrichment 5.0 wt% ^{235}U (ppmb)
MPC-37	All 14x14 and 16x16A, B, C, E	1,000	1,600 (Note 3)	1,300	1,800
	All 15x15 and 17x17	1,500	2,000	1,800	2,300
MPC-32ML	16x16D	1,500	2,000	1,600	2,100

Note:

1. For maximum initial enrichments between 4.0 wt% and 5.0 wt% ^{235}U, the minimum soluble boron concentration may be determined by linear interpolation between the minimum soluble boron concentrations at 4.0 wt% and 5.0 wt% ^{235}U.
2. If burnup credit is used (as described in Section 2.1.7), these soluble boron requirements do not apply.
~~2.~~3. For 16x16E assembly class, the soluble boron requirement is 1,500 ppmb.

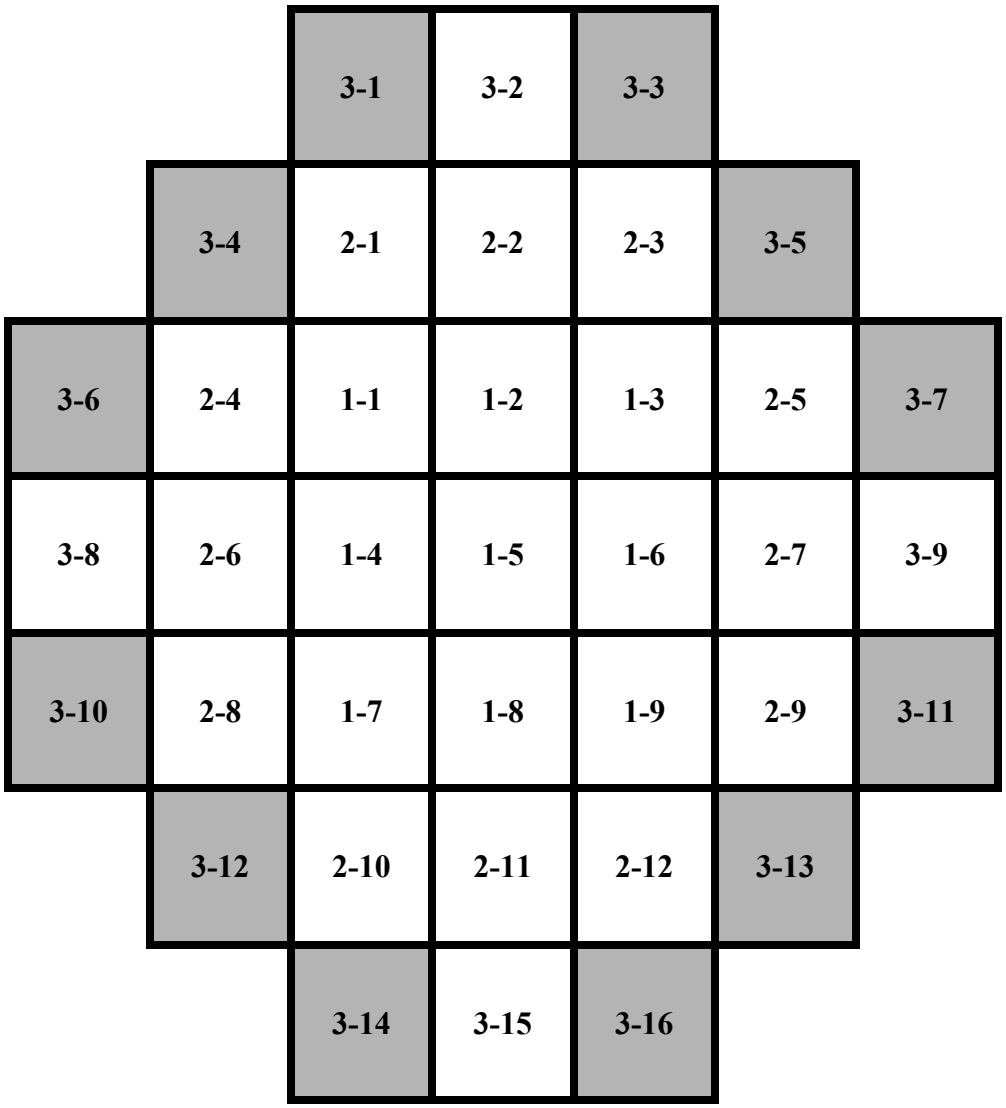

Figure 2.1.1a Location of DFCs for Damaged Fuel or Fuel Debris
in the MPC-37(Shaded Cells)

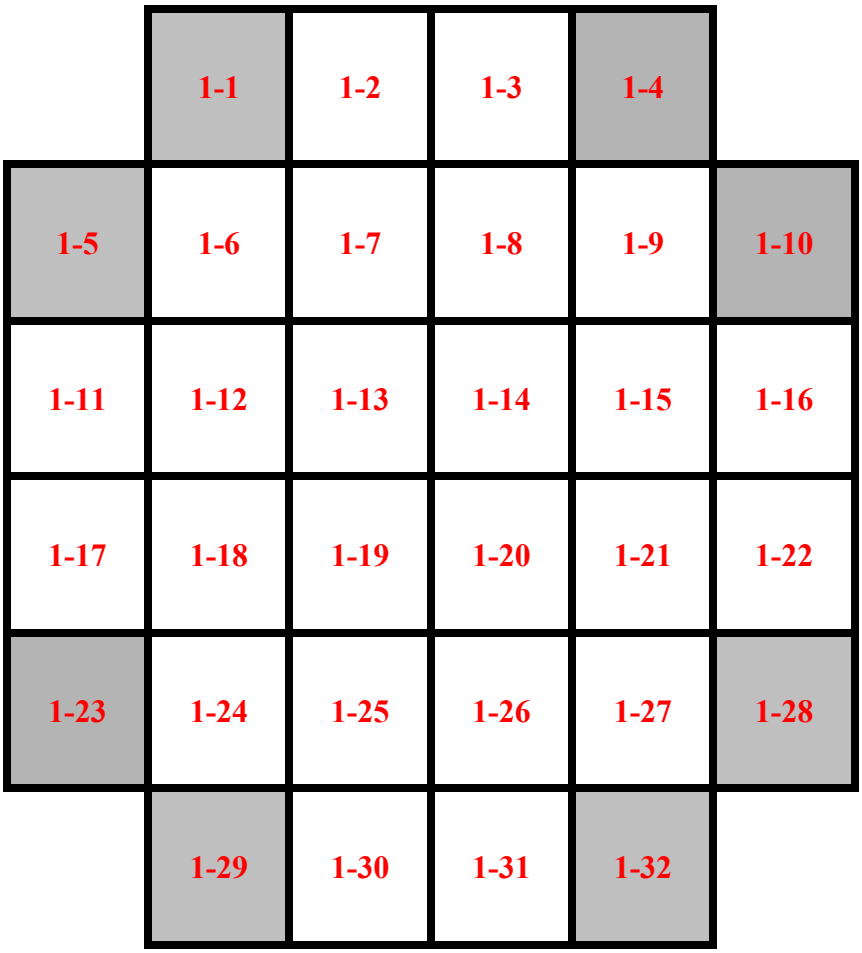

Figure 2.1.1b Location of DFCs for Damaged Fuel or Fuel Debris in the MPC-32ML (Shaded Cells)

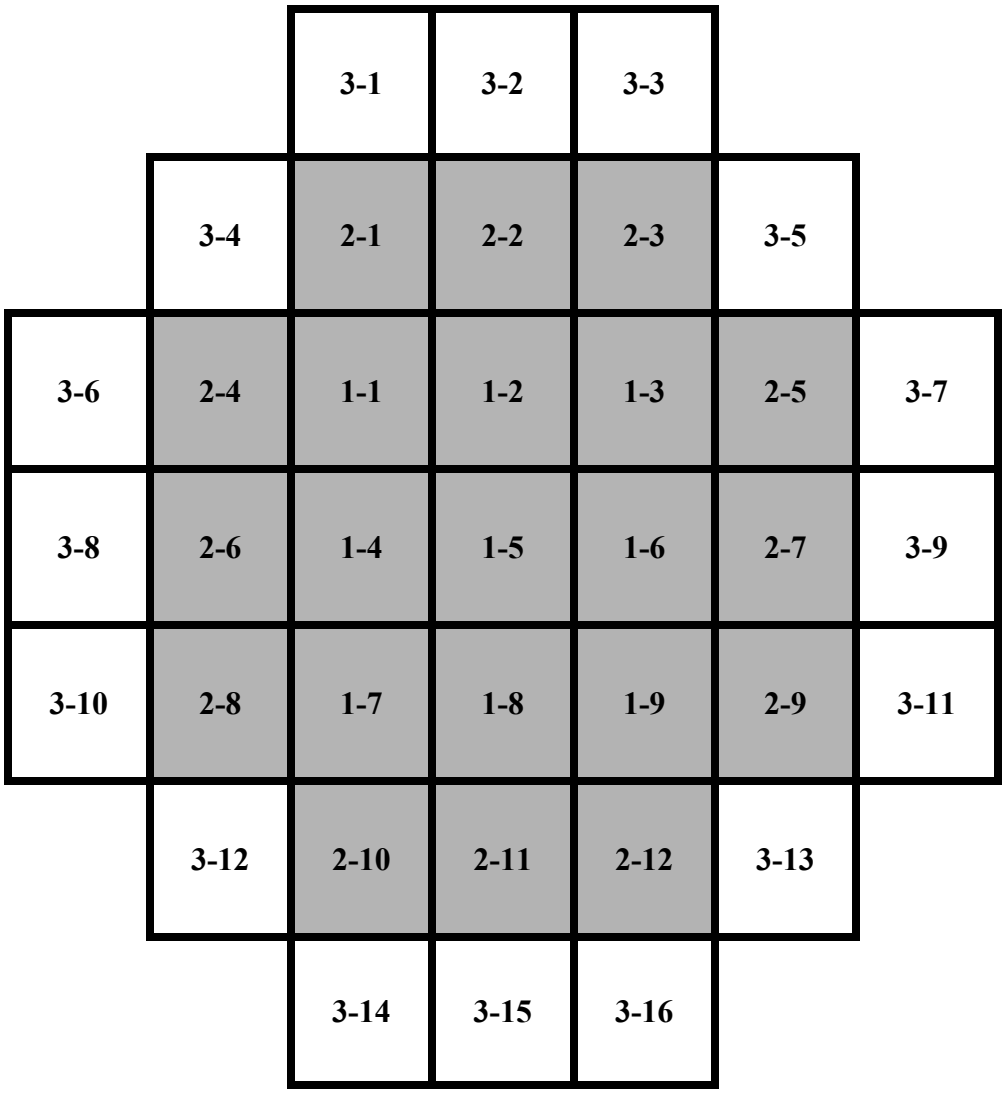

Figure 2.1.5a: Location of NSAs, APSRs, RCCAs, CEAs, and CRAs in the MPC-37 (Shaded Cells)

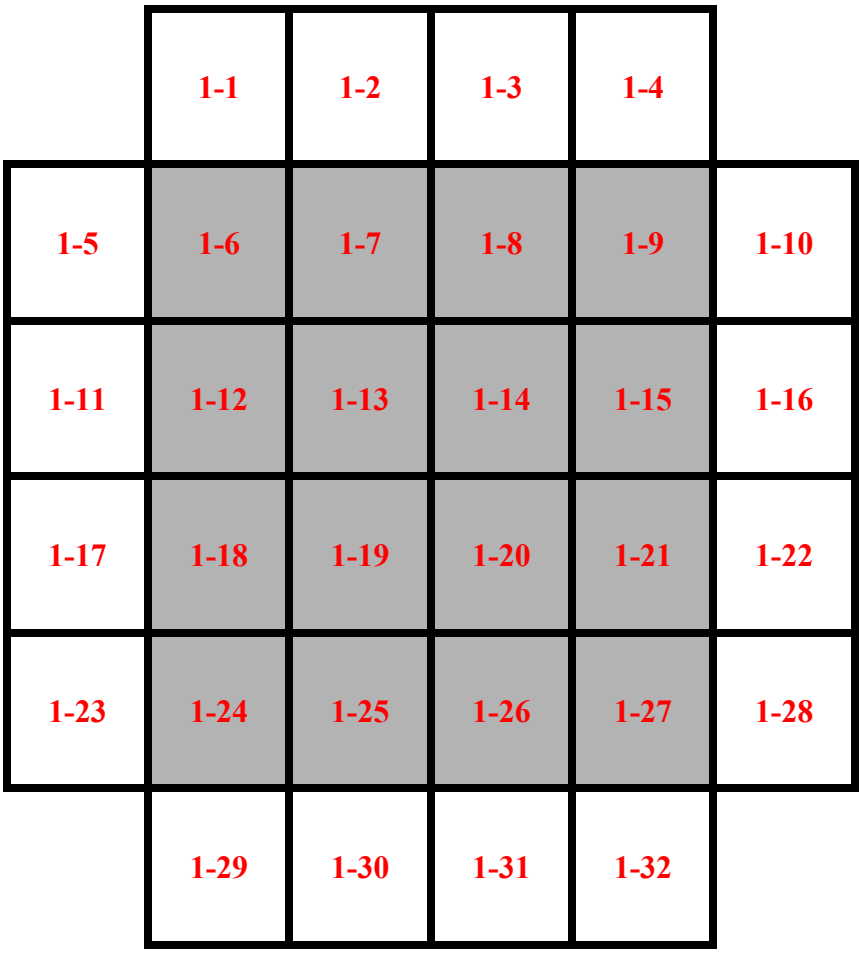

Figure 2.1.5b: Location of NSAs, APSRs, RCCAs, CEAs, and CRAs in the MPC-32ML (Shaded Cells)

[Withheld in Accordance with 10 CFR 2.390]

Figure 2.1.6: Damaged Fuel Container (Typical)

Table 2.2.1

DESIGN PRESSURES

Pressure Location	Condition	Pressure (psig)
MPC Internal Pressure	Normal	100
	Short-Term Operations	115
	Off-Normal~~/Short-Term~~	120
	Accident	200
MPC External Pressure	Normal	(0) Ambient
	Off-Normal/Short-Term	(0) Ambient
	Accident	55
HI-TRAC Water Jacket Internal Pressure	Accident	65
Overpack External Pressure	Normal	(0) Ambient
	Off-Normal/Short-Term	(0) Ambient
	Accident	See Paragraph 3.1.2.1.d

3.1 STRUCTURAL DESIGN

3.1.1 Discussion

The HI-STORM FW system consists of the Multi-Purpose Canister (MPC) and the storage overpack (Figure 1.1.1). The components subject to certification on this docket consist of the HI-STORM FW system components and the HI-TRAC VW transfer cask (please see Table 1.0.1). A complete description of the design details of these three components are provided in Section 1.2. This section discusses the structural aspects of the MPC, the storage overpack, and the HI-TRAC VW transfer cask. Detailed licensing drawings for each component are provided in Section 1.5.

(i) The Multi-Purpose Canister (MPC)

The design of the MPC seeks to attain three objectives that are central to its functional adequacy:

- Ability to Dissipate Heat: The thermal energy produced by the stored spent fuel must be transported to the outside surface of the MPC to maintain the fuel cladding and fuel basket metal walls below the regulatory temperature limits.

- Ability to Withstand Large Impact Loads: The MPC, with its payload of nuclear fuel, must withstand the large impact loads associated with the non-mechanistic tipover event.

- Restraint of Free End Expansion: The MPC structure is designed so that membrane and bending (primary) stresses produced by constrained thermal expansion of the fuel basket do not arise.

As stated in Chapter 1, the MPC Enclosure Vessel is a confinement vessel designed to meet the stress limits in ASME Code, Section III, Subsection NB. The enveloping canister shell, baseplate, and the lid system form a complete Confinement Boundary for the stored fuel that is referred to as the "Enclosure Vessel". Within this cylindrical shell confinement vessel is an egg-crate assemblage of Metamic-HT plates that form prismatic cells with square cross sectional openings for fuel storage, referred to as the fuel basket. All multi-purpose canisters designed for deployment in the HI-STORM FW have identical external diameters. The essential difference between the different MPCs lies in the fuel baskets, each of which is designed to house different types of fuel assemblies. All fuel basket designs are configured to maximize structural integrity through extensive inter-cell connectivity. Although all fuel basket designs are structurally similar, analyses for each of the MPC types is carried out separately to ensure structural compliance.

The design criteria of components in the HI-STORM FW system important to safety are defined in Chapter 2.

The principal structural functions of the MPC in storage mode are:

i. To position the fuel in a subcritical configuration, and

ii. To provide a leak tight Confinement Boundary.

The key structural functions of the overpack during storage are:

i. To serve as a missile barrier for the MPC,

ii. To provide flow paths for natural convection,

iii. To provide a kinematically stable SNF storage configuration,

iv. To provide fixed and reliable radiation shielding, and

v. To allow safe translocation of the overpack with a loaded MPC inside.

Some structural features of the MPCs that allow the system to perform these functions are summarized below:

- There are no gasketed ports or openings in the MPC. The MPC does not rely on any mechanical sealing arrangement except welding. The absence of any gasketed or flanged joints makes the MPC structure immune from joint leaks. The Confinement Boundary contains no valves or other pressure relief devices.

- The closure system for the MPCs consists of two components, namely, the MPC lid and the closure ring. The MPC lid can be either a single thick circular plate continuously welded to the MPC shell along its circumference or a two-piece lid, dual lids welded around their common periphery. When using a two piece lid only the top portion of the lid is considered as part of the closure system, the bottomportion is only for shielding purposes. The MPC closure system is shown in the licensing drawings in Section 1.5. The MPC lid is equipped with vent and drain ports, which are used both for evacuating moisture and air from the MPC following fuel loading and subsequent backfilling with an inert gas (helium) at a specified mass. The vent and drain ports are covered by a cover plate and welded before the closure ring is installed. The closure ring is a circular annular plate edge-welded to the MPC lid and shell. The two closure members are interconnected by welding around the inner diameter of the ring. Lift points for the MPC are provided on the MPC lid.

- The MPC fuel baskets consist of an array of interconnecting plates. The number of storage cells formed by this interconnection process varies depending on the type of fuel being stored. Basket configurations designed for both PWR and BWR fuel are explained in detail in Section 1.2. All baskets are designed to fit into the same MPC shell.

- The MPC basket is separated from its lateral supports (basket shims) by a small, calibrated gap designed to prevent thermal stressing associated with the thermal expansion mismatches between the fuel basket and the basket support structure. The gap is designed to ensure that the basket remains unconstrained when subjected to the thermal heat generated by the spent nuclear fuel.

The MPC fuel basket maintains the spent nuclear fuel in a subcritical arrangement. Its safe operation is assured by maintaining the physical configuration of the storage cell cavities intact in the aftermath of a non-mechanistic tipover event. This requirement is satisfied if the MPC fuel basket plates undergo a minimal deflection (see Table 2.2.11). The fuel basket strains are shown in Subsection 3.4.4.1.4 to remain ~~essentially~~ largely elastic with only localized areas of plastic strain. Moreover, from the simulation results it is demonstrated that the cross-section of the storage cell, throughout the active fuel length, remains essentially unchanged. ~~, and, t~~Therefore, there is no impairment in the recoverability or retrievability of the fuel and the subcriticality of the stored fuel is unchallenged.

The MPC Confinement Boundary contains no valves or other pressure relief devices. In addition, the analyses presented in Subsections 3.4.3, 3.4.4.1.5, and 3.4.4.1.6 show that the MPC Enclosure Vessel meets the stress intensity criteria of the ASME Code, Section III, Subsection NB for all service conditions. Therefore, the demonstration that the MPC Enclosure Vessel meets Subsection NB stress limits ensures that there will be no discernible release of radioactive materials from the MPC.

(ii) Storage Overpack

The HI-STORM FW storage overpack is a steel cylindrical structure consisting of inner and outer low carbon steel shells, a lid, and a baseplate. Between the two shells is a thick cylinder of un-reinforced (plain) concrete. Plain concrete is also installed in the lid to minimize skyshine. The storage overpack serves as a missile and radiation barrier, provides flow paths for natural convection, provides kinematic stability to the system, and acts as a shock absorber for the MPC in the event of a postulated tipover accident. The storage overpack is not a pressure vessel since it contains cooling vents. The structural steel weldment of the HI-STORM FW overpack is designed to meet the stress limits of the ASME Code, Section III, Subsection NF, Class 3 for normal and off-normal loading conditions and Regulatory Guide 3.61 for handling conditions.

As discussed in Chapters 1 and 2, the principal shielding material utilized in the HI-STORM FW overpack is plain concrete. The plain concrete in the HI-STORM FW serves a structural function only to the extent that it may participate in supporting direct compressive or punching loads. The allowable compression/bearing resistance is defined and quantified in ACI -318-05 [3.3.5]. Strength analyses of the HI-STORM FW overpack and its confined concrete have been carried out in Subsections 3.4.4.1.3 and 3.4.4.1.4 to show that the concrete is able to perform its radiation protection function and that retrievability of the MPC subsequent to any postulated accident condition of storage or handling is maintained.

The HI-STORM FW system is exposed to the fluctuating thermal state of the ambient environment. Effect of wind and relative humidity also play a role in affecting the temperature of the cask components. However, the most significant effects are the large thermal inertia of the system and the relatively low heat transfer coefficients that act to smooth out the daily temperature cycles. As a result, the amplitude of the cyclic stresses, to the extent that they are developed, remains orders of magnitude below the cask material's Endurance Limit.

The second causative factor, namely, pressure pulsation, is limited to the only pressure vessel in the system – the MPC. Pressure produces several types of stresses in the MPC (see Table 3.1.10), all of which are equally effective in causing fatigue expenditure in the metal. However, the amplitude of stress from the pressure cycling (due to the changes in the ambient conditions) is quite small and well below the endurance limit of the stainless steel material.

Therefore, failure from fatigue is not a credible concern for the HI-STORM FW system components.

3.1.2.6 Buckling

Buckling is caused by a compressive stress acting on a slender section. In the HI-STORM FW system, the steel weldment in the overpack is not slender; its height-to-diameter ratio being less than 2. There is no source of compressive stress except from the self-weight of the shell and the overpack weight of the HI-TRAC VW in the stacked condition, which produces a modest state of compressive stress. The state of a small compressive stress combined with a low slenderness ratio makes the HI-STORM FW overpack safe from the buckling mode of failure. The same statement also applies to the HI-TRAC VW transfer cask, which is a radially buttressed triple shell (in comparison to the dual shell construction in HI-STORM FW) structure.

The MPC Enclosure Vessel is protected from buckling of by the permanent tensile stress in both hoop and longitudinal directions due to internal pressure.

Finally, the fuel basket, which is an egg-crate structure, as shown in Figures 1.1.6 and1.1.7 (an intrinsically resistant structural form to buckling from axial compressive loads), is subject to minor compressive stresses from its own weight. The absence of buckling in the Metamic-HT fuel basket is based on the fact that there are no causative scenarios (normal or accident) that produce a significant in-plane compressive stress in the basket structure. A lower bound Euler Buckling strength for the Metamic-HT fuel basket can be obtained by assuming that the basket walls are fully continuous[1] over the entire height of the MPC fuel basket, neglecting the strengthening effect of the honeycomb completely, and treating the Metamic-HT basket wall as an end-loaded plate 199.5" high by 8.94" wide by 0.59" thick (corresponding to the maximum height MPC-37 fuel basket). The top and

1 In reality, the basket walls are not fully continuous in the vertical direction since the fuel basket is assembled by vertically stacking narrow width Metamic-HT panels in a honeycomb pattern (see drawing 6506 in Chapter 1 of HI-STORM FW SAR). For the above buckling strength evaluation, the assumption that the basket walls are continuous over the full height of the fuel basket is extremely conservative since the critical buckling load is inversely proportional to the square of the height.

bottom edges are assumed to be pinned and the lateral edges are assumed to be free to minimize the permissible buckling load (a particularly severe modeling artifice to minimize buckling strength). The Euler buckling load for this geometry is given by (see Timoshenko et al., "Theory of Elastic Stability", 2nd Edition):

$$P_{cr} = \frac{\pi^2 EI}{h^2} = 125.2 lbf$$

where E = Young's Modulus of Metamic-HT at 500ºC = 3,300 ksi,
I = moment of inertia of 8.94" wide by 0.59" thick plate = 0.153 in^4,
h = maximum height of fuel basket = 199.5"

The corresponding compressive axial stress is given by:

$$\sigma_{cr} = \frac{P_{cr}}{A} = \frac{125.2 lbf}{(8.94 in)(0.59 in)} = 23.7\, psi$$

The factor of safety against buckling is given by (where σ_b is the compressive stress in the basket due to ~~self-weight~~self-weight):

$$SF = \frac{\sigma_{cr}}{\sigma_b} = \frac{23.7\, psi}{19.5\, psi} = 1.21$$

Thus, even with an exceedingly conservative model, the safety margin against buckling is more than 20%.

Therefore, buckling is ruled out as a credible failure mechanism in the HI-STORM FW system components. Nevertheless, a Design Basis Load consisting of external pressure is specified in Table 2.2.1 with the (evidently, non-mechanistic) conservative assumption that the internal pressure, which will counteract buckling behavior, is zero psig. (In reality, internal pressure cannot be zero because of the positive helium fill pressure established at the time of canister backfill.)

3.1.2.7 Consideration of Manufacturing and Material Deviations

Departure from the assumed values of material properties in the safety analyses clearly can have a significant effect on the computed margins. Likewise, the presence of deviations in manufacturing that inevitably occur in custom fabrication of capital equipment may detract from the safety factors reported in this chapter. In what follows, the method and measures adopted to insure that deviations in material properties or in the fabricated hardware will not undermine the structural safety conclusions are summarized.

That the yield and ultimate strengths of materials used in manufacturing the HI-STORM FW components will be greater than that assumed in the structural analyses is insured by the requirement

System. Essential portions of the results for each loading case necessary to draw safety conclusions are extracted from the Calculation Packages and reported in this FSAR. Specifically, the results summarized from the finite element solutions in this chapter are self-contained to enable an independent assessment of the system's safety. Input data is provided in tabular form as suggested in ISG-21. For consistency, the following units are employed to document input data throughout this chapter:

- Time: second
- Mass: pound
- Length: inch

3.1.3.1 HI-STORM FW Overpack

The physical geometry and materials of construction of the HI-STORM FW overpack are provided in Sections 1.1 and 1.2 and the drawings in Section 1.5. The finite element simulation of the overpack consists of two discrete models, one for the overpack body and the other for the top lid.

The models are initially developed using the finite element code ANSYS [3.4.1], and then, depending on the load case, numerical simulations are performed either in ANSYS or in LS-DYNA [3.1.8]. For example, the handling loads (Load Case 9) and the snow load (Load Case 10) are simulated in ANSYS, and the non-mechanistic tipover event (Load Case 4) is simulated in LS-DYNA. For the non-mechanistic tipover analysis, three~~two four~~ distinct finite element models are ~~created~~developed with HI-STORM FW overpack carrying the maximum length MPC-37 (see Figure 3.4.10A) and the maximum length MPC-89 (see Figure 3.4.10B), as well as the MPC-32ML~~ and the MPC-31C~~. The overpack FE model for the MPC-32ML ~~and the MPC-31C~~ is the same as that for the MPC-37. This conservatively maximizes the weight and the angular velocity of the overpack for the non-mechanistic tipover analysis.
~~: one for the HI-STORM FW overpack carrying the maximum length MPC-37 and one for the HI-STORM FW overpack carrying the maximum length MPC-89 (Figures 3.4.10A and 3.4.10B).~~

The key attributes of the HI-STORM FW overpack models (implemented in ANSYS) are:

i. The finite element discretization of the overpack is sufficiently detailed to accurately articulate the primary membrane and bending stresses as well as the secondary stresses at locations of gross structural discontinuity. The finite element layout of the HI-STORM FW overpack body and the top lid are pictorially illustrated in Figures 3.4.3 and 3.4.5, respectively. The overpack model consists of over 70,000 nodes and 50,000 elements, which exceed the number of nodes and elements in the HI-STORM 100 tipover model utilized in [3.1.4]. Table 3.1.11 summarizes the key input data that is used to create the finite element models of the HI-STORM FW overpack body and top lid.

ii. The overpack baseplate, anchor blocks, and the lid studs are modeled with SOLID45

elements. The overpack inner and outer shells, bottom vent shells, and the lifting ribs are modeled with SHELL63 elements. A combination of SOLID45, SHELL63, and SOLSH190 elements is used to model the steel components in the HI-STORM FW lid. These element types are well suited for the overpack geometry and loading conditions, and they have been used successfully in previous cask licensing applications [3.1.10, 3.3.2].

iii. All overpack steel members are represented by their linear elastic material properties (at 300ºF) based on the data provided in Section 3.3. The concrete material in the overpack body is not explicitly modeled. Its mass, however, is accounted for by applying a uniformly distributed pressure on the baseplate annular area between the inner and outer shells (see Figure 3.4.26). The plain concrete in the HI-STORM FW lid is explicitly modeled in ANSYS using SOLID65 elements along with the input parameters listed in Table 3.1.12.

iv. To implement the ANSYS finite element model in LS-DYNA, the SOLID45, SHELL63, and SOLSH190 elements are converted to solid, shell, and thick shell elements, respectively, in LS-DYNA. The SOLID65 elements used to model the plain concrete in the HI-STORM FW lid are replaced by MAT_PSEUDO_TENSOR (or MAT_016) elements in LS-DYNA. The plain concrete in the overpack body is also modeled in LS-DYNA using MAT_PSEUDO_TENSOR elements.

v. In LS-DYNA, all overpack steel members are represented by their applicable nonlinear elastic-plastic true stress-strain relationships. The methodology used for obtaining a true stress-strain curve from a set of engineering stress-strain data (e.g., strength properties from [3.3.1]) is provided in [3.1.9], which utilizes the following power law relation to represent the flow curve of metal in the plastic deformation region:

$$\sigma = K\varepsilon^{n}$$

where n is the strain-hardening exponent and K is the strength coefficient. Table 3.1.13 provides the values of K and n ~~that~~ which are subsequently used to model the behavior of the overpack steel materials in LS-DYNA. Further details of the development of the true stress-strain relations for these materials are found in [3.4.11]. The concrete material is modeled in LS-DYNA using a non-linear material model (i.e., MAT_PSEUDO_TENSOR or MAT_016) based on the properties listed in Section 3.3.

3.1.3.2 Multi-Purpose Canister (MPC)

The two constituent parts of the MPC, namely (i) the Enclosure Vessel and (ii) the Fuel Basket, are modeled separately. The model for the Enclosure Vessel is focused to quantify its stress and strain field under the various loading conditions. The model for the Fuel Basket is focused on characterizing its strain and displacement behavior during a non-mechanistic tipover event. For the non-mechanistic tipover analysis, ~~two~~ three~~four~~ distinct finite element models are created: one for the maximum length MPC-37 ~~and~~ , one for the maximum length MPC-89, and one for the MPC-32ML~~, and one for the MPC-31C~~. The finite element models for the MPC-37 and MPC-89 enclosure

vessels are shown in Figures 3.4.11A and 3.4.11B, respectively. ~~(Figures 3.4.11 and 3.4.12).~~Note that the MPC-32ML ~~and MPC-31C~~ enclosure vessel~~s~~, carrying the PWR fuel type~~s~~, ~~are~~is identical to the MPC-37 except for the length. The finite element models for the fuel baskets, the fuel assemblies and the basket shims, for all three~~four~~ basket types are shown in Figures 3.4.12, 3.4.13 and 3.4.14, respectively.

The key attributes of the MPC finite element models (implemented in ANSYS) are:

i. The finite element layout of the Enclosure Vessel is pictorially illustrated in Figure 3.4.1. The finite element discretization of the Enclosure Vessel is sufficiently detailed to accurately articulate the primary membrane and bending stresses as well as the secondary stresses at locations of gross structural discontinuity, particularly at the MPC shell to baseplate juncture. This has been confirmed by comparing the ANSYS stress results with the analytical solution provided in [3.4.16] (specifically Cases 4a and 4b of Table 31) for the discontinuity stress at the junction between a cylindrical shell and a flat circular plate under internal pressure (100 psig). The two solutions agree within 3% indicating that the finite element mesh for the Enclosure Vessel is adequately sized. Table 3.1.14 summarizes the key input data that is used to create the finite element model of the Enclosure Vessel.

ii. The Enclosure Vessel shell, baseplate, and upper and lower lids are meshed using SOLID185 elements. The MPC lid-to-shell weld and the reinforcing fillet weld at the shell-to-baseplate juncture are also explicitly modeled using SOLID185 elements (see Figure 3.4.1).

iii. Consistent with the drawings in Section 1.5, the MPC lid is modeled as two separate plates, which are joined together along their perimeter edge. The upper lid is conservatively modeled as 4.5” thick, which is less than the minimum thickness specified on the licensing drawing (see Section 1.5). “Surface-to-surface” contact is defined over the interior interface between the two lid plates using CONTA173 and TARGE170 contact elements.

iv. The materials used to represent the Enclosure Vessel are assumed to be isotropic and are assigned linear elastic material properties based on the Alloy X material data provided in Section 3.3. The Young’s modulus value varies throughout the model based on the applied temperature distribution, which is shown in Figure 3.4.27 and conservatively bounds the normal operating temperature distribution for the maximum length MPC-37 as determined by the thermal analyses in Chapter 4.

v. The fuel basket models (Figures 3.4.12A ~~and~~ , 3.4.12B, ~~3.4.12C~~ and 3.4.12~~D~~C), which are implemented in LS-DYNA, are assembled from intersecting plates per the licensing drawings in Section 1.5, include all potential contacts and allow for relative rotations between intersecting plates. ~~For conservatism, a bounding gap is assumed at contact interfaces between any two perpendicular basket plates to allow for impacts and, therefore, maximize the stress and deformation of the fuel basket plate.~~ The fuel basket plates are modeled in LS-DYNA using thick shell elements, which behave like solid elements in contact, but can also accurately simulate the bending behavior of the fuel basket plates. To

ensure numerical accuracy, full integration thick shell elements with 10 through-thickness integration points are used. This modeling approach is consistent with the approach taken in [3.1.10] to qualify the F-32 and F-37 fuel baskets.

vi. In LS-DYNA, the fuel basket plates are represented by their applicable nonlinear elastic-plastic true stress-strain relationships in the same manner as the steel members of the HI-STORM FW overpack (see Subsection 3.1.3.1). Table 3.1.13 provides the values of K and n ~~that~~ which are subsequently used to model the behavior of the fuel basket plates in LS-DYNA. Details of the development of the true stress-strain relations are found in [3.4.11].

3.1.3.3 HI-TRAC VW Transfer Cask

The stress analysis of the transfer cask addresses three performance features that are of safety consequence. They are:

i. Performance of the water jacket as a pressure retaining enclosure under an accident condition leading to overheating of water.
ii. Performance of the threaded anchor locations in the HI-TRAC VW top flange under the maximum lifted load.
iii. Performance of the HI-TRAC VW bottom lid under its own self weight plus the weight of the heaviest MPC.

The above HI-TRAC VW components are analyzed separately using strength of materials formula, the details of which are provided in Subsections 3.4.3 and 3.4.4.

3.2 WEIGHTS AND CENTERS OF GRAVITY

As stated in Chapter 1, while the diameters of the MPC, HI-STORM FW, and HI-TRAC VW are fixed, their height is dependent on the length of the fuel assembly. The MPC cavity height (which determines the external height of the MPC) is set equal to the nominal fuel length (along with control components, if any) plus Δ, where Δ is between 1.5" (minimum), 2.0" (maximum), Δ is increased above 1.5" so that the MPC cavity height is a full inch or half-inch number. Thus, for the PWR reference fuel (Table 1.0.4), whose length including control components is 167.2" (Table 2.1.1), Δ = 1.8" so that the MPC cavity height, c, becomes 169". Δ is provided to account for irradiation and thermal growth of the fuel in the reactor. Table 3.2.1 provides the height of the internal cavities and bottom-to-top external dimension of all system components. Table 3.2.2 provides the parameters that affect the weight of cask components and their range of values assumed in this FSAR.

The cavity heights of the HI-STORM FW overpack and the HI-TRAC VW transfer cask are set greater than the MPC height by fixed amounts to account for differential thermal expansion and manufacturing tolerances. Table 3.2.1 provides the height data on HI-STORM FW, HI-TRAC VW, and the MPC as the adder to the MPC cavity length.

Table 3.2.5 provides the reference weight of the HI-STORM FW overpack for storing MPC-37 and MPC-89 containing reference PWR and BWR fuel, respectively. Conservatively, the HI-STORM FW overpack storing MPC-32ML ~~and MPC-31C, both~~ carrying PWR fuel, uses the same PWR reference weights listed in Table 3.2.5. The weight of the HI-STORM FW overpack body is provided for two discrete concrete densities and for two discrete heights for PWR and BWR fuel. The weight at any other density and any other height can be obtained by linear interpolation. Similarly the weight of the HI-STORM FW lid is provided for two discrete values of concrete density. The weight corresponding to any other density can be computed by linear interpolation.

As discussed in Section 1.2, the weight of the HI-TRAC VW transfer cask is maximized for a particular site to take full advantage of the plant's crane capacity within the architectural limitations of the Fuel Building. Accordingly, the thickness of the lead shield and outer diameter of the water jacket can be increased to maximize shielding. The weight of the empty HI-TRAC VW cask in Table 3.2.4 is provided for three lengths corresponding to PWR fuel. Using the data for three lengths, the transfer cask's weight corresponding to any other length can be obtained by linear interpolation (or extrapolation). For MPC-89, the weight data is provided for the minimum and reference fuel lengths, as well as the reference fuel assembly with a DFC and therefore likewise the transfer cask's weight corresponding to any other length can be obtained by linear interpolation (or extrapolation).

The approximate change in the empty weight of HI-TRAC VW (in kilo pounds) of a certain height, h (inch), by virtue of changing the thickness of the lead by an amount, δ (inch), is given by the formula:

$$\Delta W_{lead} = 0.1128(h - 13.5)\,\delta$$

Table 3.2.3

MPC WEIGHT DATA (COMPUTED NOMINAL VALUES)

Item	BWR Fuel Based on length below			PWR Fuel Based on length below (see Note 2)		
	Reference	Shortest from Table 3.2.2	Longest from Table 3.2.2	Reference	Shortest from Table 3.2.2	Longest from Table 3.2.2
Enclosure Vessel	27,500	27,100	27,800	28,600	25,600	31,100
Fuel Basket	8,600	8,300	8,800	7,900	7,000	9,400
Water in the MPC @ SG = 1 (See Note 1)	16,700	16,200	18,900	15,400	14,000	18,700
Water mass displaced by a closed MPC Enclosure Vessel (SG = 1)	30,800	29,900	31,600	29,300	26,600	34,500

SG = Specific Gravity

Notes 1: Water weight in the MPC assumes that water volume displaced by the fuel is equal to the fuel weight divided by an average fuel assembly density of 0.396 lb/in^3. The fuel weights used for calculating the fuel volumes for Reference/Shortest/Longest PWR and BWR fuel assemblies are 1750/1450/2050 and 750/700/850 pounds respectively.

2: Weight data for the MPC-32ML ~~and the MPC-31C are~~is bounded by values for the longest PWR fuel.

Table 3.2.4

HI-TRAC VW WEIGHT DATA (COMPUTED NOMINAL VALUES)

Item	BWR Fuel Based on length below			PWR Fuel Based on length below (see Note 1)		
	Reference	Shortest from Table 3.2.2	Longest from Table 3.2.2	Reference	Shortest from Table 3.2.2	Longest from Table 3.2.2
HI-TRAC VW Body (no Bottom Lid, water jacket empty)	84,000	81,700	86,200	85,200	78,000	99,600
HI-TRAC VW Bottom Lid	11,300	11,300	11,300	11,300	11,300	11,300
MPC with Basket	36,100	35,400	36,600	36,500	32,600	40,500
Fuel Weight (assume 50% with control components or channels, as applicable)	66,800 (750 lb per assembly average)	64,600 (725 lb per assembly average)	71,200 (800 lb per assembly average)	62,000 (1,675 lb per assembly average)	53,700 (1,450 lb per assembly average)	69,400 (1,875 lb per assembly average)
Water in the Annulus	600	600	600	600	600	700
Water in the Water Jacket	8,800	8,500	9,000	8,400	7,600	9,900
Displaced Water Mass by the Cask in the Pool (Excludes MPC)	18,900	18,400	19,400	18,600	17,500	21,600

Notes: 1: HI-TRAC VW weight data for the longest PWR fuel is bounding for the HI-TRAC carrying the MPC-32ML ~~and MPC-31C~~.

The penetration results for the small and intermediate missile are summarized in Table 3.4.6.

3.4.4.1.4 Load Case 4: Non-Mechanistic Tipover

The non-mechanistic tipover event, as described in Subsection 2.2.3(b), is site-dependent only to the extent that the stiffness of the target (ISFSI pad) affects the severity of the impact impulse. To bound the majority of ISFSI pad sites, the tipover analyses are performed using a stiff target foundation, which is defined in Table 2.2.9. The objectives of the analyses are to demonstrate that the plastic deformation in the fuel basket is sufficiently limited to permit the stored SNF to be retrieved by normal means and that there is no significant loss of radiation shielding in the storage system. Furthermore, the maximum lateral deflection of the lateral surface of the fuel basket is within the limit assumed in the criticality analyses (Chapter 6), and therefore, the lateral deflection does not have an adverse effect on criticality safety.

The tipover event is an artificial construct wherein the HI-STORM FW overpack is assumed to be perched on its edge with its C.G. directly over the pivot point A (Figure 3.4.8). In this orientation, the overpack begins its downward rotation with zero initial velocity. Towards the end of the tip-over, the overpack is horizontal with its downward velocity ranging from zero at the pivot point (point A) to a maximum at the farthest point of impact. The angular velocity at the instant of impact defines the downward velocity distribution along the contact line.

In the following, an explicit expression for calculating the angular velocity of the cask at the instant when it impacts on the ISFSI pad is derived. Referring to Figure 3.4.8, let r be the length AC where C is the cask centroid. Therefore,

$$r = \left(\frac{d^2}{4} + h^2 \right)^{1/2}$$

The mass moment of inertia of the HI-STORM FW system, considered as a rigid body, can be written about an axis through point A, as

$$I_A = I_c + \frac{W}{g} r^2$$

where I_c is the mass moment of inertia about a parallel axis through the cask centroid C, and W is the weight of the cask (W = Mg).

Let $\theta_1(t)$ be the rotation angle between a vertical line and the line AC. The equation of motion for rotation of the cask around point A, during the time interval prior to contact with the ISFSI pad, is

$$I_A \frac{d^2 \theta_1}{dt^2} = Mgr \sin \theta_1$$

This equation can be rewritten in the form

$$\frac{I_A}{2} \frac{d(\dot{\theta}_1)^2}{d\theta_1} = Mgr \sin \theta_1$$

which can be integrated over the limits $\theta_1 = 0$ to $\theta_1 = \theta_{2f}$ (Figure 3.4.8). The final angular velocity θ_1 at the time instant just prior to contact with the ISFSI pad is given by the expression

$$\dot{\theta}_1(t_B) = \sqrt{\frac{2\,Mgr}{I_A}(1 - \cos\theta_{2f})}$$

where, from Figure 3.4.8,

$$\theta_{2f} = \cos^{-1}\left(\frac{d}{2r}\right)$$

This equation establishes the initial conditions for the final phase of the tip-over analysis; namely, the portion of the motion when the cask is decelerated by the resistive force at the ISFSI pad interface. Using the data germane to HI-STORM FW (Table 3.4.11) and the above equations, the angular velocity of impact is calculated as

$$\dot{\theta}_1(t_B) = 1.45 \text{ rad/sec}$$

The LS-DYNA analysis to characterize the response of the HI-STORM FW system under the non-mechanistic tipover event is focused on two principal demonstrations, namely:

(i) The lateral deformation of the basket panels in the active fuel region is less than the limiting value in Table 2.2.11.

(ii) The impact between the MPC guide tubes and the MPC does not cause a thru-wall penetration of the MPC shell.

~~Two Four~~Three LS-DYNA finite element models are developed to simulate the postulated tipover event of HI-STORM FW storage cask with loaded MPC-37, ~~and~~ MPC-89~~,~~ and MPC-32ML ~~and MPC-31C,~~ respectively. The ~~two four~~three LS-DYNA models are constructed according to the

dimensions specified in the licensing drawings included in Section 1.5; the tallest configuration for each MPC enclosure type is considered to ensure a bounding tipover analysis. Because of geometric and loading symmetries, a half model of the loaded cask and impact target (i.e., the ISFSI pad) is considered in the analysis. The LS-DYNA models of the HI-STORM FW overpack and the MPC are described in Subsections 3.1.3.1 and 3.1.3.2, respectively.

The ISFSI pad LS-DYNA model, which consists of a 320"×100"×36" concrete pad and the underlying subgrade (800"×275"×470" in size) with non-reflective lateral and bottom surface boundaries, is identical to that used in the HI-STORM 100 tipover analysis documented in the HI-STORM 100 FSAR [3.1.4]. All structural members of the loaded cask are explicitly modeled so that any violation of the acceptance criteria can be found by examining the LS-DYNA simulation results (note: the fuel assembly, which is not expected to fail in a tipover event, is modeled as an elastic rectangular body). This is an improvement compared with the approach taken in the HI-STORM 100 tipover analysis, where the loaded MPC was modeled as a cylinder and therefore the structural integrity of the MPC and fuel basket had to be analyzed separately based on the rigid body deceleration result of the cask. Except for the fuel basket, which is divided into four parts based on the temperature distribution of the basket, each structural member of the cask is modeled as an independent part in the LS-DYNA model. Note that the critical weld connection between the MPC shell and the MPC lid is treated as a separate part and modeled with solid elements. Each of the two LS-DYNA models consists of forty-two parts, which are discretized with sufficiently high mesh density; very fine grids are used in modeling the MPC enclosure vessel, especially in the areas where high stress gradients are expected (e.g., initial impact location with the overpack). To ensure numerical accuracy, full integration thin shell and thick shell elements with 10 though-thickness integration points or multi-layer solid elements are used. The LS-DYNA tipover model consists of over 470,000 nodes and 255,000 elements for HI-STORM FW with loaded MPC-37, and the model for the cask with loaded MPC-89 consists of over 689,000 nodes and 350,000 elements. The tipover model with loaded MPC-32ML consists of 451,310~~464,200~~ nodes and 278,646 ~~280,500~~ elements~~, and the model MPC-31C consists of over 346,900 nodes and 199,000 elements~~.

The same ISFSI concrete pad material model used for the HI-STORM 100 tipover analysis reported in [3.1.4] is repeated for the HI-STORM FW tipover analysis. Specifically, the concrete pad behavior is characterized using the same LS-DYNA material model (i.e., MAT_PSEUDO_TENSOR or MAT_016) as for the end drop and tipover analyses of the HI-STORM 100 storage cask (the only difference between the HI-STORM FW reference ISFSI concrete pad model and the model of the HI-STORM 100 Set B ISFSI concrete pad is thickness). Moreover, the subgrade is also conservatively modeled as an elastic material as before. Note that this ISFSI pad material modeling approach was originally taken in the USNRC approved storage cask tipover and end drop LS-DYNA analyses [3.4.5] where a good correlation was obtained between the analysis results and the test results.

To assess the potential damage of the cask caused by the tipover accident, an LS-DYNA nonlinear material model with strain rate effect is used to model the responses of all HI-STORM FW cask structural members based on the true stress-strain curves of the corresponding materials. Note that the strain rate effect for the fuel basket material, i.e., Metamic HT, is not considered for

conservatism.

Figures 3.4.9A throughe 3.4.9CD14 depict the threefourtwo finite-element tipover analysis models developed for the bounding HI-STORM FW cask configurations with loaded MPC-37, and MPC-89, and MPC-32ML and MPC-31C, respectively.

As shown in Figure 3.4.15, the fuel basket does not experience significant plastic deformation in the active fuel region to exceed the acceptable limits; plastic deformation is essentially limited locally in cells near the top of the basket beyond the active fuel region for the both MPCMPC-37 and, MPC-89 and, MPC-32ML and MPC-31C baskets. Note that the basket corner welds are not considered in the tip-over analysis for conservatism.. The fuel basket is considered to be structurally safe since it can continue maintaining appropriate spacing between fuel assemblies after the tipover event. The MPC enclosure vessel experiences minor plastic deformation at the impact locations with the overpack guide tubes; the maximum local plastic strain (9.910.9%, see Figure 3.4.16) is well below the failure strain of the material and smaller than the plastic strain limit (i.e., at least 0.2 for stainless steel) recommended by [3.4.6] for ASME NB components. Similarly, local plastic deformation occurs in the overpack shear ring near the cask-to-pad impact location as shown in Figure 3.4.17. However, the shielding capacity of overpack will not be compromised by the tipover accident and there is no gross plastic deformation in the overpack inner shell to affect the retrievablilty of the MPC. In addition, the cask closure lid bolts are demonstrated to be structurally safe after the tipover event, only a negligibly small plastic strain is observed in the bolt near the impact location (see Figure 3.4.18). Therefore, the cask lid will not dislodge after the tipover event. Finally, Figures 3.4.19 and 3.4.20 present the deceleration time history results of the cask lid predicted by LS-DYNA. The peak rigid body decelerations, measured for the HI-STORM FW lid concrete, are shown to be 65.41.75 g's in the vertical direction and 19.316.71 g's in the horizontal direction, respectively. Note that the deceleration time histories are filtered using the LS-DYNA built-in Butterworth filter with a cut-off frequency of 350 Hz; the same filter was used for the HI-STORM 100 non-mechanistic tipover analysis [3.1.4].

The structural integrity of the HI-STORM FW lid cannot be ascertained from the LS-DYNA tipover analyses since some components of the lid, namely the lid outer shell and the lid gussets,gussets are defined as rigid members in order to simplify the modeling effort and maintain proper connectivity. Therefore, a separate tipover analysis has been performed for the HI-STORM FW lid using ANSYS, wherein a bounding peak rigid body deceleration established based on LS-DYNA tipover analysis results is statically applied to the lid. The finite element model is identical to the one used in Subsection 3.4.3 to simulate a vertical lift of the HI-STORM FW lid (Figure 3.4.5), except that the eight circumferential gussets are conservatively neglected (i.e., deleted from the finite element model).

The resulting stress distribution in the HI-STORM FW lid is shown in Figure 3.4.21. Per Subsection 2.2.3, the HI-STORM FW lid should not suffer any gross loss of shielding as a result of the non-mechanistic tipover event. To satisfy this criterion, the primary membrane stresses in the lid components are compared against the material yield strength. The most heavily loaded component is the upper shim plate closest to the point of impact (Figure 3.4.21). In order to determine the

primary membrane stress in the upper shim plate, the stresses are linearized along a path that follows the outside vertical edge of the upper shim plate (see Figure 3.4.21 for path definition). Figure 3.4.22 shows the linearized stress results. Since the membrane stress is less than the yield strength of the material at 300ºF (Table 3.3.6), it is concluded that the lid will not suffer any gross loss of shielding as a result of the non-mechanistic tipover event. The complete details of the lid tipover analysis are provided in [3.4.13].

Finally, to evaluate the potential for crack propagation and growth for the MPC fuel baskets under the non-mechanistic tipover event, a conservative crack propagation analysis is carried out for ~~both MPC-37 and MPC-89~~all of the fuel baskets using the same methodology utilized in Attachment D of [1.2.6] to evaluate the HI-STAR 180 F-37 fuel basket in support of the HI-STAR 180 SAR [3.1.10]. The crack propagation analysis is bounding since the maximum tensile strength of the basket material (28.2 ksi) documented in Table 1.2.8 is conservatively considered as the maximum tensile stress experienced by the Metamic fuel baskets in the tip-over accident and used as input to the following crack propagation analysis.

Per [1.2.6] the critical stress intensity factor of Metamic-HT panels is estimated to be

$$K_{IC} = 30ksi\sqrt{in}$$

based on Charpy V-notch absorbed energy (CVE) correlations for steels. The estimated value is consistent with the range for aluminum alloys, which is 20 to 50 $MPa\sqrt{m}$ or 18.2 to 45 $ksi\sqrt{in}$ per Table 3 of [3.4.19]. Next the minimum crack size, a_{min}, for crack propagation to occur is calculated below using the formula for a through-thickness edge crack given in [3.1.5]. Although the formula is derived for a straight-edge specimen, the use of the maximum tensile strength of the fuel basket material as the maximum tensile stress experienced by the basket well compensates for the geometric difference between the basket panel and the specimen. Moreover, the maximum size of a pre-existing crack (1/16") in the fuel basket panel is less than 1/~~59~~th of the minimum basket panel thickness (0.~~59~~35"). Thus, the assumption of a through-thickness edge crack is very conservative. The result is

$$a_{\min} = \frac{\left(\frac{K_{IC}}{1.12\sigma_{\max}}\right)^2}{\pi} = \frac{\left[\frac{30ksi\sqrt{in}}{1.12(28.2ksi)}\right]^2}{\pi} = 0.287in$$

And the safety factor against crack propagation (based on a 1/16" minimum detectable flaw size) is

$$SF = \frac{a_{\min}}{a_{\det}} = \frac{0.287in}{0.0625in} = 4.595$$

The calculated minimum crack size is about 4.6 times the maximum possible pre-existing crack size in the fuel basket (based on 100% surface inspection of each panel). The large safety factor ensures

3.4.4.1.11 Load Case 11: MPC Reflood Event

During a MPC reflood event, water is introduced to the MPC cavity through the lid drain line to cooldown the MPC internals and support fuel unloading. This quenching operation induces thermal stresses and strains in the fuel rod cladding, which are maximum at the boundary interface between the rising water and the dry (gaseous) cavity. The following analysis demonstrates that the maximum total strain in the fuel cladding due to the reflood event is well below the failure strain limit of the material. Thus, the fuel rod cladding will not be breached due to the MPC reflood event.

The analysis is carried out using the finite element code ANSYS [3.4.1]. The model, which is shown in Figure 3.4.37, is constructed using 4-node plastic large strain elements (SHELL43) based on the cladding dimensions of the PWR reference fuel type. The overall length of the model is equal to 30 times the outside diameter of the fuel cladding. As seen in Figure 3.4.37, the mesh size is reduced at the boundary between the wetted fuel rod and the dry fuel rod, where the highest stresses and strains occur. To account for the gas pressure inside the fuel rod, the top end of the fuel rod is fixed in the vertical direction, and an equivalent axial force is applied at the bottom end. A radial pressure is also applied to the inside surface of the fuel cladding (see Figure 3.4.38). The fuel cladding material is modeled as a bi-linear isotropic hardening material with temperature dependent properties. The key input data used to develop the finite element model are summarized in Table 3.4.14A.

The MPC reflood pressure, which is restricted to below the normal condition pressure limit, is too low to have any~~d~~ adverse effect on the fuel cladding. Moreover,~~,~~ the reflood water pressure acts to produce compressive hoop stresses which help reduce the tensile hoop stress (albeit by a small amount) from the internal gas pressure in the rods. Therefore, the MPC flooding pressure has no ~~harmful~~ adverse consequence to the fuel cladding and is neglected in the analysis.

At t = 0 sec, the uniform temperature throughout the entire fuel rod is set at 752ºF (400ºC), which equals the fuel cladding temperature limit under normal operating conditions. At t = 0.1 sec, the temperature assigned to the lower half of the fuel rod model is suddenly reduced to 80ºF to simulate the water quenching (see Figure 3.4.39). The resulting stress and strain distributions in the fuel rod are shown in Figures 3.4.40 and 3.4.41, respectively. The maximum stress and strain values are summarized in Table 3.4.15A. The maximum total strain in the fuel rod is well below the failure strain limit of 1.7% for the cladding material per [3.4.20]. In fact, the maximum stress and strain in the fuel rod remain in the elastic range.

The analysis described above makes a number of assumptions that significantly overstate the computed thru-wall strain in the fuel cladding. The major assumptions are:

1. Even though the peak cladding temperature occurs at a localized location, the fuel rod is modeled as a pressurized tube with closed ends at a uniform temperature that is greater than the maximum peak cladding temperature value reported in Chapter 4 when the MPC is in the HI-TRAC under the Design Basis heat load condition.
2. The rapid thermal straining of the pressurized tube (fuel rod) due to the quenching effect of water is simulated as a step transient wherein the temperature of the quenched portion of the

tube is assumed to drop down to the injected water temperature (assumed to be 80ºF) causing a step change in the cladding wall temperature in the longitudinal direction at its interface with the "dry" portion of the tube. This assumption is extremely conservative because in actuality the immersed portion of the fuel rod is blanketed by vapor which acts to retard the severity of the thermal transient.

3. Even though, as the rod is gradually immersed in water, the axial heat conduction will tend to cool the un-immersed portion of the tube thus reducing the ΔT at the quenched/dry interface, no credit for axial conduction is taken.
4. The cooling of the fuel rod by gradual immersion in the water has the beneficial effect of reducing the internal pressure (per the ideal gas law) and thus the magnitude of pressure induced stress in the fuel cladding. As the peak cladding temperature in the MPC is reached in the upper half of the fuel rods (see Chapter 4), a substantial amount of rod is cooled by water (as its level gradually rises inside the MPC) before the vulnerable zone (where the peak cladding temperature exists) is subjected to the thermal transient from quenching. No credit for this amelioration of the pressure stresses due to the gradual cooling of the rod is taken in the analysis.

The same analysis approach is repeated for the MPC-32ML ~~and MPC-31C~~ to reflect fuel rod geometry~~ies~~ specific to ~~these~~this PWR fuel type~~s~~. The geometric data, used in the re-flooding analysis, for this~~ese~~ ~~two~~ fuel type~~s~~ is summarized in Table 3.4.14B. The governing results for the fuel type~~s~~ used in MPC-32ML ~~and MPC-31C~~ are presented in Table 3.4.15B. The governing stress and strains for the governing fuel rods are presented in Figure~~s~~ 3.4.42 ~~and 3.4.43~~.

In summary, even though the analysis presented above is highly conservative, the maximum stress and strain in the fuel rod remain elastic. Moreover, the maximum strain is less than the failure strain limit by a factor of 6. Thus, the MPC reflood event will not cause a breach of the fuel rod cladding.

3.4.5 Cold

A discussion of the resistance to failure due to brittle fracture is provided in Subsection 3.1.2.

The value of the ambient temperature has two principal effects on the HI-STORM FW system, namely:

i. The steady-state temperature of all material points in the cask system will go up or down by the amount of change in the ambient temperature.

ii. As the ambient temperature drops, the absolute temperature of the contained helium will drop accordingly, producing a proportional reduction in the internal pressure in accordance with the Ideal Gas Law.

In other words, the temperature gradients in the system under steady-state conditions will remain the same regardless of the value of the ambient temperature. The internal pressure, on the other hand, will decline with the lowering of the ambient temperature. Since the stresses under normal storage

All transfer cask materials that come in contact with the spent fuel pool are coated to facilitate decontamination. The HI-TRAC VW is designed for repeated normal condition handling operations with high factor of safety to assure structural integrity. The resulting cyclic loading produces stresses that are well below the endurance limit of the cask's materials, and therefore, will not lead to a fatigue failure in the transfer cask. All other off-normal or postulated accident conditions are infrequent or one-time occurrences that do not contribute significantly to fatigue. In addition, the transfer cask utilizes materials that are not susceptible to brittle fracture during the lowest temperature permitted for loading, as discussed in Subsection 8.4.3.

Chapter 8 provides further discussions on chemical and galvanic reactions, material compatibility and operating environments.

Material Degradation

As discussed in Chapter 8, all transfer cask materials that are susceptible to corrosion are coated. The controlled environment in which the HI-TRAC VW is used mitigates damage due to direct exposure to corrosive chemicals that may be present in other industrial applications. The infrequent use and relatively low neutron flux to which the HI-TRAC VW materials are subjected do not result in radiation embrittlement or degradation of the HI-TRAC's shielding materials that could impair the HI-TRAC's intended safety function. The HI-TRAC VW transfer cask materials are selected for durability and wear resistance for their deployment.

Maintenance and Inspection Provisions

The requirements for periodic inspection and maintenance of the HI-TRAC VW transfer cask throughout the 60-year design life are defined in Chapter 10. These requirements include provisions for routine inspection of the HI-TRAC VW transfer cask for damage prior to each use, including an annual inspection of the lifting attachments. Precautions are taken during lid handling operations to protect the sealing surfaces of the bottom lid. The leak tightness of the liquid neutron shield is verified periodically. The water jacket pressure rupture discs and other fittings used can be easily removed.

3.4.8 MPC Service Life

The term of the 10CFR72, Subpart L C of C, granted by the NRC (i.e., licensed life) is 20 years. Nonetheless, the HI-STORM FW MPCs are designed for 60 years of design life, while satisfying the conservative design requirements defined in Chapter 2, including the regulatory requirements of 10CFR72. Additional assurance of the integrity of the MPC and the contained SNF assemblies throughout the 60-year life of the MPC is provided through the following:

- Design, fabrication, and inspection invoke the pertinent requirements of the ASME Code, as applicable, assures high inherent design margins in operating modes.

- Fabrication and inspection performed in accordance with the comprehensive Quality

Assurance program assures competent compliance with the fabrication requirements.

- Use of materials with known characteristics, verified through rigorous inspection and testing, as described in Chapter 10, assures component compliance with design requirements.

- Use of welding procedures in full compliance with Section III of the ASME Code ensures high-quality weld joints.

Technical Specifications, as defined in Chapter 13, have been developed and imposed on the MPC that assure that the integrity of the MPC and the contained SNF assemblies are maintained throughout the 60-year design life of the MPC.

The principal design considerations bearing on the adequacy of the MPC for the service life are summarized below.

Corrosion

All MPC materials are fabricated from corrosion-resistant austenitic stainless steel and passivated aluminum. The corrosion-resistant characteristics of such materials for dry SNF storage canister applications, as well as the protection offered by these materials against other material degradation effects, are well established in the nuclear industry. The moisture in the MPC is removed to eliminate all oxidizing liquids and gases and the MPC cavity is backfilled with dry inert helium at the time of closure to maintain an atmosphere in the MPC that provides corrosion protection for the SNF cladding throughout the dry storage period. The preservation of this non-corrosive atmosphere is assured by the inherent sealworthiness of the MPC Confinement Boundary integrity (there are no gasketed joints in the MPC).

Structural Fatigue

The passive non-cyclic nature of dry storage conditions does not subject the MPC to conditions that might lead to structural fatigue failure. Ambient temperature and insolation cycling during normal dry storage conditions and the resulting fluctuations in MPC thermal gradients and internal pressure ~~is~~ are the only mechanism for fatigue. ~~These low-stress~~These low-stress, high-cycle conditions cannot lead to a fatigue failure of the MPC that is made from stainless alloy stock (endurance limit well in excess of 20,000 psi). All other off-normal or postulated accident conditions are infrequent or one-time occurrences, which cannot produce fatigue failures. Finally, the MPC uses materials that are not susceptible to brittle fracture.

Maintenance of Helium Atmosphere

The inert helium atmosphere in the MPC provides a non-oxidizing environment for the SNF cladding to assure its integrity during long-term storage. The preservation of the helium atmosphere in the MPC is assured by the robust design of the MPC Confinement Boundary described in Section 7.1. Maintaining an inert environment in the MPC mitigates conditions that might otherwise lead to

SNF cladding failures. The required mass quantity of helium backfilled into the canister at the time of closure and the associated fabrication and closure requirements for the canister are specifically set down to assure that an inert helium atmosphere is maintained in the canister throughout the 60-year design life.

Allowable Fuel Cladding Temperatures

The helium atmosphere in the MPC promotes heat removal and thus reduces SNF cladding temperatures during dry storage. In addition, the SNF decay heat will substantially attenuate over a 60-year dry storage period. Maintaining the fuel cladding temperatures below allowable levels during long-term dry storage mitigates the damage mechanism that might otherwise lead to SNF cladding failures. The allowable long-term SNF cladding temperatures used for thermal acceptance of the MPC design are conservatively determined, as discussed in Section 4.3.

Neutron Absorber Boron Depletion

The effectiveness of the fixed borated neutron absorbing material used in the MPC fuel basket design requires that sufficient concentrations of boron be present to assure criticality safety during worst case design basis conditions over the 60-year design life of the MPC. Information on the characteristics of the borated neutron absorbing material used in the MPC fuel basket is provided in Subsection 1.2.1 and Chapter 8. The relatively low neutron flux, to which this borated material is subjected and will continue to decay over time, does not result in significant depletion of the material's available boron to perform its intended safety function. In addition, the boron content of the material used in the criticality safety analysis is conservatively based on the minimum specified boron areal density (rather than the nominal), which is further reduced by 25% for analysis purposes, as described in Section 6.1. Analysis discussed in Section ~~6.3 demonstrates~~6.3 demonstrates that the boron depletion in the neutron absorber material is negligible over a 60-year duration. Thus, sufficient levels of boron are present in the fuel basket neutron absorbing material to maintain criticality safety functions over the 60-year design life of the MPC.

The above findings are consistent with those of the NRC's Waste Confidence Decision Review, which concluded that dry storage systems designed, fabricated, inspected, and operated in the manner of the requirements set down in this document are adequate for a 100-year service life, while satisfying the requirements of 10CFR72.

3.4.9 Design and Service Life

The discussion in the preceding sections seeks to provide the logical underpinnings for setting the design life of the storage overpacks, the HI-TRAC VW transfer cask, and the MPCs as sixty years. Design life, as stated earlier, is a lower bound value for the expected performance life of a component (service life). If operated and maintained in accordance with this Safety Analysis Report, Holtec International expects the service life of HI-STORM FW casks to substantially exceed their design life values.

Table 3.4.11

INPUT DATA USED FOR CALCULATING ANGULAR VELOCITY OF OVERPACK DURING NON-MECHANISTIC TIPOVER (LOAD CASE 4)

Item	Value
Maximum weight of loaded HI-STORM FW (W)	426,300 lbf[†]
Mid-height of maximum length HI-STORM FW (h)	119.75 in
Outer diameter of HI-STORM FW (d)	140 in
Distance between cask pivot point and cask center (r)	138.709 in
Mass moment of inertia of loaded HI-STORM FW about cask pivot point (I_A)	1.076×10^{10} lb-in^2

Note: The bounding parameters defined above are only used for computing the maximum angular velocity imparted during a tip over event involving the HI-STORM FW overpack along with its contents. Also, the term "h" represents the nominal height of the maximum length of the HI-STORM FW.

[†] Bounds value in Table 3.2.8.

Table 3.4.14A

KEY INPUT DATA FOR FUEL ROD INTEGRITY ANALYSIS DURING MPC REFLOOD EVENT (LOAD CASE 11)

Item	Input Value	Source
Cladding Thickness (for reference PWR fuel), in	0.022	SAR Tables 1.0.4 and 2.1.2
Cladding OD (for reference PWR fuel), in	0.377	SAR Tables 1.0.4 and 2.1.2
Fuel Rod Pressure, psi	2,000	Ref. [3.4.24] (upper bound value)
Yield Strength of Zircaloy, psi	100,000 (at 80°F) 50,500 (at 750°F)	Ref. [3.4.21]
Tensile Strength of Zircaloy, psi	112,100 (at 80°F) 68,200 (at 750°F)	Ref. [3.4.21]
Elastic Modulus of Zircaloy, $\times 10^6$ psi	13.42 (at 80°F) 10.4 (at 750°F)	Ref. [3.4.21]
Coefficient of Thermal Expansion of Zircaloy, $\times 10^{-6}$ in/in/°F	3.3 (at 80°F) 4.5 (at 750°F)	Ref. [3.4.22]
Poisson's Ratio of Zircaloy	0.4	Appendix C of Ref. [3.4.23]

Table 3.4.14B†

KEY INPUT DATA FOR MPC-32ML ~~AND MPC-31C~~ FUEL TYPE~~S~~

Item	MPC-32ML ~~MPC-31C~~
Cladding Thickness, in	0.0285 ~~0.027~~
Cladding OD, in	0.423 ~~0.358~~

† The other input parameters such as the pressure loading, the fuel cladding thermal expansion coefficient and the cladding strength properties remain identical to that defined in Table 3.4.14A. These bounding parameters ensure that a conservative analysis is performed for th~~es~~e MPC-32ML ~~and MPC-31C~~ fuel type~~s~~.

The fuel geometric information is obtained from Table 2.1.2 of this SAR.

Table 3.4.15A

MAXIMUM RESULTS FOR FUEL ROD INTEGRITY ANALYSIS
DURING MPC REFLOOD EVENT (LOAD CASE 11)

Result	Value
Maximum Stress in Fuel Rod Cladding	29,995 psi
Maximum Strain in Fuel Rod Cladding	2.66×10^{-3}

Table 3.4.15B

MAXIMUM RESULTS FOR FUEL ROD INTEGRITY ANALYSIS
DURING MPC REFLOOD EVENT (LOAD CASE 11) – FOR MPC-32ML ~~AND MPC-31C~~[‡]

Result	Value
Maximum Stress in Fuel Rod Cladding	28,349 psi
Maximum Strain in Fuel Rod Cladding	2.54×10^{-3}

[‡] ~~Only the results for the bounding fuel rod (i.e. Fuel used in MPC-32ML) are summarized here.~~

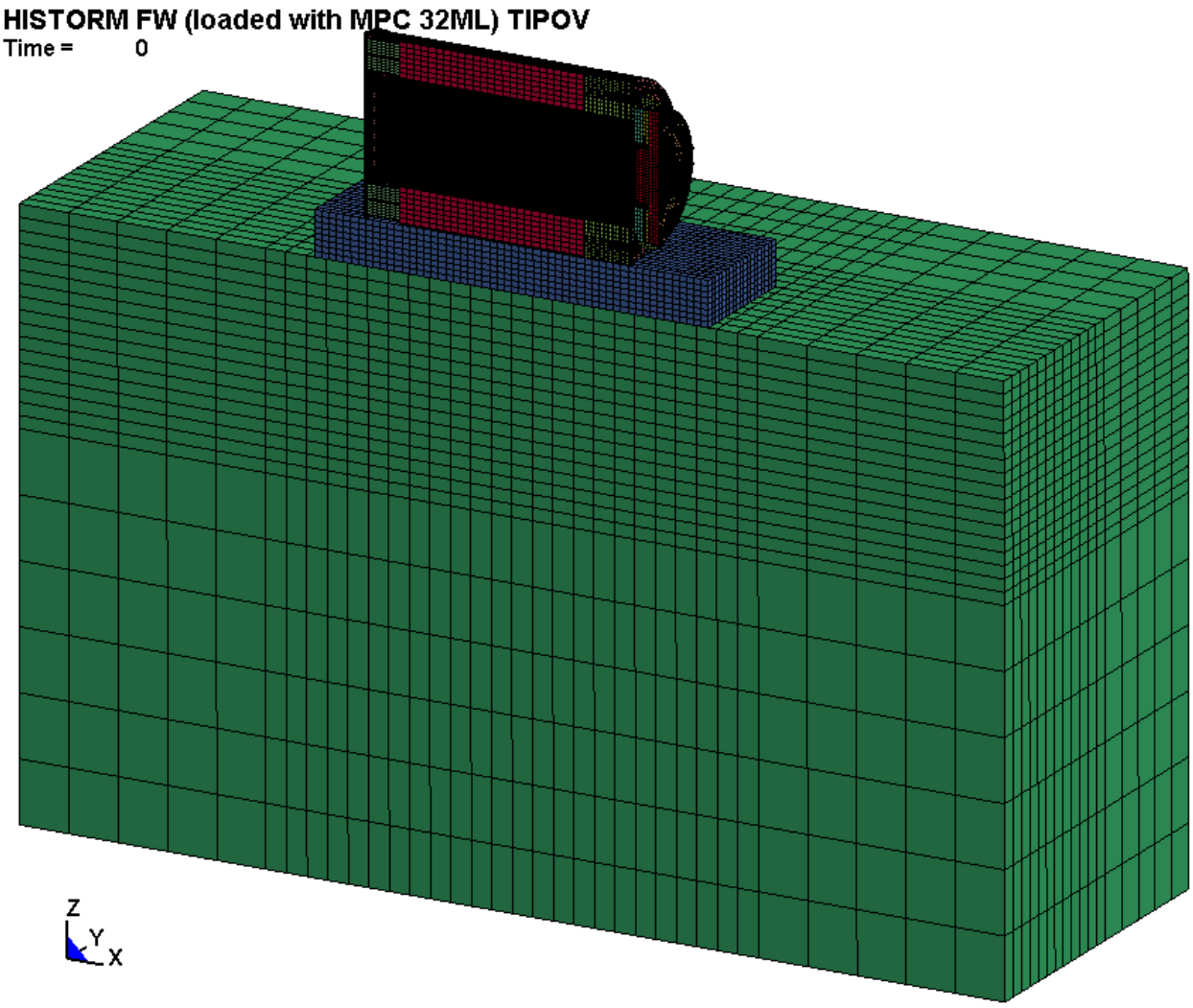

Figure 3.4.9C: LS-DYNA Tipover Model – HI-STORM FW Loaded with MPC-32ML

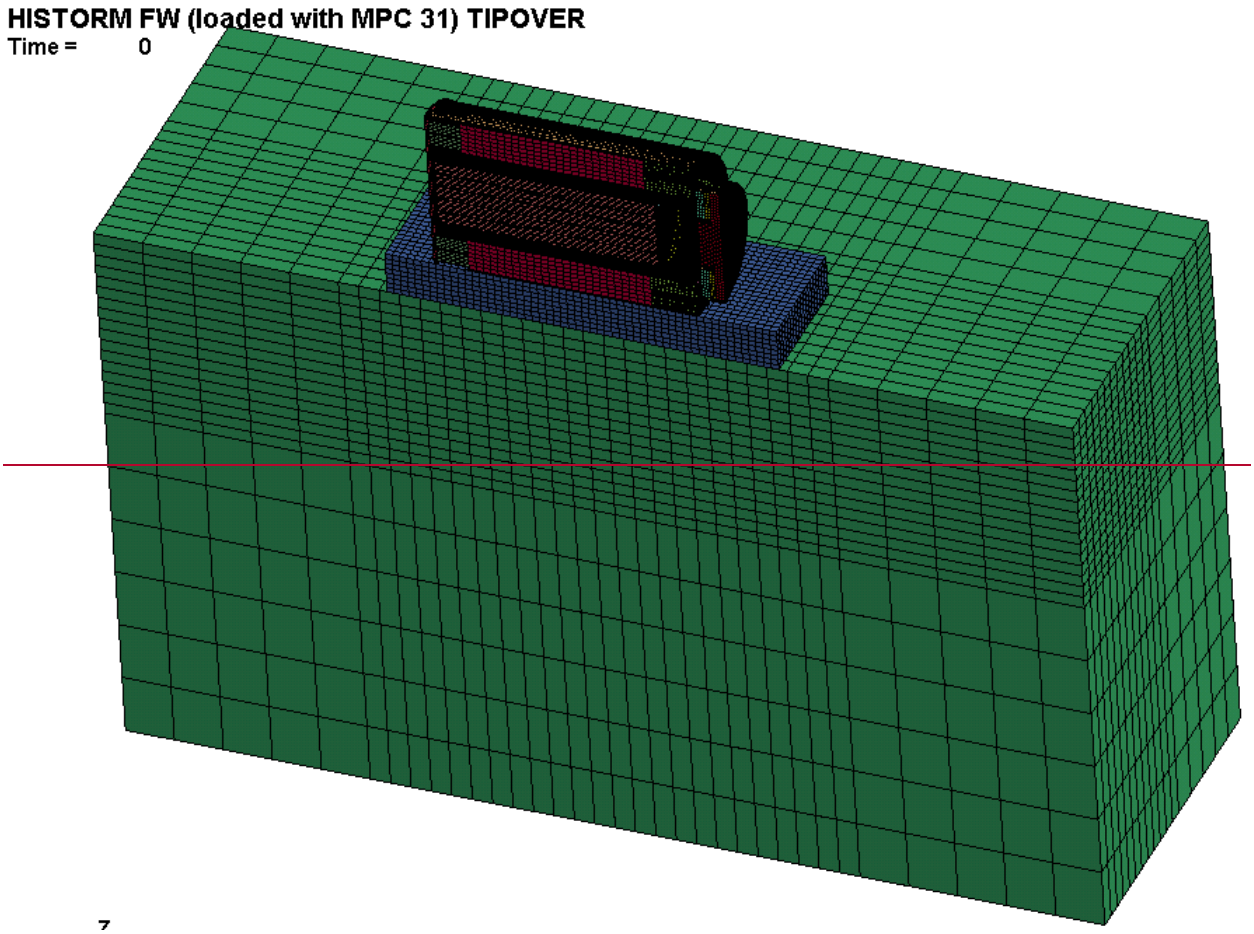

~~**Figure 3.4.9D: LS-DYNA Tipover Model – HI-STORM FW Loaded with MPC-31C**~~

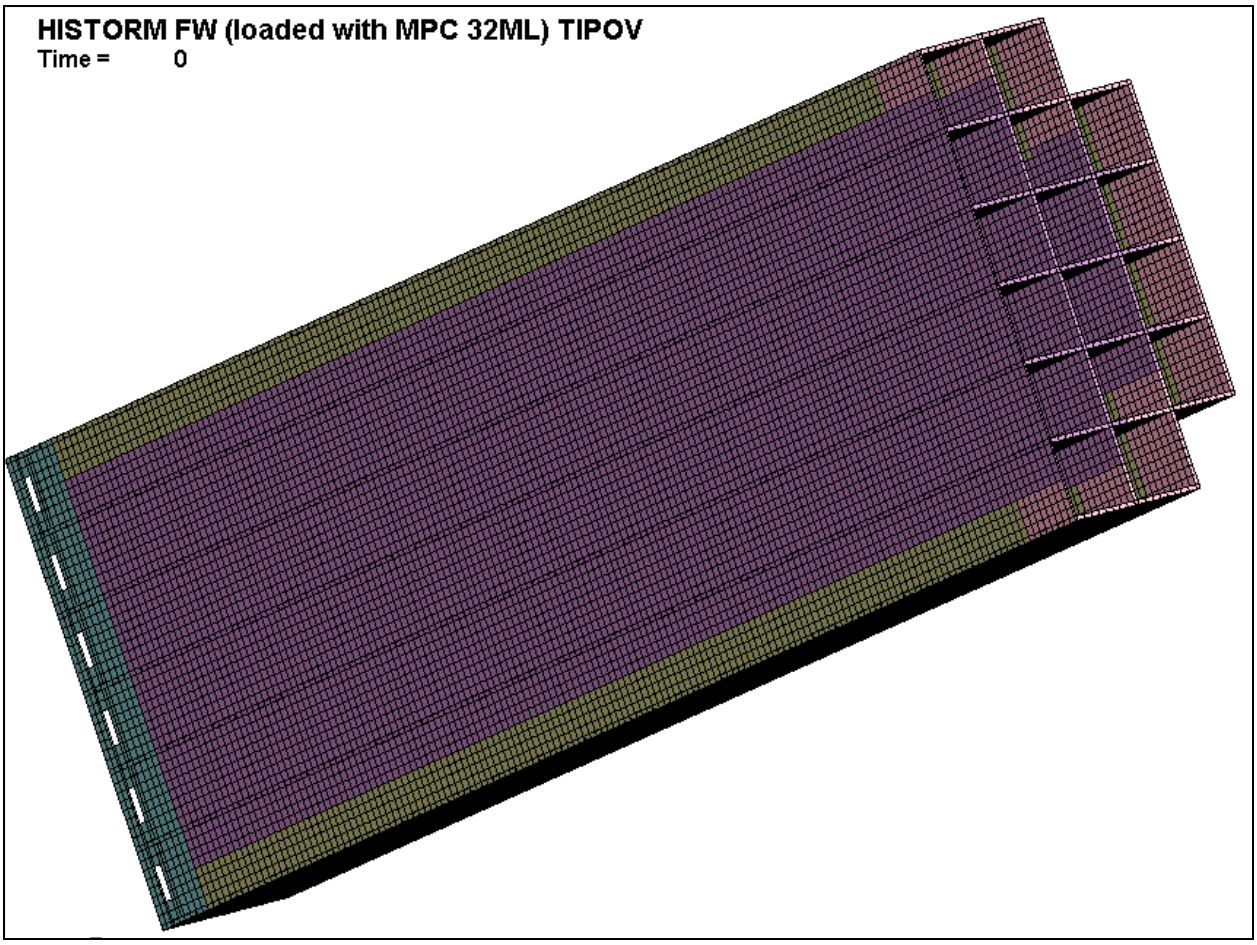

Figure 3.4.12C: LS-DYNA Model – MPC-32ML Fuel Basket
(note: the different colors represent regions with bounding temperatures of 350°C, 325°C and 200°C, respectively)

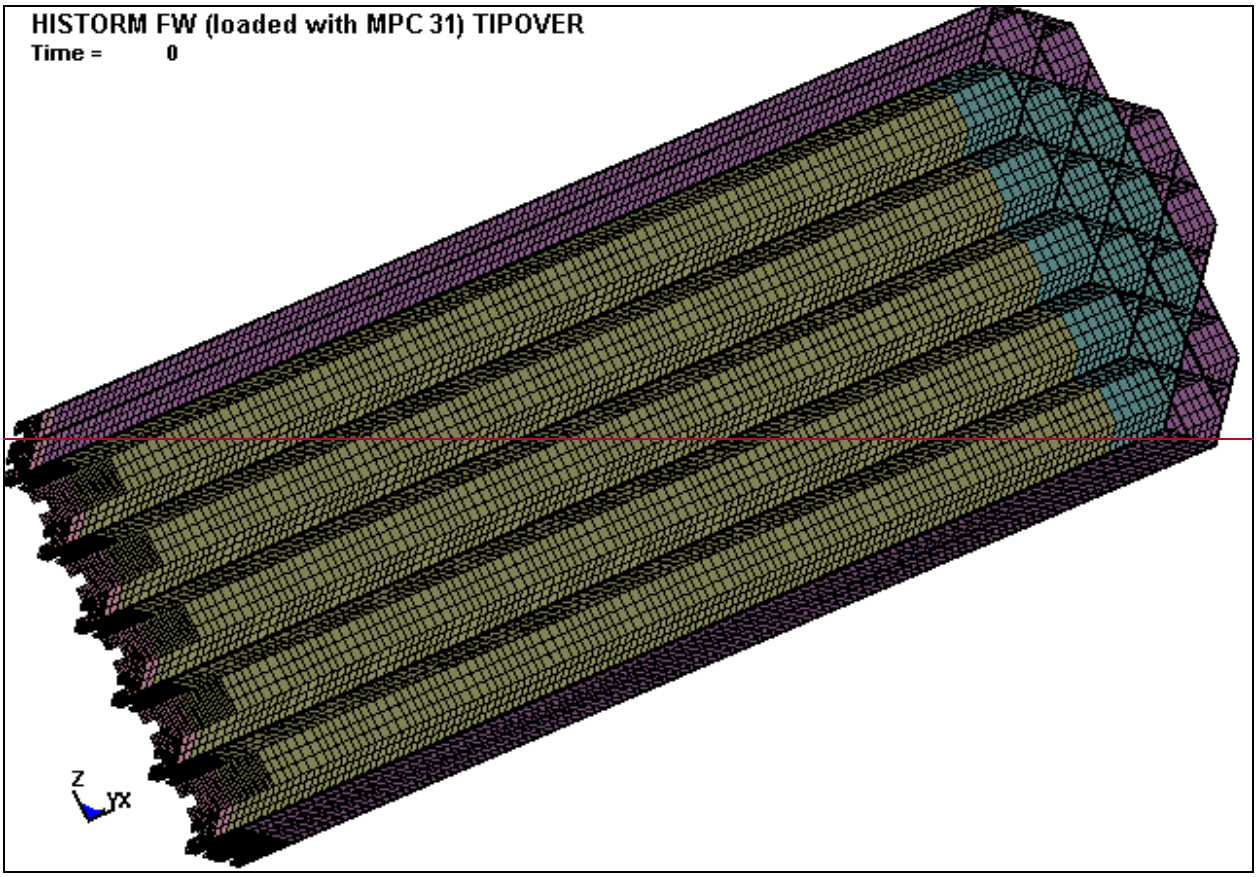

~~Figure 3.4.12B: LS-DYNA Model – MPC-31C Fuel Basket~~
~~(note: the different colors represent regions with bounding temperatures of 295°C, 255°C and 200°C, respectively)~~

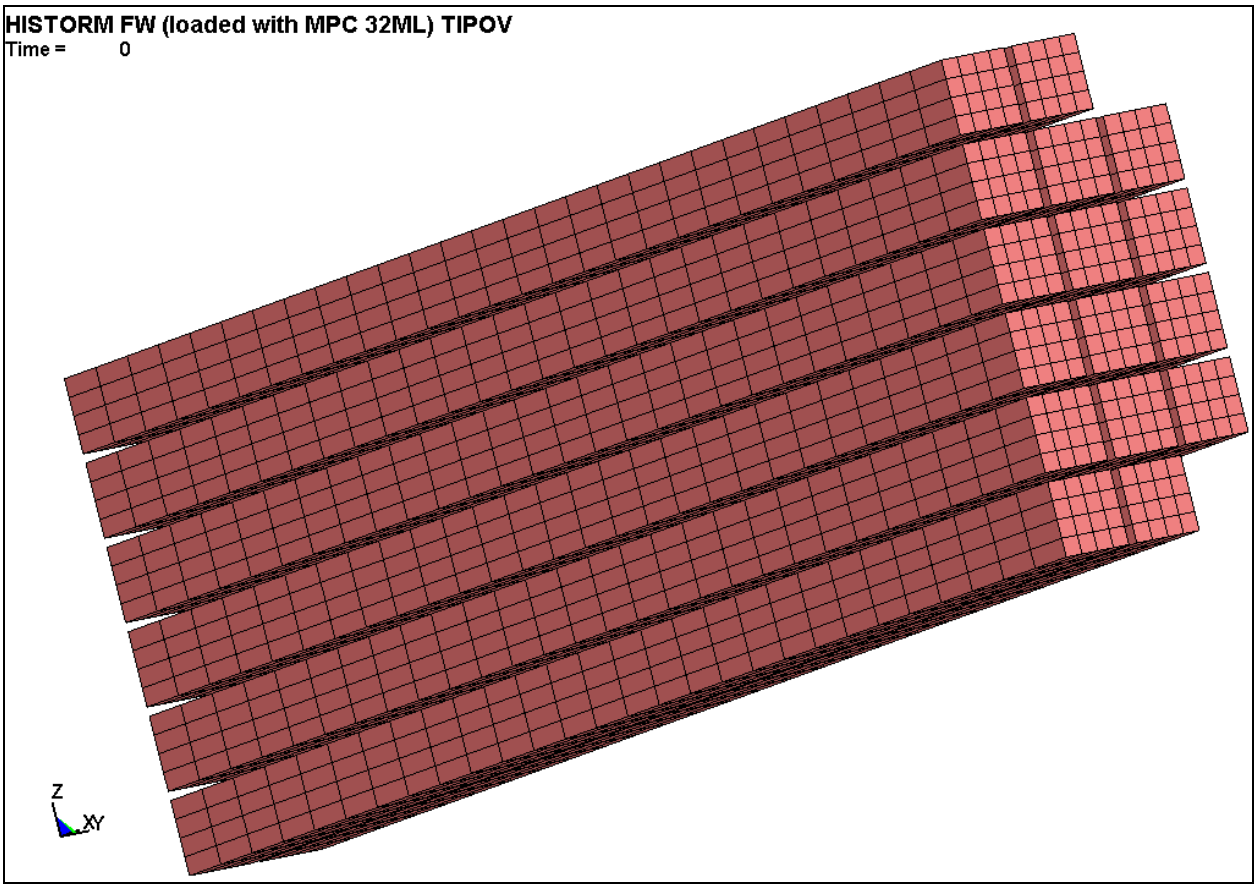

Figure 3.4.13C: LS-DYNA Model – PWR Fuel Assemblies Fuel Assemblies Loaded into MPC-32ML

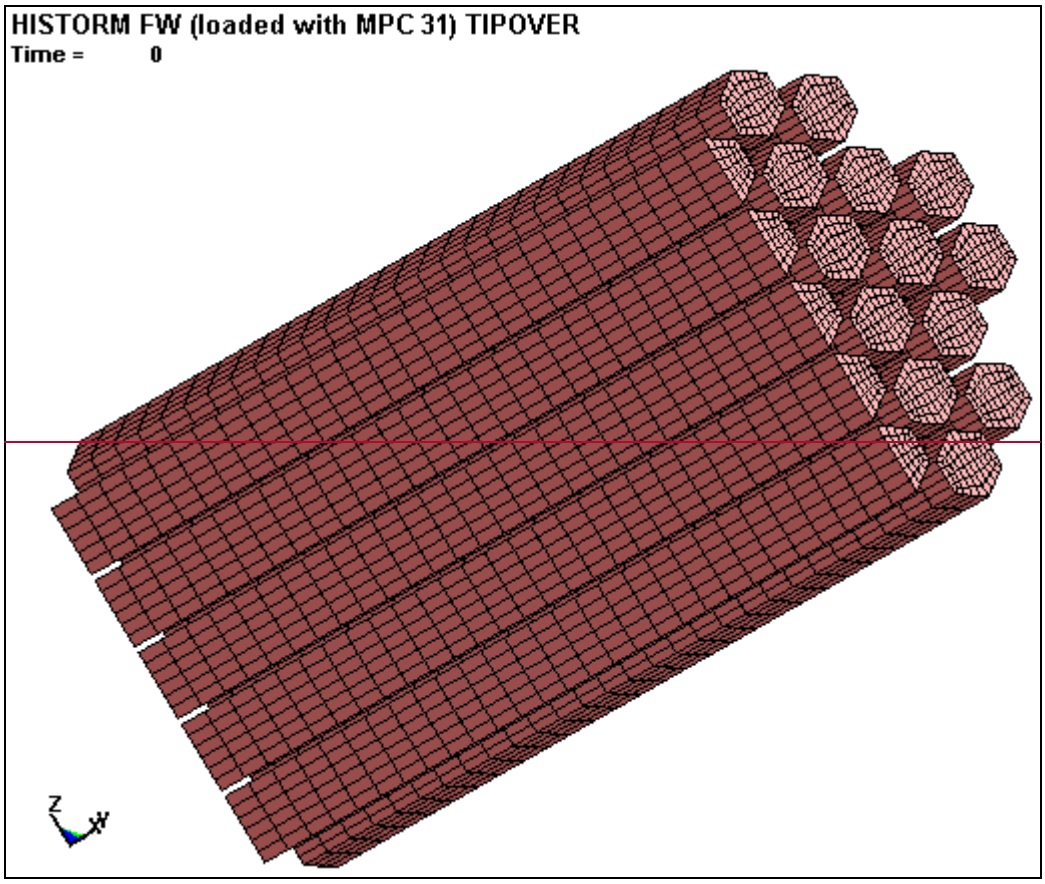

~~Figure 3.4.13D: LS-DYNA Model – PWR Fuel Assemblies Fuel Assemblies Loaded into MPC-31C~~

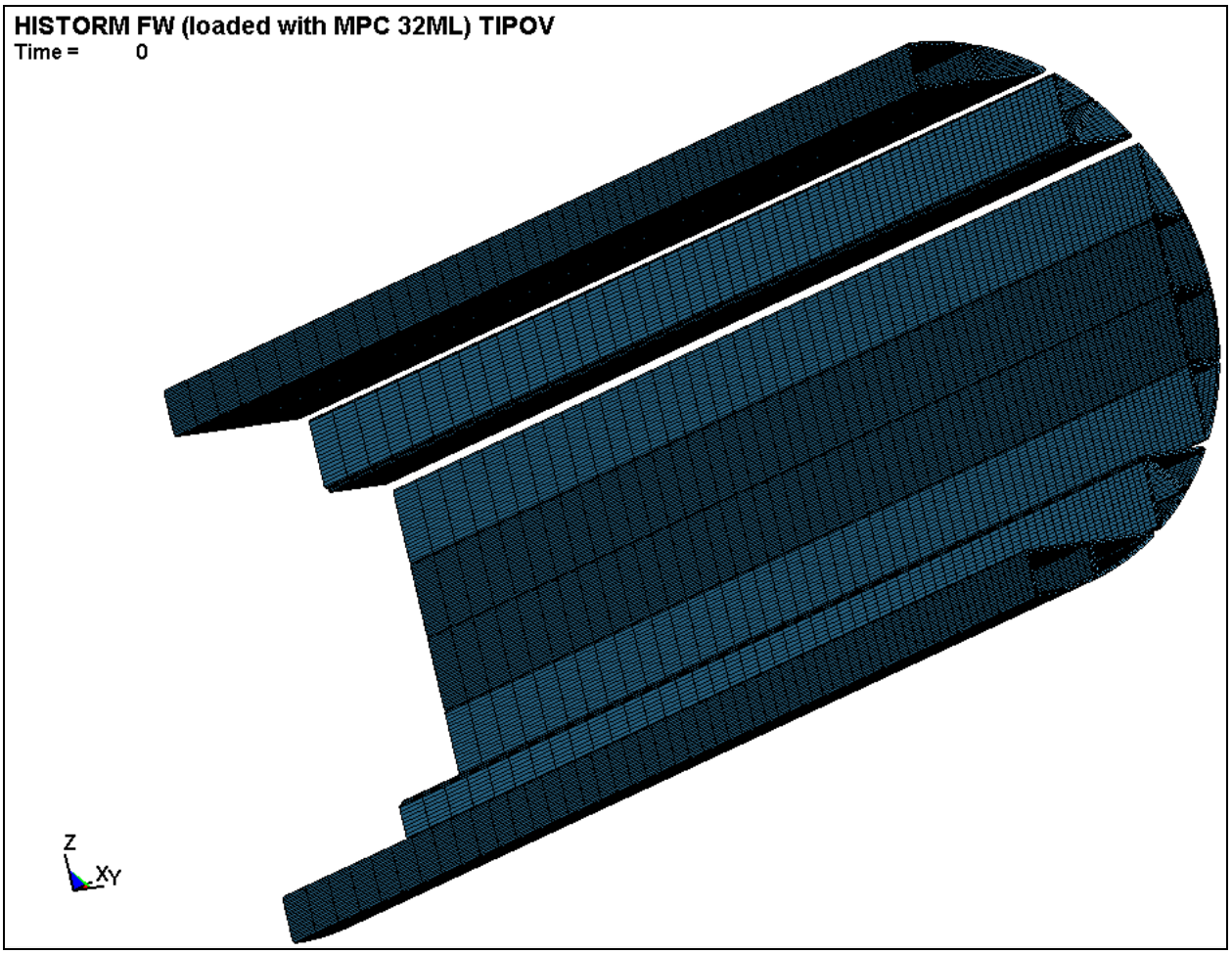

Figure 3.4.14C: LS-DYNA Model – MPC-32ML Fuel Basket Shims

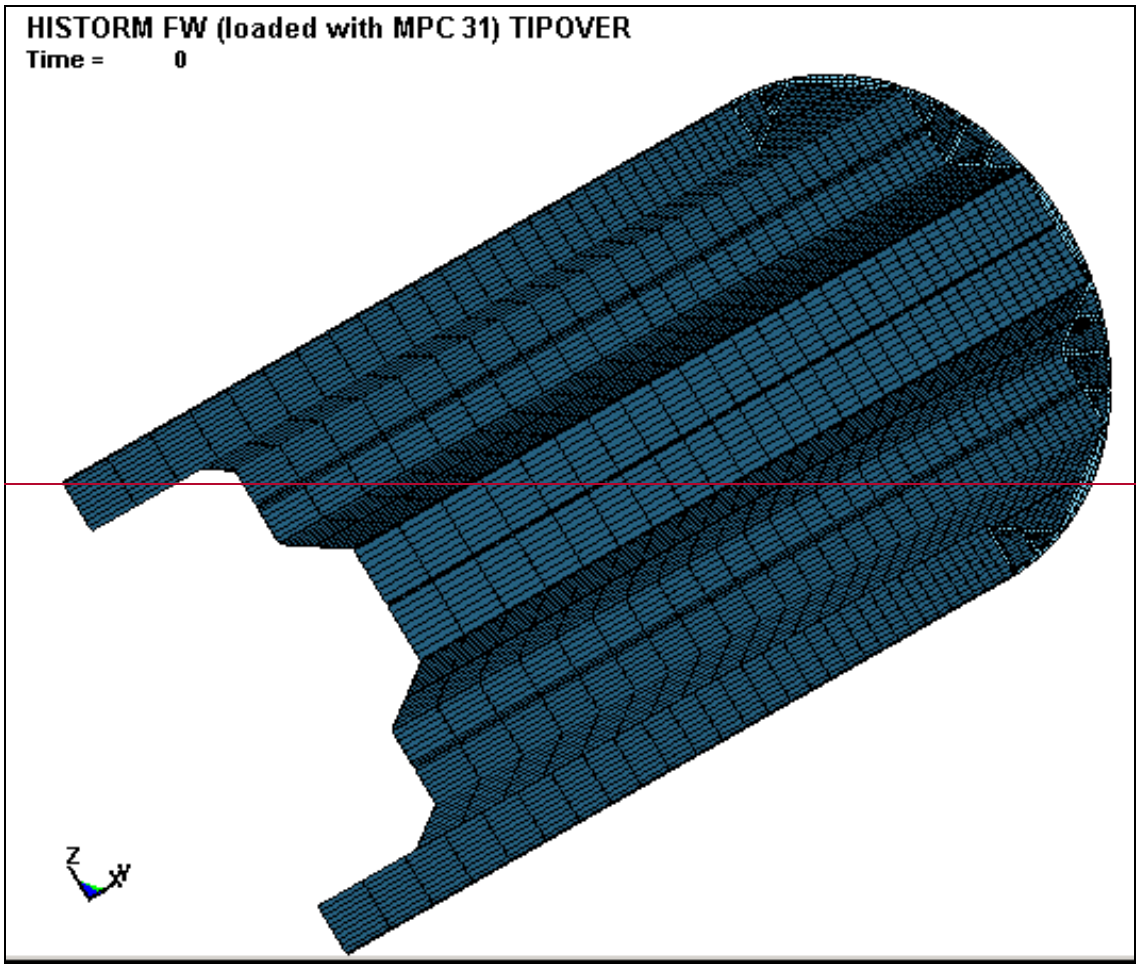

~~Figure 3.4.14D: LS-DYNA Model – MPC-31C Fuel Basket Shims~~

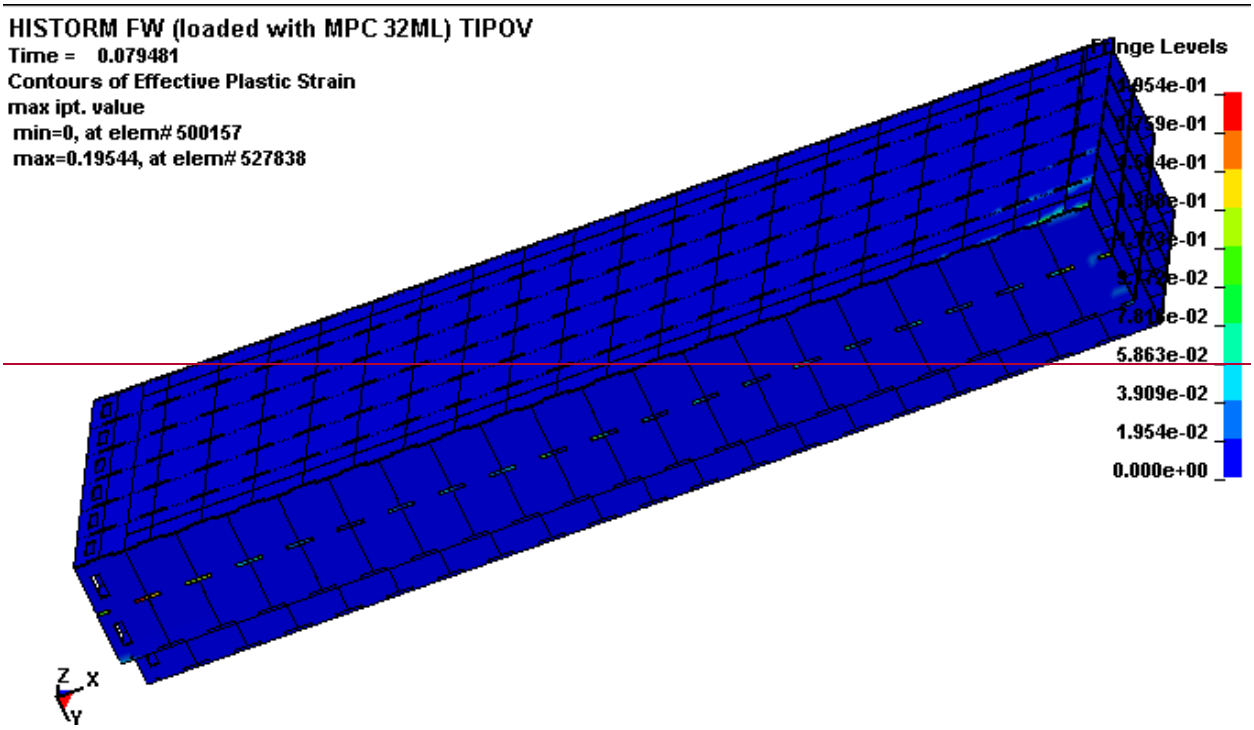
HISTORM FW (loaded with MPC 32ML) TIPOV
Time = 0.079481
Contours of Effective Plastic Strain
max ipt. value
min=0, at elem# 500157
max=0.19544, at elem# 527838
Fringe Levels
5.863e-02
3.909e-02
1.954e-02
0.000e+00
Z
X
Y

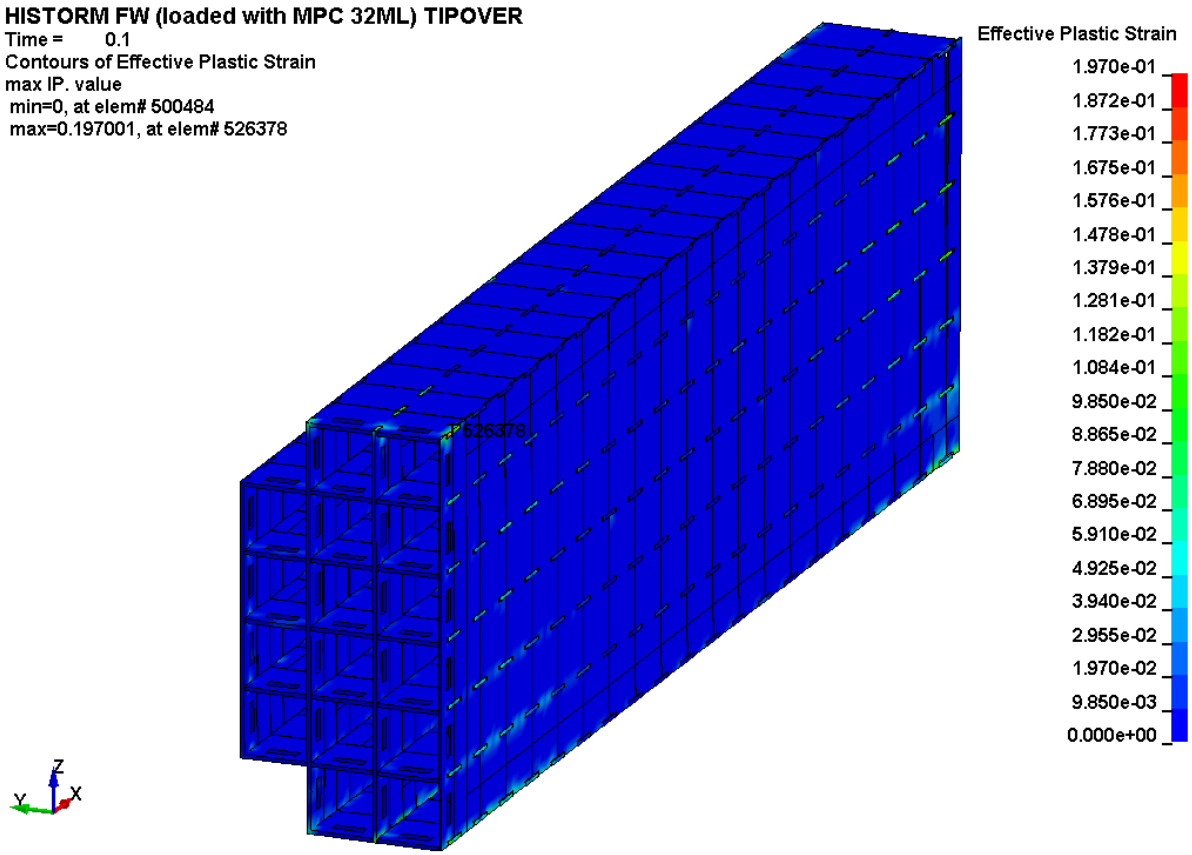
HISTORM FW (loaded with MPC 32ML) TIPOVER
Time = 0.1
Contours of Effective Plastic Strain
max IP. value
min=0, at elem# 500484
max=0.197001, at elem# 526378
Effective Plastic Strain
1.970e-01
1.872e-01
1.773e-01
1.675e-01
1.576e-01
1.478e-01
1.379e-01
1.281e-01
1.182e-01
1.084e-01
9.850e-02
8.865e-02
7.880e-02
6.895e-02
5.910e-02
4.925e-02
3.940e-02
2.955e-02
1.970e-02
9.850e-03
0.000e+00
Z
Y
X

Figure 3.4.15C: Maximum Plastic Strain – MPC-32ML Fuel Basket

HOLTEC INTERNATIONAL COPYRIGHTED MATERIAL

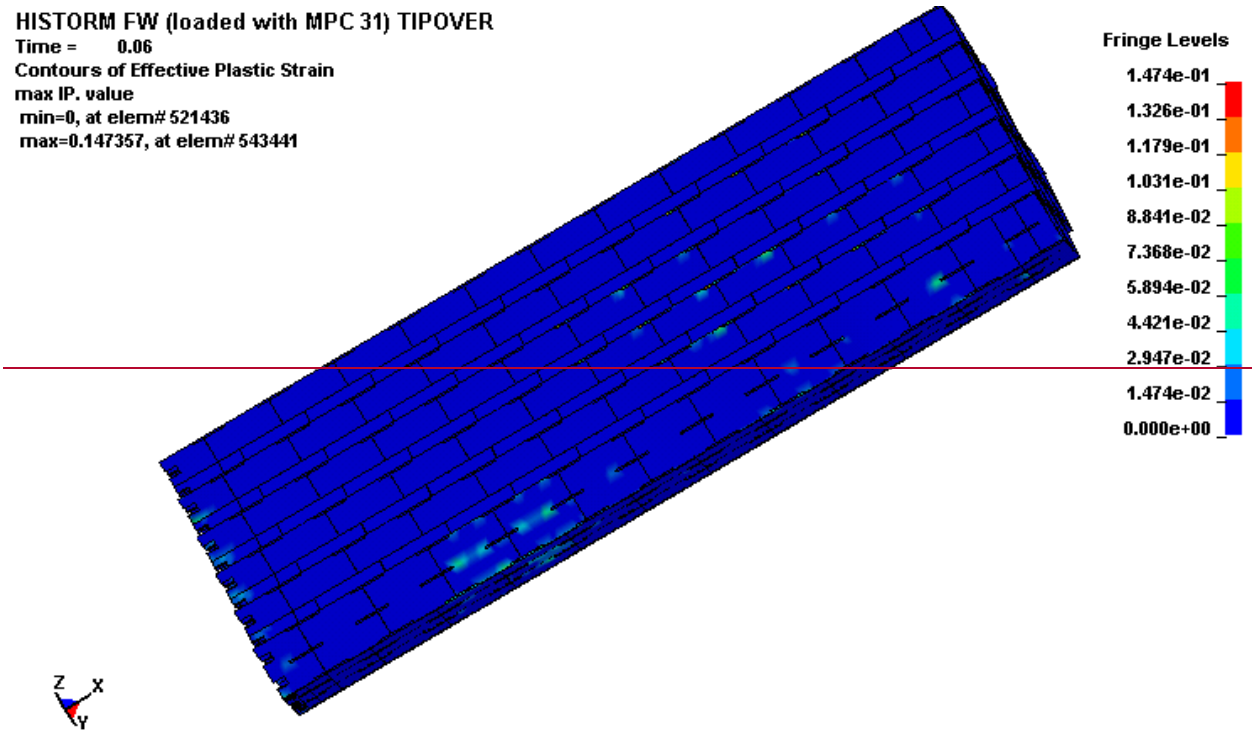

~~Figure 3.4.15D: Maximum Plastic Strain – MPC-31C Fuel Basket~~

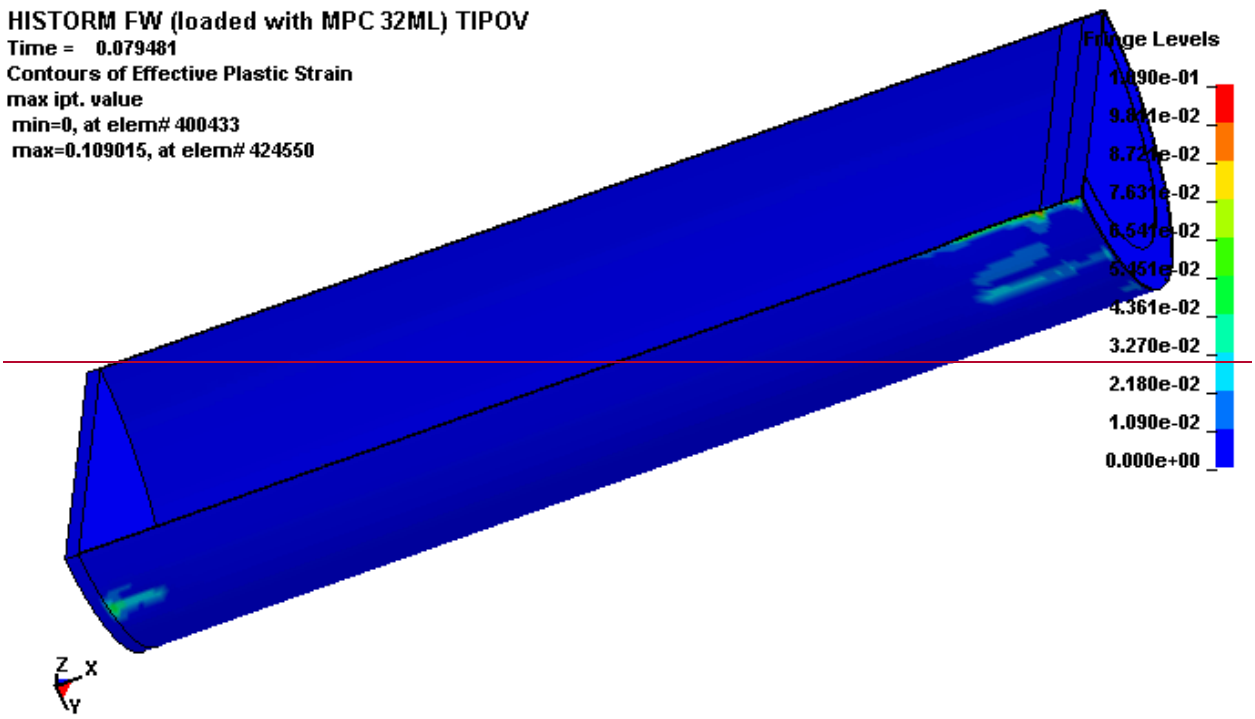
HISTORM FW (loaded with MPC 32ML) TIPOV
Time = 0.079481
Contours of Effective Plastic Strain
max ipt. value
min=0, at elem# 400433
max=0.109015, at elem# 424550
Fringe Levels
1.090e-01
9.814e-02
8.724e-02
7.631e-02
6.541e-02
5.451e-02
4.361e-02
3.270e-02
2.180e-02
1.090e-02
0.000e+00
Z
X
Y

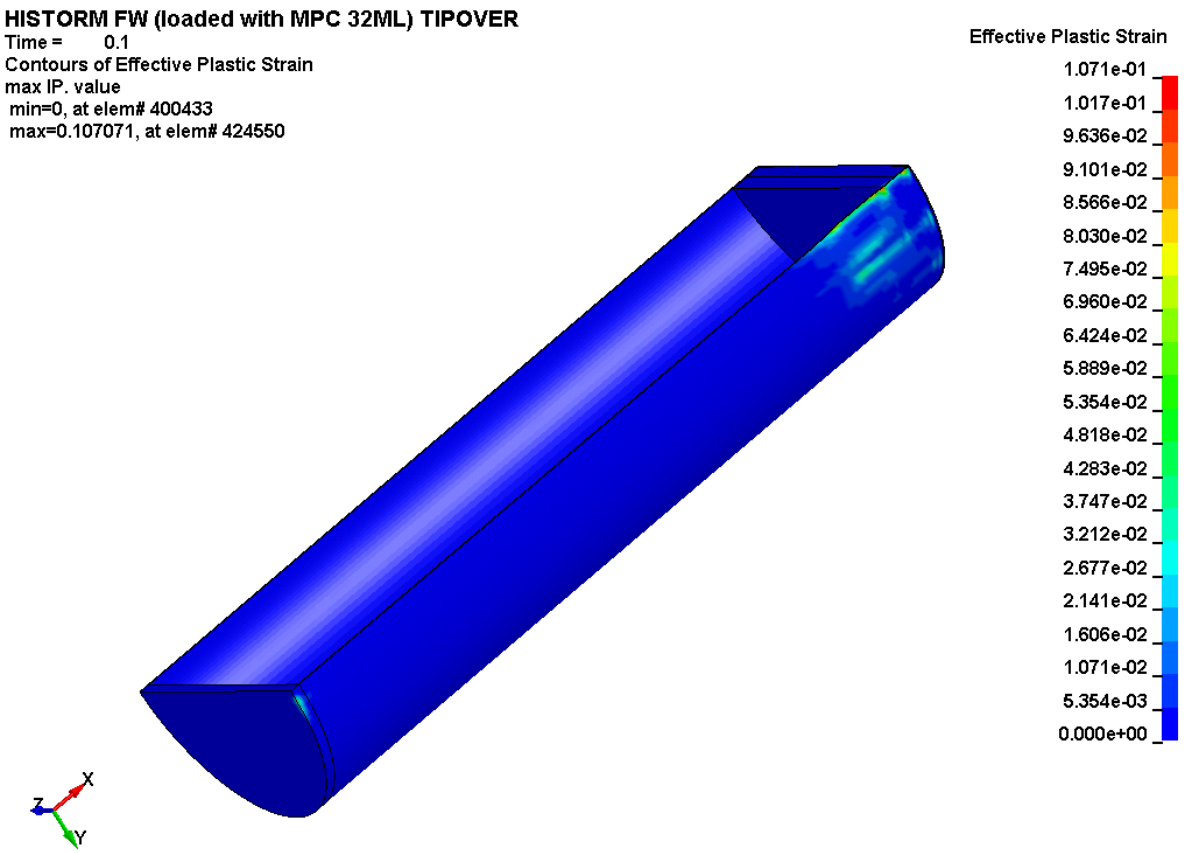

Figure 3.4.16C: Maximum Plastic Strain – MPC-32ML Enclosure Vessel

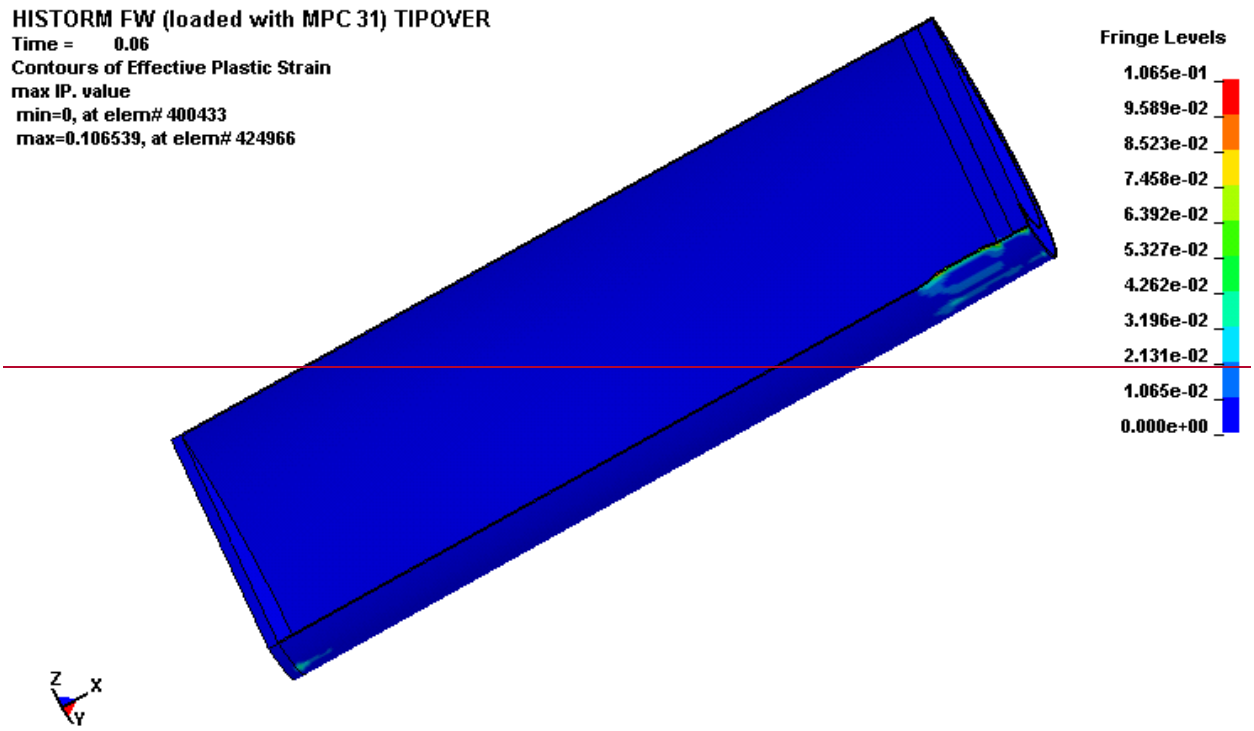

~~Figure 3.4.16D: Maximum Plastic Strain – MPC-31C Enclosure Vessel~~

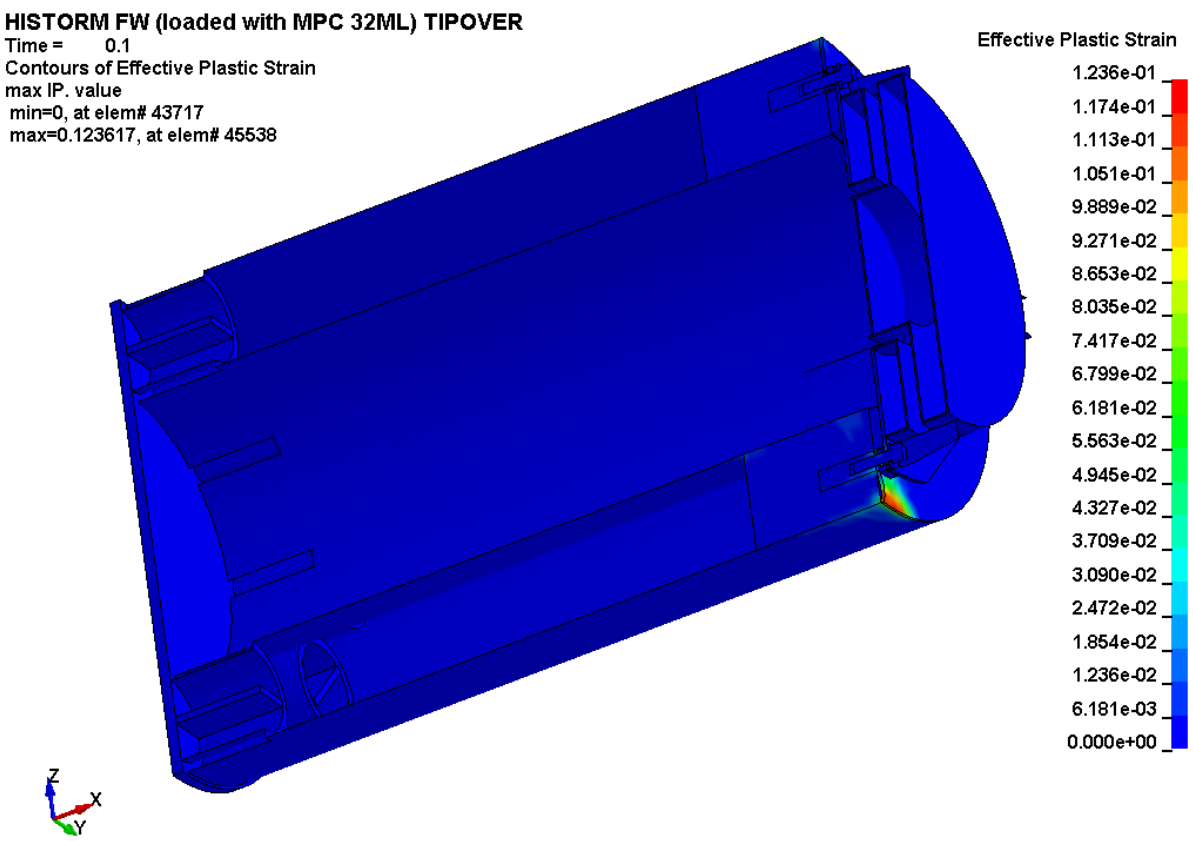

Figure 3.4.17C: Maximum Plastic Strain – HI-STORM FW Overpack
(for MPC-32ML, Excluding MPC Guide Tubes)

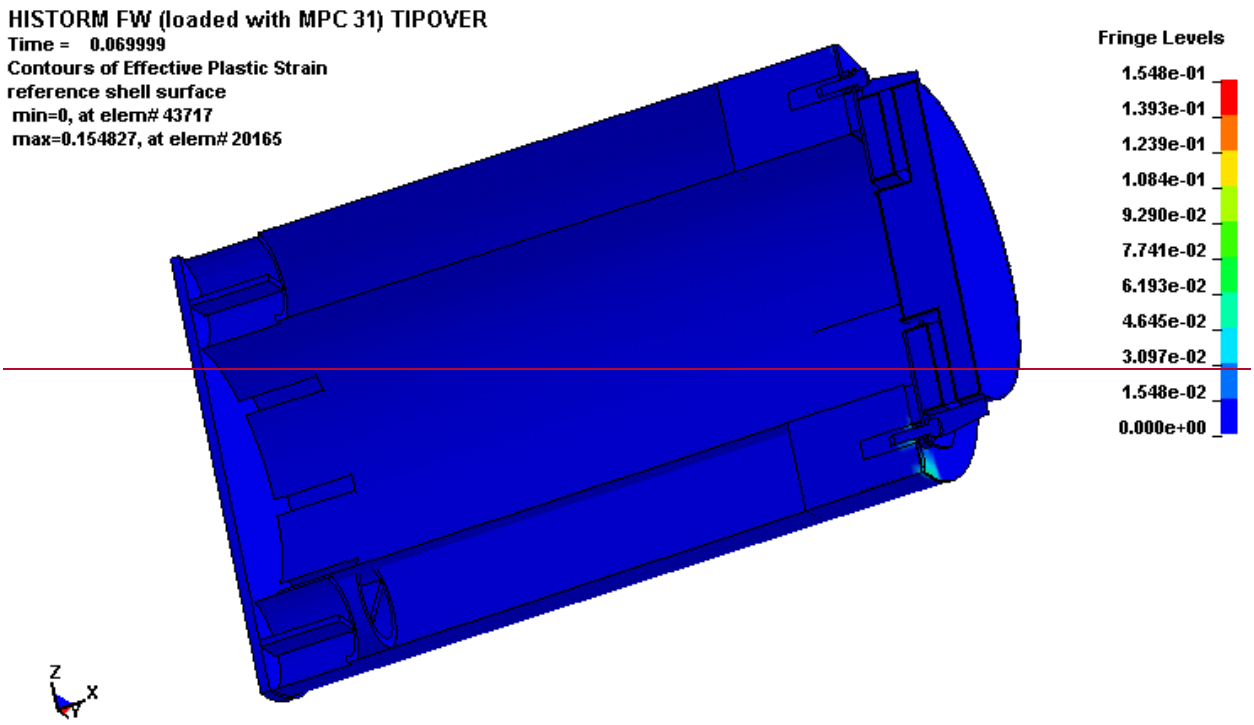

~~Figure 3.4.17D: Maximum Plastic Strain – HI-STORM FW Overpack (for MPC-31C, Excluding MPC Guide Tubes)~~

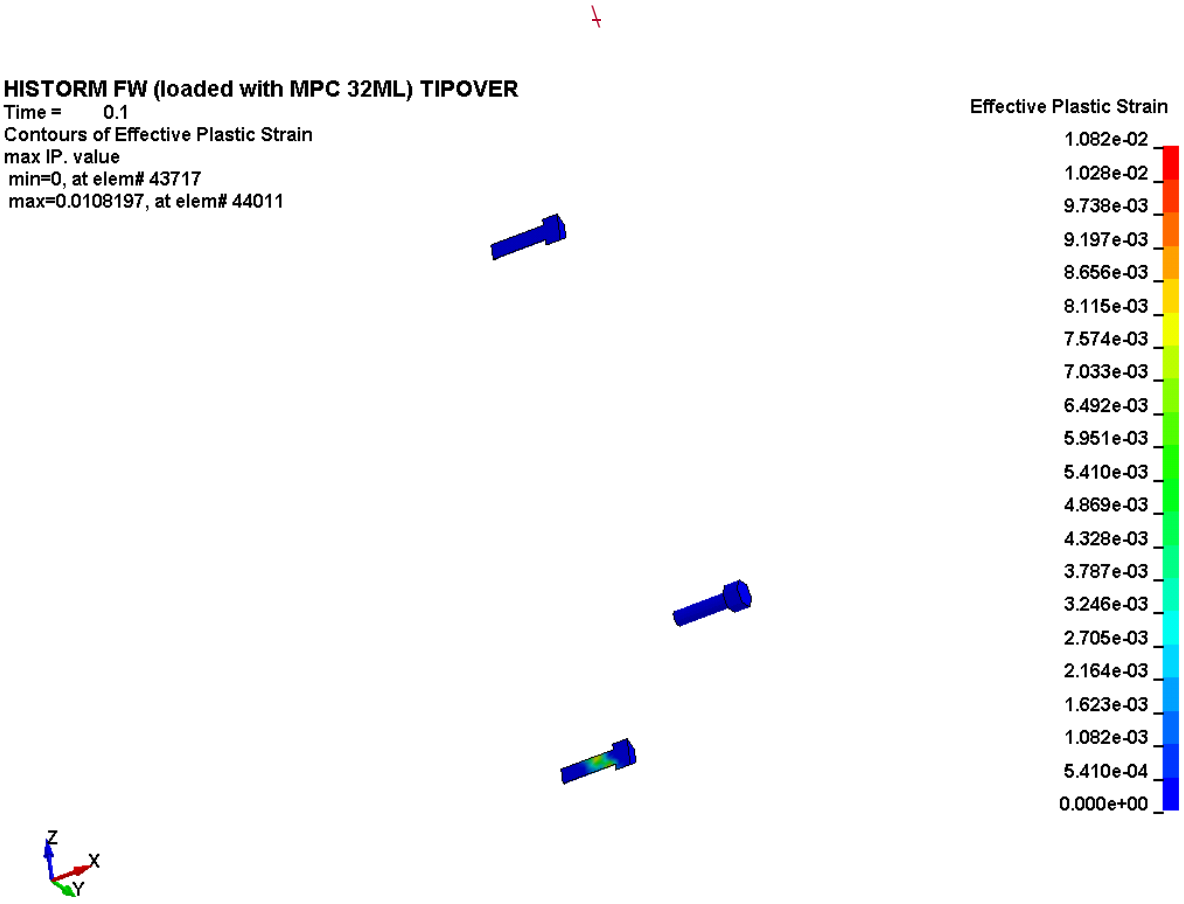

Figure 3.4.18C: Maximum Plastic Strain –
HI-STORM FW Overpack (for MPC-32ML) Closure Lid Bolts

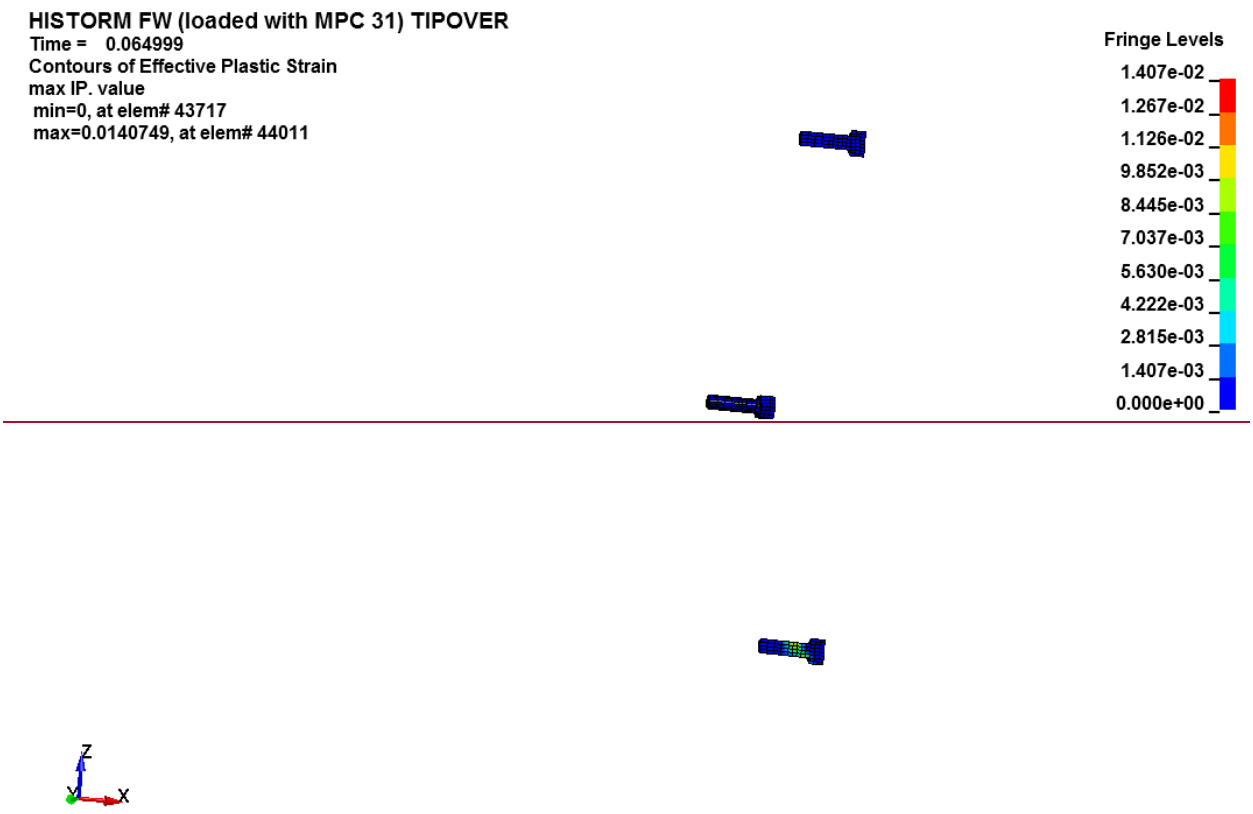

~~Figure 3.4.18D: Maximum Plastic Strain –~~
~~HI-STORM FW Overpack (for MPC-31C) Closure Lid Bolts~~

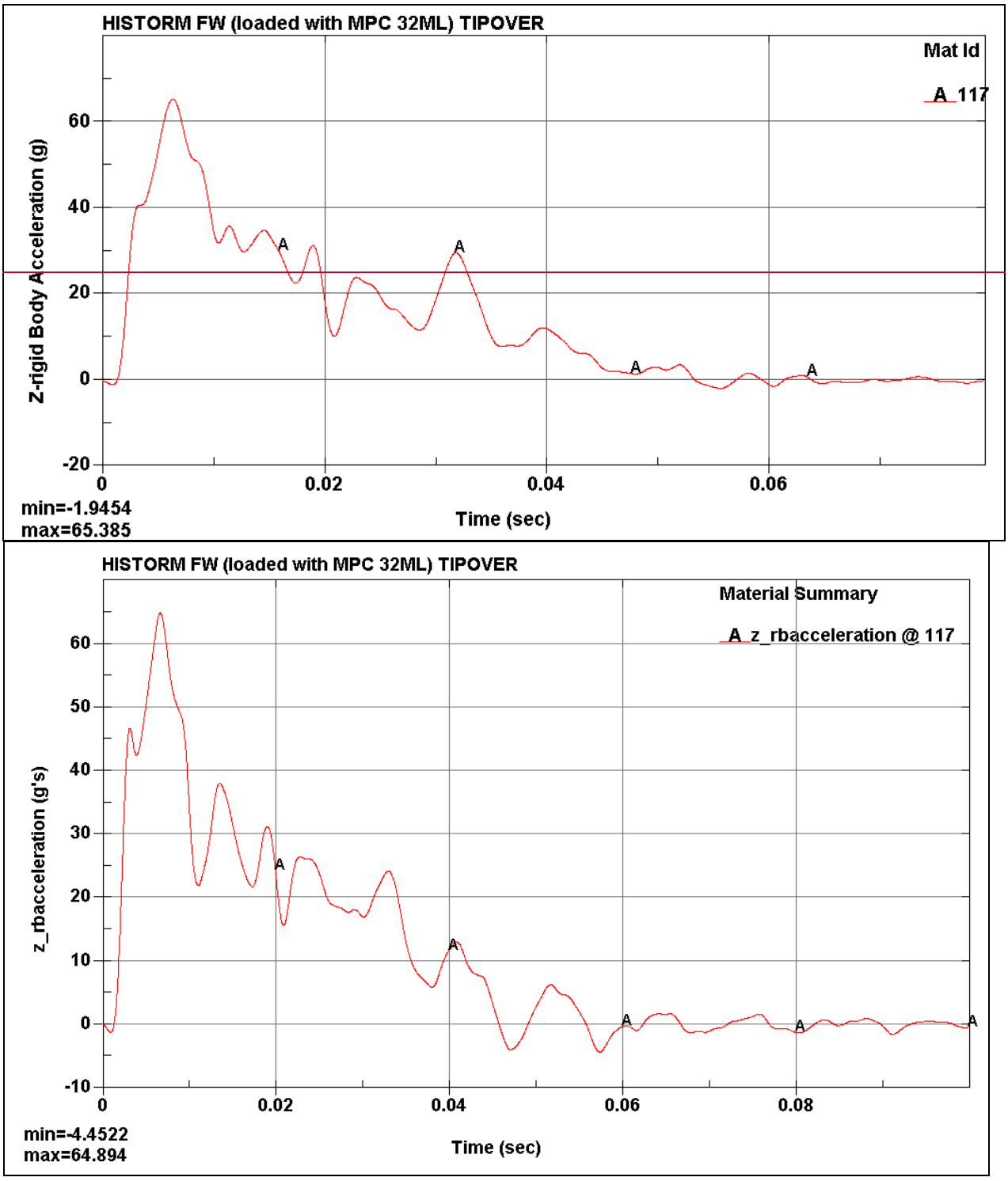

Figure 3.4.19C: Vertical Rigid Body Deceleration Time History – Cask Lid Concrete (for HI-STORM FW Loaded with MPC-32ML)

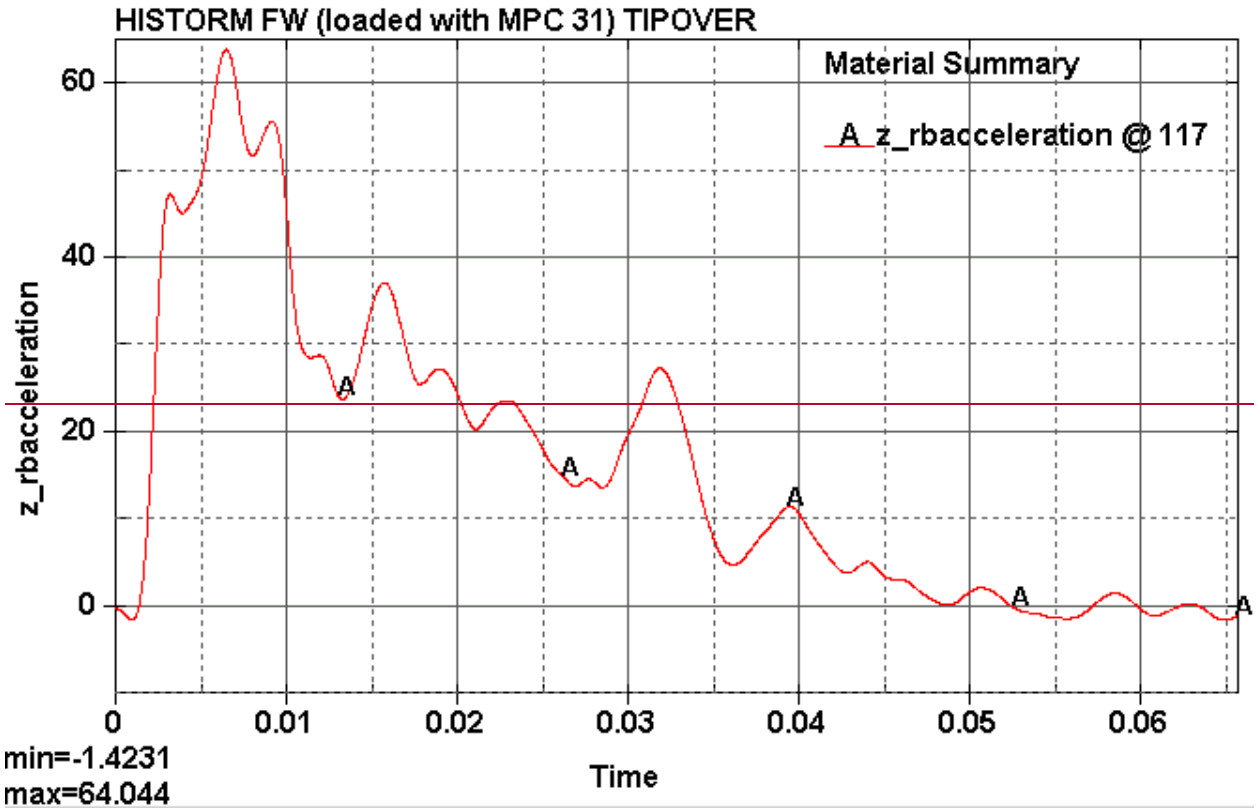

~~Figure 3.4.19D: Vertical Rigid Body Deceleration Time History – Cask Lid Concrete (for HI-STORM FW Loaded with MPC-31C)~~

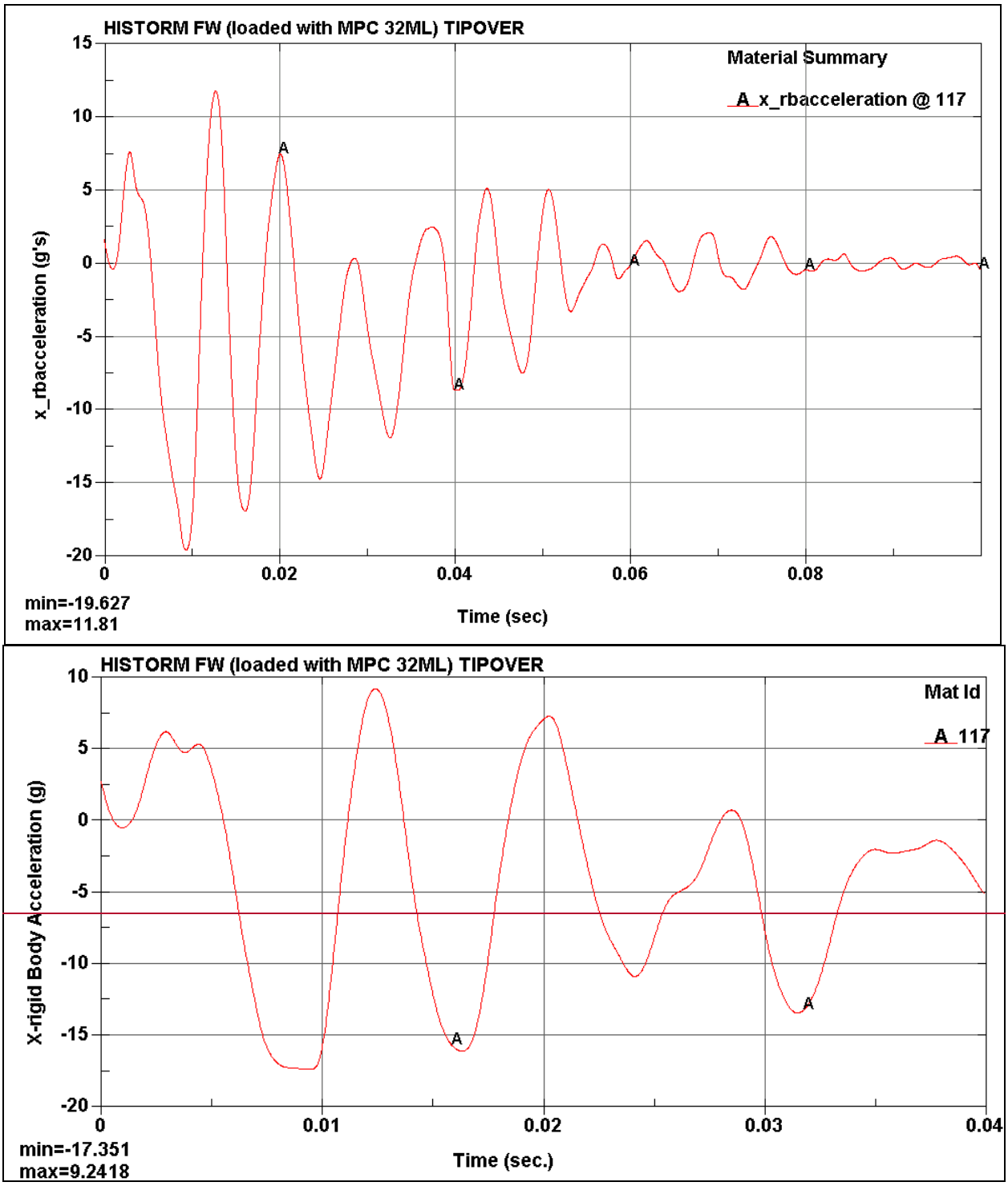

Figure 3.4.20C: Horizontal Rigid Body Deceleration Time History – Cask Lid Concrete (for HI-STORM FW Loaded with MPC-32ML)

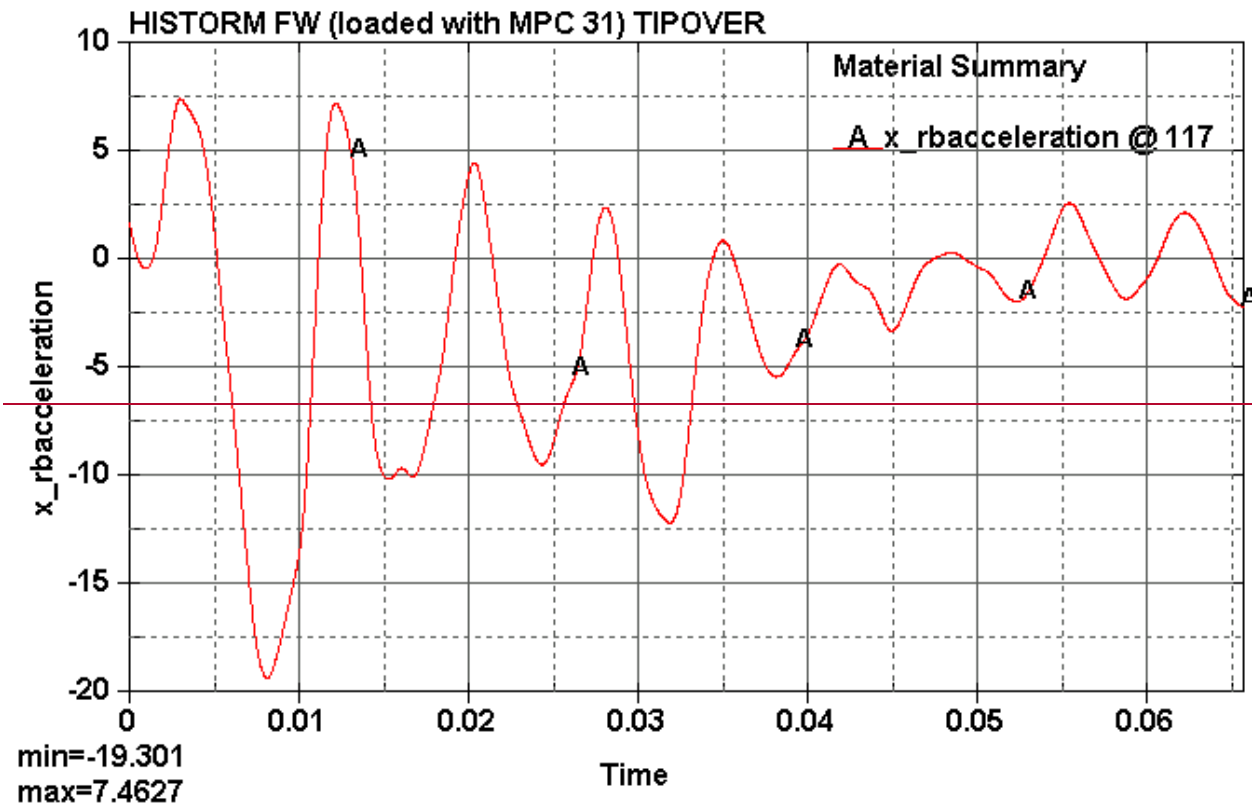

~~Figure 3.4.20D: Horizontal Rigid Body Deceleration Time History – Cask Lid Concrete (for HI-STORM FW Loaded with MPC-31C)~~

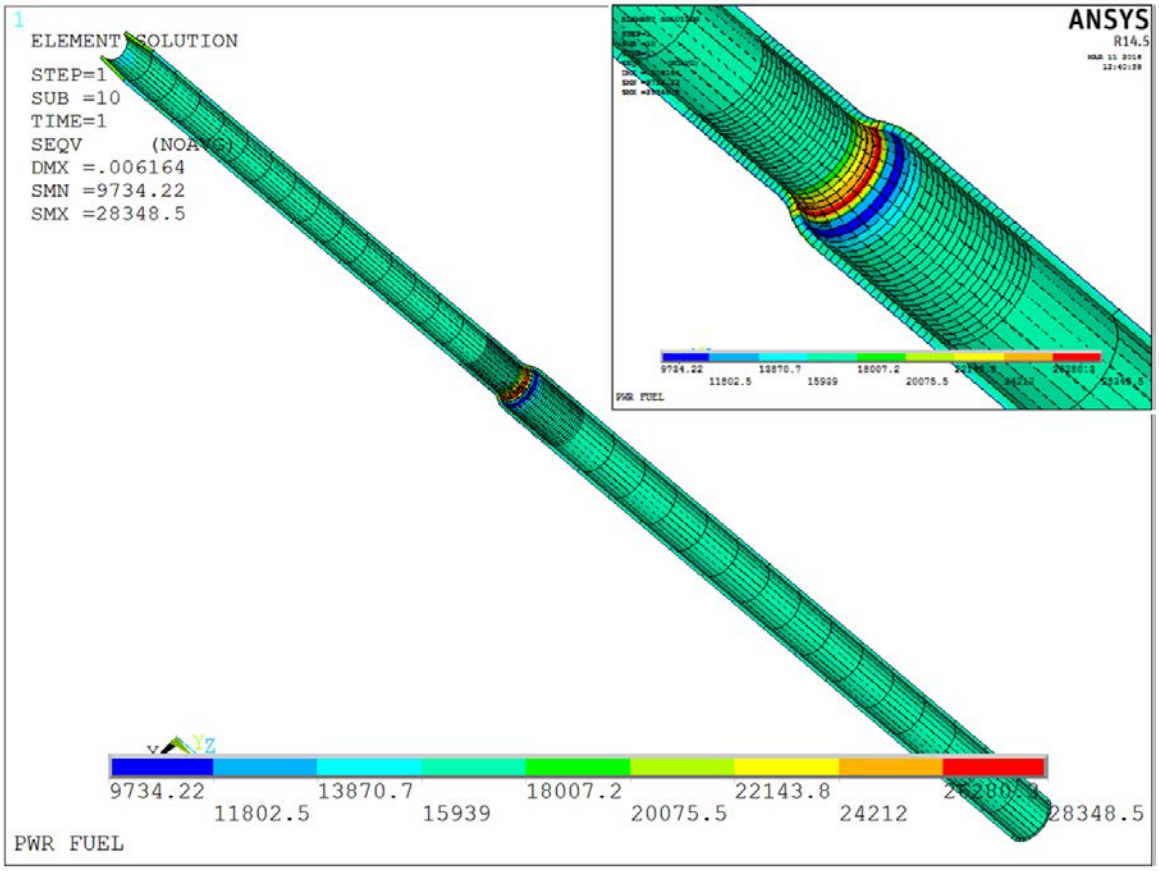

Figure 3.4.42: Stress Distribution in Fuel Rod Due to MPC Reflood (Load Case 11) – For MPC-32ML Fuel Type

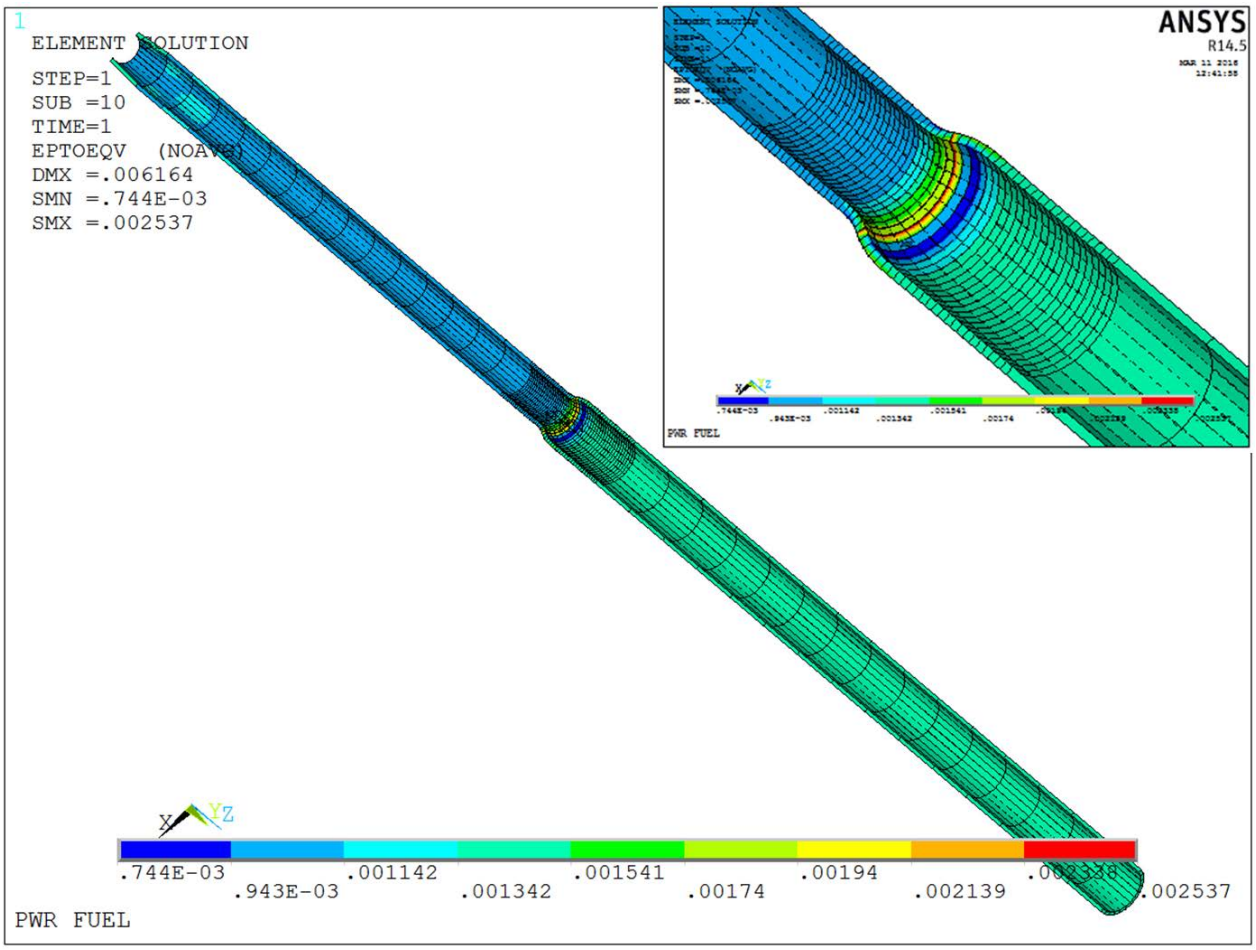

Figure 3.4.43: Strain Distribution in Fuel Rod Due to MPC Reflood (Load Case 11) – For MPC-32ML Fuel Type

3.8 REFERENCES

[3.1.1] NUREG-0612, "Control of Heavy Loads at Nuclear Power Plants," United States Nuclear Regulatory Commission.

[3.1.2] ANSI N14.6-1993, "American National Standard for Special Lifting Devices for Shipping Containers Weighing 10000 Pounds (4500 kg) or More for Nuclear Materials," American National Standards Institute, Inc.

[3.1.3] D. Burgreen, “Design Methods for Power Plant Structures”, Arcturus Publishers, 1975.

[3.1.4] HI-STORM 100 FSAR, Holtec Report No. HI-2002444, Revision 7 [USNRC Docket 72-1014].

[3.1.5] NUREG/CR-1815, “Recommendations for Protecting Against Failure by Brittle Fracture in Ferritic Steel Shipping Containers Up to Four Inches Thick”

[3.1.6] Aerospace Structural Metals Handbook, Manson.

[3.1.7] SHAKE2000, A Computer Program for the 1-D Analysis of Geotechnical Earthquake Engineering Problems, G.A. Ordonez, Dec. 2000.

[3.1.8] LS-DYNA, Version 971, Livermore Software Technology, 2006.

[3.1.9] "Construction of True-Stress-True-Strain Curves for LS-DYNA Simulations," Holtec Proprietary Position Paper DS-307, Revision 2.*

[3.1.10] HI-STAR 180 SAR, Holtec Report No. HI-2073681, Revision 3 [USNRC Docket 71-9325].

[3.3.1] ASME Boiler & Pressure Vessel Code, Section II, Part D, 2007.

[3.3.2] HI-STAR 60 SAR, Holtec Report No. HI-2073710, Revision 2 [USNRC Docket 71-9336].

[3.3.3] Properties of Aluminum Alloys, Tensile, Creep, and Fatigue Data at High and Low Temperatures, ASM International, November 2006.

* Supporting document submitted with the HI-STORM FW License Application (Docket 72-1032).

[3.3.4] Holtec Proprietary Report HI-2043162, “Spent Fuel Storage Expansion at Diablo Canyon Power Plant for Pacific Gas and Electric Co.”, Revision 1 (USNRC Docket Nos. 50-275 and 50-323).

[3.3.5] American Concrete Institute, ACI-318-05.

[3.3.6] American Concrete Institute, "Code Requirements for Nuclear Safety Related Structures" (ACI-349-85) and Commentary (ACI-349R-85).

[3.3.7] J.H. Evans, "Structural Analysis of Shipping Casks, Volume 8, Experimental Study of Stress-Strain Properties of Lead Under Specified Impact Conditions", ORNL/TM-1312, Vol. 8, ORNL, Oak Ridge, TN, August, 1970.

[3.3.8] ASTM Specification B221M-07, “Standard Specification for Aluminum and Aluminum-Alloy Extruded Bars, Rods, Wire, Profiles, and Tubes (Metric)”.

[3.4.1] ANSYS 11.0, ANSYS, Inc., 2007.

[3.4.2] ASME Boiler & Pressure Vessel Code, Section III, Subsection NF, 2007.

[3.4.3] ASME Boiler & Pressure Vessel Code, Section III, Appendices, 2007.

[3.4.4] ASME Boiler & Pressure Vessel Code, Section III, Subsection NB, 2007.

[3.4.5] Witte, M., et al., “Evaluation of Low-Velocity Impacts Tests of Solid Steel Billet onto Concrete Pads, and Application to Generic ISFSI Storage Cask for Tipover and Side Drop”, Lawrence Livermore National Laboratory, UCRL-ID-126295, Livermore, California, March 1997.

[3.4.6] Doug Ammerman and Gordon Bjorkman, “Strain-Based Acceptance Criteria for Section III of the ASME Boiler and Pressure Vessel Code”, Proceedings of the 15th International Symposium on the Packaging and Transportation of Radioactive Materials, PATRAM 2007, October 21-26, 2007, Miami, Florida, USA.

[3.4.7] NUREG/CR-6865, “Parametric Evaluation of Seismic Behavior of Freestanding Spent Fuel Dry Storage Systems,” 2005.

[3.4.8] NUREG-0800, “Standard Review Plan for the Review of Safety Analysis Reports for Nuclear Power Plants,” Section No. 3.7.1, 1989.

[3.4.9] Bechtel Topical Report BC-TOP-9A, “Design of Structures for Missile Impact”, Revision 2 (September 1974).

[3.4.10] 10CFR71, Waste Confidence Decision Review, USNRC, September 11, 1990.

[3.4.11] Holtec Proprietary Report HI-2094353, “Analysis of the Non-Mechanistic Tipover Event of the Loaded HI-STORM FW Storage Cask”, Latest Revision.

[3.4.12] Oberg, E. et. al., Machinery’s Handbook, Industrial Press Inc., 27th Edition.

[3.4.13] Holtec Proprietary Report HI-2094418, “Structural Calculation Package for HI-STORM FW System”, Latest Revision.

[3.4.14] EPRI NP-440, Full Scale Tornado Missile Impact Tests, 1977.

[3.4.15] Holtec Proprietary Report HI-2094392, “Tornado Missile Analysis for HI-STORM FW System”, Latest Revision.

[3.4.16] Young, W., Roark’s Formulas for Stress & Strain, McGraw Hill Book Company, 6th Edition.

[3.4.17] Interim Staff Guidance - 15, “Materials Evaluation”, Revision 0.

[3.4.18] Timoshenko, S., Strength of Materials (Part II), Third Edition, 1958.

[3.4.19] “Mechanical Testing and Evaluation”, ASM Handbook, Volume 8, 2000.

[3.4.20] Adkins, H.E., Koeppel, B.J., Tang, D.T., “Spent Nuclear Fuel Structural Response When Subject to an End Drop Impact Accident,” Proceedings ASME/JSME Pressure Vessels and Piping Conference, PVP-Vol. 483, American Society of Mechanical Engineers, New York, New York, 2004.

[3.4.21] Chun, R., Witte, M., Schwartz, M., "Dynamic Impact Effects on Spent Fuel Assemblies", Lawrence Livermore National Laboratory, Report UCID-21246, 1987.

[3.4.22] Rust, J.H., Nuclear Power Plant Engineering, Haralson Publishing Company, 1979.

[3.4.23] NUREG/CR-1864, “A Pilot Probabilistic Risk Assessment of a Dry Cask Storage System at a Nuclear Power Plant”, USNRC, Washington D.C., 2007.

[3.4.24] EPRI TR-103949, “Temperature Limit Determination for the Inert Dry Storage of Spent Nuclear Fuel”, May 1994.

[3.4.25] Holtec Proprietary Report HI-2166998, “Analysis of the Non-Mechanistic Tipover Event of the Loaded HI-STORM FW Storage Cask Loaded with MPC-32ML and MPC-31C”, Latest Revision.

[3.6.1] Visual Nastran 2004, MSC Software, 2004.

compliance with ISG-11 and with NUREG-1536 guidelines, subject to the exceptions and clarifications discussed in Chapter 1, Table 1.0.3.

As explained in Section 1.2, the storage of SNF in the fuel baskets in the HI-STORM FW system is configured for a three-region storage system under regionalized storage and uniform storage. Figures 1.2.1a, 1.2.1b~~, 1.2.1c~~ and 1.2.2 provide the information on the location of the regions and Tables 1.2.3a, 1.2.3b~~, 1.2.3c~~ and 1.2.4 provide the permissible specific heat load (heat load per fuel assembly) in each region for the PWR and BWR MPCs, respectively. The Specific Heat Load (SHL) values under regionalized storage are defined for two patterns that in one case maximizes ALARA (Table 1.2.3a, Pattern A and Table 1.2.4) and in the other case maximizes heat dissipation (Table 1.2.3a, Pattern B). The ALARA maximized fuel loading is guided by the following considerations:

- Region 1: Located in the core region of the basket is permitted to store fuel with medium specific heat load.
- Region 2: This is the intermediate region flanked by the core region (Region I) from the inside and the peripheral region (Region III) on the outside. This region has the maximum SHL in the basket.
- Region 3: Located in the peripheral region of the basket, this region has the smallest SHL. Because a low SHL means a low radiation dose emitted by the fuel, the low heat emitting fuel around the periphery of the basket serves to block the radiation from the Region II fuel, thus reducing the total quantity of radiation emanating from the MPC in the lateral direction.

Thus, the 3-region arrangement defined above serves to minimize radiation dose from the MPC and peak cladding temperatures mitigated by avoiding placement of hot fuel in the basket core.

To address the needs of cask users having high heat load fuel inventories, fuel loading Pattern B is defined in Table 1.2.3a to maximize heat dissipation by locating hotter fuel in the cold peripheral Region 3 and in this manner minimize cladding temperatures. This has the salutary effect of minimizing core temperature gradients in the radial direction and thermal stresses in the fuel and fuel basket.

The salutary consequences of all regionalized loading arrangements become evident from the computed peak cladding temperatures in this chapter, which show margin to the ISG-11 limit discussed earlier.

The safety analyses summarized in this chapter demonstrate acceptable margins to the allowable limits under all design basis loading conditions and operational modes. Minor changes to the design parameters that inevitably occur during the product's life cycle which are treated within the purview of 10CFR72.48 and are ascertained to have an insignificant effect on the computed safety factors may not prompt a formal reanalysis and revision of the results and associated data in the tables of this chapter unless the cumulative effect of all such unquantified changes on the reduction of any of the computed safety margins cannot be deemed to be insignificant. For purposes of this determination, an insignificant loss of safety margin with reference to an

stresses due to restraint on basket periphery thermal growth is eliminated by providing adequate basket-to-canister shell gaps to allow for basket thermal growth during all operational modes.

[

PROPRIETARY INFORMATION WITHHELD PER 10 CFR 2.390

]

The MPCs uniform & regionalized fuel storage scenarios are defined in Figures 1.2.1a, 1.2.1b~~,~~ ~~1.2.1c~~ and 1.2.2 in Chapter 1 and design maximum decay heat loads for storage of zircaloy clad fuel are listed in Tables 1.2.3a, 1.2.3b~~, 1.2.3c~~ and 1.2.4. The axial heat distribution in each fuel assembly is conservatively assumed to be non-uniformly distributed with peaking in the active fuel mid-height region (see axial burnup profiles in Figures 2.1.3 and 2.1.4). Table 4.1.1 summarizes the principal operating parameters of the HI-STORM FW system.

The fuel cladding temperature limits that the HI-STORM FW system is required to meet are discussed in Section 4.3 and given in Table 2.2.3. Additionally, when the MPCs are deployed for storing High Burnup Fuel (HBF) further restrictions during certain fuel loading operations (vacuum drying) are set forth herein to preclude fuel temperatures from exceeding the normal temperature limits. To ensure explicit compliance, a specific term “short-term operations” is defined in Chapter 2 to cover all fuel loading activities. ISG-11 fuel cladding temperature limits are applied for short-term operations.

The HI-STORM FW system (i.e., HI-STORM FW overpack, HI-TRAC VW transfer cask and MPC) is evaluated under normal storage (HI-STORM FW overpack), during off-normal and accident events and during short-term operations in a HI-TRAC VW. Results of HI-STORM FW thermal analysis during normal (long-term) storage are obtained and reported in Section 4.4. Results of HI-TRAC VW short-term operations (fuel loading, on-site transfer and vacuum drying) are reported in Section 4.5. Results of off-normal and accident events are reported in Section 4.6.

Table 4.1.1 HI-STORM FW OPERATING CONDITION PARAMETERS	
Condition	**Value**
MPC Decay Heat, max.	Tables 1.2.3a, 1.2.3b~~, 1.2.3c~~ and 1.2.4
MPC Operating Pressure	Note 1
Normal Ambient Temperature	Table 2.2.2
Helium Backfill Pressure	Table 4.4.8
Note 1: The MPC operating pressure used in the thermal analysis is based on the minimum helium backfill pressure specified in Table 4.4.8 and MPC cavity average temperature.	

Table 4.2.1

SUMMARY OF HI-STORM FW SYSTEM MATERIALS
THERMAL PROPERTY REFERENCES

Material	Emissivity	Conductivity	Density	Heat Capacity
Helium	N/A	Handbook [4.2.2]	Ideal Gas Law	Handbook [4.2.2]
Air	N/A	Handbook [4.2.2]	Ideal Gas Law	Handbook [4.2.2]
Zircaloy	[4.2.3], [4.2.17], [4.2.18], [4.2.7]	NUREG [4.2.17]	Rust [4.2.4]	Rust [4.2.4]
UO_2	Note 1	NUREG [4.2.17]	Rust [4.2.4]	Rust [4.2.4]
Stainless Steel (machined forgings)[Note 2]	Kern [4.2.5]	ASME [4.2.8]	Marks' [4.2.1]	Marks' [4.2.1]
Stainless Steel Plates[Note 3]	ORNL [4.2.11], [4.2.12]	ASME [4.2.8]	Marks' [4.2.1]	Marks' [4.2.1]
Carbon Steel	Kern [4.2.5]	ASME [4.2.8]	Marks' [4.2.1]	Marks' [4.2.1]
Concrete	Note 1	Marks' [4.2.1]	Appendix 1.D of HI-STORM 100 FSAR [4.1.8]	Handbook [4.2.2]
Lead	Note 1	Handbook [4.2.2]	Handbook [4.2.2]	Handbook [4.2.2]
Water	Note 1	ASME [4.2.10]	ASME [4.2.10]	ASME [4.2.10]
Metamic-HT	Test Data Table 1.2.8	Test Data Table 1.2.8	Test Data Table 1.2.8	Test Data Table 1.2.8
Aluminum Alloy 2219	~~Test Data Table 1.2.8~~Note 4	ASM [4.2.19]	ASM [4.2.19]	ASM [4.2.19]

Note 1: Emissivity not reported as radiation heat dissipation from these surfaces is conservatively neglected.

Note 2: Used in the MPC lid.

Note 3: Used in the MPC shell and baseplate.

Note 4: [PROPRIETARY INFORMATION WITHHELD PER 10CFR2.390]

Table 4.2.4

SUMMARY OF MATERIALS SURFACE EMISSIVITY DATA*

Material	**Emissivity**
Zircaloy	0.80
Painted surfaces	0.85
Stainless steel (machined forgings)	0.36
Stainless Steel Plates	0.587**
Carbon Steel	0.66
Metamic-HT***	Table 1.2.8
Extruded Shims (Aluminum Alloy 2219)‡	Table 1.2.9 [PROPRIETARY INFORMATION WITHHELD PER 10CFR2.390]
Solid Shims (Aluminum Alloy)‡	Table 1.2.9

* See Table 4.2.1 for cited references.

** Lower bound value from the cited references in Table 4.2.1.

*** [PROPRIETARY INFORMATION WITHHELD PER 10CFR2.390

]

4.4 THERMAL EVALUATION FOR NORMAL CONDITIONS OF STORAGE

The HI-STORM FW Storage System (i.e., HI-STORM FW overpack and MPC) and HI-TRAC VW transfer cask thermal evaluation is performed in accordance with the guidelines of NUREG-1536 [4.4.1] and ISG-11 [4.1.4]. To ensure a high level of confidence in the thermal evaluation, 3-dimensional models of the MPC, HI-STORM FW overpack and HI-TRAC VW transfer cask are constructed to evaluate fuel integrity under normal (long-term storage), off-normal and accident conditions and in the HI-TRAC VW transfer cask under short-term operation and hypothetical accidents. The principal features of the thermal models are described in this section for HI-STORM FW and Section 4.5 for HI-TRAC VW. Thermal analyses results for the long-term storage scenarios are obtained and reported in this section. The evaluation addresses the design basis thermal loadings defined in Chapter 1, Tables 1.2.3a (MPC-37, Patterns A and B) 1.2.3b (MPC-32ML)~~, 1.2.3c (MPC-31C)~~ and 1.2.4 (MPC-89). Based on these evaluations the limiting thermal loading condition is defined in Subsection 4.4.4 and adopted for evaluation of on-site transfer in the HI-TRAC (Section 4.5) and off-normal and accident events defined in Section 4.6.

4.4.1 Overview of the Thermal Model

As illustrated in the drawings in Section 1.5, the basket is a matrix of interconnected square compartments designed to hold the fuel assemblies in a vertical position under long term storage conditions. The basket is a honeycomb structure of Metamic-HT plates that are slotted and arrayed in an orthogonal configuration to form an integral basket structure. [

PROPRIETARY INFORMATION WITHHELD PER 10CFR2.390

]

Thermal analysis of the HI-STORM FW System is performed for all heat load scenarios defined in Chapter 1 for regionalized storage (Figures 1.2.1a and 1.2.2) and uniform storage (Figure~~s~~ 1.2.1b~~ and 1.2.1c~~). Each fuel assembly is *assumed to be generating heat at the maximum permissible rate (Tables 1.2.3a, 1.2.3b~~, 1.2.3c~~ and 1.2.4)*. While the assumption of limiting heat generation in each storage cell imputes a certain symmetry to the cask thermal problem, it grossly overstates the total heat duty of the system in most cases because it is unlikely that any basket would be loaded with fuel emitting heat at their limiting values in *each* storage cell. Thus, the thermal model for the HI-STORM FW system is inherently conservative for real life applications. Other noteworthy features of the thermal analyses are:

i. While the rate of heat conduction through metals is a relatively weak function of temperature, radiation heat exchange increases rapidly as the fourth power of absolute temperature.

ii. Heat generation in the MPC is axially non-uniform due to non-uniform axial burnup profiles in the fuel assemblies.

iii. Inasmuch as the transfer of heat occurs from inside the basket region to the outside, the temperature field in the MPC is spatially distributed with the lowest values reached at the periphery of the basket.

As noted in Chapter 1 and in Section 3.2, the height of the PWR MPC cavity can vary within a rather large range to accommodate spent nuclear fuel of different lengths in the MPC-37 and MPC-89[1]. The heat load limits in Table 1.2.3 (PWR MPC) and Table 1.2.4 (BWR MPC) for regionalized storage are, however, fixed regardless of the fuel (and hence MPC cavity) length. Because it is not a'priori obvious whether the shortest or the longest fuel case will govern, thermal analyses are performed for the minimum[2], reference and maximum height MPCs. Table 2.1.1 allows two different fuel assembly lengths under "minimum" category for PWR fuel. Unless specified in this chapter, the term "minimum" or "short" is used for all short fuel assembly arrays except 15x15I short fuel defined in Chapter 2.

4.4.1.1 Description of the 3-D Thermal Model

i. Overview

The HI-STORM FW System is equipped with four~~two~~ MPC designs, MPC-37, MPC-32ML, MPC-31C and MPC-89 engineered to store 37, 32~~, 31~~ PWR and 89~~ PWR and~~ BWR fuel assemblies respectively. The interior of the MPC is a 3-D array of square shaped cells inside an irregularly shaped basket outline confined inside the cylindrical space of the MPC cavity. To ensure an adequate representation of these features, a 3-D geometric model of the MPC is constructed using the FLUENT CFD code pre-processor [4.1.2]. Because the fuel basket is made of a single isotropic material (Metamic-HT), the 3-D thermal model requires no idealizations of the fuel basket structure. However, since it is impractical to model every fuel rod in every stored fuel assembly explicitly, the cross-section bounded by the inside of the storage cell (inside of the fuel channel in the case of BWR MPCs), which surrounds the assemblage of fuel rods and the interstitial helium gas (also called the "rodded region"), is replaced with an "equivalent" square ~~or hexagonal (MPC-31C)~~ homogeneous section characterized by an effective thermal conductivity. Homogenization of the cell cross-section is discussed under item (ii) below. For thermal-hydraulic simulation, each fuel assembly in its storage cell is represented by an equivalent porous medium. For BWR fuel, the presence of the fuel channel divides the storage cell space into two distinct axial flow regions, namely, the in-channel (rodded) region and the square prismatic annulus region (in the case of PWR fuel this modeling complication does not exist). The methodology to represent the spent fuel storage space as a homogeneous region with equivalent conductivities is identical to that used in the HI-STORM 100 Docket No. 72-1014 [4.1.8].

1 MPC-32ML and MPC-31C are fixed fuel length canisters for storing a specific fuel defined in Table 2.1.1b.
2 Both allowable PWR fuel assembly lengths under "minimum" category as shown in Table 2.1.1 are evaluated in this chapter.

ii. Details of the 3-D Model

The HI-STORM FW fuel basket is modeled in the same manner as the model described in the HI-STAR 180 SAR (NRC Docket No. 71-9325) [4.1.11]. Modeling details are provided in the following:

Fuel Basket 3D Model

The MPC-37, MPC-32ML and MPC-89 fuel baskets are essentially an array of square cells ~~and MPC-31C hexagonal cells~~ within an irregularly shaped basket outline. The fuel basket is confined inside a cylindrical cavity of the MPC shell. Between the fuel basket-to-shell spaces, thick Aluminum basket shims are installed to facilitate heat dissipation. To ensure an adequate representation of the fuel basket a geometrically accurate 3D model of the array of square cells and Metamic-HT plates is constructed using the FLUENT pre-processor. Other than the representation of fuel assemblies inside the storage cell spaces as porous region with effective thermal-hydraulic properties as described in the next paragraph, the 3D model includes an explicit articulation of other canister parts. The basket shims are explicitly modeled in the peripheral spaces. The fuel basket is surrounded by the MPC shell and outfitted with a solid welded lid above and a baseplate below. All of these physical details are explicitly articulated in a quarter-symmetric 3D thermal model of the HI-STORM FW as shown in Figures 4.4.2a, 4.4.2b~~, 4.4.2c~~ and 4.4.3.

Fuel Region Effective Planar Conductivity

In the HI-STORM FW thermal modeling, the cross section bounded by the inside of a PWR storage cell and the channeled area of a BWR storage cell is replaced with an "equivalent" square section characterized by an effective thermal conductivity in the planar and axial directions. Figure 4.4.1 pictorially illustrates this concept. The two conductivities are unequal because while in the planar direction heat dissipation is interrupted by inter-rod gaps; in the axial direction heat is dissipated through a continuous medium (fuel cladding). The equivalent planar conductivity of the storage cell space is obtained using a 2D conduction-radiation model of the bounding PWR and BWR fuel storage scenarios defined in the table below. The fuel geometry, consisting of an array of fuel rods with helium gaps between them residing in a storage cell, is constructed using QA validated computer codes~~the~~ (ANSYS code [4.1.1] and FLUENT[1] [4.1.2]) and lowerbound conductivities under the assumed condition of stagnant helium (no-helium-flow-condition) are obtained. In the axial direction, an area-weighted average of the cladding and helium conductivities is computed. Axial heat conduction in the fuel pellets is conservatively ignored.

The effective fuel conductivity is computed under four bounding fuel storage configurations for PWR fueled MPC-37, ~~one each~~ MPC-32ML ~~and MPC-31C~~ for specific PWR fuel and one bounding scenario for BWR fueled MPC-89. The fuel storage configurations are defined below:

[1] NRC has accepted FLUENT code for evaluation of fuel conductivities in the HI-STAR 180D licensing (Docket No. 71-9367).

Storage Scenario	MPC	Fuel
PWR: 15x15I Short Fuel	Minimum Height MPC-37 for 15x15I fuel assembly array	15x15I in Table 2.1.2
PWR: Short Fuel	Minimum Height MPC-37 for all fuel assembly arrays except 15x15I	14x14 Ft. Calhoun
PWR: Standard Fuel	Reference Height MPC-37	W-17x17
PWR: XL Fuel	Maximum Height MPC-37	AP1000
PWR: 16x16D	MPC-32ML	16x16D
~~PWR: V10A/V10B~~	~~MPC-31C~~	~~VVER 1000~~
BWR	MPC-89	GE-10x10

The fuel region effective conductivity is defined as the calculated equivalent conductivity of the fuel storage cell due to the combined effect of conduction and radiation heat transfer in the manner of the approach used in the HI-STORM 100 system (Docket No. 72-1014). Because radiation is proportional to the fourth power of absolute temperature, the effective conductivity is a strong function of temperature. ~~The~~ ANSYS and FLUENT computer codes~~finite element model~~ have been~~is~~ used to characterize fuel resistance at several representative storage cell temperatures and the effective thermal conductivity as a function of temperature obtained for all storage configurations defined above and tabulated in Table 4.4.1.

Heat Rejection from External Surfaces

The exposed surfaces of the HI-STORM FW dissipate heat by radiation and external natural convection heat transfer. Radiation is modeled using classical equations for radiation heat transfer (Rohsenow & Hartnett [4.2.2]). Jakob and Hawkins [4.2.9] recommend the following correlations for natural convection heat transfer to air from heated vertical and horizontal surfaces:

Turbulent range:

$$h = 0.19(\Delta T)^{1/3} \text{ (Vertical, } GrPr > 10^9)$$

$$h = 0.18(\Delta T)^{1/3} \text{ (Horizontal Cylinder, } GrPr > 10^9)$$

(in conventional U.S. units)

Laminar range:

$$h = 0.29\left(\frac{\Delta T}{L}\right)^{1/4} \text{ (Vertical, } GrPr < 10^9)$$

$$h = 0.27\left(\frac{\Delta T}{D}\right)^{1/4} \text{ (Horizontal Cylinder, } GrPr < 10^9)$$

(in conventional U.S. Units)

a) The fuel storage spaces are modeled as porous media having effective thermal-hydraulic properties.

b) In the case of BWR MPC-89, the fuel bundle and the small surrounding spaces inside the fuel "channel" are replaced by an equivalent porous media having the flow impedance properties computed using a conservatively articulated 3-D CFD model [4.4.2]. The space between the BWR fuel channel and the storage cell is represented as an open flow annulus. The fuel channel is also explicitly modeled. The channeled space within is also referred to as the "rodded region" that is modeled as a porous medium. The fuel assembly is assumed to be positioned coaxially with respect to its storage cell. The MPC-89 storage cell occupied with channeled BWR fuel is shown in Figure 4.4.4.

   In the case of the PWR CSF, the porous medium extends to the entire cross-section of the storage cell. As described in [4.4.2], the CFD models for both the BWR and PWR storage geometries are constructed for the Design Basis fuel defined in Table 2.1.4. The model contains comprehensive details of the fuel which includes grid straps, BWR water rods and PWR guide and instrument tubes (assumed to be plugged for conservatism).

c) The effective conductivities of the MPC storage spaces are computed for bounding fuel storage configurations defined in Paragraph 4.4.1.1(ii). The in-plane thermal conductivities are obtained using ANSYS [4.1.1] and FLUENT [4.4.2] computer~~finite element~~ models of an array of fuel rods enclosed by a square box. Radiation heat transfer from solid surfaces (cladding and box walls) is enabled in these models. Using these models the effective conduction-radiation conductivities are obtained and reported in Table 4.4.1. For heat transfer in the axial direction an area weighted mean of cladding and helium conductivities are computed (see Table 4.4.1). Axial conduction heat transfer in the fuel pellets and radiation heat dissipation in the axial direction are conservatively ignored. Thus, the thermal conductivity of the rodded region, like the porous media simulation for helium flow, is represented by a 3-D continuum having effective planar and axial conductivities. In the interest of conservatism, thermal analysis of normal storage condition in HI-STORM FW and normal onsite transfer condition in HI-TRAC VW (Section 4.5) are performed with a 10% reduced effective thermal conductivity of fuel region.

d) The internals of the MPC, including the basket cross-section, aluminum shims, bottom flow holes, top plenum, and circumferentially irregular downcomer formed by the annulus gap in the aluminum shims are modeled explicitly. For simplicity, the flow holes are modeled as rectangular openings with an understated flow area.

e) The inlet and outlet vents in the HI-STORM FW overpack are modeled explicitly to incorporate any effects of non-axisymmetry of inlet air passages on the system's thermal performance.

f) The air flow in the HI-STORM FW/MPC annulus is simulated by the k-ω turbulence model with the transitional option enabled. The adequacy of this turbulence model is confirmed in the Holtec benchmarking report [4.1.6]. The annulus grid size is selected to ensure a converged solution.(See Section 4.4.1.6).

g) A limited number of fuel assemblies defined in Table 1.2.1 ~~(upto 12 in MPC-37 and upto 16 in MPC-89)~~ classified as damaged fuel are permitted to be stored in the MPC inside Damaged Fuel Containers (DFCs). A DFC can be stored in the outer peripheral locations of ~~both~~ MPC-37, MPC-32ML~~, MPC-31C~~ and MPC-89 as shown in Figures 2.1.1a, 2.1.1b~~, 2.1.1c~~ and 2.1.2, respectively. DFC emplaced fuel assemblies have a higher resistance to helium flow because of the debris screens. However, DFC fuel storage does not affect temperature of hot fuel stored in the core of the basket because DFC storage is limited by Technical Specifications for placement in the peripheral storage locations away from hot fuel. For this reason the thermal modeling of the fuel basket under the assumption of all storage spaces populated with intact fuel is justified.

h) As shown in HI-STORM FW drawings in Section 1.5 the HI-STORM FW overpack is equipped with an optional heat shield to protect the inner shell and concrete from radiation heating by the emplaced MPC. The inner and outer shells and concrete are explicitly modeled. All the licensing basis thermal analyses explicitly include the heat shields. A sensitivity study is performed as described in paragraph 4.4.1.9 to evaluate the absence of heat shield on the overpack inner shell and overpack lid.

i) To maximize lateral resistance to heat dissipation in the fuel basket, 0.8 mm full length inter- panel gaps are conservatively assumed to exist at all intersections. This approach is identical to that used in the thermal analysis of the HI-STAR 180 Package in Docket 71-9325. The shims installed in the MPC peripheral spaces (See MPC-37, MPC-32ML~~, MPC-31C~~ and MPC-89 drawings in Section 1.5) are explicitly modeled. For conservatism bounding as-built gaps (3 mm basket-to-shims and 3 mm shims-to-shell) are assumed to exist and incorporated in the thermal models.

j) The thermal models incorporate all modes of heat transfer (conduction, convection and radiation) in a conservative manner.

k) The Discrete Ordinates (DO) model, previously utilized in the HI-STAR 180 docket (Docket 71-9325), is deployed to compute radiation heat transfer.

l) Laminar flow conditions are applied in the MPC internal spaces to obtain a lowerbound rate of heat dissipation.

The 3-D model described above is illustrated in the cross-section for the MPC-89, MPC-32ML~~,~~ ~~MPC-31C~~ and MPC-37 in Figures 4.4.2a, 4.4.2b~~, 4.4.2c~~ and 4.4.3, respectively. A closeup of the fuel cell spaces which explicitly include the channel-to-cell gap in the 3-D model applicable to BWR fueled basket (MPC-89) is shown in Figure 4.4.4. The principal 3-D modeling conservatisms are listed below:

1) The storage cell spaces are loaded with high flow resistance design basis fuel assemblies (See Table 2.1.4).
2) Each storage cell is generating heat at its limiting value under the regionalized storage scenarios defined in Chapter 2, Section 2.1.
3) Axial dissipation of heat by conduction in the fuel pellets is neglected.
4) Dissipation of heat from the fuel rods by radiation in the axial direction is neglected.
5) The fuel assembly channel length for BWR fuel is overstated.
6) The most severe environmental factors for long-term normal storage ~~—~~ ambient temperature of 80°F and 10CFR71 insolation levels ~~—~~ were coincidentally imposed on the system.
7) Reasonably bounding solar absorbtivity of HI-STORM FW overpack external surfaces is applied to the thermal models.
8) To understate MPC internal convection heat transfer, the helium pressure is understated.
9) No credit is taken for contact between fuel assemblies and the MPC basket wall or between the MPC basket and the basket supports.
10) Heat dissipation by fuel basket peripheral supports is neglected.
11) Lowerbound fuel basket emissivity function defined in the Metamic-HT Sourcebook [4.2.6] is adopted in the thermal analysis.
12) Lowerbound stainless steel emissivity obtained from cited references (See Table 4.2.1) are applied to MPC shell.
13) The k-ω model used for simulating the HI-STORM FW annulus flow yields uniformly conservative results [4.1.6].
14) Fuel assembly length is conservatively modeled equal to the height of the fuel basket.

The effect of crud resistance on fuel cladding surfaces has been evaluated and found to be negligible [4.1.8]. The evaluation assumes a thick crud layer (130 μm) with a bounding low conductivity (conductivity of helium). The crud resistance increases the clad temperature by a very small amount (~0.1°F) [4.1.8]. Accordingly this effect is neglected in the thermal evaluations.

iv. Principal Attributes of MPC-32ML 3D Thermal Model

The 3-D thermal model implemented to analyze MPC-32ML in HI-STORM FW system follows the same methodology as MPC-37 discussed previously in this sub-section. A summary of the modeling attributes is provided below:

a) The fuel storage spaces are modeled as porous media having effective thermal-hydraulic properties.

b) The entire cross-section of the storage cell is modeled as porous medium. The flow resistance through the storage cell is discussed in Paragraph 4.4.1.10.

c) The effective conductivities of the MPC-32ML storage spaces are computed for bounding fuel storage configuration defined in Paragraph 4.4.1.1(ii). The in-plane thermal conductivities are obtained using FLUENT [4.4.2] computer models of an array of fuel rods enclosed by a square box and reported in Table 4.4.1. For heat transfer in the axial direction an area weighted mean of cladding and helium conductivities are computed (see Table 4.4.1). In the interest of conservatism, thermal analysis of normal storage condition in HI-STORM FW is performed with a 10% reduced effective thermal conductivity of fuel region.

d) Similar to MPC-37, the internals of the MPC, including the basket cross-section, aluminum shims, bottom flow holes, top plenum, and circumferentially irregular downcomer formed by the annulus gap in the aluminum shims are modeled explicitly. For simplicity, the flow holes are modeled as rectangular openings with an understated flow area.

e) The thermal model and methodology outside the MPC is same as that adopted for MPC-37.

f) A limited number of fuel assemblies defined in Table 1.2.1 classified as damaged fuel are permitted to be stored in the MPC inside Damaged Fuel Containers (DFCs). DFC storage is restricted to outer peripheral locations of MPC-32ML as shown in Figure 2.1.1b.

g) To maximize lateral resistance to heat dissipation in the fuel basket, 0.8 mm inter-panel gaps are conservatively assumed to exist at all intersections. This approach is identical to that used in the thermal analysis of MPC-37 basket. The shims installed in the MPC peripheral spaces (See MPC-32ML drawings in Section 1.5) are explicitly modeled. For conservatism bounding as-built gaps (3 mm basket-to-shims and 3 mm shims-to-shell) are assumed to exist and incorporated in the thermal models.

h) The thermal models incorporate all modes of heat transfer (conduction, convection and radiation) in a conservative manner.

i) Laminar flow conditions are applied in the MPC internal spaces to obtain a lowerbound rate of heat dissipation.

4.4.1.2 Fuel Assembly 3-Zone Flow Resistance Model[1]

The HI-STORM FW System is evaluated for storage of representative PWR and BWR fuel assemblies determined by a separate analysis, to provide maximum resistance to the axial flow of helium. These are (i) PWR fuel: W17x17 and (ii) BWR fuel: GE10x10. During fuel storage helium enters the MPC fuel cells from the bottom plenum and flows upwards through the open spaces in the fuel storage cells and exits in the top plenum. Because of the low flow velocities the helium flow in the fuel storage cells and MPC spaces is in the laminar regime (Re < 100). The bottom and top plenums are essentially open spaces engineered in the fuel basket ends to facilitate helium circulation. In the case of BWR fuel storage, a channel enveloping the fuel bundle divides the flow in two parallel paths. One flow path is through the in-channel or rodded region of the storage cell and the other flow path is in the square annulus area outside the channel. In the global thermal modeling of the HI-STORM FW System the following approach is adopted:

(i) In BWR fueled MPCs, an explicit channel-to-cell gap is modeled.
(ii) The fuel assembly enclosed in a square envelope (fuel channel for BWR fuel or fuel storage cell for PWR fuel) is replaced by porous media with equivalent flow resistance.

The above modeling approach is illustrated in Figure 4.4.4.

In the FLUENT program, porous media flow resistance is modeled as follows:

$$\Delta P/L = D\mu V \qquad \text{(Eq. 1)}$$

where $\Delta P/L$ is the hydraulic pressure loss per unit length, D is the flow resistance coefficient, μ is the fluid viscosity and V is the superficial fluid velocity. In the HI-STORM FW thermal models the fuel storage cell length between the bottom and top plenums[2] is replaced by porous media. As discussed below the porous media length is partitioned in three zones with discrete flow resistances.

[1] This Sub- section duplicates the methodology used in the HI-STORM FSAR, Rev. 7, supporting CoC Amendment # 5 in Docket 72-1014 [4.1.8].
[2] These are the flow hole openings at the lower end of the fuel basket and a top axial gap to facilitate helium circulation. The flow holes are explicitly included in the 3D thermal models with an understated flow area.

explicit calculations for the case of MPC-37 are performed to quantify the conservatism introduced by using the "bounding" resistance data in the FLUENT analysis.

4.4.1.4 Evaluation of Flow Resistance in Enlarged Cell MPCs

The flow resistance factors used in the porous media model are bounding for all fuel types and MPC baskets. This was accomplished for the PWR fueled MPC-37 by placing the most resistive Westinghouse 17x17 fuel assembly in the smaller cell opening MPC-32 approved under the HI-STORM 100 Docket 72-1014, CoC Amendment No. 5 and computing the flow resistance factors. In the case of BWR fueled MPC-89 the most resistive GE-10x10 fuel assembly in the channeled configuration is explicitly modeled in the MPC-89 fuel storage spaces as shown in Figure 4.4.4. The channeled space occupied by the GE-10x10 fuel assembly is modeled as a porous region with effective flow resistance properties computed by deploying an independent 3D FLUENT model of the array of fuel rods and grid spacers.

In the PWR fuel resistance modeling case physical reasoning suggests that the flow resistance of a fuel assembly placed in the larger MPC-37 storage cell will be less than that computed using the (smaller) counterpart cells cavities in the MPC-32. However to provide numerical substantiation FLUENT calculations are performed for the case of W-17x17 fuel placed inside the MPC-32 cell opening of 8.79" and the enlarged MPC-37 cell opening of 8.94". The FLUENT results for the cell pressure drops under the baseline (MPC-32) and enlarged cell opening (MPC-37) scenarios are shown plotted in Figure 4-4-7. The plot shows that, as expected, the larger cell cross section case (MPC-37) yields a smaller pressure loss. Therefore, the MPC-37 flow resistance is bounded by the MPC-32 flow resistance used in the FLUENT simulations in the SAR. This evaluation is significant because the MPC-37 basket is determined as the limiting MPC and therefore the licensing basis HI-STORM FW temperatures by use of higher-than-actual resistance are overstated.

However, as mentioned in Sub-section 4.4.1.2, a flow resistance of $1x10^6$ m^{-2} through PWR fuel assemblies is used in the thermal analysis.

4.4.1.5 Screening Calculations to Ascertain Limiting Storage Scenario

To define the thermally most limiting HI-STORM FW storage scenario the following cases are evaluated under the limiting heat load patterns defined in Tables ~~1.2.3a, 1.2.3b,~~ 1.2.3a~~c~~[1], 1.2.3b and 1.2.4:

(i) MPC-89
(ii) Minimum height MPC-37
(iii) Reference height MPC-37
(iv) Maximum height MPC-37
(v) MPC-32ML

[1] Pattern A defined in Table 1.2.3a is the limiting fuel storage pattern (See Subsection 4.4.4.1).

~~(vi) MPC-31C~~

To evaluate the above scenarios, 3D FLUENT screening models of the HI-STORM FW cask are constructed, Peak Cladding Temperatures (PCT) computed and tabulated in Table 4.4.2. The results of the calculations yield the following:

(a) Fuel storage in MPC-37 produces a higher peak cladding temperature than that in MPC-89
(b) Fuel storage in the minimum height MPC-37 is limiting (produces the highest peak cladding temperature).

To bound the HI-STORM FW storage temperatures the limiting scenario ascertained above is adopted for evaluation of all normal, off-normal and accident conditions.

4.4.1.6 Grid Sensitivity Studies

To achieve grid independent CFD results, a grid sensitivity study is performed on the HI-STORM FW thermal model. The grid refinement is performed in the entire domain i.e. for both fluid and solid regions in both axial and radial directions. Non-uniform meshes with grid cells clustered near the wall regions are generated to resolve the boundary flow near the walls.

A number of grids are generated to study the effect of mesh refinement on the fuel and component temperatures. All sensitivity analyses were carried out for the case of MPC-37 with minimum fuel length under the bounding heat load pattern A. Following table gives a brief summary of the different sets of grids evaluated and PCT results.

Mesh No	Total Mesh Size	PCT (^oC)	Permissible Limit (^oC)	Clad Temperature Margin (^oC)
1 (Licensing Basis Mesh)	1,536,882	373	400	27
2	3,354,908	372	400	28
3	7,315,556	372	400	28
Note: Because the flow field in the annulus between MPC shell and overpack inner shell is in the transitional turbulent regime, the value of y^+ at the wall-adjacent cell is maintained on the order of 1 to ensure the adequate level of mesh refinement is reached to resolve the viscosity affected region near the wall.				

As can be seen from the above table, the PCT is essentially the same for all the meshes. The solutions from the different grids used are in the asymptotic range. Therefore, it can be concluded that the Mesh 1 is reasonably converged. To provide further assurance of convergence, the sensitivity results are evaluated in accordance with the ASME V&V 20-2009 [4.4.3]. Towards this end, the Grid Convergence Index (GCI), which is a measure of the solution uncertainty, is computed to be 0.181% for these meshes. The apparent order of the method

calculated as 2.1, is similar to the order of the method.

Based on the above results, Run No 1 grid layout is adopted for the thermal analysis of the HI-STORM FW. The thermal evaluations of MPC-32ML are performed using a mesh with similar mesh density as the licensing basis converged mesh for MPC-37.

4.4.1.7 Evaluation of 15x15I Short Fuel Assembly

i) Overview

The various fuel assembly types allowed for storage are discussed in Chapter 2. Table 2.1.1 specifically provides a classification of fuel assembly based on its length – minimum, reference and maximum. Due to the unique design of 15x15I short fuel, the thermal evaluation for 15x15I short fuel is separately discussed in this subsection. All the thermal evaluations for MPC-37 discussed previously in this section are applicable to all fuel assembly arrays/classes except the 15x15I fuel defined in Table 2.1.2. The nominal length of 15x15I short fuel with fuel shim is 150 inches (See Table 2.1.1). Therefore, the corresponding height of the MPC, HI-STORM and HI-TRAC are determined based on 150" fuel length.

ii) Evaluation of Flow Resistance through Fuel Assemblies

As discussed in Sub-section 4.4.1, the fuel bundle inside a fuel cell for the PWR fuel assemblies is replaced by an equivalent porous media with a flow resistance. The flow resistance used in the licensing basis evaluations in this chapter is based on design basis fuel assemblies W-17x17. A flow resistance of $1x10^6$ m^{-2} adopted for thermal hydraulic analysis in Docket 72-1014 CoC amendment 9 is used for PWR fuel assemblies. However, the flow resistance through fuel assemblies will be lower for smaller fuel assemblies i.e. those with lesser fuel rods. Physical reasoning suggests that the flow resistance of a smaller fuel assembly placed in the MPC storage cell will be less than that computed using the design basis W17x17 fuel assemblies. The flow impedance properties for a specific fuel assembly can be computed using the following procedure:

Step 1: Compute the flow areas A1 and A2 in the bare rods region and grids region of the licensing basis fuel assembly† and the specific fuel assembly of interest.

Step 2: Compute the hydraulic diameter D1 and D2 of the bare rods region and grids region of the licensing basis fuel assembly and the specific fuel assembly of interest.

Step 3: Compute the resistance multiplier factor α defined as the ratio of specific fuel resistance to licensing basis fuel assembly resistance in the following manner.

† The fuel characteristics of the licensing basis fuel assembly are in Reference [4.1.9]. The flow resistance through this licensing basis fuel assembly is one million (m^{-2}) [4.1.8].

HI-STORM FW overpack is equipped with a heat shield on the overpack inner shell and underneath the overpack lid concrete. They are optional features engineered to protect the overpack body concrete and overpack lid concrete from excessive temperature rise due to radiant heat from the MPC. Absence of the heat shields will have an adverse impact on the overpack temperatures. To quantify the impact, a thermal evaluation is performed for a HI-STORM overpack without the heat shields. The thermal model is exactly the same as the converged mesh discussed above in paragraph 4.4.1.6 except that heat shields are removed from the thermal model. The results of this thermal evaluation are discussed in paragraph 4.4.4.4.

4.4.1.10 Evaluation of 16x16D ~~and VVER-1000~~ Fuel Assembly

~~(a)~~ ~~16x16D~~

This fuel type is defined in Table 2.1.1b for storage in MPC-32ML. As the number of rods in this fuel type is bounded by W-17x17 fuel physical reasoning will suggest flow resistance would be bounded by it. As a due diligence measure the methodology defined in Para 4.4.1.7 is adopted to evaluate 16x16D flow resistance. The flow resistance computes ~50% of the reference W-17x17 fuel [4.1.9]. However, in the interest of conservatism a robustly bounding value of $1x10^{6}$ m^{-2} is adopted in the thermal analysis.

~~(b) VVER-1000 fuel~~

~~This is a unique fuel type that features a triangular rods pitch and a hexagonal cross-section that renders it not suitable for referencing to W-17x17 fuel. As an over-arching measure of conservatism axial flow of helium in VVER-1000 fuel assemblies situated in MPC-31C is conservatively neglected.~~

4.4.2 Effect of Neighboring Casks

HI-STORM FW casks are typically stored on an ISFSI pad in regularly spaced arrays (See Section 1.4, Figures 1.4.1 and 1.4.2). Relative to an isolated HI-STORM FW the heat dissipation from a HI-STORM FW cask placed in an array is somewhat disadvantaged. However, as the analysis in this Sub-section shows, the effect of the neighboring casks on the peak cladding temperature in the “surrounded” cask is insignificant.

(i) Effect of Insolation

The HI-STORM FW casks are subject to insolation heating during daytime hours. Presence of surrounding casks has the salutary effect of partially blocking insolation flux. This effect, results in lower temperatures and in the interest of conservatism is ignored in the analysis.

(ii) Effect of Radiation Blocking

The presence of surrounding casks has the effect of partially blocking radiation heat dissipation from the Overpack cylindrical surfaces. Its effect is evaluated in Sub-section 4.4.2.1.

(iii) Effect of Flow Area Reduction

The principal results of the hypothetical square cavity thermal model are tabulated below and compared with the baseline thermal results tabulated in Section 4.4.4.

Model	Peak Clad Temperature (°F)	Margin-to-Limit (°F)
Single Cask Model	703	49
Hypothetical Square Cavity Thermal Model	702.1	50
Peak cladding temperature reported for the limiting heat load MPC-37 Pattern A (See Subsection 4.4.4.1)		

The results show that the presence of surrounding casks has essentially no effect on the fuel cladding temperatures (the difference in the results is within the range of numerical round-off). These results are in line with prior thermal evaluations of the effect of surrounding casks in the NRC approved HI-STORM 100 System in Docket 72-1014.

4.4.3 Test Model

The HI-STORM FW thermal analysis is performed on the FLUENT [4.1.2] Computational Fluid Dynamics (CFD) program. To ensure a high degree of confidence in the HI-STORM FW thermal evaluations, the FLUENT code has been benchmarked using data from tests conducted with casks loaded with irradiated SNF ([4.1.3],[4.1.7]). The benchmark work is archived in QA validated Holtec reports ([4.1.5],[4.1.6]). These evaluations show that the FLUENT solutions are conservative in all cases. In view of these considerations, additional experimental verification of the thermal design is not necessary. FLUENT has also been used in all Holtec International Part 71 and Part 72 dockets since 1996.

4.4.4 Maximum and Minimum Temperatures

4.4.4.1 Maximum Temperatures

The 3-D model from the previous subsection is used to determine temperature distributions under long-term normal storage conditions for both BWR canisters (MPC-89) and PWR canisters (MPC-37 and~~,~~ MPC-32ML~~ and MPC-31C~~). Tables 4.4.2, 4.4.3 and 4.4.5 provide key thermal and pressure results from the FLUENT simulations, respectively. Tables 4.4.12 and 4.4.13 respectively provide the temperature and pressure results from the FLUENT simulation of the 15x15I short fuel assembly height based on the methodology discussed in Sub-Section 4.4.1.7. The peak fuel cladding result in these tables is actually overstated by the fact that the 3-D FLUENT cask model incorporates the effective conductivity of the fuel assembly sub-model.

[1] The lower computed temperature is an artifact of the use of overstated inlet and outlet loss coefficients in the single cask model. The result supports the conclusion that surrounding casks have essentially no effect on the Peak Cladding Temperatures.

Therefore the FLUENT models report the peak temperature *in the fuel storage cells*. Thus, as the fuel assembly models include the fuel pellets, the FLUENT calculated peak temperatures are actually peak pellet centerline temperatures which bound the peak cladding temperatures with a modest margin.

The following observations can be derived by inspecting the temperature field obtained from the thermal models:

- The fuel cladding temperatures are below the regulatory limit (ISG-11 [4.1.4]) under all uniform and regionalized storage scenarios defined in Chapter 1 (Figures 1.2.1a, 1.2.1b~~, 1.2.1c~~ and 1.2.2) and thermal loading scenarios defined in Tables 1.2.3a, 1.2.3b~~, 1.2.3c~~ and 1.2.4.

- The limiting fuel temperatures are reached under the Pattern A thermal loading condition defined in Table 1.2.3a in the MPC-37. Accordingly this scenario is adopted for thermal evaluation under on-site transfer (Section 4.5) and under off-normal and accident conditions (Section 4.6).

- The maximum temperature of the basket structural material is within its design limit.

- The maximum temperatures of the MPC pressure boundary materials are below their design limits.

- The maximum temperatures of concrete are within the guidance of the governing ACI Code (see Table 2.2.3).

- The calculated fuel temperature for the 15x15I short fuel assembly (Table 4.4.12) is bounded by the thermal evaluations for the minimum MPC-37 for short fuel (Table 4.4.3). The temperatures of other cask components are similar. It is reasonable to conclude that the temperatures and pressure for the minimum height MPC-37 (short fuel) bounds all scenarios.

The above observations lead us to conclude that the temperature field in the HI-STORM FW System with a loaded MPC containing heat emitting SNF complies with all regulatory temperature limits (Table 2.2.3). In other words, the thermal environment in the HI-STORM FW System is in compliance with Chapter 2 Design Criteria.

Also, all the licensing basis thermal evaluations documented in this chapter are performed for the most limiting thermal scenarios i.e. minimum MPC-37 with heat load pattern A.

4.4.4.2 Minimum Temperatures

A survey of the elevation of nuclear plants in the U.S. shows that nuclear plants are situated near about sea level or elevated slightly (~1000 ft). The effect of the elevation on peak fuel cladding temperatures is evaluated by performing calculations for a HI-STORM FW system situated at an elevation of 1500 feet. At this elevation the ambient temperature would decrease by approximately 5°F (See Table above). The peak cladding temperatures are calculated under the reduced ambient temperature and pressure at 1500 feet elevation for the limiting regionalized storage scenario evaluated in Table 4.4.2. The results are presented in Table 4.4.9.

These results show that the PCT, including the effects of site elevation, continues to be well below the regulatory cladding temperature limit of 752°F. In light of the above evaluation, it is not necessary to place ISFSI elevation constraints for HI-STORM FW deployment at elevations up to 1500 feet. If, however, an ISFSI is sited at an elevation greater than 1500 feet, the effect of altitude on the PCT shall be quantified as part of the 10 CFR 72.212 evaluation for the site using the site ambient conditions.

4.4.4.4 Evaluation of Overpack Heat Shields

As discussed in Sub-section 4.4.1.9 above, a thermal evaluation is performed to evaluate the effect of removal of heat shields from a HI-STORM overpack. The predicted temperatures from this sensitivity study of normal condition of storage are summarized in Table 4.4.14. The peak cladding temperature, basket and MPC component temperatures decrease due to removal of heat shields. As expected, the results demonstrate an increase in overpack component temperatures. However, the overpack component temperatures are below their respective normal temperature limits with significant margins. Therefore, removal of heat shields does not have a detrimental effect on the system' thermal performance.

The temperatures of overpack components increase due to removal of heat shields under normal conditions of storage. This temperature increase is then added to the predicted temperatures of all the off-normal and accident conditions discussed in Section 4.6. The resulting temperatures are still well below their respective temperature limits which demonstrate that safety conclusions made for all the off-normal and accident condition evaluations in Section 4.6 remain valid even after the removal of heat shields from the HI-STORM overpack.

4.4.5 Maximum Internal Pressure

4.4.5.1 MPC Helium Backfill Pressure

The quantity of helium emplaced in the MPC cavity shall be sufficient to yield design operating pressures defined in Table 4.4.15.~~produce an operating pressure of 7.1 and 7.0 atmospheres (absolute) respectively for loading patterns A and B during normal storage conditions defined in Table 4.1.1.~~ Thermal analyses performed on the different MPC designs indicate that this operating pressure requires a certain minimum helium backfill pressure (P_b) specified at a reference temperature (70°F). The minimum backfill pressure for each MPC type is provided in

Table 4.4.7. A theoretical upper limit on the helium backfill pressure also exists and is defined by the design pressure of the MPC vessel (Table 2.2.1). The upper limit of P_b is also reported in Table 4.4.7. To bound the minimum and maximum backfill pressures listed in Table 4.4.7 with a margin, a helium backfill specification is set forth in Table 4.4.8.

To provide additional helium backfill range for less than design basis heat load canisters a Sub-Design-Basis (SDB) heat load scenario is defined below:

(i) MPC-37 under 80% Pattern A Heat Load (Table 1.2.3)
(ii) MPC-37 under 90% Pattern A Heat Load (Table 1.2.3)
(iii) MPC-89 under 80% Design Heat Load (Table 1.2.4)
(iv) MPC-37 under vacuum drying threshold heat load in Table 4.5.1[1].
(v) MPC-89 under vacuum drying threshold heat load in Table 4.5.1[1]~~*~~.

The storage cell and MPC heat load limits under the SDB scenario (i), (ii) & (iii) are specified in Table 4.4.11. Calculations for bounding scenarios (i), (ii) & (iii) show that the maximum cladding temperature under the SDB scenario meet the ISG-11 temperature limits. The helium backfill pressure limits supporting this scenario are defined in Table 4.4.10. These backfill limits maybe optionally adopted by a cask user if the decay heats of the loaded fuel assemblies meet the SDB decay heat limits stipulated above.

Two methods are available for ensuring that the appropriate quantity of helium has been placed in an MPC:

i. By pressure measurement
ii. By measurement of helium backfill volume (in standard cubic feet)

The direct pressure measurement approach is more convenient if the FHD method of MPC drying is used. In this case, a certain quantity of helium is already in the MPC. Because the helium is mixed inside the MPC during the FHD operation, the temperature and pressure of the helium gas at the MPC's exit provides a reliable means to compute the inventory of helium. A shortfall or excess of helium is adjusted by a calculated raising or lowering of the MPC pressure such that the reference MPC backfill pressure is within the range specified in Table 4.4.8 or Table 4.4.10 (as applicable).

When vacuum drying is used as the method for MPC drying, then it is more convenient to fill the MPC by introducing a known quantity of helium (in standard cubic feet) by measuring the quantity of helium introduced using a calibrated mass flow meter or other measuring apparatus. The required quantity of helium is computed by the product of net free volume and helium specific volume at the reference temperature (70°F) and a target pressure that lies in the mid-range of the Table 4.4.8 pressures.

[1] Threshold scenarios (iv) and (v) are bounded by scenarios (i) and (iii) respectively because the core Region 1 assembly heat loads and total cask heat loads are bounded by the Sub-Design Basis heat loads in Table 4.4.11.

The net free volume of the MPC is obtained by subtracting B from A, where

A = MPC cavity volume in the absence of contents (fuel and non-fuel hardware) computed from nominal design dimensions

B = Total volume of the contents (fuel including DFCs, if used) based on nominal design dimensions

Using commercially available mass flow totalizers or other appropriate measuring devices, an MPC cavity is filled with the computed quantity of helium.

4.4.5.2 MPC Pressure Calculations

The MPC is initially filled with dry helium after fuel loading and drying prior to installing the MPC closure ring. During normal storage, the gas temperature within the MPC rises to its maximum operating basis temperature. The gas pressure inside the MPC will also increase with rising temperature. The pressure rise is determined using the ideal gas law. The MPC gas pressure is also subject to substantial pressure rise under hypothetical rupture of fuel rods and large gas inventory non-fuel hardware (PWR BPRAs). To minimize MPC gas pressures the number of BPRA containing fuel assemblies must be limited to that specified in Chapter 2, Section 2.1~~30~~.

Table 4.4.4 presents a summary of the MPC free volumes determined for the fixed height MPC-89~~, and~~ lowerbound height MPC-37 and~~,~~ MPC-32ML ~~and MPC-31C~~ fuel storage scenarios. The MPC maximum gas pressure is computed for a postulated release of fission product gases from fuel rods into this free space. For these scenarios, the amounts of each of the release gas constituents in the MPC cavity are summed and the resulting total pressures determined from the ideal gas law. A concomitant effect of rod ruptures is the increased pressure and molecular weight of the cavity gases with enhanced rate of heat dissipation by internal helium convection and lower cavity temperatures. As these effects are substantial under large rod ruptures the 100% rod rupture accident is evaluated with due credit for increased heat dissipation under increased pressure and molecular weight of the cavity gases. Based on fission gases release fractions (NUREG 1536 criteria [4.4.1]), rods' net free volume and initial fill gas pressure, maximum gas pressures with 1% (normal), 10% (off-normal) and 100% (accident condition) rod rupture are given in Table 4.4.5. The results of the calculations support the following conclusions:

(i) The maximum computed gas pressures reported in Table 4.4.5 under all design basis thermal loadings defined in Section 4.4 are all below the MPC internal design pressures for normal, off-normal and accident conditions specified in Table 2.2.1.

(ii) The MPC gas pressure obtained under loading Pattern A is essentially same as in Pattern B. Accordingly Pattern A loading condition for pressure boundary evaluation of MPC in the HI-TRAC and under off-normal and accident conditions is retained.

Evaluation of Non-Fuel Hardware

The inclusion of PWR non-fuel hardware (BPRA control elements and thimble plugs) to the PWR basket influences the MPC internal pressure through two distinct effects. The presence of non-fuel hardware increases the effective basket conductivity, thus enhancing heat dissipation and lowering fuel temperatures as well as the temperature of the gas filling the space between fuel rods. The gas volume displaced by the mass of non-fuel hardware lowers the cavity free volume. These two effects, namely, temperature lowering and free volume reduction, have opposing influence on the MPC cavity pressure. The first effect lowers gas pressure while the second effect raises it. In the HI-STORM FW thermal analysis, the computed temperature field (with non-fuel hardware excluded) has been determined to provide a conservatively bounding temperature field for the PWR baskets. The MPC cavity free space is computed based on conservatively computed volume displacement by fuel with non-fuel hardware included. This approach ensures conservative bounding pressures.

During in-core irradiation of BPRAs, neutron capture by the B-10 isotope in the neutron absorbing material produces helium. Two different forms of the neutron absorbing material are used in BPRAs: Borosilicate glass and B_4C in a refractory solid matrix ($A\iota_2O_3$). Borosilicate glass (primarily a constituent of Westinghouse BPRAs) is used in the shape of hollow pyrex glass tubes sealed within steel rods and supported on the inside by a thin-walled steel liner. To accommodate helium diffusion from the glass rod into the rod internal space, a relatively high void volume (~40%) is engineered in this type of rod design. The rod internal pressure is thus designed to remain below reactor operation conditions (2,300 psia and approximately 600°F coolant temperature). The B_4C- Al_2O_3 neutron absorber material is principally used in B&W and CE fuel BPRA designs. The relatively low temperatures of the poison material in BPRA rods (relative to fuel pellets) favor the entrapment of helium atoms in the solid matrix.

Several BPRA designs are used in PWR fuel. They differ in the number, diameter, and length of poison rods. The older Westinghouse fuel (W-14x14 and W-15x15) has used 6, 12, 16, and 20 rods per assembly BPRAs and the later (W-17x17) fuel uses up to 24 rods per BPRA. The BPRA rods in the older fuel are much larger than the later fuel and, therefore, the B-10 isotope inventory in the 20-rod BPRAs bounds the newer W-17x17 fuel. Based on bounding BPRA rods internal pressure, a large hypothetical quantity of helium (7.2 g-moles/BPRA) is assumed to be available for release into the MPC cavity from each BPRA containing fuel assembly. For a bounding evaluation the maximum permissible number of BPRA containing fuel assemblies (see discussion at the beginning of this Section) are assumed to be loaded. The MPC cavity pressures (including helium from BPRAs) are summarized in Table 4.4.5 for the bounding MPC-37 (minimum MPC height and heat load Patterns A and B), MPC-32ML~~, MPC-31C~~ and MPC-89 (design heat load) storage scenarios.

4.4.6 Engineered Clearances to Eliminate Thermal Interferences

Thermal stress in a structural component is the resultant sum of two factors, namely: (i) restraint of free end expansion and (ii) non-uniform temperature distribution. To minimize thermal

Table 4.4.1

EFFECTIVE FUEL PROPERTIES UNDER BOUNDING FUEL STORAGE CONFIGURATIONS[Note 1]

	Conductivity (Btu/hr-ft-°F)			
	PWR: Short Fuel		**PWR: Standard Fuel**	
Temperature (°F)	Planar	Axial	Planar	Axial
200	0.247	0.813	0.231	0.759
450	0.443	0.903	0.387	0.845
700	0.730	1.016	0.601	0.951
	PWR: XL Fuel		**BWR Fuel**	
	Planar	Axial	Planar	Axial
200	0.239	0.787	0.283	0.897
450	0.393	0.875	0.426	0.988
700	0.599	0.984	0.607	1.104

PWR: 15x15I Short Fuel		
Temperature (°F)	Planar	Axial
200	0.226	0.763
450	0.386	0.848
700	0.601	0.955

Thermal Inertia Properties		
	Density (lb/ft^3)	Heat Capacity (Btu/lb-°F)[Note 2]
PWR: 15x15I Short Fuel	194.5	0.056
PWR: Short Fuel	165.8	0.056
PWR: Standard Fuel	176.2	0.056
PWR: XL Fuel	187.5	0.056
BWR Fuel	255.6	0.056

Note 1: Bounding fuel storage configurations defined in 4.4.1.1(ii).
Note 2: The lowerbound heat capacity of principal fuel assembly construction materials tabulated in Table 4.2.5 (UO_2 heat capacity) is conservatively adopted.
Note 3: The fuel properties tabulated herein are used in screening calculations to define the limiting scenario for fuel storage (See Table 4.4.2).
(continued next page)

Table 4.4.1 (continued)

EFFECTIVE FUEL PROPERTIES UNDER BOUNDING FUEL STORAGE CONFIGURATIONS

	Conductivity (Btu/hr-ft-°F)	
	PWR: 16x16D ~~**PWR: VVER-1000**~~	
Temperature (°F)	Planar	Axial ~~Planar~~ ~~Axial~~
212	0.251	0.854 ~~0.229~~ ~~0.983~~
450	0.418	0.935 ~~0.308~~ ~~1.073~~
700	0.678	1.042 ~~0.341~~ ~~1.194~~

Thermal Inertia Properties		
	Density (lb/ft^3)	Heat Capacity (Btu/lb-°F)[Note ~~2~~1]
PWR: 16x16D	184.5	0.059
~~PWR: VVER-1000~~	~~183.8~~	~~0.06~~

Note ~~2~~1: The lowerbound heat capacity of principal fuel assembly construction materials tabulated in Table 4.2.5 (UO_2 heat capacity) is conservatively adopted.

Note ~~3~~2: The fuel properties tabulated herein are used in screening calculations to define the limiting scenario for fuel storage (See Table 4.4.2).

Table 4.4.2

RESULTS OF SCREENING CALCULATIONS UNDER NORMAL STORAGE CONDITIONS

Storage Scenario	Peak Cladding Temperature, °C (°F)
MPC-37	
Minimum Height[1]	**353 (667)**
Reference Height	342 (648)
Maximum Height	316 (601)
MPC-89	333 (631)

Notes:

(1) The highest temperature highlighted above is reached under the case of minimum height MPC-37 designed to store the short height Ft. Calhoun 14x14 fuel. This scenario is adopted in Chapter 4 for the licensing basis evaluation of fuel storage in the HI-STORM FW system.

(2) All the screening calculations were performed using a reference coarse mesh [4.1.9] and flow resistance based on the calculations in Holtec report [4.4.2].

1 Bounding scenario adopted in this Chapter for all thermal evaluations.

Table 4.4.3

MAXIMUM TEMPERATURES IN HI-STORM FW
UNDER LONG-TERM NORMAL STORAGE[1]

Component	**Temperature, ºC (ºF) Pattern A / Pattern B**	**MPC-32ML Temperature, ºC (ºF)**
Fuel Cladding	373 (703) / 368 (694)	349 (660)
MPC Basket	358 (676) / 354 (669)	334 (633)
Basket Periphery	290 (554) / 292 (558)	271 (520)
Aluminum Basket Shims	267 (513) / 267 (513)	256 (493)
MPC Shell	240 (464) / 242 (468)	217 (423)
MPC Lid[Note 1]	235 (455) / 232 (450)	220 (428)
Overpack Inner Shell	126 (259) / 127 (261)	108 (226)
Overpack Outer Shell	65 (149) / 65 (149)	63 (145)
Overpack Body Concrete[Note 1]	89 (192) / 90 (194)	80 (176)
Overpack Lid Concrete[Note 1]	111 (232) / 112 (234)	102 (216)
Area Averaged Air outlet[2]	103 (217) / 103 (217)	99 (210)
Note 1: Maximum section average temperature is reported.		

1 The temperatures reported in this table (all for short fuel scenarios of MPC-37) are below the design temperatures specified in Table 2.2.3, Chapter 2. These temperatures bound MPC-89 temperatures.

2 Reported herein for the option of temperature measurement surveillance of outlet ducts air temperature as set forth in the Technical Specifications.

Table 4.4.4 MINIMUM MPC FREE VOLUMES		
Item	**Lowerbound Height MPC-37 (ft^3)**	**MPC-89 (ft^3)**
Net Free Volume*	211.89	210.12
	MPC-32ML (ft^3) ~~**MPC-31C (ft^3)**~~	
Net Free Volume*	278.7~~291.23~~ ~~277.52~~	
**Net free volumes are obtained by subtracting basket, fuel, aluminum shims, spacers, basket supports and DFCs metal volume from the MPC cavity volume.*		

Table 4.4.5 SUMMARY OF MPC INTERNAL PRESSURES UNDER LONG-TERM STORAGE*		
Condition	**MPC-37 (psig) Pattern A/Pattern B**	**MPC-89 (psig)**
Initial maximum backfill** (at 70°F)	45.5/46.0	47.5
Normal: intact rods 1% rods rupture	 96.6/97.9 97.7/99.0	 98.4 99.0
Off-Normal (10% rods rupture)	107.5/108.9	104.0
Accident (100% rods rupture)	191.5/194.4	155.0
* Per NUREG-1536, pressure analyses with ruptured fuel rods (including BPRA rods for PWR fuel) is performed with release of 100% of the ruptured fuel rod fill gas and 30% of the significant radioactive gaseous fission products.		

** Conservatively assumed at the Tech. Spec. maximum value (see Table 4.4.8).
(continued next page)

Table 4.4.5 (continued)

SUMMARY OF MPC INTERNAL PRESSURES UNDER LONG-TERM STORAGE*

Condition	**MPC-32ML (psig) ~~MPC-31C (psig)~~**
Initial backfill** (at 70°F)	45.5 ~~45.5~~
Normal: intact rods 1% rods rupture	91.1 91.8 ~~91.5~~ ~~92.2~~
Off-Normal (10% rods rupture)	98.7~~3~~ ~~98.7~~
Accident (100% rods rupture)	167.5~~3.7~~ ~~163.9~~

* Per NUREG-1536, pressure analyses with ruptured fuel rods (including BPRA rods for PWR fuel) is performed with release of 100% of the ruptured fuel rod fill gas and 30% of the significant radioactive gaseous fission products.
** Conservatively assumed at the Tech. Spec. maximum value (see Table 4.4.8).

Table 4.4.6

SUMMARY OF HI-STORM FW DIFFERENTIAL THERMAL EXPANSIONS

Gap Description	**Cold Gap U (in)**	**Differential Expansion δ_i (in)**	**Is Free Expansion Criterion Satisfied (i.e., U > δ_i)**
Fuel Basket-to-MPC Radial Gap	0.125	0.112	Yes
Fuel Basket-to-MPC Minimum Axial Gap	1.5	0.421	Yes
MPC-to-Overpack Radial Gap	5.5	0.128	Yes
MPC-to-Overpack Minimum Axial Gap	3.5	0.372	Yes

Table 4.4.7

THEORETICAL LIMITS* OF MPC HELIUM BACKFILL PRESSURE**

MPC	**Minimum Backfill Pressure (psig)**	**Maximum Backfill Pressure (psig)**
MPC-37 Pattern A	41.0	47.3
MPC-37 Pattern B	40.8	47.1
MPC-89	41.9	48.4
MPC-32ML	39.7	50.6
~~MPC-31C~~	~~40.6~~	~~50.3~~

* The helium backfill pressures are set forth in the Technical Specifications with a margin (see Table 4.4.8).

** The pressures tabulated herein are at 70°F reference gas temperature.

Table 4.4.8 MPC HELIUM BACKFILL PRESSURE SPECIFICATIONS		
MPC	**Item**	**Specification**
MPC-37 Pattern A	Minimum Pressure	42.0 psig @ 70°F Reference Temperature
	Maximum Pressure	45.5 psig @ 70°F Reference Temperature
MPC-37 Pattern B	Minimum Pressure	41.0 psig @ 70°F Reference Temperature
	Maximum Pressure	46.0 psig @ 70°F Reference Temperature
MPC-89	Minimum Pressure	42.5 psig @ 70°F Reference Temperature
	Maximum Pressure	47.5 psig @ 70°F Reference Temperature
MPC-32ML	Minimum Pressure	41.5 psig @ 70°F Reference Temperature
	Maximum Pressure	45.5 psig @ 70°F Reference Temperature

Table 4.4.9 MAXIMUM HI-STORM FW TEMPERATURES AT ELEVATED SITES[1]	
Component	**Temperature, °C (°F)**
Fuel Cladding	374 (705)
MPC Basket	360 (680)
Aluminum Basket Shims	275 (527)
MPC Shell	246 (475)
MPC Lid[Note 1]	242 (468)
Overpack Inner Shell	126 (259)
Overpack Body Concrete[Note 1]	86 (187)
Overpack Lid Concrete[Note 1]	112 (234)
Note 1: Maximum section average temperature is reported.	

1 The temperatures reported in this table (all for the bounding scenario defined in Table 4.4.2) are below the design temperatures specified in Table 2.2.3, Chapter 2.

Table 4.4.15 DESIGN OPERATING ABSOLUTE PRESSURES[Note 1]	
MPC-37 Loading Pattern A Loading Pattern B	 7.1 atm 7 atm
MPC-32ML	6.5 atm
~~MPC-31C~~	~~6.3 atm~~
MPC-89	7 atm
Note 1: Table 4.4.8 helium backfill specifications ensure MPC operating pressures meet or exceed design values tabulated herein.	

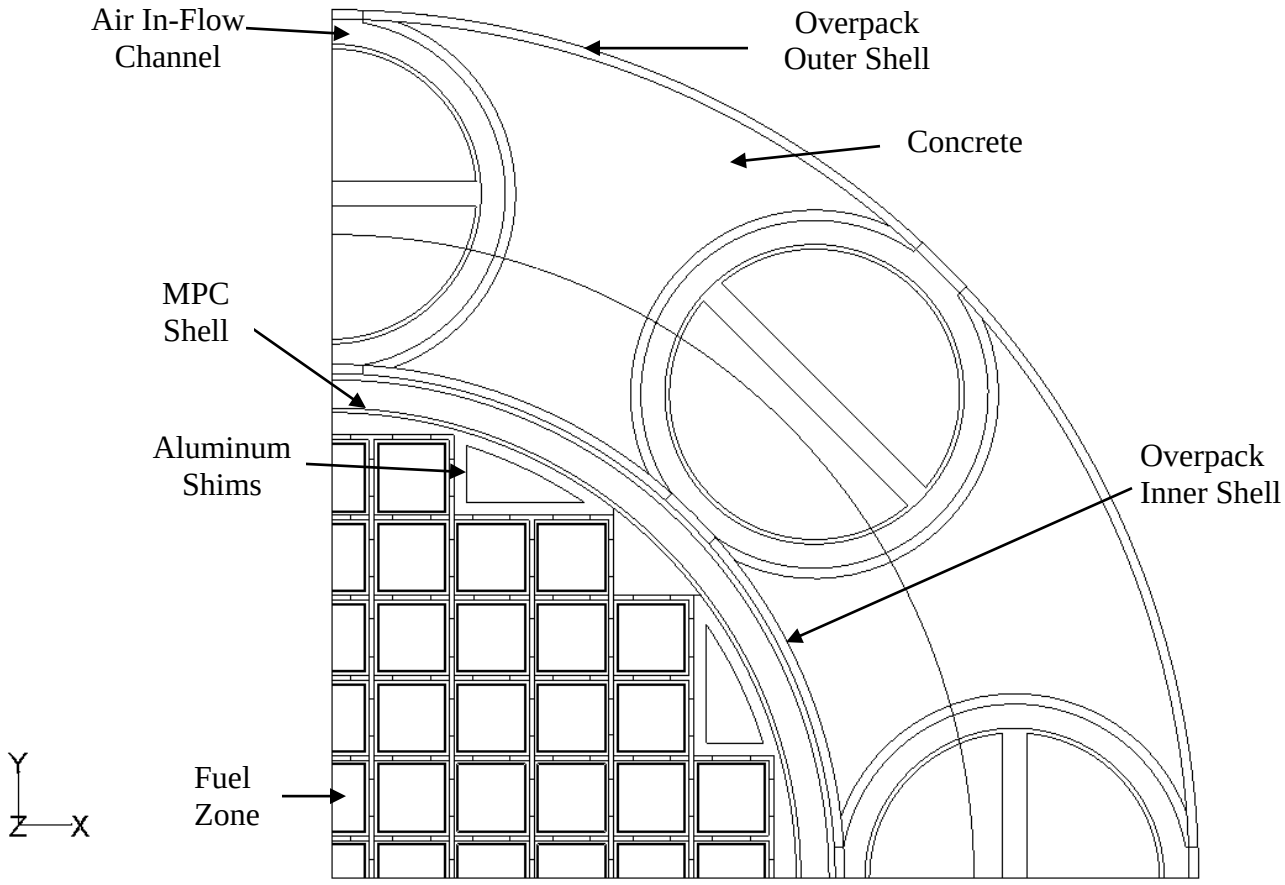

Figure 4.4.2a: Planar View of HI-STORM FW MPC-89 Quarter Symmetric 3-D Model

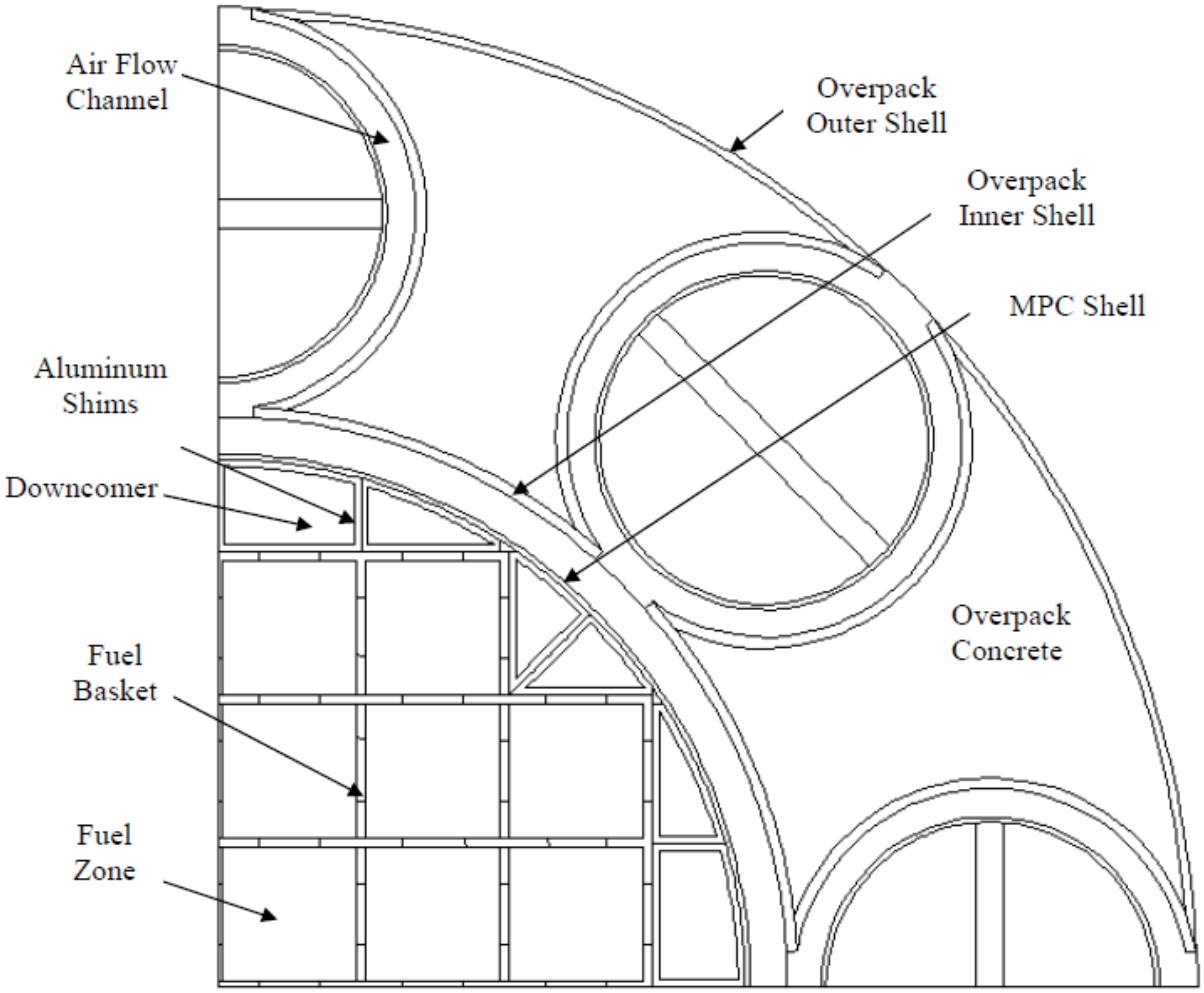

Figure 4.4.2b: Planar View of HI-STORM FW MPC-32ML Quarter Symmetric 3-D Model

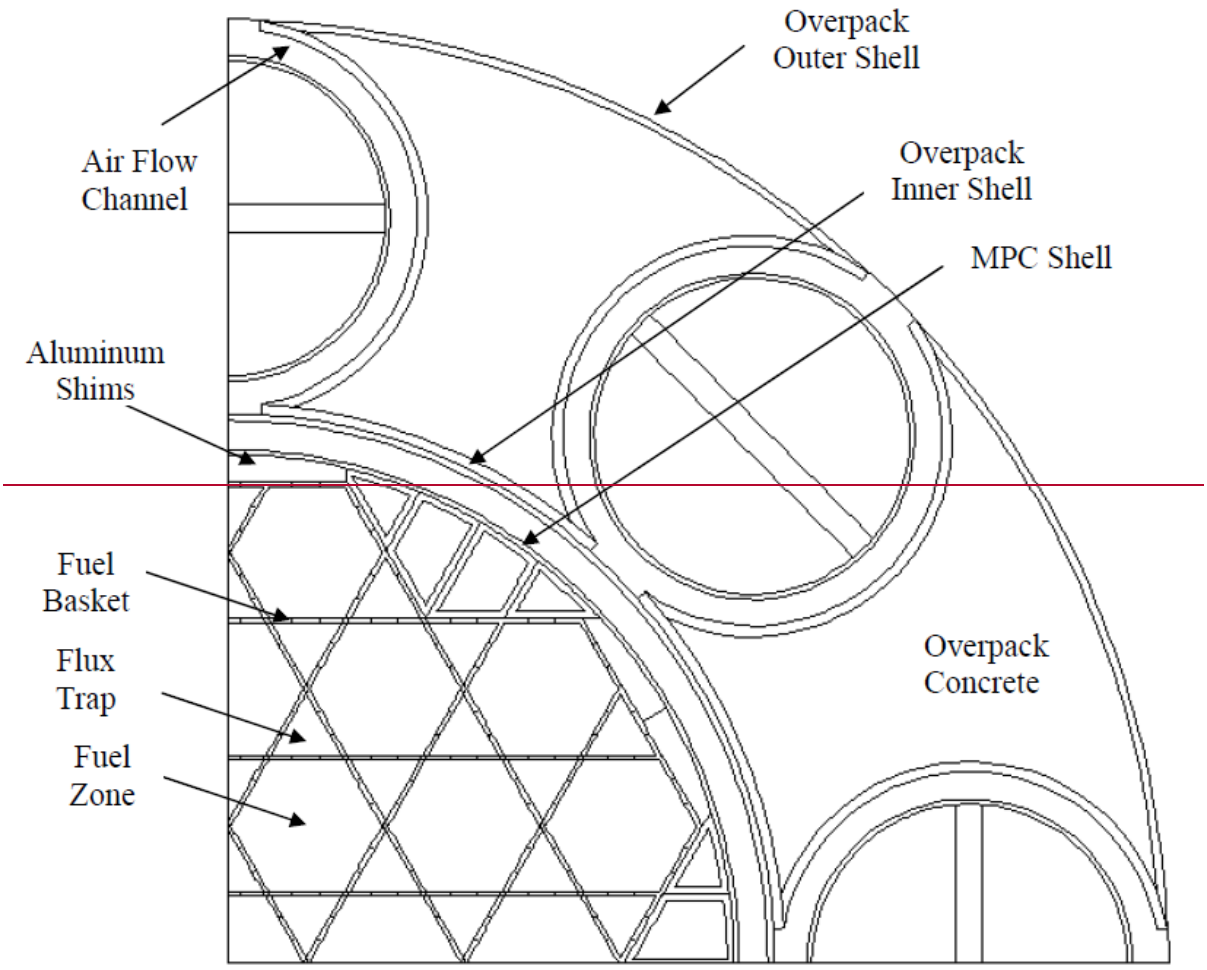

~~Figure 4.4.2c: Planar View of HI-STORM FW MPC-31C Quarter Symmetric 3-D Model~~

Mesh No	Total Mesh Size	PCT (°C)	Permissible Limit (°C)	Clad Temperature Margin (°C)
1 (Licensing Basis Mesh)	1,267,474	389	400	11
2	2,678,012	390	400	10
3	5,797,030	389	400	11

The solutions from these grids are in the asymptotic range. The finest mesh (Mesh 3) has about 4.6 times the total mesh size of the licensing basis mesh (Mesh 1). Even with such a large mesh refinement, the PCT is essentially same for all the three meshes. Since the difference of PCT for all these meshes is close to zero, it indicates that an oscillatory convergence or that the "exact" solution has been attained [4.5.1]. To provide further assurance of convergence, grid convergence index (GCI), which is a measure of the solution uncertainty, is computed as 0.566%. The apparent order of the method is calculated as 1.2.

Based on the above results, it can be concluded that the Mesh 1 is reasonably converged and is adopted as the licensing basis converged mesh.

4.5.2.3 Vacuum Drying

The initial loading of SNF in the MPC requires that the water within the MPC be drained and replaced with helium. For MPC-37, MPC-32ML and MPC-89~~s~~ containing moderate burnup fuel assemblies only, this operation may be carried out using the conventional vacuum drying approach upto design basis heat load. In this method, removal of moisture from the MPC cavity is accomplished by evacuating the MPC after completion of MPC draining operation. Vacuum drying of ~~MPC-31C loaded with moderate or high burnup fuel and~~ MPC-37, MPC-32ML and~~&~~ MPC-89~~s~~ containing high burnup fuel assemblies is permitted up to threshold heat loads defined in Table 4.5.1 and 4.5.16. High burnup f~~High burnup fF~~uel drying in MPC~~ss~~ generating greater than~~–~~ threshold heat load is performed by a ~~s require implementation of site specific vacuum drying time limits. Where such restrictions are deemed not practical theis performed by a~~ forced flow helium drying process as discussed in Section 4.5.4 ~~is mandatory~~.

Prior to the start of the MPC draining operation, both the HI-TRAC VW annulus and the MPC are full of water. The presence of water in the MPC ensures that the fuel cladding temperatures are lower than design basis limits by large margins. As the heat generating active fuel length is uncovered during the draining operation, the fuel and basket mass will undergo a gradual heat up from the initially cold conditions when the heated surfaces were submerged under water. To minimize fuel temperatures during vacuum drying operations the HI-TRAC VW annulus must be water filled. The necessary operational steps required to ensure this requirement are set forth in Chapter 9.

A 3-D FLUENT thermal model of the MPC is constructed in the same manner as described in Section 4.41. The principal input to this model is the effective conductivity of fuel under vacuum drying operations. To bound the vacuum drying operations the effective conductivity of fuel is computed assuming the MPC is filled with water vapor at a very low pressure (1 torr). The methodology for computing the effective conductivity is given in Section 4.4.1 and effective properties of design basis fuel under vacuum conditions tabulated in Table 4.5.8. To ensure a conservative evaluation the thermal model is incorporated with the following assumptions:

i. Bounding steady-state condition is reached with the MPC decay heat load set equal to the limiting heat load (Pattern A in Table 1.2.3a and 1.2.4) for MPCs fueled with Moderate Burnup Fuel and threshold heat load defined in Table 4.5.1 for MPCs fueled with one or more High Burnup fuel assemblies.

ii. The external surface of the MPC shell is postulated to be at the boiling temperature of water 100°C (212°F).

iii. The bottom surface of the MPC is insulated.

iv. MPC internal convection heat transfer is suppressed.

Results of vacuum condition analyses are provided in Subsection 4.5.4.1.

4.5.3 Maximum Time Limit During Wet Transfer Operations

In accordance with NUREG-1536, water inside the MPC cavity during wet transfer operations is not permitted to boil. This requirement is met by imposing time limits for fuel to remain submerged in water after a loaded HI-TRAC VW cask is removed from the pool.

Fuel loading operations are typically conducted with the HI-TRAC VW and its contents (water filled MPC) submerged in pool water. Under these conditions, the HI-TRAC VW is essentially at the pool water temperature. When the HI-TRAC VW transfer cask and the loaded MPC under water-flooded conditions is removed from the pool, the water, fuel, MPC and HI-TRAC VW metal absorb the decay heat emitted by the fuel assemblies. This results in a slow temperature rise of the HI-TRAC VW with time, starting from an initial (pool water) temperature. The rate of temperature rise is limited by the thermal inertia of the HI-TRAC VW system. To enable a bounding heat-up rate determination, the following conservative assumptions are utilized:

i. Heat loss by natural convection and radiation from the exposed HI-TRAC VW surfaces to ambient air is neglected (i.e., an adiabatic heat-up calculation is performed).

1 The MPC thermal model adopted for vacuum drying analysis in this sub-section includes the gap between the intersecting basket panels as 0.4 mm. A sensitivity study of the most limiting thermal scenario (least margins to fuel temperature limit) of vacuum drying condition is performed with this gap as 0.8 mm and discussed in Sub-section 4.5.4.4.

from the MPC cavity. In this case, relatively cooler water will enter via MPC lid ports and heated water will exit from the vent port. The minimum water flow rate required to maintain the MPC cavity water temperature below boiling with an adequate subcooling margin is determined as follows:

$$M_W = \frac{Q}{C_{pW}(T_{max} - T_{in})}$$

where:

M_W = minimum water flow rate (lb/hr)
C_{pw} = water heat capacity (Btu/lb-°F)
T_{max} = suitably limiting temperature below boiling (°F)
T_{in} = water supply temperature to MPC

4.5.4 Analysis of Limiting Thermal States During Short-Term Operations

4.5.4.1 Vacuum Drying

The vacuum drying option is evaluated for the two limiting scenarios defined in Section 4.5.2.2 to address Moderate Burnup Fuel under limiting heat load (Pattern A) and High Burnup Fuel under threshold heat load defined in Table 4.5.1 (MPC-37 and MPC-89) and Table 4.5.16 (MPC-32ML ~~and MPC-31C~~). The principle objective of the analysis is to ensure compliance with ISG-11 temperature limits. For this purpose 3-D FLUENT thermal models of the MPC-37, MPC-32ML~~, MPC-31C~~ and MPC-89 canisters are constructed as described in Section 4.5.2.2 and bounding steady state temperatures computed. The results are tabulated in Tables 4.5.6~~, and~~ 4.5.7 and~~,~~ 4.5.17 ~~and 4.5.18~~. The results show that the cladding temperatures comply with the ISG-11 limits for moderate and high burnup fuel in Table 4.3.1 by robust margins. The analysis presented above supports MPC drying options as summarized in Table 4.5.18~~9~~.

4.5.4.2 Forced Helium Dehydration

To reduce moisture to trace levels in the MPC using a Forced Helium Dehydration (FHD) system, a conventional, closed loop dehumidification system consisting of a condenser, a demoisturizer, a compressor, and a pre-heater is utilized to extract moisture from the MPC cavity through repeated displacement of its contained helium, accompanied by vigorous flow turbulation. Demoisturization to the 3 torr vapor pressure criteria required by NUREG 1536 is assured by verifying that the helium temperature exiting the demoisturizer is maintained at or below the psychrometric threshold of 21°F for a minimum of 30 minutes. Appendix 2.B of [4.1.8] provides a detailed discussion of the design criteria and operation of the FHD system.

The FHD system provides concurrent fuel cooling during the moisture removal process through forced convective heat transfer. The attendant forced convection-aided heat transfer occurring during operation of the FHD system ensures that the fuel cladding temperature will remain below the applicable peak cladding temperature limit in Table 2.2.3. Because the FHD operation induces a state of forced convection heat transfer in the MPC, (in contrast to the quiescent mode

Table 4.5.8

EFFECTIVE CONDUCTIVITY OF DESIGN BASIS FUEL~~Note 1~~ UNDER VACUUM DRYING OPERATIONS

(Btu/hr-ft-°F)

Ft. Calhoun 14x14Note 1		
Temperature (°F)	Planar	Axial
200	0.111	0.737
450	0.273	0.805
700	0.538	0.900
1000	0.977	1.040
Note 1: Ft. Calhoun 14x14 fuel is defined as the design basis fuel under the limiting condition of fuel storage in the minimum height MPC-37 (See Table 4.4.2).		
16x16DNote 2		
Temperature (°F)	Planar	Axial
212	0.095	0.8
450	0.229	0.867
700	0.458	0.962
785	0.558	1.003
~~VVER-1000~~Note 3		
~~Temperature (°F)~~	~~Planar~~	~~Axial~~
~~212~~	~~0.085~~	~~0.86~~
~~450~~	~~0.154~~	~~0.927~~
~~700~~	~~0.206~~	~~1.025~~
Note 2: Design Basis MPC-32ML fuel ~~Note 3: Design Basis MPC-31C fuel~~		

Table 4.5.16

THRESHOLD HEAT LOADS FOR VACUUM DRYING

MPC Type		Decay Heat Limit per Cell, kW	Number of Cells	Total Decay Heat Limit, kW
MPC-32ML (Note 1)	High Burnup Fuel	0.897	32	28.704

Note 1: Vacuum drying of Moderate Burnup Fuel permitted upto Design Basis heat load defined in Table 1.2.3b.

Table 4.5.17 MAXIMUM COMPONENT TEMPEARTURES UNDER VACUUM DRYING OPERATIONS OF MPC-32ML		
Component	**Temperature @ Threshold Heat (HBF) ºC (ºF)**	**Temperature @ Design Maximum Heat (MBF) ºC (ºF)**
Fuel Cladding	384 (723)	481 (898)
MPC Basket	368 (694)	461 (862)
Basket Periphery	304 (579)	369 (696)
Aluminum Basket Shims	263 (505)	314 (597)
MPC Shell	160 (320)	178 (352)
MPC Lid[1]	100 (212)	102 (216)

1 Maximum section average temperature is reported.

Table 4.5.18 MAXIMUM COMPONENT TEMPEARTURES DURING VACUUM DRYING OPERATIONS OF MPC-31C		
Component	**Temperature @ HBF Threshold Heat °C (°F)**	**Temperature @ MBF Threshold Heat °C (°F)**
Fuel Cladding	386 (727)	539 (1002)
MPC Basket	351 (664)	475 (887)
Basket Periphery	206 (403)	264 (507)
Aluminum Basket Shims	180 (356)	222 (432)
MPC Shell	131 (268)	144 (291)
MPC Lid[1]	100 (212)	112 (234)

1 Maximum section average temperature is reported.

Table 4.5.18~~9~~
MPC DRYING OPERATIONS

MPC Type	Fuel	Heat Load Limit (kW)	Method of Drying
MPC-32ML	MBF	44.16 (Note 1)	FHD/Vacuum Drying without Time Limit
	HBF	44.16 (Note 1)	FHD
		28.704	FHD/Vacuum Drying without Time Limit
MPC-37	MBF	44.09 (Pattern A) 45.0 (Pattern B) (Note 1)	FHD/Vacuum Drying without Time Limit
	HBF	44.09 (Pattern A) 45.0 (Pattern B) (Note 1)	FHD
		34.36	FHD/Vacuum Drying without Time Limit
MPC-89	MBF	46.36 (Note 1)	FHD/Vacuum Drying without Time Limit
	HBF	46.36 (Note 1)	FHD
		34.75	FHD/Vacuum Drying without Time Limit

Note 1: Design Basis heat load.
Note 2:Cyclic drying under time limited vacuum drying operations is permitted in accordance with ISG-11, Rev. 3 requirements by limiting number of cycles to less than 10 and cladding temperature variations to less than 65°C (117°F). Suitable time limits for these cycles shall be evaluated based on site specific conditions and thermal methodology defined in Section 4.5.

[4.2.4] Rust, J.H., "Nuclear Power Plant Engineering," Haralson Publishing Company, (1979).

[4.2.5] Kern, D.Q., "Process Heat Transfer," McGraw Hill Kogakusha, (1950).

[4.2.6] "Metamic-HT Qualification Sourcebook", Holtec Report HI-2084122, Latest Revision.

[4.2.7] "Spent Nuclear Fuel Effective Thermal Conductivity Report," US DOE Report BBA000000-01717-5705-00010 REV 0, (July 11, 1996).

[4.2.8] ASME Boiler and Pressure Vessel Code, Section II, Part D, (1995).

[4.2.9] Jakob, M. and Hawkins, G.A., "Elements of Heat Transfer," John Wiley & Sons, New York, (1957).

[4.2.10] ASME Steam Tables, 3rd Edition (1977).

[4.2.11] "Nuclear Systems Materials Handbook, Vol. 1, Design Data", ORNL TID 26666.

[4.2.12] "Scoping Design Analyses for Optimized Shipping Casks Containing 1-, 2-, 3-, 5-, 7-, or 10-Year-Old PWR Spent Fuel", ORNL/CSD/TM-149 TTC-0316, (1983).

[4.2.13] Not used.

[4.2.14] Not used.

[4.2.15] Not used.

[4.2.16] USNRC Docket no 72-1027, TN-68 FSAR & Docket no 72-1021 TN-32 FSAR.

[4.2.17] Hagrman, Reymann and Mason, "MATPRO-Version 11 (Revision 2) A Handbook of Materials Properties for Use in the Analysis of Light Water Reactor Fuel Rod Behavior," NUREG/CR-0497, Tree 1280, Rev. 2, EG&G Idaho, August 1981.

[4.2.18] "Effective Thermal Conductivity and Edge Conductance Model for a Spent-Fuel Assembly," R. D. Manteufel & N. E. Todreas, Nuclear Technology, 105, 421- 440, (March 1994).

[4.2.19] Aluminum Alloy 2219 Material Data Sheet, ASM Aerospace Specification Metals, Inc., Pompano Beach, FL.

[4.2.20] "Spacecraft Thermal Control Coatings References", NASA Publication NASA/TP-2005-212792, December 2005.

[4.2.21] "Thermal Radiation Heat Transfer", Third Edition, Robert Siegel and John R. Howell.

[4.4.1] NUREG-1536, "Standard Review Plan for Dry Cask Storage Systems," USNRC, (January 1997).

[4.4.2] "Pressure Loss Charactersistics for In-Cell Flow of Helium in PWR and BWR Storage Cells", Holtec Report HI-2043285, Revision 6, Holtec International, Marlton, NJ, 08053.

[4.4.3] "Standard for Verification and Validation in Computational Fluid Dynamics and Heat Transfer", ASME V&V 20-2009.

[4.5.1] "Procedure for Estimating and Reporting of Uncertainty due to Discretization in CFD Applications", I.B. Celik, U. Ghia, P.J. Roache and C.J. Freitas (Journal of Fluids Engineering Editorial Policy on the Control of Numerical Accuracy).

[4.6.1] United States Code of Federal Regulations, Title 10, Part 71.

[4.6.2] Gregory, J.J. et. al., "Thermal Measurements in a Series of Large Pool Fires", SAND85-1096, Sandia National Laboratories, (August 1987).

CHAPTER 5†: SHIELDING EVALUATION

5.0 INTRODUCTION

The shielding analysis of the HI-STORM FW system is presented in this chapter. As described in Chapter 1, the HI-STORM FW system is designed to accommodate both PWR and BWR MPCs within HI-STORM FW overpacks (see Table 1.0.1).

In addition to storing intact PWR and BWR fuel assemblies, the HI-STORM FW system is designed to store BWR and PWR damaged fuel assemblies and fuel debris. Damaged fuel assemblies and fuel debris are defined in Subsection 2.1. Both damaged fuel assemblies and fuel debris are required to be loaded into Damaged Fuel Containers (DFCs).

As described in Chapter 2 (see Table 2.1.1), MPC-37 and MPC-32ML are designed to store various PWR fuel assembly classes. In this chapter, shielding analyses are mainly performed for MPC-37 (for PWR fuel assemblies) since most PWR fuel assemblies can be loaded into MPC-37. Nevertheless, shielding analysis for adjacent and 1-m dose rates for HI-STORM FW cask with MPC-32ML loaded with 16x16D fuel assemblies are included in this chapter, to show the radiation shielding features of the cask system is enough to meet the requirements of 10CFR72.104 and 72.106. Site specific analyses need to use the site specific MPC and fuel type for controlled area boundary dose calculations to show the site's compliance with 10 CFR 72.104. Also, as discussed in Section 5.1, the burnup and cooling times selected for accident conditions represent reasonable upper bound limit, and the heavy metal mass in MPC-32ML is comparable to that in MPC-37. -This is confirmed by source terms for accident-condition design basis fuel burnup, cooling time combination, as provided in Section 5.2 for fuel assembly in MPC-37 and MPC-32ML. Therefore, it is concluded that the accident condition evaluated in this chapter for MPC-37 is reasonably conservative, and no further site's compliance with 10 CFR 72.106 is required for MPC-32ML, except for the fuel assemblies in MPC-32ML with a higher burnup than the design basis accident-condition burnup. More detail is provided in Subsection 5.1.2.

PWR fuel assemblies may contain burnable poison rod assemblies (BPRAs), with any number of full-length rods and thimble plug rodlets in the locations without a full-length rod, thimble plug devices (TPDs), control rod assemblies (CRAs) or axial power shaping rod assemblies (APSRs), neutron source assemblies (NSAs), or similarly named devices. These non-fuel hardware devices are an integral yet removable part of PWR fuel assemblies and therefore the HI-STORM FW

† This chapter has been prepared in the format and section organization set forth in Regulatory Guide 3.61. However, the material content of this chapter also fulfills the requirements of NUREG-1536. Pagination and numbering of sections, figures, and tables are consistent with the convention set down in Chapter 1, Section 1.0, herein. Finally, all terms-of-art used in this chapter are consistent with the terminology of the glossary and component nomenclature of the Bill-of-Materials (Section 1.5).

system has been designed to store PWR fuel assemblies with or without these devices. Since each device occupies the same location within a fuel assembly, a single PWR fuel assembly will not contain multiple devices, with the exception of instrument tube tie rods (ITTRs), which may be stored in the assembly along with other types of non-fuel hardware.

As described in Chapter 1(see Tables 1.2.3 and 1.2.4), the loading of fuel in all HI-STORM FW MPCs will follow specific heat load limitations.

In order to offer the user more flexibility in fuel storage, the HI-STORM FW System offers two heat load patterns, each with a three-region loading configuration, in the MPC-37. The MPC-89 has one heat load pattern with a three-region loading configuration. The regionalized storage patterns are guided by the considerations of minimizing occupational and site boundary dose to comply with ALARA principles.

The sections that follow will demonstrate that the design of the HI-STORM FW dry cask storage system fulfills the following acceptance criteria outlined in the Standard Review Plan, NUREG-1536 [5.2.1]:

Acceptance Criteria

1. The minimum distance from each spent fuel handling and storage facility to the controlled area boundary must be at least 100 meters. The “controlled area” is defined in 10CFR72.3 as the area immediately surrounding an ISFSI or monitored retrievable storage (MRS) facility, for which the licensee exercises authority regarding its use and within which ISFSI operations are performed.

2. The system designer must show that, during both normal operations and anticipated occurrences, the radiation shielding features of the proposed dry cask storage system are sufficient to meet the radiation dose requirements in Sections 72.104(a). Specifically, the vendor must demonstrate this capability for a typical array of casks in the most bounding site configuration. For example, the most bounding configuration might be located at the minimum distance (100 meters) to the controlled area boundary, without any shielding from other structures or topography.

3. Dose rates from the cask must be consistent with a well established “as low as reasonably achievable” (ALARA) program for activities in and around the storage site.

4. After a design-basis accident, an individual at the boundary or outside the controlled area shall not receive a dose greater than the limits specified in 10CFR72.106.

5. The proposed shielding features must ensure that the dry cask storage system meets the regulatory requirements for occupational and radiation dose limits for individual members of the public, as prescribed in 10CFR Part 20, Subparts C and D.

Consistent with the Standard Review Plan, NUREG-1536, this chapter contains the following information:

- A description of the shielding features of the HI-STORM FW system, including the HI-TRAC transfer cask.
- A description of the source terms.
- A general description of the shielding analysis methodology.
- A description of the analysis assumptions and results for the HI-STORM FW system, including the HI-TRAC transfer cask.
- Analyses are presented for each MPC showing that the radiation dose rates follow As-Low-As-Reasonably-Achievable (ALARA) practices.
- Analyses to show that the 10CFR72.106 controlled area boundary radiation dose limits can be met during accident conditions of storage for non-effluent radiation from illustrative ISFSI configurations at a minimum distance of 100 meters. Since only representative dose rate values for normal conditions are presented for this chapter, compliance with the radiation and exposure objectives of 10CFR72.104 is not being evaluated herein but will be performed as part of the site specific evaluations.

Chapter 2 contains a detailed description of structures, systems, and components important to safety.

Chapter 7 contains a discussion on the release of radioactive materials from the HI-STORM FW system. Therefore, this chapter only calculates the dose from direct neutron and gamma radiation emanating from the HI-STORM FW system.

Chapter 11, Radiation Protection, contains the following information:

- A discussion of the estimated occupational exposures for the HI-STORM FW system, including the HI-TRAC transfer cask.
- A summary of the estimated radiation exposure to the public.

The safety analyses summarized in this chapter demonstrate that under accident conditions, acceptable margins to allowable limits exist under all design basis loading conditions. For normal and off-normal conditions, the analyses in this chapter simply provide a generic evaluation that demonstrates that the dose requirements as specified in 10CFR72.104 can be met under site specific conditions. Minor changes to the design parameters that inevitably occur during the product's life cycle which are treated within the purview of 10CFR72.48 and are ascertained to have an insignificant effect on the computed dose rates in this chapter may not prompt a formal

reanalysis and revision of the results and associated data in the tables of this chapter unless the cumulative effect of all such unquantified changes cannot be deemed any more to be insignificant. For accident conditions, the dose limit as specified in 10CFR72.106 is 5 rem. The only accident which impacts dose rates is the loss of water in the water jacket for the HI-TRAC VW. For the purposes of determining if the changes to the HI-TRAC VW are insignificant, an insignificant loss of margin with reference to the 5 rem acceptance criteria is defined as the estimated reduction that is no more than one order of magnitude less than the available margin reported in the FSAR. For normal and off-normal conditions, site specific dose evaluations are required to demonstrate compliance with 10CFR72.104. Incorporating any minor changes into those site specific evaluations is only warranted if it would be expected, on a site specific basis, that those changes could result in a situation where the limits are no longer met and where therefore other compensatory measures are required, such as a change in the loading plan or the concrete density. Incorporating changes into the analyses in this chapter for normal and off-normal conditions will only be performed under extenuating circumstances, e.g. major changes to the shielding design, in order to provide an updated template for the site specific dose analyses.

To ensure rigorous configuration control, the information in the Licensing drawings in Section 1.5 should be treated as the authoritative source for numerical analysis at all times. Reliance on the input data and associated results in this chapter for additional mathematical computations may not be appropriate as they serve the sole purpose of establishing safety compliance in accordance with the acceptance criteria set down in Chapter 2 and in this chapter.

5.1 DISCUSSION AND RESULTS

The principal sources of radiation in the HI-STORM FW system are:

- Gamma radiation originating from the following sources:

  1. Decay of radioactive fission products
  2. Secondary photons from neutron capture in fissile and non-fissile nuclides
  3. Hardware activation products generated during core operations

- Neutron radiation originating from the following sources

  1. Spontaneous fission
  2. α,n reactions in fuel materials
  3. Secondary neutrons produced by fission from subcritical multiplication
  4. γ,n reactions (this source is negligible)

During loading, unloading, and transfer operations, shielding from gamma radiation is provided by the stainless steel structure and the basket of the MPC and the steel, lead, and water in the HI-TRAC transfer cask. For storage, the gamma shielding is provided by the MPC, and the steel and concrete ("Metcon" structure) of the overpack. Shielding from neutron radiation is provided by the concrete of the overpack during storage and by the water of the HI-TRAC transfer cask during loading, unloading, and transfer operations. It is worth noting that the models, used to evaluate the dose calculations in this chapter, are constructed with minimum concrete densities and minimum lead thicknesses.

The shielding analyses were performed with MCNP5 [5.1.1] developed by Los Alamos National Laboratory (LANL). The source terms for the design basis fuels were calculated with the SAS2H and ORIGEN-S sequences from the SCALE 5 system [5.1.2, 5.1.3]. A detailed description of the MCNP models and the source term calculations are presented in Sections 5.3 and 5.2, respectively.

The design basis zircaloy clad fuel assemblies used for calculating the dose rates presented in this chapter are Westinghouse (W) 17x17 and the General Electric (GE) 10x10, for PWR (in MPC-37) and BWR fuel types, respectively. 16x16D is the design basis fuel assembly for PWR in MPC-32ML. Required site specific shielding evaluations will verify whether those assemblies and assembly parameters are appropriate for the site-specific analyses. Subsection 2.1 specifies the acceptable fuel characteristics, including the acceptable maximum burnup levels and minimum cooling times for storage of fuel in the HI-STORM FW MPCs.

The following presents a discussion that explains the rationale behind the burnup and cooling time combinations that are evaluated in this chapter for normal and accident conditions.

10CFR72 contains two sections that set down main dose rate requirements: §104 for normal and off-normal conditions, and §106 for accident conditions. The relationship of these requirements to the analyses in this Chapter 5, and the burnup and cooling times selected for the various analyses, are as follows:

- 10CFR72.104 specifies the dose limits from an ISFSI (and other operations) at a site boundary under normal and off-normal conditions. Compliance with §104 can therefore only be demonstrated on a site-specific basis, since it depends not only on the design of the cask system and the loaded fuel, but also on the ISFSI layout, the distance to the site boundary, and possibly other factors such as use of higher density concrete or the terrain around the ISFSI. The purpose of this chapter is therefore to present a general overview over the expected dose rates, next to the casks and at various distances, to aid the user in applying ALARA considerations and planning of the ISFSI. To that extent, it is sufficient to present reasonably conservative dose rate values, based on a reasonable conservative choice of burnups and cooling times of the assemblies.
- For the accident dose limit in 10CFR72.106 it is desirable to show compliance in this Chapter 5 on a generic basis, so that calculations on a site-by-site basis are not required.[†] To that extend, a burnup and cooling time calculation that maximizes the dose rate under accident conditions needs to be selected.

The HI-STORM FW System offers three-region loading configurations for MPC-37 and MPC-89 as shown in Table 1.2.3a and Table 1.2.4 in Chapter 1. The uniform loading configuration for MPC-32ML is shown in Table 1.2.3b.

- For the MPC-37, there are two heat load patterns, each with a three-region loading configuration – Loading Pattern A and Loading Pattern B. An important difference between Pattern A and Pattern B loading is the loading is the maximum allowed heat load of the cells on the periphery of the MPC-37. Pattern A contains the cells with the lowest decay heat on the periphery, while Pattern B contains the cells with the highest decay heat on the periphery. In Pattern A, fuel assemblies with higher heat loads are loaded in the inner region allowing the user to take advantage of self-shielding from the fuel assemblies with lower heat loads in the outer regions. However, for Pattern B, the fuel assemblies with the higher heat loads could be loaded in the outer region (Region 3). Based on this difference it is expected that Pattern B will have higher dose rates than Pattern A. Therefore, for dose calculations Pattern B is selected, as it is the more limiting of the two loading patterns. Furthermore, uniform loading of MPC-37 cells is assumed for dose calculations. The burnup and cooling time combination is selected as representative of the cells on the periphery. This is a conservative approach, as it assumes that all thirty seven cells have a decay heat per cell equal to or slightly exceeding the decay heat of the periphery cells.

[†] As it is discussed in Subsection 5.1.2, a site-specific shielding evaluation may be required for accident-condition of MPC-32ML.

- For the MPC-89, there is only one heat load pattern with a three-region loading configuration. Based on the configuration for the MPC-89, fuel assemblies with higher heat loads would be loaded in the inner region allowing the user to take advantage of self-shielding from fuel assemblies with lower heat loads in the outer regions (see Table 1.2.4). However, for simplification, the shielding analyses are performed for a single region, i.e. assuming all assemblies in the basket have the same burnup and cooling time. In the case of the MPC-89 the burnup and cooling time combination is selected as a representative average for the entire basket.

- For the MPC-32ML, there is only one heat load pattern with a uniform loading configuration. The design basis burnup, enrichment, cooling time combination has the same burnup and enrichment as the design basis fuel combination for MPC-37, but with slightly longer cooling time. The fuel combination heat load is more than the decay heat limit per cell. Furthermore, since different burnup, enrichment and cooling time combinations may produce same decay heat, but different source terms, additional regionalized shielding analysis is performed by dividing the basket cells into Regions 1 to 3, where Region 1 is the innermost cells, and Region 3 is the outermost cells. The detail of this additional analysis is provided in Subsection 5.4.6.

While Loading Pattern B for the MPC-37 allows assemblies with higher heat loads and therefore higher source terms in the outer region (Region 3) of the MPC, the guiding principle in selecting fuel loading should still be to preferentially place assemblies with higher source terms in the inner regions of the basket as far as reasonably possible.

It is recognized that for a given heat load, an infinite number of burnup and cooling time combination could be selected, which would result in slightly different dose rate distributions around the cask. For a high burnup with a corresponding longer cooling time, dose locations with a high neutron contribution would show higher dose values, due to the non-linear relationship between burnup and neutron source term. At other locations dose rates are more dominated by contribution from the gamma sources. In these cases, short cooling time and lower burnup combinations with heat load comparable to the higher burnup and corresponding longer cooling time combinations would result in higher dose rates. However, in those cases, there would always be a compensatory effect, since for each dose location, higher neutron dose rates would be partly offset by lower gamma dose rates and vice versa.

Based on these considerations, average burnup and cooling time values are selected for all calculations for normal conditions, i.e values that are away from the extreme values. The selected values are shown in Table 5.0.1, and are based on a total heat loads presented in Table 1.2.3. For the accident conditions however, it is recognized that the bounding accident condition is the loss of water in the HI-TRAC VW, a condition that is neutron dominated due to the removal of the principal neutron absorber in the HI-TRAC VW (water). For this case, the upper bound burnup is selected, in order to maximize the neutron source strength of all assemblies in the basket, and a corresponding higher cooling time is selected in order to meet the overall heat load limit in the cask. The resulting burnup and cooling times values for accidents are therefore different from

those for normal conditions and are listed in Table 5.0.2. In all cases, low initial enrichments are selected, which further increases the neutron source terms from the assemblies

With the burnup and cooling times selected based on above considerations, dose rates calculated for normal conditions will be reasonably conservative, while for accident conditions those will represent reasonable upper bound limits.

Table 5.0.1

DESIGN BASIS FUEL BURNUP, COOLING TIME AND ENRICHMENT FOR NORMAL CONDITIONS

Design Basis Burnup and Cooling Times Zircaloy Clad Fuel		
MPC-37	**MPC-89**	**MPC-32ML**
45,000 MWD/MTU 4.5 Year Cooling 3.6 wt% U-235 Enrichment	45,000 MWD/MTU 5 Year Cooling 3.2 wt% U-235 Enrichment	45,000 MWD/MTU 4.6 Year Cooling 3.6 wt% U-235 Enrichment

Table 5.0.2

DESIGN BASIS FUEL BURNUP, COOLING TIME AND ENRICHMENT FOR ACCIDENT CONDITIONS

Design Basis Burnup and Cooling Times Zircaloy Clad Fuel		
MPC-37	**MPC-89**	**MPC-32ML**
65,000 MWD/MTU 8 Year Cooling 4.8 wt% U-235 Enrichment	65,000 MWD/MTU 10 Year Cooling 4.8 wt% U-235 Enrichment	62,500 MWD/MTU 8 Year Cooling 4.6 wt% U-235 Enrichment

5.1.1 Normal and Off-Normal Operations

Chapter 12 discusses the potential off-normal conditions and their effect on the HI-STORM FW system. None of the off-normal conditions have any impact on the shielding analysis. Therefore, off-normal and normal conditions are identical for the purpose of the shielding evaluation.

The 10CFR72.104 criteria for radioactive materials in effluents and direct radiation during normal operations are:

1. During normal operations and anticipated occurrences, the annual dose equivalent to any real individual who is located beyond the controlled area, must not exceed 25 mrem to the whole body, 75 mrem to the thyroid and 25 mrem to any other critical organ.

2. Operational restrictions must be established to meet as low as reasonably achievable (ALARA) objectives for radioactive materials in effluents and direct radiation.

10CFR20 Subparts C and D specify additional requirements for occupational dose limits and radiation dose limits for individual members of the public. Chapter 11 specifically addresses these regulations.

In accordance with ALARA practices, design objective dose rates are established for the HI-STORM FW system and presented in Table 2.3.2.

Figure 5.1.1 identifies the locations of the dose points referenced in the dose rate summary tables for the HI-STORM FW overpack. Dose Point #2 is located on the side of the cask at the axial mid-height. Dose Points #1 and #3 are the locations of the inlet and outlet air ducts, respectively. The dose values reported for these locations (adjacent and 1 meter) were averaged over the duct opening. Dose Point #4 is the dose location on the overpack lid. The dose values reported at the locations shown on Figure 5.1.1 are averaged over a region that is approximately 1 foot in width.

Figure 5.1.2 identifies the location of the dose points for the HI-TRAC VW transfer cask. Dose Point Locations #1 and #3 are situated below and above the water jacket, respectively. Dose Point #4 is the dose location on the HI-TRAC VW lid and dose rates below the HI-TRAC VW are estimated with Dose Point #5. Dose Point Location #2 is situated on the side of the cask at the axial mid-height.

The total dose rates presented are presented for two cases: with and without BPRAs. The dose from the BPRAs was conservatively assumed to be the maximum calculated in Subsection 5.2.4.

Tables 5.1.1 and 5.1.2 provides dose rates adjacent to and one meter from the HI-TRAC VW during normal conditions for the MPC-37 and MPC-89. The dose rates listed in Table 5.1.1 correspond to the normal condition in which the MPC is dry and the HI-TRAC water jacket is filled with water.

Tables 5.1.5 ~~and~~, 5.1.6 and 5.1.10 provide the design basis dose rates adjacent to the HI-STORM FW overpack during normal conditions for the MPC-37 ~~and~~, MPC-89 and MPC-32ML. Tables 5.1.7 ~~and~~, 5.1.8 and 5.1.11 provide the design basis dose rates at one meter from the HI-STORM FW overpack containing the MPC-37, ~~and~~ MPC-89 and MPC-32ML, respectively.

It should be noted that since adjacent and 1-m dose rates of HI-STORM FW with MPC-32ML are comparable with those with MPC-37, it is concluded that the dose rates around the HI-TRAC VW with MPC-32ML are also comparable with those with MPC-37. Also, the lead thickness of the HI-TRAC VW varies from one plant to another plant. Thus, no additional shielding calculation is performed in this chapter for HI-TRAC VW with MPC-32ML.

The dose to any real individual at or beyond the controlled area boundary is required to be below 25 mrem per year. The minimum distance to the controlled area boundary is 100 meters from the ISFSI. Table 5.1.3 presents the annual dose to an individual from a single HI-STORM FW cask and various storage cask arrays, assuming an 8760 hour annual occupancy at the dose point location. The minimum distance required for the corresponding dose is also listed. It is noted that these data are provided for illustrative purposes only. A detailed site-specific evaluation of dose at the controlled area boundary must be performed for each ISFSI in accordance with 10CFR72.212. The site-specific evaluation will consider dose from other portions of the facility and will consider the actual conditions of the fuel being stored (burnup and cooling time).

Figure 5.1.3 is an annual dose versus distance graph for the HI-STORM FW cask array configurations provided in Table 5.1.3. This curve, which is based on an 8760 hour occupancy, is provided for illustrative purposes only and will be re-evaluated on a site-specific basis.

Subsection 5.2.3 discusses the BPRAs, TPDs, CRAs and APSRs that are permitted for storage in the HI-STORM FW system. Subsection 5.4.4 discusses the increase in dose rate as a result of adding non-fuel hardware in the MPCs.

The analyses summarized in this section demonstrate that the HI-STORM FW system is in compliance with the radiation and exposure objectives of 10CFR72.106. Since only representative dose rate values for normal conditions are presented in this chapter, compliance with 10CFR72.104 is not being evaluated. This will be performed as part of the site specific evaluations.

5.1.2 Accident Conditions

The 10CFR72.106 radiation dose limits at the controlled area boundary for design basis accidents are:

> Any individual located on or beyond the nearest boundary of the controlled area may not receive from any design basis accident the more limiting of a total effective dose equivalent of 5 Rem, or the sum of the deep-dose equivalent and the committed dose

equivalent to any individual organ or tissue (other than the lens of the eye) of 50 Rem. The lens dose equivalent shall not exceed 15 Rem and the shallow dose equivalent to skin or to any extremity shall not exceed 50 Rem. The minimum distance from the spent fuel or high-level radioactive waste handling and storage facilities to the nearest boundary of the controlled area shall be at least 100 meters.

Structural evaluations, presented in Chapter 3, shows that a freestanding HI-STORM FW storage overpack containing a loaded MPC remains standing during events that could potentially lead to a tip-over event. Therefore, the tip-over accident is not considered as part of the shielding evaluation.

Design basis accidents which may affect the HI-STORM FW overpack can result in limited and localized damage to the outer shell and radial concrete shield. As the damage is localized and the vast majority of the shielding material remains intact, the effect on the dose at the site boundary is negligible. Therefore, the site boundary doses for the loaded HI-STORM FW overpack for accident conditions are equivalent to the normal condition doses, which meet the 10CFR72.106 radiation dose limits. However the adjacent and one meter dose rates may be increased, which should be considered in any post-accident activities near the affected cask.

The design basis accidents analyzed in Chapter 11 have one bounding consequence that affects the shielding materials of the HI-TRAC transfer cask. It is the potential for damage to the water jacket shell and the loss of the neutron shield (water). In the accident consequence analysis, it is conservatively assumed that the neutron shield (water) is completely lost and replaced by a void.

Throughout all design basis accident conditions the axial location of the fuel will remain fixed within the MPC because of the MPC's design features (see Chapter 1). Further, the structural evaluation of the HI-TRAC VW in Chapter 3 shows that the inner shell, lead, and outer shell remain intact throughout all design basis accident conditions. Localized damage of the HI-TRAC outer shell is possible; however, localized deformations will have only a negligible impact on the dose rate at the boundary of the controlled area.

The complete loss of the HI-TRAC neutron shield significantly affects the dose at mid-height (Dose Point #2) adjacent to the HI-TRAC. Loss of the neutron shield has a small effect on the dose at the other dose points. To illustrate the impact of the design basis accident, the dose rates at Dose Point #2 (see Figure 5.1.2) are provided in Table 5.1.4 (MPC-37) for the HI-TRAC VW at a distance of 1 meter and at a distance of 100 meters. The normal condition dose rates are provided for reference. The dose for a period of 30 days is shown in Table 5.1.9, where 30 days is used to illustrate the radiological impact for a design basis accident. Based on this dose rate and the short duration of use for the loaded HI-TRAC transfer cask, it is evident that the dose as a result of the design basis accident cannot exceed 5 rem at the controlled area boundary for the short duration of the accident.

Analyses summarized in this section demonstrate that the HI-STORM FW system, including the HI-TRAC VW transfer cask, is in compliance with the 10CFR72.106 limits. It should be noted

that, as a defense in depth, site-specific shielding evaluation shall be performed if there is any fuel to be loaded into MPC-32ML with a burnup more than the design basis accident-condition burnup for MPC-32ML in Table 5.0.2.

Table 5.1.1

DOSE RATES FROM THE HI-TRAC VW FOR NORMAL CONDITIONS
MPC-37 DESIGN BASIS FUEL
45,000 MWD/MTU AND 4.5-YEAR COOLING

Dose Point Location	Fuel Gammas (mrem/hr)	(n,γ) Gammas (mrem/hr)	^{60}Co Gammas (mrem/hr)	Neutrons (mrem/hr)	Totals (mrem/hr)	Totals with BPRAs (mrem/hr)
ADJACENT TO THE HI-TRAC VW						
1	975	25	808	67	1874	1874
2	2939	75	<1	154	3169	3169
3	20	5	339	6	371	561
4	98	1	530	225	854	1147
5	940	3	2074	1022	4038	4038
ONE METER FROM THE HI-TRAC VW						
1	695	12	99	30	835	835
2	1382	22	10	58	1472	1474
3	268	6	142	9	425	501
4	80	<1	295	73	449	613
5	470	1	1129	297	1897	1897

Notes:

- Refer to Figure 5.1.2 for dose locations.
- Values are rounded to nearest integer.
- Dose rates are based on no water within the MPC, an empty annulus, and a water jacket full of water. For the majority of the duration that the HI-TRAC bottom lid is installed, the MPC cavity will be flooded with water. The water within the MPC greatly reduces the dose rate.
- Streaming may occur through the annulus. However, during handling/operations the annulus is filled with water and lead snakes are typically present to reduce the streaming effects. Further, operators are not present on top of the transfer cask.
- The "Fuel Gammas" category includes gammas from the spent fuel, ^{60}Co from the spacer grids, and ^{60}Co from the BPRAs in the active fuel region.

Table 5.1.2

DOSE RATES FROM THE HI-TRAC VW FOR NORMAL CONDITIONS
MPC-89 DESIGN BASIS FUEL
45,000 MWD/MTU AND 5-YEAR COOLING

Dose Point Location	Fuel Gammas (mrem/hr)	(n,γ) Gammas (mrem/hr)	^{60}Co Gammas (mrem/hr)	Neutrons (mrem/hr)	Totals (mrem/hr)
ADJACENT TO THE HI-TRAC VW					
1	244	18	2247	40	2549
2	2466	107	<1	219	2793
3	3	3	581	4	591
4	25	<1	505	138	669
5	132	2	2135	720	2989
ONE METER FROM THE HI-TRAC VW					
1	411	13	291	29	744
2	1142	30	21	74	1267
3	119	5	280	8	412
4	16	<1	300	43	360
5	79	<1	1202	202	1484

Notes:

- Refer to Figure 5.1.2 for dose locations.
- Values are rounded to nearest integer.
- Dose rates are based on no water within the MPC, an empty annulus, and a water jacket full of water. For the majority of the duration that the HI-TRAC bottom lid is installed, the MPC cavity will be flooded with water. The water within the MPC greatly reduces the dose rate.
- Streaming may occur through the annulus. However, during handling/operations the annulus is filled with water and lead snakes are typically present to reduce the streaming effects. Further, operators are not present on top of the transfer cask.
- The "Fuel Gammas" category includes gammas from the spent fuel and ^{60}Co from the spacer grids.

Table 5.1.3

DOSE RATES FOR ARRAYS OF HI-STORM FWs with MPC-37

Array Configuration	1 cask	2x2	2x3	2x4	2x5
HI-STORM FW Overpack					
45,000 MWD/MTU AND 4.5-YEAR COOLING					
Annual Dose (mrem/year)	18	15	23	11	14
Distance to Controlled Area Boundary (meters)	300	400	400	500	500

Notes:

- Values are rounded to nearest integer.
- 8760 hour annual occupancy is assumed.
- Dose location is at the center of the long side of the array.

Table 5.1.4

DOSE RATES FROM HI-TRAC VW WITH MPC-37
FOR ACCIDENT CONDITIONS
AT BOUNDING BURNUP AND COOLING TIMES

Dose Point Location	Fuel Gammas (mrem/hr)	(n,γ) Gammas (mrem/hr)	^{60}Co Gammas (mrem/hr)	Neutrons (mrem/hr)	Totals (mrem/hr)	Totals with BPRAs (mrem/hr)
ONE METER FROM HI-TRAC VW						
65,000 MWD/MTU AND 8-YEAR COOLING						
2 (Accident Condition)	1735	3	13	2651	4403	4407
2 (Normal Condition)	893	50	7	122	1071	1074
100 METERS FROM HI-TRAC VW						
65,000 MWD/MTU AND 8-YEAR COOLING						
2 (Accident Condition)	0.7	<0.1	0.1	1.4	2.3	2.4

Notes:

- Refer to Figure 5.1.2 for dose locations.
- Values are rounded to nearest integer where appropriate.
- The "Fuel Gammas" category includes gammas from the spent fuel, ^{60}Co from the spacer grids, and ^{60}Co from the BPRAs in the active fuel region.

Table 5.1.5

DOSE RATES ADJACENT TO HI-STORM FW OVERPACK
FOR NORMAL CONDITIONS
MPC-37
BURNUP AND COOLING TIME
45,000 MWD/MTU AND 4.5-YEAR COOLING

Dose Point Location	Fuel Gammas (mrem/hr)	(n,γ) Gammas (mrem/hr)	^{60}Co Gammas (mrem/hr)	Neutrons (mrem/hr)	Totals (mrem/hr)	Totals with BPRAs (mrem/hr)
1	273	2	14	4	292	292
2	135	1	<1	1	141	141
3 (surface)	11	1	25	2	39	53
3 (overpack edge)	13	<1	63	1	78	113
4 (center)	<1	1	<1	<1	<4	<4
4 (mid)	1	1	4	1	7	10
4 (outer)	10	<1	30	<1	42	59

Notes:

- Refer to Figure 5.1.1 for dose locations.
- Values are rounded to nearest integer where appropriate.
- Dose location 3 (surface) is at the surface of the outlet vent. Dose location 3 (overpack edge) is in front of the outlet vent, but located radially above the overpack outer diameter.
- Dose location 4 (center) is at the center of the top surface of the top lid. Dose location 4 (mid) is situated directly above the vertical section of the outlet vent. Dose location 4 (outer) is extended along the top plane of the top lid, located radially above the overpack outer diameter.
- The "Fuel Gammas" category includes gammas from the spent fuel, ^{60}Co from the spacer grids, and ^{60}Co from the BPRAs in the active fuel region.

Table 5.1.6

DOSE RATES ADJACENT TO HI-STORM FW OVERPACK
FOR NORMAL CONDITIONS
MPC-89
BURNUP AND COOLING TIME
45,000 MWD/MTU AND 5-YEAR COOLING

Dose Point Location	**Fuel Gammas (mrem/hr)**	**(n,γ) Gammas (mrem/hr)**	**^{60}Co Gammas (mrem/hr)**	**Neutrons (mrem/hr)**	**Totals (mrem/hr)**
1	172	2	31	3	208
2	92	2	<1	1	96
3 (surface)	3	<1	29	2	35
3 (overpack edge)	5	<1	69	<1	76
4 (center)	0.1	0.4	0.4	0.1	1
4 (mid)	0.2	0.5	4.3	0.5	6
4 (outer)	2	<1	33	<1	37

Notes:

- Refer to Figure 5.1.1 for dose locations.
- Values are rounded to nearest integer where appropriate.
- Dose location 3 (surface) is at the surface of the outlet vent. Dose location 3 (overpack edge) is in front of the outlet vent, but located radially above the overpack outer diameter.
- Dose location 4 (center) is at the center of the top surface of the top lid. Dose location 4 (mid) is situated directly above the vertical section of the outlet vent. Dose location 4 (outer) is extended along the top plane of the top lid, located radially above the overpack outer diameter.
- The "Fuel Gammas" category includes gammas from the spent fuel and ^{60}Co from the spacer grids.

Table 5.1.7

DOSE RATES AT ONE METER FROM HI-STORM FW OVERPACK
FOR NORMAL CONDITIONS
MPC-37
BURNUP AND COOLING TIME
45,000 MWD/MTU AND 4.5-YEAR COOLING

Dose Point Location	**Fuel Gammas (mrem/hr)**	**(n,γ) Gammas (mrem/hr)**	**^{60}Co Gammas (mrem/hr)**	**Neutrons (mrem/hr)**	**Totals (mrem/hr)**	**Totals with BPRAs (mrem/hr)**
1	57	1	4	1	62	62
2	75	1	1	1	77	78
3	6	<1	5	<1	13	15
4 (center)	0.6	0.3	1.0	0.2	2.1	2.7

Notes:

- Refer to Figure 5.1.1 for dose locations.
- Values are rounded to nearest integer where appropriate.
- The "Fuel Gammas" category includes gammas from the spent fuel, ^{60}Co from the spacer grids, and ^{60}Co from the BPRAs in the active fuel region.

Table 5.1.8

DOSE RATES AT ONE METER FROM HI-STORM FW OVERPACK
FOR NORMAL CONDITIONS
MPC-89
BURNUP AND COOLING TIME
45,000 MWD/MTU AND 5-YEAR COOLING

Dose Point Location	**Fuel Gammas (mrem/hr)**	**(n,γ) Gammas (mrem/hr)**	**^{60}Co Gammas (mrem/hr)**	**Neutrons (mrem/hr)**	**Totals (mrem/hr)**
1	38	<1	7	<1	47
2	47	<1	<1	<1	50
3	3	<1	5	<1	10
4 (center)	0.2	0.2	1	0.1	2

Notes:

- Refer to Figure 5.1.1 for dose locations.
- Values are rounded to nearest integer where appropriate.
- The "Fuel Gammas" category includes gammas from the spent fuel and ^{60}Co from the spacer girds.

Table 5.1.9

DOSE FROM HI-TRAC VW WITH MPC-37
FOR ACCIDENT CONDITIONS
AT 100 METERS
65,000 MWD/MTU AND 8-YEAR COOLING

Dose Point Location	**Dose Rate (rem/hr)**	**Accident Duration (days)**	**Total Dose (rem)**	**Regulatory Limit (rem)**	**Time to Reach Regulatory Limit (days)**
2 (Accident Condition)	2.3E-3	30	1.66	5	90

Notes:

- Refer to Figure 5.1.2 for dose locations.
- Values are rounded to nearest integer where appropriate.
- Dose rates used to evaluated " Total Dose (rem)" are from Table 5.1.4
- Regulatory Limit is from 10CFR72.106.

Table 5.1.10

DOSE RATES ADJACENT TO HI-STORM FW OVERPACK
FOR NORMAL CONDITIONS
MPC-32MLWITH 16X16D FUEL
BURNUP AND COOLING TIME
45,000 MWD/MTU AND 4.6-YEAR COOLING

Dose Point Location	Fuel Gammas (mrem/hr)	(n,γ) Gammas (mrem/hr)	^{60}Co Gammas (mrem/hr)	Neutrons (mrem/hr)	Totals (mrem/hr)	Totals with BPRAs (mrem/hr)
1	177	1	79	2	260	260
2	132	2	< 1	1	135	135
3 (surface)	16	1	16	2	35	45
3 (overpack edge)	13	< 1	38	1	51	75
4 (center)	0.1	0.4	0.3	0.1	1.0	1.2
4 (mid)	4	< 1	1	< 1	5	6
4 (outer)	8	< 1	20	< 1	29	42

Notes:

- Refer to Figure 5.1.1 for dose locations.
- Values are rounded to nearest integer where appropriate.
- Dose location 3 (surface) is at the surface of the outlet vent. Dose location 3 (overpack edge) is in front of the outlet vent, but located radially above the overpack outer diameter.
- Dose location 4 (center) is at the center of the top surface of the top lid. Dose location 4 (mid) is situated directly above the vertical section of the outlet vent. Dose location 4 (outer) is extended along the top plane of the top lid, located radially above the overpack outer diameter.
- The "Fuel Gammas" category includes gammas from the spent fuel, ^{60}Co from the spacer grids, and ^{60}Co from the BPRAs in the active fuel region.

Table 5.1.11

DOSE RATES AT ONE METER FROM HI-STORM FW OVERPACK
FOR NORMAL CONDITIONS
MPC-32MLWITH 16X16D FUEL
BURNUP AND COOLING TIME
45,000 MWD/MTU AND 4.6-YEAR COOLING

Dose Point Location	Fuel Gammas (mrem/hr)	(n,γ) Gammas (mrem/hr)	^{60}Co Gammas (mrem/hr)	Neutrons (mrem/hr)	Totals (mrem/hr)	Totals with BPRAs (mrem/hr)
1	40	< 1	15	< 1	56	56
2	68	1	2	1	72	72
3	7	< 1	8	< 1	15	19
4 (center)	0.7	0.2	0.7	0.2	1.8	2.2

Notes:

- Refer to Figure 5.1.1 for dose locations.
- Values are rounded to nearest integer where appropriate.
- The "Fuel Gammas" category includes gammas from the spent fuel, ^{60}Co from the spacer grids, and ^{60}Co from the BPRAs in the active fuel region.

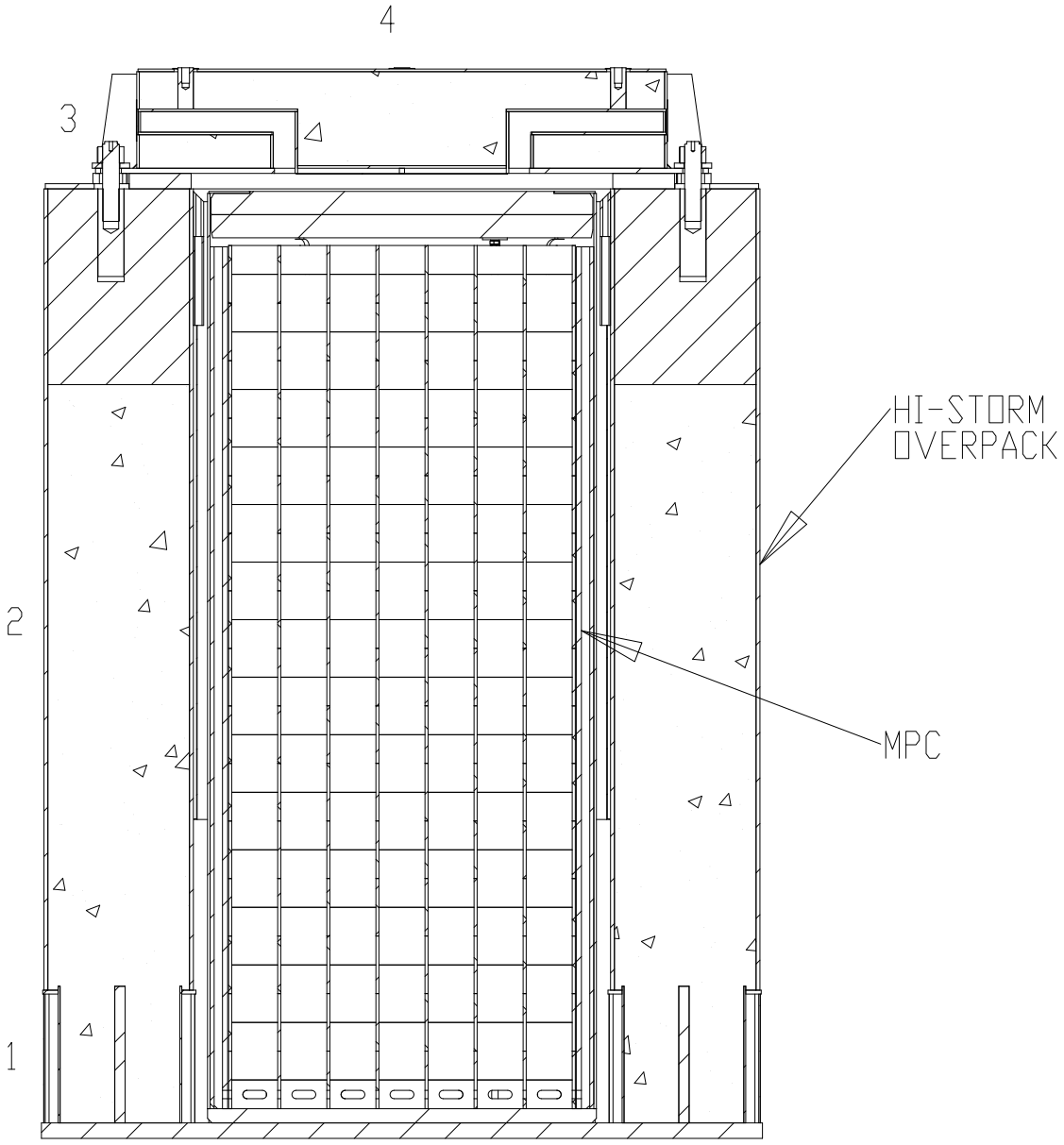

Figure 5.1.1

CROSS SECTION ELEVATION VIEW OF HI-STORM FW OVERPACK WITH DOSE POINT LOCATIONS

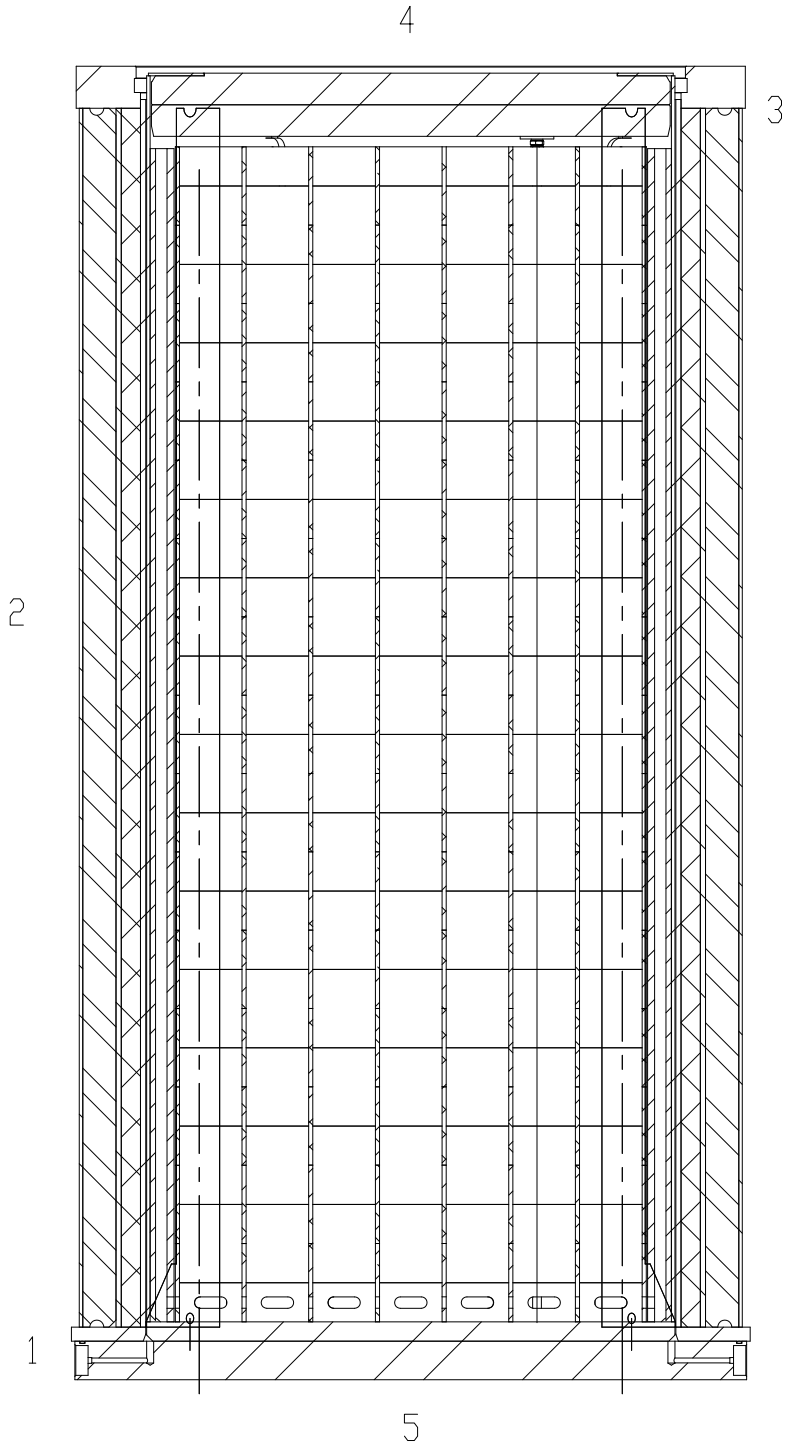

Figure 5.1.2
CROSS SECTION ELEVATION VIEW OF HI-TRAC VW TRANSFER CASK WITH DOSE POINT LOCATIONS

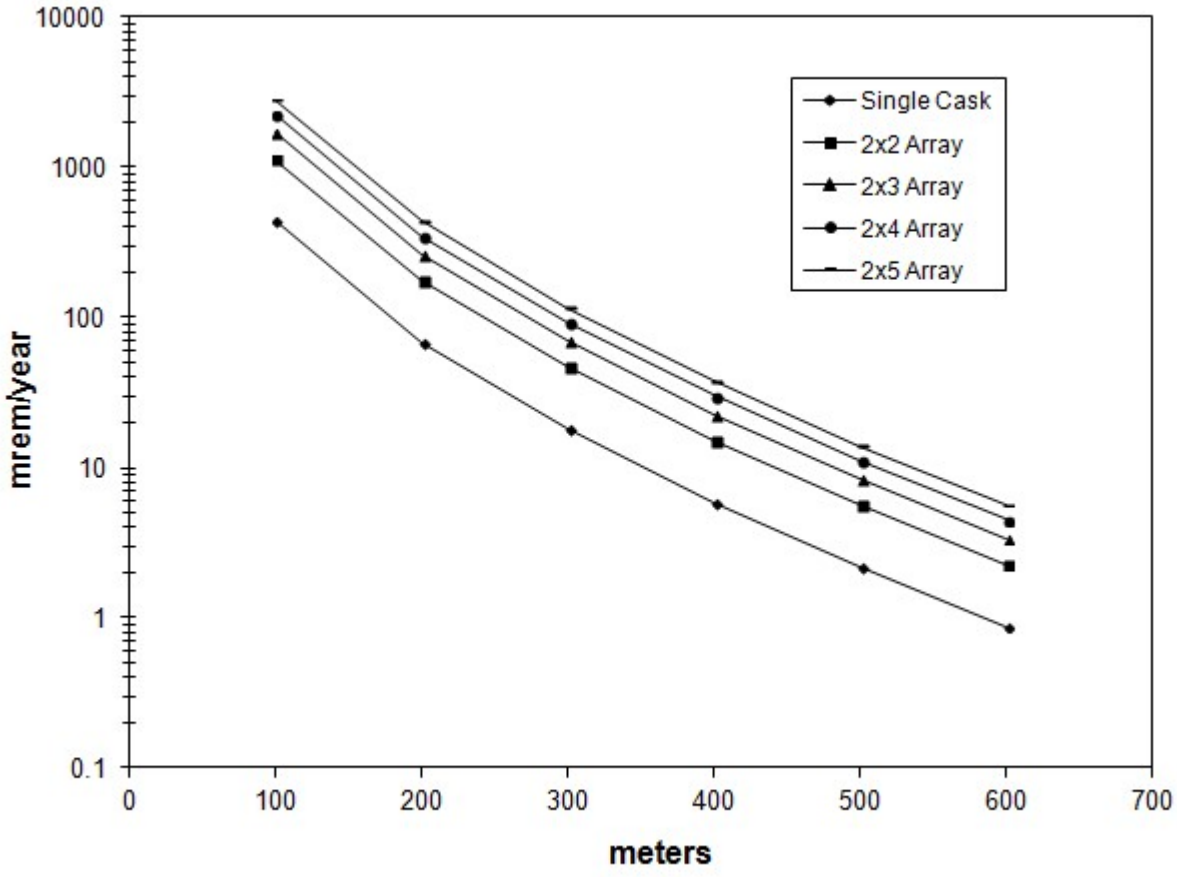

Figure 5.1.3

ANNUAL DOSE VERSUS DISTANCE FOR VARIOUS CONFIGURATIONS OF THE MPC-37 FOR 45,000 MWD/MTU AND 4.5 YEAR COOLING (8760 HOUR OCCUPANCY ASSUMED)

5.2 SOURCE SPECIFICATION

The neutron and gamma source terms, decay heat values, and quantities of radionuclides available for release were calculated with the SAS2H and ORIGEN-S modules of the SCALE 5 system [5.1.2, 5.1.3]. SAS2H has been extensively compared to experimental isotopic validations and decay heat measurements. References [5.2.8] through [5.2.12] and [5.2.15] present isotopic comparisons for PWR and BWR fuels for burnups ranging to 47 GWD/MTU and reference [5.2.13] presents results for BWR measurements to a burnup of 57 GWD/MTU. A comparison of calculated and measured decays heats is presented in reference [5.2.14]. All of these studies indicate good agreement between SAS2H and measured data. Additional comparisons of calculated values and measured data are being performed by various institutions for high burnup PWR and BWR fuel. These new results, when published, are expected to further confirm the validity of SAS2H for the analysis of PWR and BWR fuel.

Sample input files for SAS2H and ORIGEN-S are provided in Appendix 5.A. The gamma source term is actually comprised of three distinct sources. The first is a gamma source term from the active fuel region due to decay of fission products. The second source term is from ^{60}Co activity of the stainless steel structural material in the fuel element above and below the active fuel region. The third source is from (n,γ) reactions described below.

A description of the design basis fuel in MPC-37 and MPC-89 for the source term calculations is provided in Table 5.2.1, and in Table 5.2.17 for design basis fuel in MPC-32ML. Subsection 5.2.5 discusses, in detail, the determination of the design basis fuel assemblies.

In performing the SAS2H and ORIGEN-S calculations, a single full power cycle was used to achieve the desired burnup. This assumption, in conjunction with the above-average specific powers listed in Tables 5.2.1 and 5.2.17 resulted in conservative source term calculations.

5.2.1 Gamma Source

Tables 5.2.2 through 5.2.5 and Table 5.2.19 provide the gamma source in MeV/s and photons/s as calculated with SAS2H and ORIGEN-S for the design basis zircaloy clad fuel at the burnups and cooling times used for normal and accident conditions.

Previous analyses were performed for the HI-STORM 100 system to determine the dose contribution from gammas as a function of energy [5.2.17]. The results of these analyses have revealed that, due to the magnitude of the gamma source at lower energies, photons with energies as low as 0.45 MeV must be included in the shielding analysis, but photons with energies below 0.45 MeV are too weak to penetrate the HI-STORM overpack or HI-TRAC. The effect of gammas with energies above 3.0 MeV, on the other hand, was found to be insignificant. This is due to the fact that the source of gammas in this range (i.e., above 3.0 MeV) is extremely low. Therefore, all photons with energies in the range of 0.45 to 3.0 MeV are included in the shielding calculations.

The primary source of activity in the non-fuel regions of an assembly arises from the activation of ^{59}Co to ^{60}Co. The primary source of ^{59}Co in a fuel assembly is impurities in the steel structural material above and below the fuel. The zircaloy in these regions is neglected since it does not have a significant ^{59}Co impurity level. Reference [5.2.2] indicates that the impurity level in steel is 800 ppm or 0.8 gm/kg. Therefore, inconel and stainless steel in the non-fuel regions are both assumed to have the same 0.8 gm/kg impurity level.

Some of the PWR fuel assembly designs (B&W and WE 15x15) utilized inconel in-core grid spacers while other PWR fuel designs use zircaloy in-core grid spacers. In the mid 1980s, the fuel assembly designs using inconel in-core grid spacers were altered to use zircaloy in-core grid spacers. Since both designs may be loaded into the HI-STORM FW system, the gamma source for the PWR zircaloy clad fuel assembly includes the activation of the in-core grid spacers. Although BWR assembly grid spacers are zircaloy, some assembly designs have inconel springs in conjunction with the grid spacers. The gamma source for the BWR zircaloy clad fuel assembly includes the activation of these springs associated with the grid spacers.

The non-fuel data listed in Table 5.2.1 were taken from References [5.2.2], [5.2.4], and [5.2.5]. As stated above, a Cobalt-59 impurity level of 0.8 gm/kg was used for both inconel and stainless steel. Therefore, there is little distinction between stainless steel and inconel in the source term generation and since the shielding characteristics are similar, stainless steel was used in the MCNP calculations instead of inconel. The BWR masses for an 8x8 fuel assembly were used. These masses are also appropriate for the 10x10 assembly since the masses of the non-fuel hardware from a 10x10 and an 8x8 are approximately the same. The masses listed are those of the steel components. The zircaloy in these regions was not included because zircaloy does not produce significant activation.

The masses in Table 5.2.1 and Table 5.2.17 were used to calculate a ^{59}Co impurity level in the fuel assembly material. The grams of impurity were then used in ORIGEN-S to calculate a ^{60}Co activity level for the desired burnup and decay time. The methodology used to determine the activation level was developed from Reference [5.2.3] and is described here.

1. The activity of the ^{60}Co is calculated using ORIGEN-S. The flux used in the calculation was the in-core fuel region flux at full power.

2. The activity calculated in Step 1 for the region of interest was modified by the appropriate scaling factors listed in Table 5.2.6 and Table 5.2.20. These scaling factors were taken from Reference [5.2.3].

Tables 5.2.7 through 5.2.10 provide the ^{60}Co activity utilized in the shielding calculations for normal and accident conditions for the non-fuel regions of the assemblies in the MPC-37 and the MPC-89. Table 5.2.21 provide those data for the assemblies in the MPC-32ML.

In addition to the two sources already mentioned, a third source arises from (n,γ) reactions in the material of the MPC and the overpack. This source of photons is properly accounted for in

MCNP when a neutron calculation is performed in a coupled neutron-gamma mode.

5.2.2 Neutron Source

It is well known that the neutron source strength increases as enrichment decreases, for a constant burnup and decay time. This is due to the increase in Pu content in the fuel, which increases the inventory of other transuranium nuclides such as Cm. The gamma source also varies with enrichment, although only slightly. Because of this effect and in order to obtain conservative source terms, low initial fuel enrichments of 3.2 and 3.6 wt% were chosen for the BWR and PWR design basis fuel assemblies under normal conditions, respectively. For the accident conditions, ~~a~~ fuel enrichments of 4.8 wt% ~~was chosen~~ for the BWR and PWR (MPC-37), and 4.6 wt% for the PWR (MPC-32ML) were chosen to accommodate the higher burnups of the selected source terms (see Table 5.0.2) in accordance with Table 5.2.24 of reference [5.2.17].

The neutron source calculated for the design basis fuel assemblies for the MPCs and the design basis fuel are listed in Tables 5.2.11 through 5.2.14, and Table 5.2.22 in neutrons/s for the selected burnup and cooling times used in the shielding evaluations for normal and accident conditions. The neutron spectrum is generated in ORIGEN-S.

5.2.3 Non-Fuel Hardware

Burnable poison rod assemblies (BPRAs), thimble plug devices (TPDs), control rod assemblies (CRAs), and axial power shaping rods (APSRs) are permitted for storage in the HI-STORM FW system as an integral part of a PWR fuel assembly. BPRAs and TPDs may be stored in any fuel location while CRAs and APSRs are restricted as specified in Subsection 2.1.

5.2.3.1 BPRAs and TPDs

Burnable poison rod assemblies (BPRA) (including wet annular burnable absorbers) and thimble plug devices (TPD) (including orifice rod assemblies, guide tube plugs, and water displacement guide tube plugs) are an integral, yet removable, part of a large portion of PWR fuel. The TPDs are not used in all assemblies in a reactor core but are reused from cycle to cycle. Therefore, these devices can achieve very high burnups. In contrast, BPRAs are burned with a fuel assembly in core and are not reused. In fact, many BPRAs are removed after one or two cycles before the fuel assembly is discharged. Therefore, the achieved burnup for BPRAs is not significantly different from that of a fuel assembly. Vibration suppressor inserts are considered to be in the same category as BPRAs for the purposes of the analysis in this chapter since these devices have the same configuration (long non-absorbing thimbles which extend into the active fuel region) as a BPRA without the burnable poison.

TPDs are made of stainless steel and contain a small amount of inconel. These devices extend down into the plenum region of the fuel assembly but typically do not extend into the active fuel region. Since these devices are made of stainless steel, there is a significant amount of cobalt-60

produced during irradiation. This is the only significant radiation source from the activation of steel and inconel.

BPRAs are made of stainless steel in the region above the active fuel zone and may contain a small amount of inconel in this region. Within the active fuel zone the BPRAs may contain 2-24 rodlets which are burnable absorbers clad in either zircaloy or stainless steel. The stainless steel clad BPRAs create a significant radiation source (Co-60) while the zircaloy clad BPRAs create a negligible radiation source. Therefore, the stainless steel clad BPRAs are bounding.

SAS2H and ORIGEN-S were used to calculate a radiation source term for the TPDs and BPRAs. In the ORIGEN-S calculations the cobalt-59 impurity level was conservatively assumed to be 0.8 gm/kg for stainless steel and 4.7 gm/kg for inconel. These calculations were performed by irradiating the appropriate mass of steel and inconel using the flux calculated for the design basis W 17x17 fuel assembly. The mass of material in the regions above the active fuel zone was scaled by the appropriate scaling factors listed in Table 5.2.6 in order to account for the reduced flux levels above the fuel assembly. The total curies of cobalt were calculated for the TPDs and BPRAs as a function of burnup and cooling time.

Since the HI-STORM FW cask system is designed to store many varieties of PWR fuel, a representative TPD and BPRA had to be determined for the purposes of the analysis. This was accomplished in the HI-STORM 100 FSAR [5.2.17] by analyzing all of the BPRAs and TPDs (Westinghouse and B&W 14x14 through 17x17) found in references [5.2.5] and [5.2.7] to determine the TPD and BPRA which produced the highest Cobalt-60 source term and decay heat for a specific burnup and cooling time. The TPD was determined to be the Westinghouse 17x17 guide tube plug and the BPRA was actually determined by combining the higher masses of the Westinghouse 17x17 and 15x15 BPRAs into a single hypothetical BPRA. The masses of these devices are listed in Table 5.2.15.

Table 5.2.16 shows the curies of Co-60 that were calculated for BPRAs and TPDs in each region of the fuel assembly (e.g. incore, plenum, top). A burnup and cooling time, separate from the fuel assemblies, is used for BPRAs and TPDs. Table 2.1.25 of the HI-STORM 100 [5.2.17] lists the allowable burnups and cooling times for non-fuel hardware that corresponds to the BPRA. These burnup and cooling times assure that the Co-60 activity remains below the levels specified above. For specific site boundary evaluations, these levels/values can be used if they are bounding. Alternatively, more realistic values can be used.

The HI-STORM 100 [5.2.17] presents dose rates for both BPRAs and TPDs. The results indicate that BPRAs are bounding, therefore all dose rates in this chapter will contain a BPRA in every PWR fuel location. However, Section 5.4 also contains a quantitative dose rates comparison from BPRAs and TPDs to validate this approach. Subsection 5.4.4 discusses the increase in the cask dose rates due to the insertion of BPRAs into fuel assemblies.

It should be noted that 16x16D fuel assemblies may actually not use BPRAs, but same BPRAs are conservatively considered in MPC-32ML shielding calculations to demonstrate compliance with the applicable safety limits.

5.2.3.2 CRAs and APSRs

Control rod assemblies (CRAs) (including control element assemblies and rod cluster control assemblies) and axial power shaping rod assemblies (APSRs) are an integral portion of a PWR fuel assembly. These devices are utilized for many years (upwards of 20 years) prior to discharge into the spent fuel pool. The manner in which the CRAs are utilized vary from plant to plant. Some utilities maintain the CRAs fully withdrawn during normal operation while others may operate with a bank of rods partially inserted (approximately 10%) during normal operation. Even when fully withdrawn, the ends of the CRAs are present in the upper portion of the fuel assembly since they are never fully removed from the fuel assembly during operation. The result of the different operating styles is a variation in the source term for the CRAs. In all cases, however, only the lower portion of the CRAs will be significantly activated. Therefore, when the CRAs are stored with the PWR fuel assembly, the activated portion of the CRAs will be in the lower portion of the cask. CRAs are fabricated of various materials. The cladding is typically stainless steel, although inconel has been used. The absorber can be a single material or a combination of materials. AgInCd is possibly the most common absorber although B_4C in aluminum is used, and hafnium has also been used. AgInCd produces a noticeable source term in the 0.3-1.0 MeV range due to the activation of Ag. The source term from the other absorbers is negligible, therefore the AgInCd CRAs are the bounding CRAs.

APSRs are used to flatten the power distribution during normal operation and as a result these devices achieve a considerably higher activation than CRAs. There are two types of B&W stainless steel clad APSRs: gray and black. According to reference [5.2.5], the black APSRs have 36 inches of AgInCd as the absorber while the gray ones use 63 inches of inconel as the absorber. Because of the cobalt-60 source from the activation of inconel, the gray APSRs produce a higher source term than the black APSRs and therefore are the bounding APSR.

Since the level of activation of CRAs and APSRs can vary, the quantity that can be stored in an MPC is being limited. These devices are required to be stored in the locations as outlined in Subsection 2.1.

Subsection 5.4.4 discusses the effect on dose rate of the insertion of APSRs or CRAs into fuel assemblies.

5.2.4 Choice of Design Basis Assembly

The Westinghouse 17x17 and GE 10x10 assemblies were selected as design basis assemblies since they are widely used throughout the industry. Site specific shielding evaluations should verify that those assemblies and assembly parameters are appropriate for the site-specific

analyses. Because of its large width, 16x16D (e.g., 16x16 Focus and 16x16 HTP fuel assemblies) was selected as design basis fuel assembly for MPC-32ML.

5.2.5 Decay Heat Loads and Allowable Burnup and Cooling Times

Subsection 2.1 describes the MPC maximum decay heat limits per assembly. The allowable burnup and cooling time limits are derived based on the allowable decay heat limits.

5.2.6 Fuel Assembly Neutron Sources

Neutron source assemblies (NSAs) are used in reactors for startup. There are different types of neutron sources (e.g. californium, americium-beryllium, plutonium-beryllium, polonium-beryllium, antimony-beryllium). These neutron sources are typically inserted into the water rod of a fuel assembly and are usually removable.

During in-core operations, the stainless steel and inconel portions of the NSAs become activated, producing a significant amount of Co-60. A detailed discussion about NSAs is provided in reference [5.2.17], where it is concluded that activation from NSAs are bounded by activation from BPRAs.

For ease of implementation in the CoC, the restriction concerning the number of NSAs is being applied to all types of NSAs. In addition, conservatively NSAs are required to be stored in the inner region of the MPC basket as specified in Subsection 2.1. Further limitations allow for only one NSA to be stored in the MPC-37 or -(see Table 2.1.1a), or MPC-32ML (see Table 2.1.1b).

Table 5.2.1

DESCRIPTION OF DESIGN BASIS CLAD FUEL

	PWR (MPC-37)	**BWR**
Assembly type/class	WE 17×17	GE 10×10
Active fuel length (in.)	144	144
No. of fuel rods	264	92
Rod pitch (in.)	0.496	0.51
Cladding material	Zircaloy-4	Zircaloy-2
Rod diameter (in.)	0.374	0.404
Cladding thickness (in.)	0.0225	0.026
Pellet diameter (in.)	0.3232	0.345
Pellet material	UO_2	UO_2
Pellet density (gm/cc)	10.412 (95% of theoretical)	10.522 (96% of theoretical)
Enrichment (w/o ^{235}U)	3.6	3.2
Specific power (MW/MTU)	43.48	30
Weight of UO_2 (kg)††	532.150	213.531
Weight of U (kg)††	469.144	188.249
No. of Water Rods/ Guide Tubes	25	2
Water Rod/ Guide Tube O.D. (in.)	0.474	0.98
Water Rod/ Guide Tube Thickness (in.)	0.016	0.03

†† Derived from parameters in this table.

Table 5.2.1 (continued) DESCRIPTION OF DESIGN BASIS FUEL		
	PWR (MPC-37)	**BWR**
Lower End Fitting (kg)	5.9 (steel)	4.8 (steel)
Gas Plenum Springs (kg)	1.150 (steel)	1.1 (steel)
Gas Plenum Spacer (kg)	0.793 (inconel) 0.841 (steel)	N/A
Expansion Springs (kg)	N/A	0.4 (steel)
Upper End Fitting (kg)	6.89 (steel) 0.96 (inconel)	2.0 (steel)
Handle (kg)	N/A	0.5 (steel)
Incore Grid Spacers (kg)	4.9 (inconel)	0.33 (inconel springs)

Table 5.2.2

CALCULATED MPC-37 PWR FUEL GAMMA SOURCE PER ASSEMBLY FOR DESIGN BASIS BURNUP AND COOLING TIME FOR NORMAL CONDITIONS

Lower Energy	**Upper Energy**	**45,000 MWD/MTU 4.5-Year Cooling**	
(MeV)	(MeV)	(MeV/s)	(Photons/s)
0.45	0.7	2.11E+15	3.68E+15
0.7	1.0	7.67E+14	9.02E+14
1.0	1.5	1.74E+14	1.39E+14
1.5	2.0	1.45E+13	8.30E+12
2.0	2.5	1.01E+13	4.47E+12
2.5	3.0	4.05E+11	1.47E+11
Total		3.08E+15	4.73E+15

Table 5.2.3

CALCULATED MPC-37 PWR FUEL GAMMA SOURCE PER ASSEMBLY FOR BURNUP AND COOLING TIME FOR ACCIDENT CONDITIONS

Lower Energy	**Upper Energy**	**65,000 MWD/MTU 8-Year Cooling**	
(MeV)	(MeV)	(MeV/s)	(Photons/s)
0.45	0.7	2.05E+15	3.56E+15
0.7	1.0	4.16E+14	4.89E+14
1.0	1.5	1.30E+14	1.04E+14
1.5	2.0	8.66E+12	4.95E+12
2.0	2.5	6.46E+11	2.87E+11
2.5	3.0	4.49E+10	1.63E+10
Total		2.60E+15	4.16E+15

Table 5.2.4

CALCULATED MPC-89 BWR FUEL GAMMA SOURCE PER ASSEMBLY FOR DESIGN BASIS BURNUP AND COOLING TIME FOR NORMAL CONDITIONS

Lower Energy	**Upper Energy**	**45,000 MWD/MTU 5-Year Cooling**	
(MeV)	(MeV)	(MeV/s)	(Photons/s)
0.45	0.7	7.52E+14	1.31E+15
0.7	1.0	2.40E+14	2.82E+14
1.0	1.5	5.53E+13	4.42E+13
1.5	2.0	4.15E+12	2.37E+12
2.0	2.5	2.02E+12	8.97E+11
2.5	3.0	9.74E+10	3.54E+10
Total		1.05E+15	2.04E+15

Table 5.2.5

CALCULATED MPC-89 BWR FUEL GAMMA SOURCE PER ASSEMBLY FOR BURNUP AND COOLING TIME FOR ACCIDENT CONDITIONS

Lower Energy	**Upper Energy**	**65,000 MWD/MTU 10-Year Cooling**	
(MeV)	(MeV)	(MeV/s)	(Photons/s)
0.45	0.7	6.98E+14	1.21E+15
0.7	1.0	8.37E+13	9.85E+13
1.0	1.5	3.50E+13	2.80E+13
1.5	2.0	2.52E+12	1.44E+12
2.0	2.5	4.49E+10	2.00E+10
2.5	3.0	3.90E+09	1.42E+09
Total		8.19E+14	1.34E+15

Table 5.2.6

SCALING FACTORS USED IN CALCULATING THE ^{60}Co SOURCE

Region	PWR (MPC-37)	BWR
Handle	N/A	0.05
Upper End Fitting	0.1	0.1
Gas Plenum Spacer	0.1	N/A
Expansion Springs	N/A	0.1
Gas Plenum Springs	0.2	0.2
Incore Grid Spacer	1.0	1.0
Lower End Fitting	0.2	0.15

Table 5.2.7

CALCULATED MPC-37 ^{60}Co SOURCE PER ASSEMBLY FOR DESIGN BASIS FUEL AT DESIGN BASIS BURNUP AND COOLING TIME FOR NORMAL CONDITIONS

Location	**45,000 MWD/MTU and 4.5-Year Cooling (curies)**
Lower End Fitting	86.02
Gas Plenum Springs	16.77
Gas Plenum Spacer	11.91
Expansion Springs	NA
Incore Grid Spacers	357.19
Upper End Fitting	57.22
Handle	NA

Table 5.2.8

CALCULATED MPC-37 ^{60}Co SOURCE PER ASSEMBLY FOR DESIGN BASIS FUEL AT BURNUP AND COOLING TIME FOR ACCIDENT CONDITIONS

Location	**65,000 MWD/MTU and 8-Year Cooling (curies)**
Lower End Fitting	64.89
Gas Plenum Springs	12.65
Gas Plenum Spacer	8.99
Expansion Springs	NA
Incore Grid Spacers	269.46
Upper End Fitting	43.17
Handle	NA

Table 5.2.9

CALCULATED MPC-89 ^{60}Co SOURCE PER ASSEMBLY FOR DESIGN BASIS FUEL AT DESIGN BASIS BURNUP AND COOLING TIME FOR NORMAL CONDITIONS

Location	**45,000 MWD/MTU and 5-Year Cooling (curies)**
Lower End Fitting	158.66
Gas Plenum Springs	48.48
Gas Plenum Spacer	N/A
Expansion Springs	8.81
Grid Spacer Springs	72.72
Upper End Fitting	44.07
Handle	5.51

Table 5.2.10

CALCULATED MPC-89 ^{60}Co SOURCE PER ASSEMBLY FOR DESIGN BASIS FUEL AT BURNUP AND COOLING TIME FOR ACCIDENT CONDITIONS

Location	**65,000 MWD/MTU and 10-Year Cooling (curies)**
Lower End Fitting	90.17
Gas Plenum Springs	27.55
Gas Plenum Spacer	N/A
Expansion Springs	5.01
Grid Spacer Springs	41.33
Upper End Fitting	25.05
Handle	3.13

Table 5.2.11

CALCULATED MPC-37 PWR NEUTRON SOURCE PER ASSEMBLY
FOR 45,000 MWD/MTU BURNUP AND 4.5 YEAR COOLING

Lower Energy (MeV)	**Upper Energy (MeV)**	**45,000 MWD/MTU 4.5-Year Cooling (Neutrons/s)**
1.0e-01	4.0e-01	3.05E+07
4.0e-01	9.0e-01	6.64E+07
9.0e-01	1.4	6.63E+07
1.4	1.85	5.30E+07
1.85	3.0	9.88E+07
3.0	6.43	8.97E+07
6.43	20.0	8.56E+06
Totals		4.13E+08

Table 5.2.12

CALCULATED MPC-37 PWR NEUTRON SOURCE PER ASSEMBLY
FOR 65,000 MWD/MTU BURNUP AND 8 YEAR COOLING

Lower Energy (MeV)	**Upper Energy (MeV)**	**65,000 MWD/MTU 8-Year Cooling (Neutrons/s)**
1.0e-01	4.0e-01	6.80E+07
4.0e-01	9.0e-01	1.48E+08
9.0e-01	1.4	1.47E+08
1.4	1.85	1.17E+08
1.85	3.0	2.18E+08
3.0	6.43	1.98E+08
6.43	20.0	1.89E+07
Totals		9.16E+08

Table 5.2.13

CALCULATED MPC-89 BWR NEUTRON SOURCE
PER ASSEMBLY
FOR DESIGN BASIS FUEL
FOR 45,000 MWD/MTU BURNUP AND 5 YEAR COOLING

Lower Energy (MeV)	**Upper Energy (MeV)**	**45,000 MWD/MTU 5-Year Cooling (Neutrons/s)**
1.0e-01	4.0e-01	1.37E+07
4.0e-01	9.0e-01	2.99E+07
9.0e-01	1.4	2.99E+07
1.4	1.85	2.38E+07
1.85	3.0	4.44E+07
3.0	6.43	4.03E+07
6.43	20.0	3.86E+06
Totals		1.86E+08

Table 5.2.14

CALCULATED MPC-89 BWR NEUTRON SOURCE
PER ASSEMBLY
FOR DESIGN BASIS FUEL
FOR 65,000 MWD/MTU BURNUP AND 10 YEAR COOLING

Lower Energy (MeV)	**Upper Energy (MeV)**	**65,000 MWD/MTU 10-Year Cooling (Neutrons/s)**
1.0e-01	4.0e-01	2.40E+07
4.0e-01	9.0e-01	5.22E+07
9.0e-01	1.4	5.20E+07
1.4	1.85	4.15E+07
1.85	3.0	7.71E+07
3.0	6.43	7.00E+07
6.43	20.0	6.68E+06
Totals		3.24E+08

Table 5.2.15
DESCRIPTION OF DESIGN BASIS BURNABLE POISON ROD ASSEMBLY AND THIMBLE PLUG DEVICE

Region	**BPRA**	**TPD**
Upper End Fitting (kg of steel)	2.62	2.3
Upper End Fitting (kg of inconel)	0.42	0.42
Gas Plenum Spacer (kg of steel)	0.77488	1.71008
Gas Plenum Springs (kg of steel)	0.67512	1.48992
In-core (kg of steel)	13.2	N/A

Table 5.2.16
DESIGN BASIS COBALT-60 ACTIVITIES FOR BURNABLE POISON ROD
ASSEMBLIES AND THIMBLE PLUG DEVICES

Region	**BPRA**	**TPD**
Upper End Fitting (curies Co-60)	32.7	25.21
Gas Plenum Spacer (curies Co-60)	5.0	9.04
Gas Plenum Springs (curies Co-60)	8.9	15.75
In-core (curies Co-60)	848.4	N/A

Table 5.2.17 DESCRIPTION OF 16X16D DESIGN BASIS CLAD FUEL	
	PWR (MPC-32ML)
Assembly type/class	16x16D
Active fuel length (cm)	390
No. of fuel rods	236
Rod pitch (in.)	1.43
Cladding material	Zircaloy-4
Rod diameter (cm)	1.075
Cladding thickness (cm)	0.068
Pellet diameter (cm)	0.911
Pellet material	UO_2
Pellet density (g/cc)	10.45 (95.3% of theoretical)
Enrichment (w/o ^{235}U)	3.6
Specific power (MW/MTU)	36.56
Weight of UO_2 (kg)††	624.651
Weight of U (kg)††	552.703
No. of Water Rods/ Guide Tubes	20
Water Rod/ Guide Tube O.D. (cm)	1.41
Water Rod/ Guide Tube Thickness (cm)	0.077

†† Derived from parameters in this table.

Table 5.2.17 (continued) DESCRIPTION OF 16X16D DESIGN BASIS FUEL	
	PWR (MPC-32ML)
Lower End Fitting (kg)	10.795 (steel/inconel)
Gas Plenum Springs (kg)	1.474 (steel/inconel)
Gas Plenum Spacer (kg)	1.692 (steel/inconel)
Upper End Fitting (kg)	12.344 (steel/inconel)
Incore Grid Spacers (kg)	12.67 (inconel)

Table 5.2.19a

CALCULATED 16X16D (MPC-32ML) PWR FUEL GAMMA SOURCE PER ASSEMBLY FOR DESIGN BASIS BURNUP AND COOLING TIME FOR NORMAL CONDITIONS

Lower Energy	**Upper Energy**	**45,000 MWD/MTU 4.6-Year Cooling**	
(MeV)	(MeV)	(MeV/s)	(Photons/s)
0.45	0.7	2.43E+15	4.22E+15
0.7	1.0	8.74E+14	1.03E+15
1.0	1.5	2.00E+14	1.60E+14
1.5	2.0	1.58E+13	9.04E+12
2.0	2.5	9.55E+12	4.24E+12
2.5	3.0	4.06E+11	1.48E+11
Total		3.52E+15	5.42E+15

Table 5.2.19b

CALCULATED 16X16D (MPC-32ML) PWR FUEL GAMMA SOURCE PER ASSEMBLY FOR DESIGN BASIS BURNUP AND COOLING TIME FOR ACCIDENT CONDITIONS

Lower Energy	**Upper Energy**	**62,500 MWD/MTU 8-Year Cooling**	
(MeV)	(MeV)	(MeV/s)	(Photons/s)
0.45	0.7	2.30E+15	3.99E+15
0.7	1.0	4.63E+14	5.44E+14
1.0	1.5	1.49E+14	1.19E+14
1.5	2.0	1.00E+13	5.72E+12
2.0	2.5	6.57E+11	2.92E+11
2.5	3.0	4.68E+10	1.70E+10
Total		2.92E+15	4.66E+15

Table 5.2.20

SCALING FACTORS USED IN CALCULATING THE 16X16D (MPC-32ML) ^{60}Co SOURCE

Region	PWR (MPC-32ML)
Upper End Fitting	0.05
Gas Plenum Spacer	0.1
Gas Plenum Springs	0.2
Incore Grid Spacer	1.0
Lower End Fitting	0.2

Table 5.2.21

CALCULATED ^{60}Co SOURCE PER ASSEMBLY FOR 16X16D (MPC-32ML) DESIGN BASIS FUEL AT DESIGN BASIS BURNUP AND COOLING TIME FOR NORMAL AND ACCIDENT CONDITIONS

Location	45,000 MWD/MTU and 4.6-Year Cooling (curies)	62,500 MWD/MTU and 8-Year Cooling (curies)
Upper End Fitting	43.51	32.57
Gas Plenum Springs	11.93	8.93
Gas Plenum Spacer	20.78	15.56
Incore Grid Spacers	893.18	668.57
Lower End Fitting	152.20	113.93

Table 5.2.22

CALCULATED 16X16D (MPC-32ML) PWR NEUTRON SOURCE PER ASSEMBLY DESIGN BASIS BURNUP AND COOLING TIME FOR NORMAL AND ACCIDENT CONDITIONS

Lower Energy (MeV)	**Upper Energy (MeV)**	**45,000 MWD/MTU 4.6-Year Cooling (Neutrons/s)**	**62,500 MWD/MTU 8-Year Cooling (Neutrons/s)**
1.0e-01	4.0e-01	3.65E+07	7.42E+07
4.0e-01	9.0e-01	7.96E+07	1.62E+08
9.0e-01	1.4	7.95E+07	1.61E+08
1.4	1.85	6.35E+07	1.29E+08
1.85	3.0	1.19E+08	2.39E+08
3.0	6.43	1.08E+08	2.17E+08
6.43	20.0	1.03E+07	2.07E+07
Totals		4.96E+08	1.00E+09

5.3 MODEL SPECIFICATIONS

The shielding analysis of the HI-STORM FW system was performed with MCNP5 [5.1.1]. MCNP is a Monte Carlo transport code that offers a full three-dimensional combinatorial geometry modeling capability including such complex surfaces as cones and tori. This means that no gross approximations were required to represent the HI-STORM FW system, including the HI-TRAC transfer casks, in the shielding analysis. A sample input file for MCNP is provided in Appendix 5.A.

As discussed in Subsection 5.1.1, off-normal conditions do not have any implications for the shielding analysis. Therefore, the MCNP models and results developed for the normal conditions also represent the off-normal conditions. Subsection 5.1.2 discussed the accident conditions and stated that the only accident that would impact the shielding analysis would be a loss of the neutron shield (water) in the HI-TRAC. Therefore, the MCNP model of the normal HI-TRAC condition has the neutron shield in place while the accident condition replaces the neutron shield with void. Subsection 5.1.2 also mentioned that there is no credible accident scenario that would impact the HI-STORM shielding analysis. Therefore, models and results for the normal and accident conditions are identical for the HI-STORM overpack.

5.3.1 Description of the Radial and Axial Shielding Configuration

Chapter 1 provides the drawings that describe the HI-STORM FW system, including the HI-TRAC transfer cask. These drawings, using nominal dimensions, were used to create the MCNP models used in the radiation transport calculations. Modeling deviations from these drawings are discussed below. Figures 5.3.1 and 5.3.2, as well as Figures 5.3.12 and 5.3.13, show cross sectional views of the HI-STORM FW overpack, MPCs, and basket cells as they are modeled in MCNP. Figures 5.3.1 and 5.3.2 were created in VISED and are drawn to scale. The inlet and outlet vents were modeled explicitly, therefore, streaming through these components is accounted for in the calculations of the dose adjacent to the overpack and at 1 meter. Figures 5.3.3 and 5.3.4 show a cross sectional view of the HI-TRAC VW with the MPC-37 and MPC-89, respectively, as it was modeled in MCNP. These figures were created in VISED and are drawn to scale.

Figure 5.3.5 shows a cross sectional view of the HI-STORM FW overpack with the as-modeled thickness of the various materials.

Figure 5.3.6 shows the axial representation of the HI-STORM FW overpack with the various as-modeled dimensions indicated.

Figure 5.3.7 shows axial cross-sectional views of the HI-TRAC VW transfer casks with the as-modeled dimensions and materials specified. Figures 5.3.8 and 5.3.9 shows fully labeled radial cross-sectional view of the HI-TRAC VW transfer casks and each of the MPCs.

Calculations were performed for the HI-STORM 100 [5.2.17] to determine the acceptability of homogenizing the fuel assembly versus explicit modeling. Based on these calculations it was concluded that it is acceptable to homogenize the fuel assembly without loss of accuracy. The width of the PWR (in MPC-37) and BWR homogenized fuel assembly is equal to 17 times the pitch and 10 times the pitch, respectively. Homogenization results in a noticeable decrease in run time. The width of 16x16D fuel assembly in MCNP model of MPC-32ML is provided as a note under Table 5.3.1.

Several conservative approximations were made in modeling the MPC. The conservative approximations are listed below.

1. The fuel shims are not modeled because they are not needed on all fuel assembly types. However, most PWR fuel assemblies will have fuel shims. The fuel shim length for the design basis fuel assembly type determines the positioning of the fuel assembly for the shielding analysis. This is conservative since it removes steel that would provide a small amount of additional shielding.

2. The MPC basket supports are not modeled. This is conservative since it removes material that would provide a small increase in shielding.

3. The MPC cavity height, MPC height and HI-STORM FW cavity height for HI-STORM FW with MPC-32ML are calculated using the length of fuel without non-fuel hardware and/or DFC, and data provided in Table 3.2.1.

The zircaloy flow channels are included in the modeling of the BWR assemblies. The expected impact of this assumption on the dose rates is insignificant. Additionally, site specific analysis should consider site specific fuel characteristics as applicable.

5.3.1.1 Fuel Configuration

As described earlier, the active fuel region is modeled as a homogenous zone. The end fittings and the plenum regions are also modeled as homogenous regions of steel. The masses of steel used in these regions are shown in Table 5.2.1 and Table 5.2.17. The axial description of the design basis fuel assemblies is provided in Table 5.3.1. Figures 5.3.10 and 5.3.11 graphically depict the location of the PWR and BWR fuel assemblies within the HI-STORM FW system. The axial locations of the basket, inlet vents, and outlet vents are shown in these figures.

5.3.1.2 Streaming Considerations

The MCNP model of the HI-STORM overpack completely describes the inlet and outlet vents, thereby properly accounting for their streaming effect. Further, the top lid is properly modeled with its reduced diameter, which accounts for higher localized dose rates on the top surface of the HI-STORM.

The MCNP model of the HI-TRAC transfer cask accounts for the fins through the HI-TRAC water jacket, as discussed in Subsection 5.4.1, as well as the open annulus.

5.3.2 Regional Densities

Composition and densities of the various materials used in the HI-STORM FW system and HI-TRAC shielding analyses are given in Table 5.3.2. All of the materials and their actual geometries are represented in the MCNP model.

The concrete density shown in Table 5.3.2 is the minimum concrete density analyzed in this chapter. The HI-STORM FW overpacks are designed in such a way that the concrete density in the body of the overpack can be increased to approximately 3.2 g/cm^3 (200 lb/cu-ft). Increasing the density beyond the value in Table 5.3.2 would result in a significant reduction in the dose rates. This may be beneficial based on on-site and off-site ALARA considerations.

The water density inside the MPC corresponds to the maximum allowable water temperature within the MPC. The water density in the water jacket corresponds to the maximum allowable temperature at the maximum allowable pressure. As mentioned, the HI-TRAC transfer cask may be equipped with a water jacket to provide radial neutron shielding. Demineralized water (borated water) will be utilized in the water jacket. To ensure operability for low temperature conditions, ethylene glycol (25% in solution) may be added to reduce the freezing point for low temperature operations. Calculations were performed for the HI-STORM 100 system [5.2.17] to determine the effect of the ethylene glycol on the shielding effectiveness of the radial neutron shield. Based on these calculations, it was concluded that the addition of ethylene glycol (25% in solution) does not reduce the shielding effectiveness of the radial neutron shield.

Subsections 4.4 and 4.5 demonstrate that all materials used in the HI-STORM and HI-TRAC remain below their design temperatures as specified in Table 2.2.3 during all normal conditions. Therefore, the shielding analysis does not address changes in the material density or composition as a result of temperature changes.

Chapter 11 discusses the effect of the various accident conditions on the temperatures of the shielding materials and the resultant impact on their shielding effectiveness. As stated in Subsection 5.1.2, there is only one accident that has any significant impact on the shielding

configuration. This accident is the loss of the neutron shield (water) in the HI-TRAC as a result of fire or other damage. The change in the neutron shield was conservatively analyzed by assuming that the entire volume of the liquid neutron shield was replaced by void.

Table 5.3.1

DESCRIPTION OF THE AXIAL MCNP MODEL OF THE FUEL ASSEMBLIES†

Region	Start (in.)	Finish (in.)	Length (in.)	Actual Material	Modeled Material
PWR (MPC-37)					
Lower End Fitting	0.0	2.738	2.738	SS304	SS304
Space	2.738	3.738	1.0	zircaloy	void
Fuel	3.738	147.738	144.0	fuel & zircaloy	fuel & zircaloy
Gas Plenum Springs	147.738	151.916	4.178	SS304 & inconel	SS304
Gas Plenum Spacer	151.916	156.095	4.179	SS304 & inconel	SS304
Upper End Fitting	156.095	159.765	3.670	SS304 & inconel	SS304
BWR					
Lower End Fitting	0.0	7.385	7.385	SS304	SS304
Fuel	7.385	151.385	144.0	fuel & zircaloy	fuel & zircaloy
Space	151.385	157.385	6.0	zircaloy	void
Gas Plenum Springs	157.385	166.865	9.48	SS304 & zircaloy	SS304
Expansion Springs	166.865	168.215	1.35	SS304	SS304
Upper End Fitting	168.215	171.555	3.34	SS304	SS304
Handle	171.555	176	4.445	SS304	SS304

† All dimensions start at the bottom of the fuel assembly. The length of the fuel shims must be added to the distances to determine the distance from the top of the MPC baseplate.

Table 5.3.1 (Continued)

DESCRIPTION OF THE AXIAL MCNP MODEL OF THE 16X16D FUEL ASSEMBLIES†

Region	Start (cm)	Finish (cm)	Length (cm)	Actual Material	Modeled Material
PWR (MPC-32ML) (Note 1)					
Lower End Fitting	0.0	34.002	34.002	SS304	SS304
Space	34.0	38.612	4.61	zircaloy	void
Fuel	38.6	428.612	390	fuel & zircaloy	fuel & zircaloy
Gas Plenum Springs	428.6	446.189	17.577	SS304 & inconel	SS304
Gas Plenum Spacer	446.2	466.360	20.171	SS304 & inconel	SS304
Upper End Fitting	466.4	489.700	23.34	SS304 & inconel	SS304

Note 1: The width of the fuel assembly is modeled as 22.96 cm.

† All dimensions start at the bottom of the fuel assembly. The length of the fuel shims must be added to the distances to determine the distance from the top of the MPC baseplate.

Table 5.3.2

COMPOSITION OF THE MATERIALS IN THE HI-STORM FW SYSTEM

Component	Density (g/cm³)	Elements	Mass Fraction (%)
Metamic-HT†	2.61 (9% B_4C)	**Proprietary Information Withheld in Accordance with 10 CFR 2.390**	
SS304	7.94	Cr	19
		Mn	2
		Fe	69.5
		Ni	9.5
Carbon Steel	7.82	C	1.0
		Fe	99.0
Zircaloy	6.55	Zr	98.24
		Sn	1.45
		Fe	0.21
		Cr	0.10

† All B-10 loadings in the Metamic compositions are conservatively lower than the values defined in the Bill of Materials.

Table 5.3.2 (continued)

COMPOSITION OF THE MATERIALS IN THE HI-STORM FW SYSTEM

Component	Density (g/cm^3)	Elements	Mass Fraction (%)
BWR Fuel Region Mixture	4.781 (5.0 wt% U-235)	^{235}U	3.207
		^{238}U	60.935
		O	8.623
		Zr	26.752
		N	0.014
		Cr	0.027
		Fe	0.034
		Sn	0.409
PWR Fuel Region Mixture (MPC-37)	3.769 (5.0 wt% U-235)	^{235}U	3.709
		^{238}U	70.474
		O	9.972
		Zr	15.565
		Cr	0.016
		Fe	0.033
		Sn	0.230
16x16D Fuel Region Mixture (MPC-32ML)	3.7565 (5.0 wt% U-235)	^{235}U	3.6111
		^{238}U	68.612
		O	9.709
		Zr	17.750
		Cr	0.262
		Fe	0.038
		Sn	0.018

HOLTEC INTERNATIONAL COPYRIGHTED MATERIAL

Table 5.3.2 (continued)

COMPOSITION OF THE MATERIALS IN THE HI-STORM FW SYSTEM

Component	Density (g/cm^3)	Elements	Mass Fraction (%)
Lower End Fitting (PWR MPC-37)	1.849	SS304	100
Gas Plenum Springs (PWR MPC-37)	0.23626	SS304	100
Gas Plenum Spacer (PWR MPC-37)	0.33559	SS304	100
Upper End Fitting (PWR MPC-37)	1.8359	SS304	100
Lower End Fitting (BWR)	1.5249	SS304	100
Gas Plenum Springs (BWR)	0.27223	SS304	100
Expansion Springs (BWR)	0.69514	SS304	100
Upper End Fitting (BWR)	1.4049	SS304	100
Handle (BWR)	0.26391	SS304	100
Lower End Fitting (MPC-32ML)	0.6022	SS304	100
Gas Plenum Springs (MPC-32ML)	0.159	SS304	100
Gas Plenum Spacer (MPC-32ML)	0.159	SS304	100
Upper End Fitting (MPC-32ML)	1.00325	SS304	100

Table 5.3.2 (continued)

COMPOSITION OF THE MATERIALS IN THE HI-STORM FW SYSTEM

Lead	11.3	Pb	99.9
		Cu	0.08
		Ag	0.02
Water	0.919 (water jacket)	H	11.2
	0.958 (inside MPC)	O	88.8

Table 5.3.2 (continued)

COMPOSITION OF THE MATERIALS IN THE HI-STORM FW SYSTEM

Component	Density (g/cm^3)	Elements	Mass Fraction (%)
Water w/ 2000 ppm	0.958	B-10	0.036
		B-11	0.164
		H	11.17
		O	88.63
Concrete	2.4	H	1.0
		O	53.2
		Si	33.7
		Al	3.4
		Na	2.9
		Ca	4.4
		Fe	1.4

Proprietary Information Withheld in Accordance with 10 CFR 2.390

Figure 5.3.1
HI-STORM FW OVERPACK WITH MPC-37 CROSS SECTIONAL VIEW AS MODELED IN MCNP†

† This figure is drawn to scale using VISED.

Proprietary Information Withheld in Accordance with 10 CFR 2.390

Figure 5.3.2

HI-STORM FW OVERPACK WITH MPC-89 CROSS SECTIONAL VIEW AS MODELED IN MCNP†

† This figure is drawn to scale using VISED.

Proprietary Information Withheld in Accordance with 10 CFR 2.390

Figure 5.3.3

HI-TRAC VW OVERPACK WITH MPC-37 CROSS SECTIONAL VIEW AS MODELED IN MCNP†

† This figure is drawn to scale using VISED.

Proprietary Information Withheld in Accordance with 10 CFR 2.390

Figure 5.3.4

HI-TRAC VW OVERPACK WITH MPC-89 CROSS SECTIONAL VIEW AS MODELED IN MCNP†

† This figure is drawn to scale using VISED.

Proprietary Information Withheld in Accordance with 10 CFR 2.390

Figure 5.3.5
CROSS SECTION OF HI-STORM FW OVERPACK

Proprietary Information Withheld in Accordance with 10 CFR 2.390

Figure 5.3.6
HI-STORM FW OVERPACK CROSS SECTIONAL ELEVATION VIEW

Proprietary Information Withheld in Accordance with 10 CFR 2.390

Figure 5.3.7
HI-TRAC VW TRANSFER CASK WITH POOL LID CROSS SECTIONAL ELEVATION VIEW (AS MODELED)

Proprietary Information Withheld in Accordance with 10 CFR 2.390

Figure 5.3.8

HI-TRAC VW TRANSFER CASK CROSS SECTIONAL VIEW WITH MPC-37 (AS MODELED)

Proprietary Information Withheld in Accordance with 10 CFR 2.390

Figure 5.3.9

HI-TRAC VW TRANSFER CASK CROSS SECTIONAL VIEW WITH MPC-89 (AS MODELED)

Proprietary Information Withheld in Accordance with 10 CFR 2.390

Figure 5.3.10

AXIAL LOCATION OF PWR DESIGN BASIS FUEL IN THE HI-STORM FW OVERPACK

Proprietary Information Withheld in Accordance with 10 CFR 2.390

Figure 5.3.11

AXIAL LOCATION OF BWR DESIGN BASIS FUEL IN THE HI-STORM FW OVERPACK

Proprietary Information Withheld in Accordance with 10 CFR 2.390

Figure 5.3.12

CROSS SECTIONAL VIEW OF AN MPC-37 BASKET CELL AS MODELED IN MCNP

Proprietary Information Withheld in Accordance with 10 CFR 2.390

Figure 5.3.13

CROSS SECTIONAL VIEW OF AN MPC-89 BASKET CELL AS MODELED IN MCNP

5.4 SHIELDING EVALUATION

The MCNP-5 code was used for all of the shielding analyses [5.1.1]. MCNP is a continuous energy, three-dimensional, coupled neutron-photon-electron Monte Carlo transport code. Continuous energy cross section data are represented with sufficient energy points to permit linear-linear interpolation between points. The individual cross section libraries used for each nuclide are those recommended by the MCNP manual Cross section libraries are based on ENDF/B-V and ENDF/B-VI, except for Sn isotopes where the ENDL92 library is used, and uranium isotopes where LANL/T16 libraries are used. These are the default libraries for the MCNP code version used here [5.1.1]. MCNP has been extensively benchmarked against experimental data by the large user community. References [5.4.2], [5.4.3], and [5.4.4] are three examples of the benchmarking that has been performed.

The energy distribution of the source term, as described earlier, is used explicitly in the MCNP model. A different MCNP calculation is performed for each of the three source terms (neutron, decay gamma, and ^{60}Co). The axial distribution of the fuel source term is described in Table 2.1.5 and Figures 2.1.3 and 2.1.4. The PWR and BWR axial burnup distributions were obtained from References [5.4.5] and [5.4.6], respectively and have previously been utilized in the HI-STORM FSAR [5.2.17]. These axial distributions were obtained from operating plants and are representative of PWR and BWR fuel with burnups greater than 30,000 MWD/MTU. The ^{60}Co source in the hardware was assumed to be uniformly distributed over the appropriate regions.

It has been shown that the neutron source strength varies as the burnup level raised by the power of 4.2. Since this relationship is non-linear and since the burnup in the axial center of a fuel assembly is greater than the average burnup, the neutron source strength in the axial center of the assembly is greater than the relative burnup times the average neutron source strength. In order to account for this effect, the neutron source strength in each of the 10 axial nodes listed in Table 2.1.5 was determined by multiplying the average source strength by the relative burnup level raised to the power of 4.2. The peak relative burnups listed in Table 2.1.5 for the PWR and BWR fuels are 1.105 and 1.195 respectively. Using the power of 4.2 relationship results in a 37.6% ($1.105^{4.2}/1.105$) and 76.8% ($1.195^{4.2}/1.195$) increase in the neutron source strength in the peak nodes for the PWR and BWR fuel, respectively. The total neutron source strength increases by 15.6% for the PWR fuel assemblies and 36.9% for the BWR fuel assemblies.

MCNP was used to calculate doses at the various desired locations. MCNP calculates neutron or photon flux and these values can be converted into dose by the use of dose response functions. This is done internally in MCNP and the dose response functions are listed in the input file in Appendix 5.A. The response functions used in these calculations are listed in Table 5.4.1 and were taken from ANSI/ANS 6.1.1, 1977 [5.4.1].

The dose rates at the various locations were calculated with MCNP using a two-step process. The first step was to calculate the dose rate for each dose location per starting particle for each neutron and gamma group in each basket region for each axial and azimuthal dose location. The second step is to multiply the dose rate per starting particle for each energy group and basket location (i.e., tally output/quantity) by the source strength (i.e. particles/sec) in that group and sum the resulting dose rates for all groups and basket locations in each dose location. The normalization of these results and calculation of the total dose rate from neutrons, fuel gammas or Co-60 gammas is performed with the following equation.

$$T_{final} = \sum_{j=1}^{M}\left[\sum_{i=1}^{N}\frac{T_{i,j}}{Fm_i} * F_{i,j}\right] \qquad \text{(Equation 5.4.1)}$$

where,

T_{final} = Final dose rate (rem/h) from neutrons, fuel gammas, or Co-60

N = Number of groups (neutrons, fuel gammas) or Number of axial sections (Co-60 gammas)

M = Number of regions in the basket

$T_{i,j}$ = Tally quantity from particles originating in MCNP in group/section i and region j (rem/h)(particles/sec)

$F_{i,j}$ = Fuel Assembly source strength in group i and region j (particles/sec)

Fm_i = Source fraction used in MCNP for group i

Note that dividing by Fm_i (normalization) is necessary to account for the number of MCNP particles that actually start in group i. Also note that T_i is already multiplied by a dose conversion factor in MCNP.

The standard deviations of the various results were statistically combined to determine the standard deviation of the total dose in each dose location. The estimated variance of the total dose rate, S^2_{total}, is the sum of the estimated variances of the individual dose rates S^2_i. The estimated total dose rate, estimated variance, and relative error [5.1.1] are derived according to Equations 5.4.2 through 5.4.5.

$$R_i = \frac{\sqrt{S_i^2}}{T_i} \qquad \text{(Equation 5.4.2)}$$

$$S_{Total}^2 = \sum_{i=1}^{n} S_i^2 \qquad \text{(Equation 5.4.3)}$$

$$T_{Total} = \sum_{i=1}^{n} T_i \qquad \text{(Equation 5.4.4)}$$

$$R_{Total} = \frac{\sqrt{S_{Total}^2}}{T_{Total}} = \frac{\sqrt{\sum_{i=1}^{n} S_i^2}}{T_{Total}} = \frac{\sqrt{\sum_{i=1}^{n} (R_i \times T_i)^2}}{T_{Total}} \qquad \text{(Equation 5.4.5)}$$

where,

i	=	tally component index
n	=	total number of components
T_{Total}	=	total estimated tally
T_i	=	tally i component
S^2_{Total}	=	total estimated variance
S^2_i	=	variance of the i component
R_i	=	relative error of the i component
R_{Total}	=	total estimated relative error

Note that the two-step approach outlined above allows the accurate consideration of the neutron and gamma source spectrum, and the location of the individual assemblies, since the tallies are calculated in MCNP as a function of the starting energy group and the assembly location, and then in the second step multiplied with the source strength in each group in each location. It is therefore equivalent to a one-step calculation where source terms are directly specified in the MCNP input files, except for the following approximations:

The first approximation is that fuel is modeled as fresh UO_2 fuel (rather than spent fuel) in MCNP, with an upper bound enrichment. The second approximation is related to the axial burnup profile. The profile is modeled by assigning a source probability to each of the 10 axial sections of the active region, based on a representative axial burnup profile [5.2.17]. For fuel gammas, the probability is proportional to the burnup, since the gamma source strength changes essentially linearly with burnup. For neutrons, the probability is proportional to the burnup raised to the power of 4.2, since the neutron source strength is proportional to the burnup raised to about that power [5.4.7]. This is a standard approach that has been previously used in the licensing calculations for the HI-STAR 100 cask [5.4.8] and HI-STORM 100 system [5.2.17].

Tables 5.1.6 and 5.1.7 provide the design basis dose rates adjacent to the HI-STORM overpack during normal conditions for the MPC types in Table 1.0.1. Table 5.1.8 provides the design basis dose rates at one meter from the overpack containing the MPC-37. A detailed discussion of the normal, off-normal, and accident condition dose rates is provided in Subsections 5.1.1 and 5.1.2.

Table 5.4.2 shows the corresponding dose rates adjacent to and one meter away from the HI-TRAC for the fully flooded MPC-37 condition with an empty water-jacket (condition in which the HI-TRAC is removed from the spent fuel pool). Table 5.4.3 shows the dose rates adjacent to and one meter away from the HI-TRAC for the fully flooded MPC-37 condition with the water jacket filled with water (condition in which welding operations are performed). For the conditions involving a fully flooded MPC-37, the internal water level was 5 inches below the MPC lid. These dose rates represent the various conditions of the HI-TRAC during operations. Comparing these results to Table 5.1.1 (dry MPC-37 and HI-TRAC water jacket filled with water) indicates that the dose rates in the upper and lower portions of the HI-TRAC are significantly reduced with water in the MPC.

Table 5.4.4 shows the corresponding dose rates adjacent to and one meter away from the HI-TRAC for the fully flooded MPC-89 condition with an empty water-jacket. Table 5.4.5 shows the dose rates adjacent to and one meter away from the HI-TRAC for the fully flooded MPC-89 condition with the water jacket filled with water. These results demonstrate that the dose rates on contact at the top and bottom of the HI-TRAC VW are somewhat higher in the MPC-89 case than in the MPC-37 case. However, the MPC-37 produces higher dose rates than the MPC-89 at the center of the HI-TRAC, on-contact, and at locations 1 meter away from the HI-TRAC. Therefore, the MPC-37 is used for the exposure calculations in Chapter 11 of the SAR.

The calculations presented herein are using a uniform loading pattern. All MPCs, however, also offer regionalized loading patterns, as mentioned in Section 5.0 and described in Subsection 1.2. These loading patterns authorize fuel of higher decay heat (i.e., higher burnups and shorter cooling times) to be stored in certain regions of the basket. Evaluations have been performed for the HI-STORM 100 [5.2.17] where analysis of the MPC-32 and MPC-68 using the same burnup and cooling times in Region 1 and Region 2. Region 1 contains 38% of total number of assemblies for the MPC-32 and 47% for the MPC-68. The evaluations show that approximately 21% and 27% of the neutron dose at the edge of the water jacket comes from region 1 fuel assemblies in the MPC-32 and MPC-68, respectively. Further, approximately 1% and 2% of the photon dose at the edge of the water jacket comes from region 1 fuel assemblies in the MPC-32 and MPC-68, respectively. These results clearly indicate that the outer fuel assemblies shield almost the entire gamma source from the inner assemblies in the radial direction and a significant percentage of the neutron source. The conclusion from this analysis is that the total dose rate on the external radial surfaces of the cask can be greatly reduced by placing longer cooled and lower burnup fuels on the outside of the basket. Using a uniform loading pattern, rather than

employing the regionalized loading scheme, in these HI-STORM FW calculations is therefore acceptable as it produces conservative dose rate values on the radial surfaces.

Since MCNP is a statistical code, there is an uncertainty associated with the calculated values. In MCNP the uncertainty is expressed as the relative error which is defined as the standard deviation of the mean divided by the mean. Therefore, the standard deviation is represented as a percentage of the mean. The relative error for the total dose rates presented in this chapter were typically less than 5% and the relative error for the individual dose components was typically less than 10%.

5.4.1 Streaming Through Radial Steel Fins

The HI-STORM FW overpack and the HI-TRAC VW cask utilize radial steel fins for structural support and cooling. The attenuation of neutrons through steel is substantially less than the attenuation of neutrons through concrete and water. Therefore, it is possible to have neutron streaming through the fins that could result in a localized dose peak. The reverse is true for photons, which would result in a localized reduction in the photon dose.

Analysis of the steel fins in the HI-TRAC has previously been performed in the HI-STORM 100 FSAR [5.2.17] and indicates that neutron streaming is noticeable at the surface of the cask. The neutron dose rate on the surface of the steel fin is somewhat higher than the circumferential average dose rate at that location. The gamma dose rate, however, is slightly lower than the circumferential average dose rate at that location. At one meter from the cask surface there is little difference between the dose rates calculated over the fins compared to the other areas of the water jackets.

These conclusions indicate that localized neutron streaming is noticeable on the surface of the transfer casks. However, at one meter from the surface the streaming has dissipated. Since most HI-TRAC operations will involve personnel moving around the transfer cask at some distance from the cask, only surface average dose rates are reported in this chapter.

5.4.2 Damaged Fuel Post-Accident Shielding Evaluation

The Holtec Generic PWR and BWR DFCs are designed to accommodate any PWR or BWR fuel assembly that can physically fit inside the DFC. Damaged fuel assemblies under normal conditions, for the most part, resemble intact fuel assemblies from a shielding perspective. Under accident conditions, it can not be guaranteed that the damaged fuel assembly will remain intact. As a result, the damaged fuel assembly may begin to resemble fuel debris in its possible configuration after an accident.

Since damaged fuel is identical to intact fuel from a shielding perspective no specific analysis is required for damaged fuel under normal conditions. However, a generic shielding evaluation was previously performed for the HI-STORM 100 [5.2.17] to demonstrate that fuel debris under normal or accident conditions, or damaged fuel in a post-accident configuration, will not result in a significant increase in the dose rates around the 100-ton HI-TRAC. Since the 100-ton HI-TRAC and the HI-TRAC VW are similar in design, the conclusions from the 100-ton HI-RAC evaluations are also applicable to the HI-TRAC VW.

The scenario analyzed to determine the potential change in dose rate as a result of fuel debris or a damaged fuel assembly collapse in the HI-STORM 100 [5.2.17] feature fuel debris or a damaged fuel assembly that has collapsed (which can have a higher average fuel density than an intact fuel assembly). If the damaged fuel assembly would fully or partially collapse, the fuel density in one portion of the assembly would increase and the density in the other portion of the assembly would decrease. The analysis consisted of modeling the fuel assemblies in the damaged fuel locations in the MPC-24 and MPC-68 with a fuel density that was twice the normal fuel density and correspondingly increasing the source rate for these locations by a factor of two. A flat axial power distribution was used which is approximately representative of the source distribution if the top half of an assembly collapsed into the bottom half of the assembly. Increasing the fuel density over the entire fuel length, rather than in the top half or bottom half of the fuel assembly, is conservative and provides the dose rate change in both the top and bottom portion of the cask.

The results for the MPC-24 and MPC-68 calculations [5.2.17] show that the potential effect on the dose rate is not very significant for the storage of damaged fuel and/or fuel debris. This conclusion is further reinforced by the fact that the majority of the significantly damaged fuel assemblies in the spent fuel inventories are older assemblies from the earlier days of nuclear plant operations. Therefore, these assemblies will have a considerably lower burnup and longer cooling times than the assemblies analyzed in this chapter. In addition, since the dose rate change is not significant for the 100-ton HI-TRAC, the dose rate change will not be significant for the HI-TRAC VW or the HI-STORM FW overpacks.

5.4.3 Site Boundary Evaluation

NUREG-1536 [5.2.1] states that detailed calculations need not be presented since SAR Chapter 12 assigns ultimate compliance responsibilities to the site licensee. Therefore, this subsection describes, by example, the general methodology for performing site boundary dose calculations. The site-specific fuel characteristics, burnup, cooling time, and the site characteristics would be factored into the evaluation performed by the licensee.

The methodology of calculating the dose from a single HI-STORM overpack loaded with an MPC and various arrays of loaded HI-STORMs at distances equal to and greater than 100 meters is described in the HI-STORM 100 FSAR [5.2.17]. A back row factor of 0.20 was calculated in

[5.2.17], and utilized herein to calculate dose value C below, based on the results that the dose from the side of the back row of casks is approximately 16 % of the total dose.

The annual dose, assuming 100% occupancy (8760 hours), at 300 meters from a single HI-STORM FW cask is presented in Table 5.4.6 for the design basis burnup and cooling time analyzed.

The annual dose, assuming 8760 hour occupancy, at distance from an array of casks was calculated in three steps.

1. The annual dose from the radiation leaving the side of the HI-STORM FW overpack was calculated at the distance desired. Dose value = A.

2. The annual dose from the radiation leaving the top of the HI-STORM FW overpack was calculated at the distance desired. Dose value = B.

3. The annual dose from the radiation leaving the side of a HI-STORM FW overpack, when it is behind another cask, was calculated at the distance desired. The casks have an assumed 15-foot pitch. Dose value = C.

The doses calculated in the steps above are listed in Table 5.4.7. Using these values, the annual dose (at the center of the long side) from an arbitrary 2 by Z array of HI-STORM FW overpacks can easily be calculated. The following formula describes the method.

Z = number of casks along long side

Dose = ZA + 2ZB + ZC

The results for various typical arrays of HI-STORM overpacks can be found in Section 5.1. While the off-site dose analyses were performed for typical arrays of casks containing design basis fuel, compliance with the requirements of 10CFR72.104(a) can only be demonstrated on a site-specific basis, as stated earlier. Therefore, a site-specific evaluation of dose at the controlled area boundary must be performed for each ISFSI in accordance with 10CFR72.212. The site-specific evaluation will consider the site-specific characteristics (such as exposure duration and the number of casks deployed), dose from other portions of the facility and the specifics of the fuel being stored (burnup and cooling time).

5.4.4 Non-Fuel Hardware

As discussed in Subsection 5.2.3, non-fuel hardware in the form of BPRAs, TPDs, CRAs, and APSRs are permitted for storage, integral with a PWR fuel assembly, in the HI-STORM FW

system. Since each device occupies the same location within an assembly, only one device will be present in a given assembly. ITTRs, which are installed after core discharge and do not contain radioactive material, may also be stored in the assembly. BPRAs, TPDs and ITTRs are authorized for unrestricted storage in an MPC. The permissible locations of the CRAs and APSRs are shown in Figure 2.1.5.

Table 5.4.8 provides the dose rates at various locations on the surface and one meter from the HI-TRAC VW due to the BPRAs and TPDs for the MPC-37. The results in Table 5.4.8 show that the BPRAs essentially bound TPDs. All dose rates with NFH in this chapter therefore assume BPRA in every assembly. Note that, even for calculations without NFH, the dose from the active region conservatively contains the contribution of the BPRA. This mainly affects dose location 1 and 2, and results for these locations are therefore identical in most tables, and don't show the dose rate difference indicated in Table 5.4.8.

The analyses in this chapter that consider presence of BPRAs assume that a full-length rod with burnable poison is present in all principal locations. In reality, many BPRAs contain full-length poison rods in some locations, and thimble rodlets in others. The burnup and cooling time combinations listed in Table 2.1.25 of HI-STORM 100 FSAR [5.2.17] for BPRAs and TPDs were selected to ensure the Co-60 activity of those devices is below the value of 895 Ci (BPRA) and 50 Ci (TPD). These activities are used in the dose evaluations presented in this chapter. Apart from the total activity, the axial distribution of the material in those devices is important for the dose rates. This axial distribution is shown in Table 5.2.15 (masses) and 5.2.16 (activities). It can be observed from Table 5.2.16, while TPDs have a lower overall activity, their activity in the gas plenum region of the assembly is higher compared to that of the BPRAs. These activities were used to calculate the dose rates in Table 5.4.8. The results in this table show that the maximum dose effect for BPRAs is at the side of the cask, while the maximum dose effect of TPDs is near and on the top of the cask. Nevertheless, Table 5.4.8 demonstrates that even near and on the top of the cask, the TPD doses are bounded by the BPRA doses. It is to be noted that BPRAs with several thimble plugs may result higher dose rate near and on the top of the cask than that reported in Table 5.4.8. However, the potential local increase in dose near and on the top of the cask due the presence of several thimble plug rodlets instead of full length BPRA rods would be more than compensated by the reduction of the dose from the side of the cask at larger distances. Therefore, using BPRAs with all burnable poison rods in the analyses that demonstrate compliance with the site boundary dose limits would be bounding, and hence the burnup and cooling time combinations for BPRAs in Table 2.1.25 of the HI-STORM 100 FSAR [5.2.17] are conservative.

Two different configurations were analyzed for CRAs and three different configurations were analyzed for APSRs in the HI-STORM FSAR [5.2.17]. The dose rate due to CRAs and APSRs was explicitly calculated for dose locations around the HI-TRAC and results were provided for the different configurations of CRAs and APSRs, respectively, in the MPCs. These results

indicate the dose rate on the radial surfaces of the overpack due to the storage of these devices is less than the dose rate from BPRAs (the increase in dose rate on the radial surface due to CRAs and APSRs are virtually negligible). For the surface dose rate at the bottom, the value for the CRA is comparable to or higher than the value from the BPRA. The increase in the bottom dose rates due to the presence of CRAs is on the order of 10-15% (based on bounding configuration 1 in [5.2.17]). The dose rate out the top of the overpack is essentially 0. The latter is due to the fact that CRAs and APSRs do not achieve significant activation in the upper portion of the devices due to the manner in which they are utilized during normal reactor operations. In contrast, the dose rate out the bottom of the overpack is substantial due to these devices. However, these dose rates occur in an area (below the pool lid and transfer doors) which is not normally occupied.

While the evaluations described above are based on conservative assumptions, the conclusions can vary slightly depending on the number of CRAs and their operating conditions.

5.4.5 Effect of Uncertainties

The design basis calculations presented in this chapter are based on a range of conservative assumptions, but do not explicitly account for uncertainties in the methodologies, codes and input parameters, that is, it is assumed that the effect of uncertainties is small compared to the numerous conservatisms in the analyses. To show that this assumption is valid, calculations have previously been performed as "best estimate" calculations and with estimated uncertainties added [5.4.9]. In all scenarios considered (e.g., evaluation of conservatisms in modeling assumptions, uncertainties associated with MCNP as well as the depletion analysis (including input parameters), etc.), the total dose rates long with uncertainties are comparable to, or lower than, the corresponding values from the design basis calculations. This provides further confirmation that the design basis calculations are reasonable and conservative.

5.4.6 MPC-32ML with Regionalized Loading Patterns

As discussed in Section 5.2, there is only one heat load pattern with a uniform loading configuration for MPC-32ML. However, different burnup, enrichment and cooling time combinations may produce same decay heat, but different source terms. Additional regionalized shielding analysis is provided in this subsection by dividing the MPC-32ML basket cells into Regions 1 to 3, where Region 1 is the innermost cells, and Region 3 is the outermost cells. The fuel burnup, enrichment and cooling time combinations in Table 5.4.9 are used to calculate the adjacent and 1-m dose rates for HI-STORM FW with MPC-32ML. The heat load of each combination is either more than the decay heat limit per cell, or for the minimum cooling time of 3 years. Conservative enrichments are also considered for all combinations. Each burnup, enrichment, and cooling time combination can be in Region 1, Region 2, and/or Region 3 cells. The maximum adjacent and 1 m dose rates are provided in Tables 5.4.10 and 5.4.11,

respectively. Higher concrete density may be used in site specific shielding analysis to further lower the occupational dose rates.

Table 5.4.1

FLUX-TO-DOSE CONVERSION FACTORS
(FROM [5.4.1])

Gamma Energy (MeV)	**(rem/hr)/ (photon/cm^2-s)**
0.01	3.96E-06
0.03	5.82E-07
0.05	2.90E-07
0.07	2.58E-07
0.1	2.83E-07
0.15	3.79E-07
0.2	5.01E-07
0.25	6.31E-07
0.3	7.59E-07
0.35	8.78E-07
0.4	9.85E-07
0.45	1.08E-06
0.5	1.17E-06
0.55	1.27E-06
0.6	1.36E-06
0.65	1.44E-06
0.7	1.52E-06
0.8	1.68E-06
1.0	1.98E-06
1.4	2.51E-06
1.8	2.99E-06
2.2	3.42E-06

Table 5.4.1 (continued) FLUX-TO-DOSE CONVERSION FACTORS (FROM [5.4.1])	
Gamma Energy (MeV)	**(rem/hr)/ (photon/cm^2-s)**
2.6	3.82E-06
2.8	4.01E-06
3.25	4.41E-06
3.75	4.83E-06
4.25	5.23E-06
4.75	5.60E-06
5.0	5.80E-06
5.25	6.01E-06
5.75	6.37E-06
6.25	6.74E-06
6.75	7.11E-06
7.5	7.66E-06
9.0	8.77E-06
11.0	1.03E-05
13.0	1.18E-05
15.0	1.33E-05

Table 5.4.1 (continued)

FLUX-TO-DOSE CONVERSION FACTORS
(FROM [5.4.1])

Neutron Energy (MeV)	**Quality Factor**	**(rem/hr)†/(n/cm²-s)**
2.5E-8	2.0	3.67E-6
1.0E-7	2.0	3.67E-6
1.0E-6	2.0	4.46E-6
1.0E-5	2.0	4.54E-6
1.0E-4	2.0	4.18E-6
1.0E-3	2.0	3.76E-6
1.0E-2	2.5	3.56E-6
0.1	7.5	2.17E-5
0.5	11.0	9.26E-5
1.0	11.0	1.32E-4
2.5	9.0	1.25E-4
5.0	8.0	1.56E-4
7.0	7.0	1.47E-4
10.0	6.5	1.47E-4
14.0	7.5	2.08E-4
20.0	8.0	2.27E-4

† Includes the Quality Factor.

Table 5.4.2

DOSE RATES FOR THE HI-TRAC VW FOR THE FULLY FLOODED MPC CONDITION WITH AN EMPTY NEUTRON SHIELD

MPC-37 DESIGN BASIS ZIRCALOY CLAD FUEL AT 45,000 MWD/MTU AND 4.5-YEAR COOLING

Dose Point Location	Fuel Gammas (mrem/hr)	(n,γ) Gammas (mrem/hr)	^{60}Co Gammas (mrem/hr)	Neutrons (mrem/hr)	Totals (mrem/hr)	Totals with BPRAs (mrem/hr)
ADJACENT TO THE HI-TRAC VW						
1	711	<1	489	67	1268	1268
2	2242	2	<1	319	2563	2563
3	7	<1	128	2	139	210
4	15	<1	227	<1	244	371
5 (bottom lid)	465	<1	1802	79	2346	2346
ONE METER FROM THE HI-TRAC VW						
1	541	<1	61	53	657	657
2	1141	<1	5	116	1263	1264
3	191	<1	75	20	286	326
4	8	<1	127	<1	137	208
5	259	<1	985	20	1266	1266

Notes:

- Refer to Figure 5.1.2 for dose point locations.
- Values are rounded to nearest integer.
- MPC internal water level is 5 inches below the MPC lid.
- The "Fuel Gammas" category includes gammas from the spent fuel, ^{60}Co from the spacer grids, and ^{60}Co from the BPRAs in the active fuel region.

Table 5.4.3

DOSE RATES FOR THE HI-TRAC VW FOR THE FULLY FLOODED MPC CONDITION WITH A FULL NEUTRON SHIELD

MPC-37 DESIGN BASIS ZIRCALOY CLAD FUEL AT 45,000 MWD/MTU AND 4.5-YEAR COOLING

Dose Point Location	Fuel Gammas (mrem/hr)	(n,γ) Gammas (mrem/hr)	^{60}Co Gammas (mrem/hr)	Neutrons (mrem/hr)	Totals (mrem/hr)	Totals with BPRAs (mrem/hr)
ADJACENT TO THE HI-TRAC VW						
1	433	1	301	5	740	740
2	1266	5	<1	27	1298	1298
3	2	<1	69	<1	73	111
4	15	<1	227	<1	244	371
5 (bottom lid)	465	<1	1802	80	2347	2347
ONE METER FROM THE HI-TRAC VW						
1	294	1	34	4	333	334
2	657	2	3	10	671	672
3	95	<1	41	1	138	160
4	8	<1	127	<1	137	208
5	259	<1	985	20	1265	1265

Notes:

- Refer to Figure 5.1.2 for dose point locations.
- Values are rounded to nearest integer.
- MPC internal water level is 5 inches below the MPC lid.
- The "Fuel Gammas" category includes gammas from the spent fuel, ^{60}Co from the spacer grids, and ^{60}Co from the BPRAs in the active fuel region.

Table 5.4.4

DOSE RATES FOR THE HI-TRAC VW FOR THE FULLY FLOODED MPC CONDITION WITH AN EMPTY NEUTRON SHIELD

MPC-89 DESIGN BASIS ZIRCALOY CLAD FUEL AT 45,000 MWD/MTU AND 5-YEAR COOLING

Dose Point Location	Fuel Gammas (mrem/hr)	(n,γ) Gammas (mrem/hr)	^{60}Co Gammas (mrem/hr)	Neutrons (mrem/hr)	Totals (mrem/hr)
ADJACENT TO THE HI-TRAC VW					
1	195	<1	1513	43	1752
2	2435	3	<1	579	3018
3	<1	<1	351	2	355
4	3	<1	217	<1	222
5 (bottom lid)	40	<1	1530	5	1576
ONE METER FROM THE HI-TRAC VW					
1	387	<1	197	69	654
2	1180	<1	12	168	1361
3	118	<1	154	26	299
4	<1	<1	132	<1	135
5	19	<1	864	2	886

Notes:

- Refer to Figure 5.1.2 for dose point locations.
- Values are rounded to nearest integer.
- MPC internal water level is 5 inches below the MPC lid.
- The "Fuel Gammas" category includes gammas from the spent fuel and ^{60}Co from the spacer grids.

Table 5.4.5

DOSE RATES FOR THE HI-TRAC VW FOR THE FULLY FLOODED MPC CONDITION WITH A FULL NEUTRON SHIELD

MPC-89 DESIGN BASIS ZIRCALOY CLAD FUEL AT 45,000 MWD/MTU AND 5-YEAR COOLING

Dose Point Location	Fuel Gammas (mrem/hr)	(n,γ) Gammas (mrem/hr)	^{60}Co Gammas (mrem/hr)	Neutrons (mrem/hr)	Totals (mrem/hr)
ADJACENT TO THE HI-TRAC VW					
1	102	<1	926	2	1031
2	1373	10	<1	47	1431
3	<1	<1	189	<1	192
4	3	<1	217	<1	222
5 (bottom lid)	40	<1	1530	5	1576
ONE METER FROM THE HI-TRAC VW					
1	211	1	115	5	332
2	627	3	7	16	653
3	72	<1	83	1	157
4	<1	<1	132	<1	135
5	19	<1	864	2	886

Notes:

- Refer to Figure 5.1.2 for dose point locations.
- Values are rounded to nearest integer.
- MPC internal water level is 5 inches below the MPC lid.
- The "Fuel Gammas" category includes gammas from the spent fuel and ^{60}Co from the spacer grids.

Table 5.4.6

ANNUAL DOSE AT 300 METERS FROM A SINGLE HI-STORM FW OVERPACK WITH AN MPC-37 WITH DESIGN BASIS ZIRCALOY CLAD FUEL

Dose Component	**45,000 MWD/MTU 4.5-Year Cooling (mrem/yr)**
Fuel gammas	15.8
^{60}Co Gammas	2.2
Neutrons	0.2
Total	18.2

Notes:

- Gammas generated by neutron capture are included with fuel gammas.
- The Co-60 gammas include BPRAs.
- The "Fuel Gammas" category includes gammas from the spent fuel, ^{60}Co from the spacer grids, and ^{60}Co from the BPRAs in the active fuel region.

Table 5.4.7

DOSE VALUES USED IN CALCULATING ANNUAL DOSE FROM VARIOUS HI-STORM FW ISFSI CONFIGURATIONS
45,000 MWD/MTU AND 4.5-YEAR COOLING ZIRCALOY CLAD FUEL

Distance	**A Side of Overpack (mrem/yr)**	**B Top of Overpack (mrem/yr)**	**C Side of Shielded Overpack (mrem/yr)**
100 meters	396.0	44.0	79.2
200 meters	61.7	6.9	12.3
300 meters	16.4	1.8	3.3
400 meters	5.3	0.6	1.1
500 meters	2.0	0.2	0.4
600 meters	0.8	0.1	0.2

Notes:

- 8760 hour annual occupancy is assumed.
- Values are rounded to nearest integer where appropriate.

Table 5.4.8

DOSE RATES DUE TO BPRAs AND TPDs FROM THE HI-TRAC VW FOR NORMAL CONDITIONS

Dose Point Location	BPRAs (mrem/hr)	TPDs (mrem/hr)
ADJACENT TO THE HI-TRAC VW		
1	159.09	0.0
2	509.04	0.0
3	192.78	165.31
4	304.15	275.53
5	137.27	0.0
ONE METER FROM THE HI-TRAC VW		
1	122.06	0.40
2	240.70	3.10
3	128.50	86.95
4	174.25	153.49
5	63.13	0.0

Notes:

- Refer to Figure 5.1.2 for dose locations.
- Dose rates are based on no water within the MPC, an empty annulus, and a water jacket full of water. For the majority of the duration that the HI-TRAC bottom lid is installed, the MPC cavity will be flooded with water. The water within the MPC greatly reduces the dose rate
- Includes the BPRAs from both the active and non-active region.

Table 5.4.9

BURNUP, ENRICHMENT, COOLING TIME COMBINATIONS FOR
3-REGION REGIONALIZED LOADING PATTERNS

Burnup (MWD/MTU)	Initial U-235 Enrichment (wt%)	Cooling Time (years)
15000	1	3
20000	1.2	3
25000	1.4	3.2
30000	1.8	3.6
35000	1.8	4.2
40000	2.5	4.6
45000	2.7	5.4
50000	3	6.4
55000	3.1	8
60000	3.8	9.5
65000	4.1	12

Table 5.4.10

MAXIMUM DOSE RATES ADJACENT TO HI-STORM FW OVERPACK
FOR NORMAL CONDITIONS
MPC-32MLWITH 16X16D FUEL
BURNUP AND COOLING TIME
REGIONALIZED LOADING PATTERNS

Dose Point Location	Fuel Gammas (mrem/hr)	(n,γ) Gammas (mrem/hr)	^{60}Co Gammas (mrem/hr)	Neutrons (mrem/hr)	Totals (mrem/hr)	Totals with BPRAs (mrem/hr)
1	206	1	87	2	295	295
2	170	1	< 1	1	172	172
3 (surface)	16	1	18	2	37	47
3 (overpack edge)	12	< 1	45	1	57	82
4 (center)	< 1	1.0	0.2	0.2	1.5	1.7
4 (mid)	4	< 1	1	< 1	6	6
4 (outer)	10	< 1	22	< 1	33	45

Notes:

- Refer to Figure 5.1.1 for dose locations.
- Values are rounded to nearest integer where appropriate.
- Dose location 3 (surface) is at the surface of the outlet vent. Dose location 3 (overpack edge) is in front of the outlet vent, but located radially above the overpack outer diameter.
- Dose location 4 (center) is at the center of the top surface of the top lid. Dose location 4 (mid) is situated directly above the vertical section of the outlet vent. Dose location 4 (outer) is extended along the top plane of the top lid, located radially above the overpack outer diameter.
- The "Fuel Gammas" category includes gammas from the spent fuel, ^{60}Co from the spacer grids, and ^{60}Co from the BPRAs in the active fuel region.

Table 5.4.11

MAXIMUM DOSE RATES AT ONE METER FROM HI-STORM FW OVERPACK
FOR NORMAL CONDITIONS
MPC-32MLWITH 16X16D FUEL
BURNUP AND COOLING TIME
REGIONALIZED LOADING PATTERNS

Dose Point Location	Fuel Gammas (mrem/hr)	(n,γ) Gammas (mrem/hr)	^{60}Co Gammas (mrem/hr)	Neutrons (mrem/hr)	Totals (mrem/hr)	Totals with BPRAs (mrem/hr)
1	51	< 1	16	< 1	68	68
2	90	< 1	1	< 1	92	92
3	8	< 1	8	< 1	17	21
4 (center)	0.6	0.4	0.7	0.3	2.0	2.5

Notes:

- Refer to Figure 5.1.1 for dose locations.
- Values are rounded to nearest integer where appropriate.
- The "Fuel Gammas" category includes gammas from the spent fuel, ^{60}Co from the spacer grids, and ^{60}Co from the BPRAs in the active fuel region.

HOLTEC INTERNATIONAL COPYRIGHTED MATERIAL

5.5 REGULATORY COMPLIANCE

Chapters 1 and 2 and this chapter of this SAR describe in detail the shielding structures, systems, and components (SSCs) important to safety.

The shielding-significant SSCs important to safety have been valuated in this chapter and their impact on personnel and public health and safety resulting from operation of an independent spent fuel storage installation (ISFSI) utilizing the HI-STORM FW system has been evaluated.

It has been shown that the design of the shielding system of the HI-STORM FW system is in compliance with 10CFR72 and that the applicable design and acceptance criteria including 10CFR20 have been satisfied. Thus, this shielding evaluation provides reasonable assurance that the HI-STORM FW system will allow safe storage of spent fuel in full conformance with 10CFR72.

5.6 REFERENCES

[5.1.1] LA-UR-03-1987, MCNP — A General Monte Carlo N-Particle Transport Code, Version 5, April 24, 2003 (Revised 10/3/05).

[5.1.2] I.C. Gauld, O.W. Hermann, "SAS2: A Coupled One-Dimensional Depletion and Shielding Analysis Module," ORNL/TM-2005/39, Version 5.1, Vol. I, Book 3, Sect. S2, Oak Ridge National Laboratory, November 2006.

[5.1.3] I.C. Gauld, O.W. Hermann, R.M. Westfall, "ORIGEN-S: SCALE System Module to Calculate Fuel Depletion, Actinide Transmutation, Fission Product Buildup and Decay, and Associated Radiation Source Terms," ORNL/TM-2005/39, Version 5.1, Vol. II, Book 1, Sect. F7, Oak Ridge National Laboratory, November 2006.

[5.2.1] NUREG-1536, SRP for Dry Cask Storage Systems, USNRC, Washington, DC, January 1997.

[5.2.2] A.G. Croff, M.A. Bjerke, G.W. Morrison, L.M. Petrie, "Revised Uranium-Plutonium Cycle PWR and BWR Models for the ORIGEN Computer Code," ORNL/TM-6051, Oak Ridge National Laboratory, September 1978.

[5.2.3] A. Luksic, "Spent Fuel Assembly Hardware: Characterization and 10CFR 61 Classification for Waste Disposal," PNL-6906-vol. 1, Pacific Northwest Laboratory, June 1989.

[5.2.4] J.W. Roddy et al., "Physical and Decay Characteristics of Commercial LWR Spent Fuel," ORNL/TM-9591/V1&R1, Oak Ridge National Laboratory, January 1996.

[5.2.5] "Characteristics of Spent Fuel, High Level Waste, and Other Radioactive Wastes Which May Require Long-Term Isolation," DOE/RW-0184, U.S. Department of Energy, December 1987.

[5.2.6] Not Used.

[5.2.7] "Characteristics Database System LWR Assemblies Database," DOE/RW-0184-R1, U.S. Department of Energy, July 1992.

[5.2.8] O. W. Hermann, et al., “Validation of the Scale System for PWR Spent Fuel Isotopic Composition Analyses,” ORNL/TM-12667, Oak Ridge National Laboratory, March 1995.

HOLTEC INTERNATIONAL COPYRIGHTED MATERIAL

[5.2.9] M. D. DeHart and O. W. Hermann, "An Extension of the Validation of SCALE (SAS2H) Isotopic Predictions for PWR Spent Fuel," ORNL/TM-13317, Oak Ridge National Laboratory, September 1996.

[5.2.10] O. W. Hermann and M. D. DeHart, "Validation of SCALE (SAS2H) Isotopic Predictions for BWR Spent Fuel," ORNL/TM-13315, Oak Ridge National Laboratory, September 1998.

[5.2.11] "Summary Report of SNF Isotopic Comparisons for the Disposal Criticality Analysis Methodology," B00000000-01717-5705-00077 REV 00, CRWMS M&O, September 1997.

[5.2.12] "Isotopic and Criticality Validation of PWR Actinide-Only Burnup Credit," DOE/RW-0497, U.S. Department of Energy, May 1997.

[5.2.13] B. D. Murphy, "Prediction of the Isotopic Composition of UO_2 Fuel from a BWR: Analysis of the DU1 Sample from the Dodewaard Reactor," ORNL/TM-13687, Oak Ridge National Laboratory, October 1998.

[5.2.14] O. W. Hermann, et al., "Technical Support for a Proposed Decay Heat Guide Using SAS2H/ORIGEN-S Data," NUREG/CR-5625, ORNL-6698, Oak Ridge National Laboratory, September 1994.

[5.2.15] C. E. Sanders, I. C. Gauld, "Isotopic Analysis of High-Burnup PWR Spent Fuel Samples from the Takahama-3 Reactor," NUREG/CR-6798, ORNL/TM-2001/259, Oak Ridge National Laboratory, January 2003.

[5.2.16] Not Used.

[5.2.17] HI-2002444, Rev. 7, "Final Safety Analysis Report for the HI-STORM 100 Cask System", USNRC Docket 72-1014.

[5.4.1] "American National Standard Neutron and Gamma-Ray Flux-to-Dose Rate Factors", ANSI/ANS-6.1.1-1977.

[5.4.2] D. J. Whalen, et al., "MCNP: Photon Benchmark Problems," LA-12196, Los Alamos National Laboratory, September 1991.

[5.4.3] D. J. Whalen, et al., "MCNP: Neutron Benchmark Problems," LA-12212, Los Alamos National Laboratory, November 1991.

HOLTEC INTERNATIONAL COPYRIGHTED MATERIAL

[5.4.4] J. C. Wagner, et al., “MCNP: Criticality Safety Benchmark Problems,” LA-12415, Los Alamos National Laboratory, October 1992.

[5.4.5] S. E. Turner, "Uncertainty Analysis - Axial Burnup Distribution Effects," presented in "Proceedings of a Workshop on the Use of Burnup Credit in Spent Fuel Transport Casks," SAND-89-0018, Sandia National Laboratory, Oct. 1989.

[5.4.6] Commonwealth Edison Company, Letter No. NFS-BND-95-083, Chicago, Illinois.

[5.4.7] B.L. Broadhead, “Recommendations for Shielding Evaluations for Transport and Storage Packages,“ NUREG/CR-6802 (ORNL/TM-2002/31), Oak Ridge National Laboratory, May 2003.

[5.4.8] HI-2012610, Rev. 3, ”Final Safety Analysis Report for the HI-STAR 100 Cask System”, USNRC Docket 72-1008.

[5.4.9] HI-2073681, Rev. 3, “Safety Analysis Report on the HI-STAR 180 Package”, USNRC Docket 71-9325.

APPENDIX 5.A

SAMPLE INPUT FILES FOR SAS2H, ORIGEN-S, AND MCNP

Proprietary Appendix Withheld in Accordance with 10 CFR 2.390

HOLTEC INTERNATIONAL COPYRIGHTED MATERIAL

TABLE 6.1.1(a)
BOUNDING MAXIMUM k_{eff} VALUES FOR EACH ASSEMBLY CLASS IN THE MPC-37
(HI-TRAC VW)

Fuel Assembly Class	4.0 wt% ^{235}U Maximum Enrichment†		5.0 wt% ^{235}U Maximum Enrichment†	
	Minimum Soluble Boron Concentration (ppm)	Maximum k_{eff}	Minimum Soluble Boron Concentration (ppm)	Maximum k_{eff}
14x14A	1000	0.8946	1500	0.8983
14x14B	1000	0.9213	1500	0.9282
14x14C	1000	0.9211	1500	0.9277
15x15B	1500	0.9129	2000	0.9311
15x15C	1500	0.9029	2000	0.9188
15x15D	1500	0.9223	2000	0.9421
15x15E	1500	0.9206	2000	0.9410
15x15F	1500	0.9244	2000	0.9455
15x15H	1500	0.9142	2000	0.9325
15x15I	1500	0.9155	2000	0.9362
16x16A	1000	0.9275	1500	0.9366
16x16A[DFC]††	1000	0.9400	1600	0.9404
16x16B	1000	0.9258	1500	0.9334
16x16C	1000	0.9099	1500	0.9187
16x16E	1000	0.9231	1500	0.9303
17x17A	1500	0.9009	2000	0.9194
17x17B	1500	0.9181	2000	0.9380
17x17C	1500	0.9222	2000	0.9424
17x17D	1500	0.9183	2000	0.9384
17x17E	1500	0.9203	2000	0.9392

† For maximum allowable enrichments between 4.0 wt% ^{235}U and 5.0 wt% ^{235}U, the minimum soluble boron concentration may be calculated by linear interpolation between the minimum soluble boron concentrations specified for each assembly class.

†† Intact Fuel Assembly Class 16x16A loaded in DFCs in all 37 cell locations, if permitted by the certificate of compliance.

HOLTEC INTERNATIONAL COPYRIGHTED MATERIAL

TABLE 6.1.1 (bc)

BOUNDING MAXIMUM k_{eff} VALUES FOR EACH ASSEMBLY CLASS IN MPC-32ML (HI-TRAC VW)

Fuel Assembly Class	**4.0 wt% ^{235}U Maximum Enrichment†**		**5.0 wt% ^{235}U Maximum Enrichment†**	
	Minimum Soluble Boron Concentration (ppm)	**Maximum k_{eff}**	**Minimum Soluble Boron Concentration (ppm)**	**Maximum k_{eff}**
16x16D	1500	0.9256~~0.9205~~	2000	0.9427~~0.9386~~

† For maximum allowable enrichments between 4.0 wt% ^{235}U and 5.0 wt% ^{235}U, the minimum soluble boron concentration may be calculated by linear interpolation between the minimum soluble boron concentrations specified for each assembly class.

HOLTEC INTERNATIONAL COPYRIGHTED MATERIAL

TABLE 6.1.4(a)

BOUNDING MAXIMUM k_{eff} VALUES FOR THE MPC-37
WITH UP TO 12 DFCs

Fuel Assembly Class of Undamaged Fuel	**4.0 wt% ^{235}U Maximum Enrichment for Undamaged Fuel and Damaged Fuel/Fuel Debris †**		**5.0 wt% ^{235}U Maximum Enrichment for Undamaged Fuel and Damaged Fuel/Fuel Debris †**	
	Minimum Soluble Boron Concentration (ppm)	**Maximum k_{eff}**	**Minimum Soluble Boron Concentration (ppm)**	**Maximum k_{eff}**
All 14x14, 16x16††	1300	0.9155	1800	0.9305
All 15x15, all 17x17	1800	0.9032	2300	0.9276

† For maximum allowable enrichments between 4.0 wt% ^{235}U and 5.0 wt% ^{235}U, the minimum soluble boron concentration may be calculated by linear interpolation between the minimum soluble boron concentrations specified for each assembly class.

†† For assembly class 16x16A intact fuel can be loaded with or without DFCs if permitted in the certificate of compliance.

HOLTEC INTERNATIONAL COPYRIGHTED MATERIAL

TABLE 6.1.4(b~~c~~)

BOUNDING MAXIMUM k_{eff} VALUES FOR MPC-32ML
WITH UP TO 8 DFCs

Fuel Assembly Class of Undamaged Fuel	**4.0 wt% ^{235}U Maximum Enrichment for Undamaged Fuel and Damaged Fuel/Fuel Debris †**		**5.0 wt% ^{235}U Maximum Enrichment for Undamaged Fuel and Damaged Fuel/Fuel Debris †**	
	Minimum Soluble Boron Concentration (ppm)	**Maximum k_{eff}**	**Minimum Soluble Boron Concentration (ppm)**	**Maximum k_{eff}**
16x16D	1600	0.9186~~0.9149~~	2100	0.9380~~0.9347~~

† For maximum allowable enrichments between 4.0 wt% ^{235}U and 5.0 wt% ^{235}U, the minimum soluble boron concentration may be calculated by linear interpolation between the minimum soluble boron concentrations specified for each assembly class.

HOLTEC INTERNATIONAL COPYRIGHTED MATERIAL

- Fuel assemblies are predominantly characterized by the amount of fuel and the fuel-to-water (moderator) ratio. Increasing the amount of fuel, or the enrichment of the fuel, will increase the amount of fissile material, and therefore increase reactivity. Regarding the fuel-to-water ratio, it is important to note that commercial PWR and BWR assemblies are undermoderated, i.e. they do not contain enough water for a maximum possible reactivity.
- The neutron poison in the basket walls uses B-10, which is an absorber of thermal neutrons. This poison therefore also needs water (moderator) to be effective. This places a specific importance on the amount of water between the outer rows of the fuel assemblies and the basket cell walls. Note that this explains some of the differences in reactivity between the different assembly types in the same basket, even for the same enrichment, where assemblies with a smaller cross section, i.e. which have more water between the periphery of the assembly and the surrounding wall, generally have a lower reactivity.

Based on these characteristics, the following conclusions can be made:

- Since fuel assemblies are undermoderated, any changes in geometry inside the fuel assembly that increases the amount of water while maintaining the amount of fuel are expected to increase reactivity. This explains why reducing the cladding or guide tube/water rod thicknesses, or increasing the fuel rod pitch results in an increase in reactivity.
- Increasing the active length will increase the amount of fuel while maintaining the fuel-to-water ratio, and therefore increase reactivity.
- The channel of the BWR assembly is a structure located outside of the rod array. It therefore does not affect the water-to-fuel ratio within the assembly. However, it reduces the amount of water between the assembly and the neutron poison, therefore reducing the effective thermalization for the poison. Therefore, an increase of the channel wall thickness will increase reactivity.
- In respect to the effect of the fuel pellet outer diameter, several compensatory effects need to be considered. Increasing the diameter will tend to increase the reactivity due to the increase in the fuel amount. However, it will also change the fuel-to-water-ratio, and will therefore make the fuel more undermoderated, which in turn tends to reduce reactivity. The effect of this change in moderation may depend on the condition of the pellet-to-clad gap. Assuming an empty pellet-to clad gap, which would be consistent with undamaged fuel rods, the change in moderation is small, and the net effect is an increase in reactivity, since the effect of the increase in the fissionable material dominates. In this case, the maximum pellet diameter is more reactive. When the pellet-to-clad gap is conservatively flooded, as recommended by NUREG 1536 (see section 6.4.2.3), a reduction of the fuel pellet diameter will also result in an increase in the amount of water, i.e. have a double effect on the water-to-fuel ratio. In this case, it is possible that a slight reduction may result in no reduction or even an increase in reactivity. However, this is caused by a further amplification of the conservative assumption of the flooded pellet-to-clad gap, not by a positive increase in reactivity from the reduction in fuel (which would

HOLTEC INTERNATIONAL COPYRIGHTED MATERIAL

TABLE 6.2.3

EFFECT OF THE FLOODING OF THE PELLET-TO-CLAD GAP

Fuel Assembly Class	Maximum k_{eff} at 5.0 wt% ^{235}U Maximum Enrichment		
	Flooded Pellet-to-Clad Gap	Empty Pellet-to-Clad Gap	Difference
14x14A	0.8983	0.8962	-0.0021
14x14B	0.9282	0.9235	-0.0047
14x14C	0.9277	0.9237	-0.0038
15x15B	0.9311	0.9284	-0.0027
15x15C	0.9188	0.9164	-0.0024
15x15D	0.9421	0.9386	-0.0035
15x15E	0.9410	0.9371	-0.0039
15x15F	0.9455	0.9408	-0.0047
15x15H	0.9325	0.9300	-0.0025
15x15I	0.9357	0.9305	-0.0052
16x16A	0.9366	0.9284	-0.0082
16x16A[DFC]	0.9400	0.9340	-0.0060
16x16B	0.9334	0.9297	-0.0037
16x16C	0.9187	0.9144	-0.0043
16x16D	0.9427~~0.9386~~	0.9361~~0.9350~~	-0.0066~~-0.0036~~
16x16E	0.9303	0.9223	-0.0080
17x17A	0.9194	0.9160	-0.0034
17x17B	0.9380	0.9335	-0.0045
17x17C	0.9424	0.9375	-0.0049
17x17D	0.9384	0.9323	-0.0061
17x17E	0.9392	0.9346	-0.0046

HOLTEC INTERNATIONAL COPYRIGHTED MATERIAL

6.3 MODEL SPECIFICATION

6.3.1 Description of Calculational Model

Figures 6.3.1 through 6.3.~~5~~ 7 show representative cross sections of the criticality models for all considered ~~the two~~ baskets. Figures 6.3.1, 6.3.2 and 6.3.~~2~~ 6 show ~~a~~ single cell from each ~~of the two~~ basket~~s~~. Figures 6.3.3, 6.3.4 and 6.3.7~~9~~4 show the entire MPC-37, ~~and~~ MPC-89 and MPC-32ML basket, respectively. Figure 6.3.5 shows a sketch of the calculational model in the axial direction.

Full three-dimensional calculational models were used for all calculations. The calculational models explicitly define the fuel rods and cladding, the guide tubes, water rods and the channel (for the BWR assembly), the neutron absorber walls of the basket cells, and the surrounding MPC shell and overpack. For the flooded condition (loading and unloading), pure, unborated water was assumed to be present in the fuel rod pellet-to-clad gaps, since this represents the bounding condition as demonstrated in Section 6.4.2.3. Appendix 6.B provides sample input files for typical MPC basket designs

Note that the water thickness above and below the fuel is modeled as unborated water, even when borated water is present in the fuel region.

The discussion provided in Section 6.2.1 regarding the principal characteristics of fuel poison is also important for the various studies presented in this section, and supports the fact that those studies only need to be performed for a single BWR and PWR assembly type, and that the results of those studies are then generally applicable to all assembly types. The studies and the relationship to the discussion in Section 6.2.1 are listed below. Note that this approach is consistent with that used for the HI-STORM 100. The MPC-32ML basket design is very similar to the MPC-37 basket; the only major difference is the increased cell ID and, consequently, the number of storage locations is reduced. Therefore, all studies performed for MPC-37 are directly applicable to MPC-32ML, since the same behavior (reactivity effect) is expected. ~~However, MPC~~However, MPC-32ML basket specific studies are performed and discussed below.

Basket Manufacturing Tolerance: The two aspects of the basket tolerance that are evaluated are the cell wall thickness and the cell ID. The reduced cell wall thickness results in a reduced amount of poison (since the material composition of the wall is fixed), and therefore in an increase in reactivity. The reduced cell ID reduces amount of water between the fuel the poison, and therefore the effectiveness of the poison material. Both effects are simply a function of the geometry, and are independent of the fuel type.

Panel Gaps: Similar to the basket manufacturing tolerance for the cell wall thickness, this tolerance has a small effect on the overall poison amount of the basket, which would affect the reactivity of the system independent of the fuel type.

HOLTEC INTERNATIONAL COPYRIGHTED MATERIAL

Eccentric positioning (see Section 6.3.3): When a fuel assembly is located in the center of a basket cell, it is surrounded by equal amounts of water on all sides, and hence the thermalization of the neutrons that occur between the assembly and the poison in the cell wall, and hence the effectiveness of the poison, is also equal on all sides. For an eccentric positioning, the effectiveness of the poison is now reduced on those sides where the assembly is located close to the cell walls, and increased on the opposite sides. This creates a compensatory situation for a single cell, where the net effect is not immediately clear. However, for the entire basket, and for the condition where all assemblies are located closest to the center of the basket, the ~~four~~ assemblies at the center of the basket are now located close to each other, separated by poison plates with a reduced effectiveness since they are not surrounded by water on any side. This now becomes the dominating condition is terms of reactivity increase. This effect is also applicable to all assembly types, since those assemblies are all located close to the center of the basket, i.e. the eccentric position with all assemblies moved towards the center will be bounding regardless of the assembly type.

Wall thicknesses of DFCs: DFCs are used for damaged fuel and fuel debris in selected locations of the basket, but are also permitted to be used for intact fuel of the array/type 16x16A. Generally, DFCs are thin-walled containers, in order to minimize the additional weight to be supported by the basket. For damaged fuel and fuel debris calculations, a wall thickness of 0.025" is used, and studies with larger wall thicknesses show an insignificant effect. However, when DFCs are also used for intact assemblies of the 16x16A array/type, it is shown that there is a noticeable effect when a thicker wall is modeled. Consequently, for DFCs for intact 16x16A fuel, a conservative DFC wall thickness of 0.075" is used to provide manufacturing flexibility. Note that this already a rather thick wall, the same as typically used for storage racks in spent fuel pools, and would therefore present a practical upper limit for any DFC design.

The basket geometry can vary due to manufacturing tolerances and due to potential deflections of basket walls as the result of accident conditions. The basket tolerances are defined on the drawings in Chapter 1. The structural acceptance criteria for the basket during accident conditions is that the permanent deflection of the basket panels is limited to a fraction of 0.005 (0.5%) of the panel width (see Chapter 3). The analyses in Chapter 3 demonstrate that permanent deformations of the basket walls during accident conditions are far below this limit. In fact, the analyses show that the vast majority of the basket panels remain elastic during and after an accident, and therefore show no permanent deflection whatsoever, and that any deformation is limited to small localized areas. Nevertheless, it is conservatively assumed that 2 adjacent cell walls in each cell are deflected to the maximum extent possible over their entire length and width, i.e. that the cell ID is reduced by 0.5% of the cell width, or 0.045" for the MPC-37 cells and 0.030" for the MPC-89 cells. Stated differently, the minimum cell ID based on tolerances was further reduced by the amounts stated above for all cells in each basket to account for the potential deflections of basket walls during accident conditions. Assuming that all cell sizes are reduced is a simplifying, but very conservative assumption, since cell walls are shared between neighboring cells, so while the deflection of a basket wall would reduce the cell size on one side, it necessarily increases that on the other side of the wall. MCNP5 was used to determine the manufacturing tolerances and deflections that produced the most adverse effect on criticality.

HOLTEC INTERNATIONAL COPYRIGHTED MATERIAL

After the reactivity effect (positive effect with an increase in reactivity; or negative effect with a decrease in reactivity) of the manufacturing tolerances was determined, the criticality analyses were performed using the worst case conditions in the direction which would increase reactivity. For simplification, the same worst case conditions are used for both normal and accident conditions. For all calculations, fuel assemblies were assumed to be eccentrically located in the cells, since this results in higher reactivities (see Section 6.3.3). Maximum k_{eff} results (including the bias, uncertainties, or calculational statistics), along with the selected dimensions, for a number of dimensional combinations are shown in Table 6.3.2 for ~~both~~ various baskets. The cell ID is evaluated for minimum (tolerance only)~~, minimum with deformation~~, nominal~~, and an~~ increased value and a bounding with deformation. The wall thickness is evaluated for nominal and minimum values.

Based on the calculations, the conservative dimensional assumptions listed in Table 6.3.3 were determined for the basket designs. Because the reactivity effect (positive or negative) of the manufacturing tolerances is not assembly dependent, these dimensional assumptions were employed for all criticality analyses.

The basket is manufactured from individual slotted panels. The panels are expected to be in direct contact with each other (see Drawings in Chapter 1). However, to show that small gaps between panels would have essentially no effect on criticality, calculations are performed with a postulated 0.06" gap between panels, repeated in the axial direction every 10" in all panels. Since it is expected that the effect of these gaps would be small, these calculations were performed with a larger number of particles per cycle, larger number of inactive cycles, and a larger total number of cycles to improve the statistics of each run, so the real reactivity effect could be better separated from the statistical "noise". The results are summarized in Tables 6.3.6 and show that the METAMIC gap has a very small effect. Therefore, all calculations are performed without any gaps between panels.

Variations of water temperature in the cask were analyzed using CASMO-4. The analyses were performed for the assembly class 10x10A in the MPC-89, ~~and~~ for the assembly class 17x17B with 2000 ppm soluble boron in the water in the MPC-37, and for the assembly class 16x16D with 2000 ppm soluble boron in the water in the MPC-32ML. These are the same assemblies and conditions used for the fuel dimension studies in Section 6.2, and shown there to be representative of all assemblies qualified for those baskets. The results are presented in Table 6.3.1, and show that the minimum water temperature (corresponding to a maximum water density) are bounding. This condition is therefore used in all further calculations. This is expected since an increased temperature results in a reduced water density, a condition that is shown in Section 6.4 to result in reduced reactivities.

Calculations documented in Chapter 3 show that the baskets stay within the applicable structural limits during all normal and accident conditions. Furthermore, the neutron poison material is an integral and non-removable part of the basket material, and its presence is therefore not affected by the accident conditions. Except for the potential deflection of the basket walls that is already considered in the criticality models, damage to the cask under accident conditions is limited to

HOLTEC INTERNATIONAL COPYRIGHTED MATERIAL

possible loss of the water in the water jacket of ~~he~~ HI-TRAC VW. However, this condition is already considered in the calculational models. Other parameters important to criticality safety are fuel type and enrichment, which are not affected by the hypothetical accident conditions. The calculational models of the cask and basket for the accident conditions are therefore identical to the models for normal conditions, and no separate models need to be developed for accident conditions.

6.3.2 Cask Regional Densities

Composition of the various components of the principal designs of the HI-STORM FW system are listed in Table 6.3.4. The cross section set for each nuclide is listed in Table 6.3.8, and is consistent with the cross section sets used in the benchmarking calculations documented in Appendix A. Note that these are the default cross sections chosen by the code.

The HI-STORM FW system is designed such that the fixed neutron absorber will remain effective for a storage period greater than 60 years, and there are no credible means to lose it.

The continued efficacy of the fixed neutron absorber is assured by acceptance testing, documented in Subsection 10.1.6.3, to validate the ^{10}B (poison) concentration in the fixed neutron absorber. To demonstrate that the neutron flux from the irradiated fuel results in a negligible depletion of the poison material over the storage period, an evaluation of the number of neutrons absorbed in the ^{10}B was performed. The calculation conservatively assumed a constant neutron source for 60 years equal to the initial source for the design basis fuel, as determined in Section 5.2, and shows that the fraction of ^{10}B atoms destroyed is less than 10^{-7} in 60 years. Thus, the reduction in ^{10}B concentration in the fixed neutron absorber by neutron absorption is negligible. Therefore, in accordance with 10CFR72.124(b), there is no need to provide a surveillance or monitoring program to verify the continued efficacy of the neutron absorber.

6.3.3 Eccentric Positioning of Assemblies in Fuel Storage Cells

The potential reactivity effect of eccentric positioning of assemblies in the fuel storage locations is accounted for in a conservatively bounding fashion, as described further in this subsection. The calculations in this subsection serve to identify the eccentric positioning of assemblies in the fuel storage locations, which results in a higher maximum k_{eff} value than the centered positioning. For the cases where the eccentric positioning results in a higher maximum k_{eff} value, the eccentric positioning is used for all corresponding cases reported in the summary tables in Section 6.1 and the results tables in Section 6.4.

To conservatively account for eccentric fuel positioning in the fuel storage cells, three different configurations are analyzed, and the results are compared to determine the bounding configuration:

HOLTEC INTERNATIONAL COPYRIGHTED MATERIAL

TABLE 6.3.1

CASMO-4 CALCULATIONS FOR EFFECT OF TEMPERATURE

Change in Nominal Parameter	**Δk Maximum Tolerance**			**Action/Modeling Assumption**
	MPC-37, 17x17B, 5.0 wt%, Borated Water with 2000 ppm Soluble Boron	**MPC-89, 10x10A, 4.8 wt%, Fresh Water**	**MPC-32ML, 16x16D, 5.0 wt%, Borated Water with 2000 ppm Soluble Boron**	
Increase in Temperature 20°C 40°C 70°C 100°C	 Ref. -0.0008 -0.0023 -0.0042	 Ref. -0.0035 -0.0100 -0.0180	 Ref. -0.0004 -0.0012 -0.0023	Assume 20°C
10% Void in Moderator 20°C with no void 20°C 100°C	 Ref. -0.0036 -0.0096	 Ref. -0.0282 -0.0463	 Ref. -0.0010 -0.0055	Assume no void

HOLTEC INTERNATIONAL COPYRIGHTED MATERIAL

TABLE 6.3.2

EVALUATION OF BASKET MANUFACTURING TOLERANCES

Box I.D.	**Box Wall Thickness**	**Maximum k_{eff}**
MPC-37 (17x17B, 5.0% Enrichment)		
nominal (8.94")	nominal (0.59")	0.9332
nominal (8.94")	minimum (0.57”)	0.9346
increased (8.96")	minimum (0.57”)	0.9350
minimum (8.92")	minimum (0.57”)	0.9352
minimum, including deformation (8.875")	minimum (0.57”)	0.9374
MPC-89 (10x10A 4.8% Enrichment)		
nominal (6.01")	nominal (0.40")	0.9365
nominal (6.01")	minimum (0.38”)	0.9403
increased (6.03")	minimum (0.38”)	0.9396
minimum (5.99")	minimum (0.38”)	0.9417
minimum, including deformation (5.96")	minimum (0.38”)	0.9428
MPC-32ML (16x16D, 5.0% Enrichment)		
nominal (9.57")	nominal (0.59")	0.9366
nominal (9.57")	minimum (0.57”)	0.9385
increased (9.61")	minimum (0.57”)	0.9367
minimum (9.53")	minimum (0.57”)	0.9410
minimum, including deformation (9.482")	minimum (0.57”)	0.9428

HOLTEC INTERNATIONAL COPYRIGHTED MATERIAL

TABLE 6.3.3

BASKET DIMENSIONAL ASSUMPTIONS

Basket Type	Box I.D.	Box Wall Thickness
MPC-37	minimum, including deformation(8.875")	minimum (0.57”)
MPC-89	minimum, including deformation (5.96")	minimum (0.38”)
MPC-32ML	minimum, including deformation(9.482")	minimum (0.57”)

HOLTEC INTERNATIONAL COPYRIGHTED MATERIAL

TABLE 6.3.5

REACTIVITY EFFECTS OF ECCENTRIC POSITIONING OF CONTENT
(FUEL ASSEMBLIES AND DFCs) IN BASKET CELLS

CASE	Contents centered (Reference)	Content moved towards center of basket		Content moved towards basket periphery	
	Maximum k_{eff}	Maximum k_{eff}	k_{eff} Difference to Reference	Maximum k_{eff}	k_{eff} Difference to Reference
MPC-37, Undamaged Fuel	0.9327	0.9380	0.0053	0.9143	-0.0184
MPC-37, Undamaged Fuel and Damaged Fuel/Fuel Debris (12 DFCs)	0.9260	0.9276	0.0016	0.9158	-0.0102
MPC-89, Undamaged Fuel	0.9369	0.9435	0.0066	0.9211	-0.0158
MPC-89, Undamaged Fuel and Damaged Fuel/Fuel Debris (16 DFCs)	0.9415	0.9451	0.0036	0.9301	-0.0114
MPC-32ML, Undamaged Fuel	0.9390	0.9427	0.0037	0.9156	-0.0234
MPC-32ML, Undamaged Fuel and Damaged Fuel/Fuel Debris (8 DFCs)	0.9372	0.9380	0.0009	0.9223	-0.0149

TABLE 6.3.6

REACTIVITY EFFECTS GAPS IN BASKET CELL PLATES

Gaps in Metamic-HT	**MPC-37 (17x17B, 5.0% ENRICHMENT)**	**MPC-89 (10x10A, 4.8% ENRICHMENT)**	**MPC-32ML (16x16D, 5.0% ENRICHMENT**
None	0.9380	0.9435	0.9427
0.06” every 10”	0.9382	0.9439	0.9426

HOLTEC INTERNATIONAL COPYRIGHTED MATERIAL

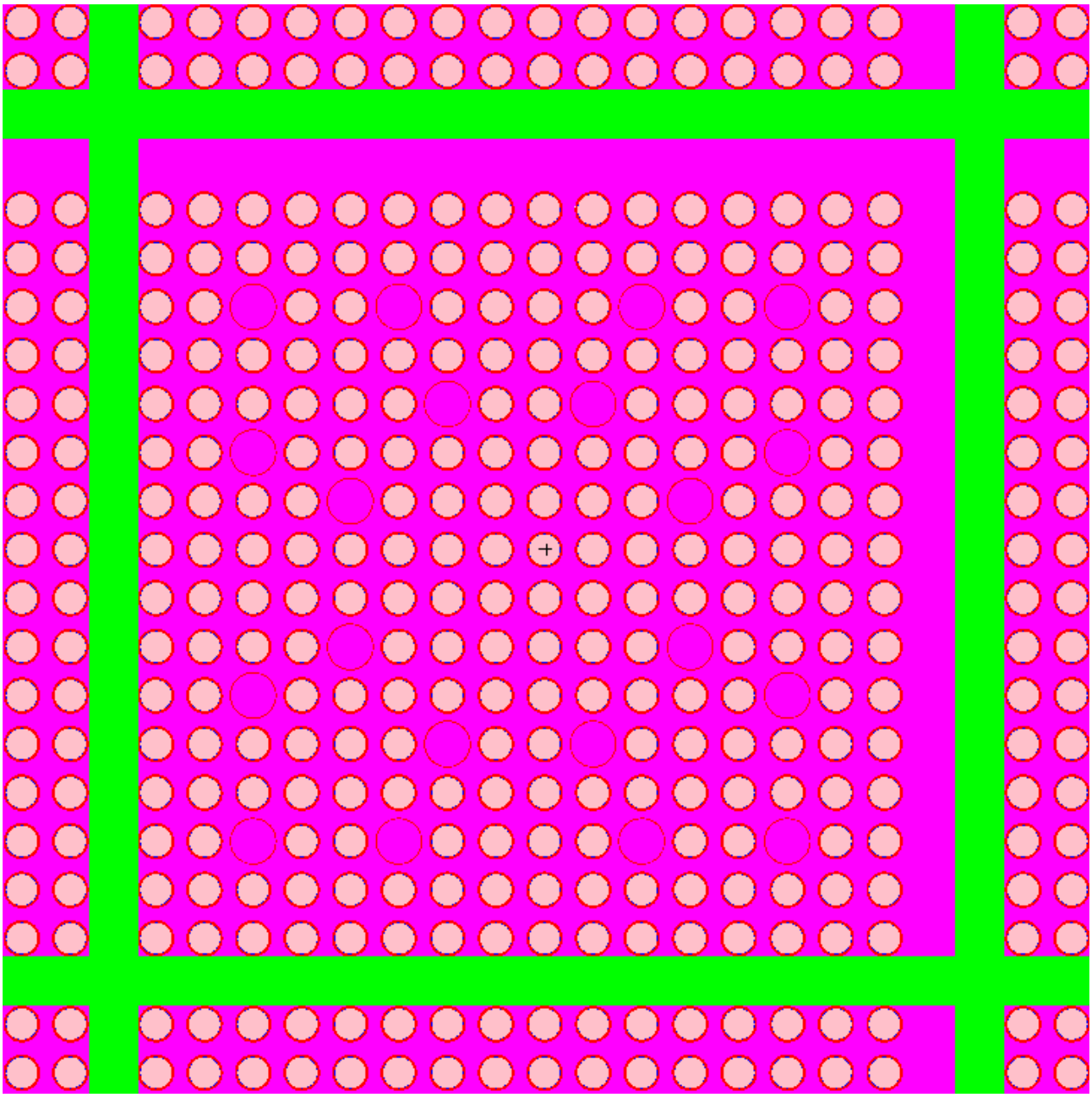

Figure generated directly from MCNP input file using the MCNP plot function. For Cell ID and Cell Wall Thickness see Table 6.3.3. For true dimensions see the drawings in Chapter 1.

Figure 6.3.6~~7~~: Typical Cell of the Calculational Model (planar cross-section) with representative fuel in MPC-32ML

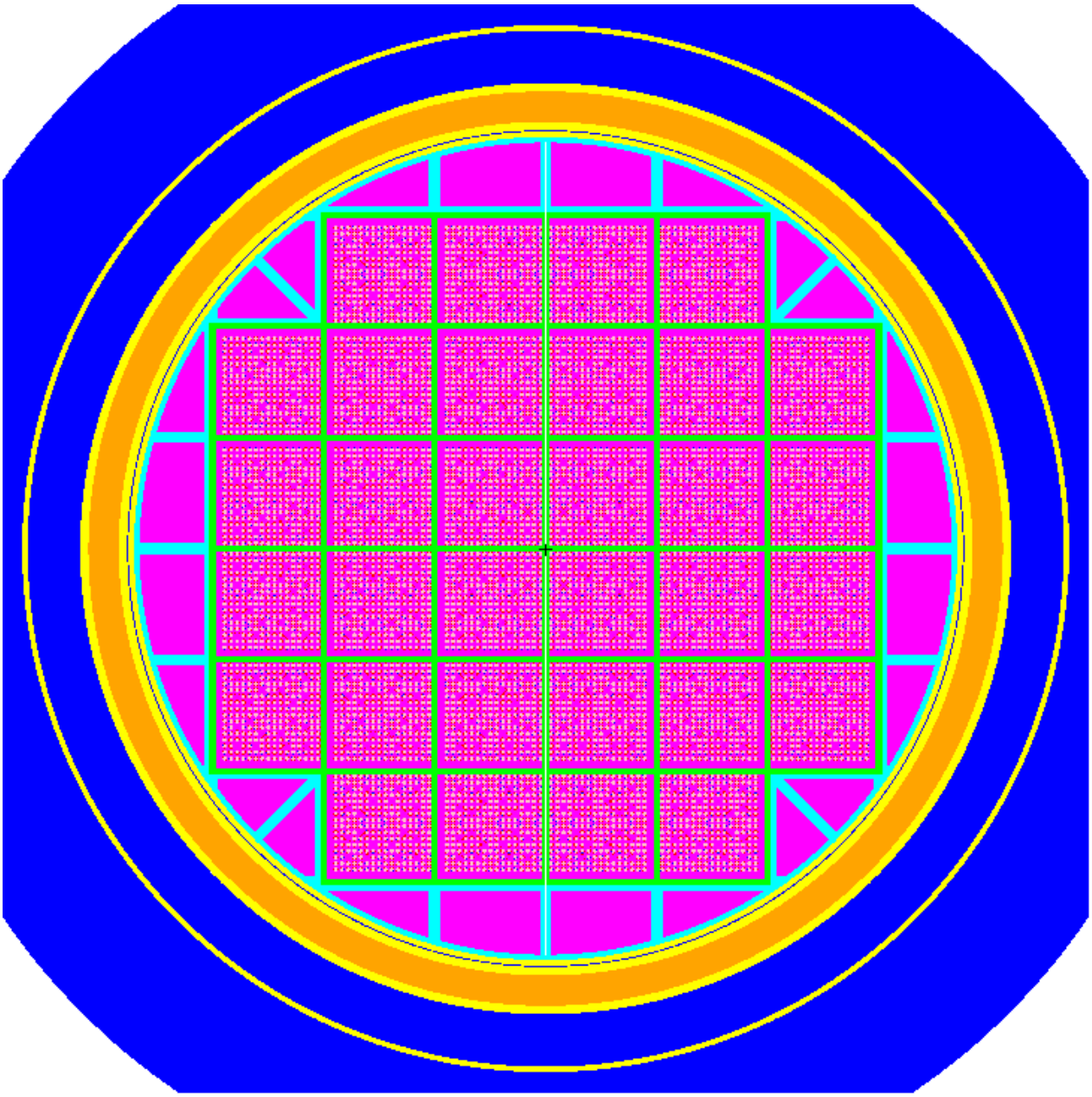

Figure generated directly from MCNP input file using the MCNP plot function. For radial dimensions of the HI-TRAC VW used in the analyses see Table 6.3.7. For true dimensions see the drawings in Chapter 1.

Figure 6.3.7~~9~~: Calculational Model (planar cross-section) of MPC-32ML

6.4 CRITICALITY CALCULATIONS

6.4.1 Calculational Methodology

The principal method for the criticality analysis is the general three-dimensional continuous energy Monte Carlo N-Particle code MCNP5 [6.1.4] developed at the Los Alamos National Laboratory. MCNP5 was selected because it has been extensively used and verified and has all of the necessary features for this analysis. MCNP5 calculations used continuous energy cross-section data distributed with the code [6.1.4].

The convergence of a Monte Carlo criticality problem is sensitive to the following parameters: (1) number of histories per cycle, (2) the number of cycles skipped before averaging, (3) the total number of cycles and (4) the initial source distribution. The MCNP5 criticality output contains a great deal of useful information that may be used to determine the acceptability of the problem convergence. Based on this information, a minimum of 20,000 histories were simulated per cycle, a minimum of 20 cycles were skipped before averaging, a minimum of 100 cycles were accumulated, and the initial source was specified as uniform over the fueled regions (assemblies). To verify that these parameters are sufficient, studies were performed where the number of particles per cycle and/or the number of skipped cycles were increased. The calculations are presented in Table 6.4.9, and show only small differences between the cases, with the statistical tolerance of those calculations. All calculations are therefore performed with the parameters stated above, except for some studies that are performed with 50000 neutrons per cycle for improved accuracy, and except for the calculations for the HI-STORM, which need less particles for convergence. Appendix 6.D provides sample input files for various ~~the MPC-37 and MPC-89~~ baskets in the HI-STORM FW system.

6.4.2 Fuel Loading or Other Contents Loading Optimization

The basket designs are intended to safely accommodate fuel with enrichments indicated in Section 2.1. The calculations were based on the assumption that the HI-STORM FW system (HI-TRAC VW transfer cask) was fully flooded with clean unborated water or water containing specific minimum soluble boron concentrations. In all cases, the calculations include bias and calculational uncertainties, as well as the reactivity effects of manufacturing tolerances, determined by assuming the worst case geometry.

The discussion provided in Section 6.2.1 regarding the principal characteristics of fuel assemblies and basket poison is also important for the various studies presented in this section, and supports the fact that those studies only need to be performed for a single BWR and PWR assembly types, and that the results of those studies are then generally applicable to all assembly types. The studies and the relationship to the discussion in Section 6.2.1 are listed below. Note that this approach is consistent with that used for the HI-STORM 100.

Internal and External Moderation (Section 6.4.2.1): The studies presented in Table 6.2.3 show that all assemblies essentially behave identical in respect to water moderation, specifically, that

HOLTEC INTERNATIONAL COPYRIGHTED MATERIAL

Note that the modeling approach for damaged fuel and fuel debris is identical to that used in the HI-STORM 100 and HI-STAR 100.

Bounding Undamaged Assemblies

The undamaged assemblies assumed in the basket in those cells not filled with DFCs are those that show the highest reactivity for each group of assemblies, namely

- 9x9E for BWR 9x9E/F, 8x8F and 10x10G assemblies
- 10x10F for BWR 10x10F assemblies
- 10x10A for all other BWR assemblies;
- 16x16A for all PWR assemblies with 14x14 and 16x16 arrays; ~~and~~
- 15x15F for all PWR assemblies with 15x15 and 17x17 arrays; and
- 16x16D for all PWR assemblies qualified for MPC-32ML..

Since the damaged fuel modeling approach results in higher reactivities, requirements of soluble boron for PWR fuel and maximum enrichment for BWR fuel are different from those for undamaged fuel only. Those limits are listed in Table 6.1.4 (PWR) and Table 6.1.5 (BWR) in Section 6.1. Note that for the calculational cases for damaged and undamaged fuel in the MPC-89, the same enrichment is used for the damage and undamaged assemblies.

Note that for the first group of BWR assemblies listed above (9x9E/F, 8x8F and 10x10G), calculations were performed for both 9x9E and 10x10G as undamaged assemblies, and assembly class 9x9E showed the higher reactivity, and is therefore used in the design basis analyses. This may seem contradictory to the results for undamaged assemblies listed in Table 6.1.2, where the 10x10G shows a higher reactivity. However, the cases in Table 6.1.2 are not at the same enrichment between those assemblies.

All calculations with damaged and undamaged fuel are performed for an active length of 150 inches. There are two assembly classes (17x17D and 17x17E) that have a larger active length for the undamaged fuel. However, the calculations for undamaged fuel presented in Table 6.1.1 show that the reactivity of those undamaged assemblies is at least 0.0050 delta-k lower than that of the assembly class 15x15F selected as the bounding assembly for the cases with undamaged and damaged fuel. The effect of the active fuel length is less than that, with a value of 0.0026 reported in Table 6.2.1 for a much larger difference in active length of 50 Inches. The difference in active length between the 17x17D/E and 15x15F is therefore more than bounded, and the 15x15F assembly class is therefore appropriate to bound all undamaged assemblies with 15x15 and 17x17 arrays.

HOLTEC INTERNATIONAL COPYRIGHTED MATERIAL

Bare Fuel Rod Arrays

A conservative approach is used to model both damaged fuel and fuel debris in the DFCs, using arrays of bare fuel rods:

- Fuel in the DFCs is arranged in regular, rectangular arrays of bare fuel rods, i.e., all cladding and other structural material in the DFC is replaced by water.

- For cases with soluble boron, additional calculations are performed with reduced water density in the DFC. This is to demonstrate that replacing all cladding and other structural material with borated water is conservative.

- The active length of these rods is assumed to be the same as for the intact fuel rods in the basket, even for more densely packed bare fuel rod arrays where it results in a total amount of fuel in the DFC that exceeds that for the intact assembly.

- To ensure the configuration with optimum moderation and highest reactivity is analyzed, the amount of fuel per unit length of the DFC is varied over a large range. This is achieved by changing the number of rods in the array and the rod pitch. The number of rods are varied between 16 (4x4) and 324 (18x18) for BWR fuel, ~~and~~ between 64 (8x8) and 576 (24x24) for PWR fuel, and between 289 (17x17) and 676 (26x26) for 16x16D.

This is a very conservative approach to model damaged fuel, and to model fuel debris configurations such as severely damaged assemblies and bundles of individual fuel rods, as the absorption in the cladding and structural material is neglected.

Further, this is a conservative approach to model fuel debris configurations such as bare fuel pellets due to the assumption of an active length of 150 inch (BWR and PWR). The actual height of bare fuel pellets in a DFC would be significantly below these values due to the limitation of the fuel mass for each basket position.

All calculations are performed for full cask models, containing the maximum permissible number of DFCs together with undamaged assemblies.

As an example of the damaged fuel model used in the analyses, Figure 6.4.1 shows the basket cell of an MPC-37 with a DFC containing a 14x14 array of bare fuel rods.

Principal results are listed in Table 6.4.6, ~~and~~ 6.4.7~~,~~ ~~6.4.11~~ and 6.4.11~~2~~ for the MPC-37, MPC-89, ~~MPC-31C~~ and MPC-~~89~~32ML, respectively. In all cases, the maximum k_{eff} is below the regulatory limit of 0.95.

For the HI-STORM 100, additional studies for damaged fuel assemblies were performed to further show that the above approach using arrays of bare fuel rods are bounding. The studies considered conditions including

HOLTEC INTERNATIONAL COPYRIGHTED MATERIAL

TABLE 6.4.1

MAXIMUM REACTIVITIES WITH REDUCED EXTERNAL WATER DENSITIES

Water Density		**Maximum k_{eff}**		
Internal	**External**	**MPC-37 (17x17B, 5.0%)**	**MPC-89 (10x10A, 4.8%)**	**MPC-32ML (16x16D, 5.0%)**
100%	100%	0.9380	0.9435	0.9427
100%	70%	0.9377	0.9432	0.9423
100%	50%	0.9399	0.9439	0.9429
100%	20%	0.9366	0.9428	0.9425
100%	10%	0.9374	0.9437	0.9426
100%	5%	0.9376	0.9435	0.9426
100%	1%	0.9383	0.9435	0.9429

HOLTEC INTERNATIONAL COPYRIGHTED MATERIAL

TABLE 6.4.2

REACTIVITY EFFECTS OF PARTIAL CASK FLOODING

MPC-37 (17x17B, 5.0% ENRICHMENT)		
Flooded Condition (% Full)	Maximum k_{eff}, Vertical Orientation	Maximum k_{eff}, Horizontal Orientation
25	0.9175	0.8306
50	0.9325	0.9093
75	0.9357	0.9349
100	0.9380	0.9380
MPC-89 (10x10A, 4.8% ENRICHMENT)		
Flooded Condition (% Full)	Maximum k_{eff}, Vertical Orientation	Maximum k_{eff}, Horizontal Orientation
25	0.9204	0.8345
50	0.9382	0.9128
75	0.9416	0.9392
100	0.9435	0.9435
MPC-32ML (16x16D, 5.0% ENRICHMENT)		
Flooded Condition (% Full)	Maximum k_{eff}, Vertical Orientation	Maximum k_{eff}, Horizontal Orientation
25	0.9203	0.8213
50	0.9374	0.9175
75	0.9411	0.9399
100	0.9427	0.9427

HOLTEC INTERNATIONAL COPYRIGHTED MATERIAL

TABLE 6.4.3

REACTIVITY EFFECT OF FLOODING THE PELLET-TO-CLAD GAP

~~Pellet-to-Clad Condition~~	~~**Maximum k_{eff}**~~	
	~~**MPC-37 (17x17B, 5.0% ENRICHMENT)**~~	~~**MPC-89 (10x10A, 4.8% ENRICHMENT)**~~
~~dry~~	~~0.9335~~	~~0.9391~~
~~flooded with unborated water~~	~~0.9380~~	~~0.9435~~
Case	**Maximum k_{eff}**	
	Dry	**Flooded with unborated water**
MPC-37 (17x17B, 5.0% Enrichment)	0.9335	0.9380
MPC-89 (10x10A, 4.8% Enrichment)	0.9391	0.9435
MPC-32ML (16x16D, 5.0% Enrichment)	0.9361~~0.9350~~	0.9427~~0.9386~~

HOLTEC INTERNATIONAL COPYRIGHTED MATERIAL

TABLE 6.4.4

REACTIVITY EFFECT OF PREFERENTIAL FLOODING OF THE DFCs

DFC Configuration	**Maximum k_{eff}**	
	Preferential Flooding	**Fully Flooded**
MPC-37 with 12 DFCs (5% Enrichment, Undamaged assembly 15x15F, 20x20 Bare Rod Array)	0.8705	0.9276
MPC-89 with 16 DFCs (4.8 % Enrichment, Undamaged assembly 10x10A, 9x9 Bare Rod Array)	0.8296	0.9464
MPC-32ML with 8 DFCs (5% Enrichment, Undamaged assembly 16x16D, 22x22 Bare Rod Array)	0.8667	0.9380

HOLTEC INTERNATIONAL COPYRIGHTED MATERIAL

TABLE 6.4.5

MAXIMUM k_{eff} VALUES WITH REDUCED WATER DENSITIES

Internal Water Density† in g/cm³	**Maximum k_{eff}**								
	MPC-89 10x10A, 4.8%	**MPC-37 (1500ppm) 17x17B, 4.0 %**		**MPC-37 (2000ppm) 17x17B, 5.0 %**		**MPC-37† (2300ppm) 15x15F and Damaged Fuel 5.0 %**		**MPC-32ML (2000ppm) 16x16D, 5.0 %**	
Guide Tubes	N/A	filled	void	filled	void	filled	void	filled	void
1.00	0.9435	0.9181	0.9071	0.9380	0.9292	0.9276	0.9265	0.9427	0.9397
0.99	0.9415	0.9181	0.9059	0.9367	0.9296	0.9271	0.9264	0.9420	0.9389
0.98	0.9391	0.9162	0.9054	0.9368	0.9279	0.9271	0.9257	0.9423	0.9376
0.97	0.9370	0.9166	0.9035	0.9364	0.9272	0.9265	0.9242	0.9422	0.9373
0.96	0.9345	0.9147	0.9005	0.9360	0.9265	0.9265	0.9232	0.9408	0.9366
0.95	0.9304	0.9148	0.9010	0.9356	0.9243	0.9253	0.9217	0.9414	0.9358
0.94	0.9280	0.9133	0.8995	0.9335	0.9238	0.9255	0.9225	0.9408	0.9346
0.93	0.9259	0.9128	0.8986	0.9355	0.9237	0.9263	0.9214	0.9423	0.9376
0.92	0.9232	0.9120	0.8955	0.9327	0.9203	0.9237	0.9204	0.9399	0.9328
0.91	0.9183	0.9105	0.8947	0.9335	0.9208	0.9229	0.9194	0.9400	0.9321
0.90	0.9169	0.9090	0.8934	0.9303	0.9189	0.9226	0.9169	0.9387	0.9307
0.85	0.9013	0.9042	0.8840	0.9272	0.9109	0.9190	0.9127	0.9352	0.9250
0.80	0.8850	0.8973	0.8733	0.9222	0.9022	0.9138	0.9040	0.9293	0.9169
0.70	0.8462	0.8813	0.8477	0.9068	0.8780	0.9000	0.8851	0.9140	0.8981
0.60	0.7980	0.8565	0.8132	0.8866	0.8478	0.8806	0.8571	0.8902	0.8695
0.40	0.6762	0.7876	0.7195	0.8244	0.7585	0.8192	0.7735	0.8082	0.7844
0.20	0.5268	0.6827	0.5806	0.7284	0.6298	0.7237	0.6517	0.6691	0.6510
0.10	0.4649	0.6206	0.5112	0.6698	0.5639	0.6669	0.5889	0.5855	0.5775

† External moderator is modeled at 100%.

† With undamaged and damaged fuel. All other cases with undamaged fuel only

HOLTEC INTERNATIONAL COPYRIGHTED MATERIAL

TABLE 6.4.10

COMPARISON OF MAXIMUM k_{eff} VALUES FOR EACH ASSEMBLY CLASS IN THE MPC-37 WITH CONDITIONS OF FILLED AND VOIDED GUIDE AND INSTRUMENT TUBES AT 5 % ENRICHMENT

Fuel Assembly Class	**Maximum k_{eff}, Filled Tubes**	**Maximum k_{eff}, Voided Tubes**
14x14A	0.8983	0.8887
14x14B	0.9282	0.9148
14x14C	0.9275	0.9277
15x15B	0.9311	0.9251
15x15C	0.9188	0.9134
15x15D	0.9421	0.9379
15x15E	0.9410	0.9365
15x15F	0.9455	0.9404
15x15H	0.9325	0.9317
15x15I	0.9357	0.9362
16x16A	0.9366	0.9320
16x16A[DFC]	0.9400	0.9404
16x16B	0.9334	0.9301
16x16C	0.9187	0.9015
16x16E	0.9303	0.9149
17x17A	0.9194	0.9135
17x17B	0.9380	0.9292
17x17C	0.9424	0.9345
17x17D	0.9384	0.9293
17x17E	0.9392	0.9314

HOLTEC INTERNATIONAL COPYRIGHTED MATERIAL

TABLE 6.4.11~~2~~

MAXIMUM k_{eff} VALUES IN MPC-32ML WITH UNDAMAGED (16x16D) AND DAMAGED FUEL

Bare Rod Array inside the DFC	**Maximum k_{eff}, 4.0 wt%**	**Maximum k_{eff}, 5.0 wt%**
17x17	0.9158~~0.9123~~	0.9337~~0.9303~~
19x19	0.9178~~0.9142~~	0.9367~~0.9332~~
20x20	0.9182~~0.9149~~	0.9377~~0.9342~~
21x21	0.9186~~0.9146~~	0.9378~~0.9344~~
22x22	0.9185~~0.9144~~	0.9380~~0.9347~~
23x23	0.9181~~0.9140~~	0.9377~~0.9336~~
24x24	0.9183~~0.9136~~	0.9367~~0.9331~~
26x26	0.9164~~0.9122~~	0.9356~~0.9315~~

HOLTEC INTERNATIONAL COPYRIGHTED MATERIAL

APPENDIX 6.B: MISCELLANEOUS INFORMATION

6.B.1 Sample Input File MPC-37
6.B.2 Sample Input File MPC-89
6.B.3 Analyzed Distributed Enrichment Patterns for Higher Enrichments
6.B.4 Assembly Cross Sections
6.B.5~~6~~ Sample Input File MPC-32ML

HOLTEC INTERNATIONAL COPYRIGHTED MATERIAL

6.B.1 Sample Input File MPC-37

PROPRIETARY INFORMATION WITHHELD PER 10CFR2.390

6.B.2 Sample Input File MPC-89

PROPRIETARY INFORMATION WITHHELD PER 10CFR2.390

6.B.3 Analyzed Distributed Enrichment Patterns

PROPRIETARY INFORMATION WITHHELD PER 10CFR2.390

6.B.4 Assembly Cross Sections

PROPRIETARY INFORMATION WITHHELD PER 10CFR2.390

6.B.5 Sample Input File MPC-31C

PROPRIETARY INFORMATION WITHHELD PER 10CFR2.390

6.B.6 Sample Input File MPC-32ML

PROPRIETARY INFORMATION WITHHELD PER 10CFR2.390